



The cyto-toxicity of some chemotherapeutic drugs on liver and kidney cell lines and the protective role of Ca^{2+} binding proteins

By

Noor Ahmed Mohammed

**A thesis Submitted to University of Birmingham in Partial Fulfilment
of the Requirement for the degree of Doctor of Philosophy**

School of Biosciences

College of Life and Environmental Sciences

University of Birmingham

September 2016

UNIVERSITY OF
BIRMINGHAM

University of Birmingham Research Archive

e-theses repository

This unpublished thesis/dissertation is copyright of the author and/or third parties. The intellectual property rights of the author or third parties in respect of this work are as defined by The Copyright Designs and Patents Act 1988 or as modified by any successor legislation.

Any use made of information contained in this thesis/dissertation must be in accordance with that legislation and must be properly acknowledged. Further distribution or reproduction in any format is prohibited without the permission of the copyright holder.

Abstract

Cancer Chemotherapy treatment involves the administration of drugs to patients, these drugs mainly work by interacting with the cell cycle or inhibiting DNA synthesis. Unfortunately, the toxicity of these chemotherapy drugs is severe and can have serious side-effects on different tissues and organs of the body. In chemotherapy treatment about 85% of cancer patients exhibit some degree of liver or kidney damage. Therefore, the aim of this study was to investigate the cytotoxicity of some of the most commonly used chemotherapy drugs; Methotrexate (MTX), Etoposide, Cisplatin and Doxorubicin (DOX) on liver and kidney cell lines (HepG2, Huh7.5, COS-7 and HK2). Therefore, our focus were on studying the molecular mechanism by which these drugs cause cell death in liver and kidney cells. This study also investigated the effects of some Ca^{2+} binding proteins (RGN, SERCA1, SERCA2b, SPCA1a, SPCA2) to test their ability to decrease the toxicity of these chemotherapeutic drugs in liver and kidney cells. The results showed that Etoposide, Cisplatin and DOX induce cell death in both kidney and liver cell lines via several different pathways such as apoptosis, necrosis, and autophagy. The results presented here also showed that several of the drugs used induced cell death by a novel new autophagic pathway in liver and kidney cells. Our data also suggested that regucalcin (RGN) and the endoplasmic reticulum Ca^{2+} pumps (SERCA1 and SERCA2b), but not the secretory pathway Ca^{2+} pumps (SPCA1a and SPCA2) were able to protect against different types of chemotherapy-induced toxicity in liver and kidney cells. These new observations will help to build up our awareness of the diverse effect of these drugs have on liver and kidney cells and may also help to develop protective interventions and strategies in the future to reduce hepatotoxicity and nephrotoxicity caused by these drugs.

Dedicated to

Peshmerga of Kurdistan and their families

Acknowledgments

I would like to show my gratitude to the Kurdistan Regional Government (KRG) for sponsoring me to do my PhD in Birmingham University which is one of the top universities in the UK.

I would like to express my gratitude and sincere thanks to my supervisor Prof. Frank Michelangeli for his everlasting support, guidance, criticism and motivations during the period of my study. It was my great fortune to have him as my supervisor.

I would also like to especially thank my co-supervisor Dr. Nik Hodges for his kindness and support during my PhD.

I express my gratitude to Prof. Chris Bunce, Dr. Farhat Khanim, Dr Scott White and every single person who held my hand in the most difficult time in my PhD.

I would like to thank all my colleagues in the 8th, 4th and 7th floor for their help and support and especially Israa Hakeem, Maiss Al-Amere and Tahira Mujtaba.

Last but not the least; I would like to especially thank my best husband Haval and my second soul, my daughter Norjan, for the endless help, love and patience along my study. Big thanks to my lovely parents, sisters and brothers for their prayers and encouragement over a growing number of years.

Table of Contents

1	Introduction	1
1.1	Chemotherapy.....	1
1.2	Classes of Chemotherapy drugs	2
1.2.1	Alkylating Agents	3
1.2.2	Antimetabolites	7
1.2.3	Anti-tumor Antibiotics.....	9
1.2.4	Topoisomerase inhibitors.....	11
1.2.5	Other Types of chemotherapy drugs.....	13
1.3	Cell Death.....	14
1.3.1	Major Forms of cell death.....	14
1.3.2	Apoptosis	14
1.3.2.1	Extrinsic apoptotic pathway	18
1.3.2.2	Intrinsic apoptotic pathway.....	18
1.3.3	Necrosis cell death	21
1.3.4	Necroptosis	23
1.3.5	Autophagy.....	23
1.4	Regucalcin	26
1.4.1	Transcription Regulation of Regucalcin expression.....	28
1.4.2	Regucalcin and apoptosis.....	29
1.4.2.1	Regucalcin role in suppressing cell death and apoptosis in liver cells ..	29
1.4.3	Regucalcin protein and Ca^{2+} Homeostasis	31
1.5	Cytoprotection	32
1.6	Calcium.....	34
1.6.1	Ca^{2+} channels and pumps	36
1.6.1.1	Inositol 1, 4, 5-triphosphate receptors (IP3Rs).....	37

1.6.1.2	Ryanodine receptors (RyRs).....	38
1.6.1.3	Mitochondrial permeability transition pore channels (MPTP).....	39
1.6.2	Ca ²⁺ Pumps	39
1.6.2.1	Overview of the Sarco (endo) plasmic reticulum Ca ²⁺ -ATPase (SERCAs)	40
1.6.2.1.1	SERCA kinetic cycle	41
1.6.2.1.2	SERCA Ca ²⁺ pumps inhibitors	42
1.6.2.2	Overview of secretory pathway Ca ²⁺ –ATPase (SPCAs).....	43
1.6.2.2.1	The multifunctions of SPCA in Eukaryotic cells	44
1.7	Aims of this study.....	45
2	Materials and Methods	47
2.1	Materials	47
2.2	Methods	50
2.2.1	Cell culture technique	50
2.2.2	Mammalian cells culture and subculturing	50
2.2.3	Mammalian cells freezing and thawing	50
2.2.4	Mammalian cells counting Via a Haemocytometer.....	51
2.2.5	Cell viability assay (MTT Assay)	51
2.2.6	Stock solution preparation	52
2.2.7	Caspase activity assay	52
2.2.8	Caspase-3 substrate activity	52
2.2.9	Necrosis inhibitor.....	53
2.2.10	Lactate Dehydrogenase (LDH) activity	53
2.2.11	LC3-GFP Autophagy transfection	53
2.2.12	Flow cytometry and cell viability	53
2.2.13	Comet Aassay	54
2.2.14	Protein estimation	55

2.2.14.1	Preparation of Cell lysates	55
2.2.14.2	Bradford protein concentration determination assay	55
2.2.14.3	SDS_PAGE	55
2.2.14.4	Western blotting.....	56
2.2.15	Transfection	57
2.2.15.1	Making Luria-Bertani (LB) and Agar Plates	57
2.2.15.2	DH5 α cells transformation and RGN plasmid preparation	57
2.2.15.3	Estimation of plasmid RGN DNA quantity	57
2.2.15.4	Transfection of COS-7 cells	57
2.2.15.5	Co-Localization of RGN.....	58
2.2.15.6	Cell proliferation and crystal violet assay	59
2.3	Statistical Analysis	59
2.4	Image analysis	59
3	Mechanisms of cell death by chemotherapeutic drug	61
3.1	Introduction	61
3.2	Cell viability and DMSO concentration	62
3.2.1	Cell viability with MTT assay	62
3.2.2	Cell Viability with Flow Cytometry	62
3.3	The effect of chemotherapy drugs on the viability of liver (HepG2, Huh7.5) and kidney cells (COS-7, HK2).....	63
3.3.1	The effect of chemotherapy drug Methotrexate on the viability of kidney cells (COS-7, HK2) and liver cells (HepG2, Huh7.5) using the MTT assay	63
3.3.2	The effect of chemotherapy drug Etoposide on the viability of kidney (COS-7, HK2) and liver cell lines (HepG2, Huh7.5) as performed using the MTT assay	69
3.3.3	The effect of chemotherapy drug Cisplatin on the viability of kidney cell lines (COS-7, HK2) and liver cell lines (HepG2, Huh7.5), as performed using the MTT assay	71

3.3.4	The effect of chemotherapy drug Doxorubicin (DOX) on the viability of kidney (COS-7, HK2) and liver cells (HepG2, Huh7.5) as performed using the MTT assay.....	72
3.4	Detection of apoptosis induced by MTX, Etoposide, Cisplatin, and Doxorubicin using caspase 3 inhibitors and the fluorogenic substrate (488 Nuc caspase-3) on kidney and liver cell lines.....	75
3.4.1	Detection of apoptosis by caspases caused by Etoposide, Cisplatin, and Doxorubicin using a caspase 3 inhibitor to detect the effects on cell viability.....	75
3.4.1.1	Effect of caspases inhibitor on Etoposide induced cell death	75
3.4.1.2	The effect of caspase inhibitor -3 on Cisplatin induced cell death ...	78
3.4.1.3	The effect of caspase inhibitor -3 on Doxorubicin induced cell death.	81
3.4.2	Detection of apoptosis by caspase activation induced by MTX, Etoposide, Cisplatin, and Doxorubicin using a fluorogenic substrate (488 Nuc caspase-3)	84
3.4.2.1	Detection of apoptosis by caspase activation induced by MTX, using a fluorogenic substrate (488 Nuc caspase-3) on kidney and liver cell lines	85
3.4.2.2	Detection of apoptosis by caspase activation induced by Etoposide, using the fluorogenic substrate (488 Nuc caspase-3) on kidney and liver cell lines	87
3.4.2.3	Detection of apoptosis by caspase activation induced by Cisplatin, using the fluorogenic substrate (488 Nuc caspase-3) on kidney and liver cell lines.....	89
3.4.2.4	Detection of apoptosis by caspase activation induced by Doxorubicin, using a fluorogenic substrate (488 Nuc caspase-3) on kidney and liver cell lines	91
3.5	Determination of Necrosis involved in the cell death process induced by the chemotherapy drugs.....	92
3.5.1	Determination of necrosis using necrosis inhibitor (necrostatin by Etoposide, Cisplatin and doxorubicin) in kidney and liver cell lines	92
3.5.1.1	Detection of regulated necrosis using necrostatin by Etoposide in kidney and liver cells.....	92

3.5.1.2	Determination of regulated necrosis induced by Cisplatin in kidney and liver cell lines.....	95
3.5.1.3	Using necrostatin to determine whether regulated necrosis is involved in cell death induced by Doxorubicin in kidney and liver lines	98
3.5.2	Lactate dehydrogenases release assay to determine necrosis through plasma membrane leakage when kidney and liver cell lines are exposed to chemotherapy agents	100
3.5.2.1	Detection of necrosis induced by Etoposide in kidney and liver cell lines using the lactate dehydrogenases release assay	100
3.5.2.2	Determination of necrosis induced by Cisplatin in kidney and liver cells using the lactate dehydrogenases assay	101
3.5.2.3	Detection of necrosis induced by doxorubicin in kidney and liver cell lines using the lactate dehydrogenases assay	102
3.6	Autophagy detection using cytosolic LC3-GFP as a biomarker for autophagosome formation	103
3.6.1	Monitoring autophagy using LC3- GFP by Etoposide in kidney and liver cells.....	104
3.6.2	Monitoring autophagy using LC3- GFP by Cisplatin in kidney and liver cells.....	105
3.6.3	Monitoring autophagy using GFP-LC3 by Doxorubicin in kidney and liver cells.....	107
3.7	Investigating DNA single strand breaks using comet assay.....	108
3.7.1	Comet assays for measuring DNA breaks in COS-7 cells treated cells with DOX.....	109
3.7.2	Comet assay for measuring DNA breaks in HepG2 cells treated cells ..	110
3.8	Discussion.....	112
3.8.1	The effect of Methotrexate (MTX) in Kidney (COS-7, HK2) and liver (HepG2, Huh7.5) cancer cell lines	112
3.8.2	The effect of Etoposide in Kidney (COS-7, HK2) and liver (HepG2, Huh7.5) cell lines.....	113

3.8.3	The effect of Cisplatin in Kidney (COS-7, HK2) and liver (HepG2, Huh7.5) cell lines.....	114
3.8.4	The effect of Doxorubicin in Kidney (COS-7, HK2) and liver (HepG2, Huh7.5) cell lines.....	116
4	RGN over-expression in COS-7 and HepG2 cells and drugs treatment	120
4.1	Introduction	120
4.2	SMP30, Over-expression, Detection, and Cytoprotection	122
4.2.1	Over-expression and Detection of SMP30	123
4.2.2	The cytoprotection of SMP30 overexpression in COS-7 and HepG2 cells exposed to chemotherapeutic drugs.....	124
4.2.2.1	The cytoprotection effect SMP30 overexpression in COS-7	124
4.2.2.2	The cytoprotection effect of SMP30 overexpression in HepG2.....	127
4.2.3	The effect of SMP30 on COS-7 cell viability and proliferation.....	128
4.2.3.1	The effect of SMP30 overexpression on COS-7 cells viability.....	128
4.2.3.2	The effect of SMP30 overexpression on COS-7 cell proliferation.....	129
4.3	RGN-GFP, Overexpression, Detection, Cytoprotection and Microscopy studies	131
4.3.1	Optimization of the transfection efficiency in COS-7 cells.....	131
4.3.2	Detecting RGN at protein level in kidney and liver cell line.....	134
4.3.3	Effect of overexpression of RGN-GFP on COS-7 cell viability following treatment with Doxorubicin.....	134
4.3.4	The effect of RGN-GFP on COS-7 cell proliferation.....	135
4.3.5	Microscopy studies of RGN-GFP treated with Doxorubicin.....	136
4.3.5.1	Time-lapse experiments with COS-7 and DOX	136
4.3.5.2	Co-localization of RGN-GFP with COS-7 cells.....	138
4.3.5.2.1	Co-localization of RGN-GFP in COS-7 cells with mitochondria and nuclei and the effects of Doxorubicin	138
4.3.5.2.2	Co-localization of RGN-GFP with COS-7 cells and Etoposide...	144

4.3.5.2.3	Co-localization of RGN-GFP within COS-7 during the early stages of Doxorubicin treatment	147
4.3.6	Treating HepG2 cells with different calcium concentration.....	150
4.3.6.1	Measuring RGN expression by western blot	150
4.4	Discussion.....	151
5	SERCA and SPCA expression in COS-7 cells and drug treatment.....	155
5.1	Introduction	155
5.2	Effect of BAPTA-AM on DOX-induced cell death in COS-7 cells	156
5.3	The effects of BAPTA-AM on Cisplatin-induced cell death in COS-7 cells.	157
5.4	SERCA detection, over-expression and cytoprotection	158
5.4.1	SERCA detection in normal cells	158
5.4.2	Overexpression of SERCA	159
5.4.3	High resolution visualisation of the localisation of SERCA-GFP using fluorescence microscopy	161
5.4.4	The effects of SERCA-GFP overexpression on COS-7 cell viability	163
5.4.4.1	The effect of SERCA1-GFP overexpression on COS-7 cell viability when treated with chemotherapy drugs	163
5.4.4.2	The effect of SERCA2b-GFP overexpression on COS-7 cell viability when treated with chemotherapy drugs	164
5.5	SPCA transfection, detection and cyto-pretecton.....	166
5.5.1	Overexpression of SPCA	166
5.5.2	The visualisation of the localisation of SPCA-GFP using fluorescence microscopy.....	167
5.5.3	The effect of overexpression of SPCA-GFP on COS-7 cells treated with chemotherapy drugs Doxorubicin and Cisplatin	169
5.5.3.1	The effect of overexpression of SPCA1a –GFP on COS-7 cells treated with Doxorubicin and Cisplatin.....	169
5.5.3.2	The effect of SPCA2-GFP overexpression on COS-7 cells treated with Doxorubicin and Cisplatin.....	170

5.6	The effect of Ca^{2+} concentrations in the culture media on SERCA expression	172
5.7	Discussion.....	174
6	General discussion and future works.....	178
6.1	General discussion.....	178
6.2	Future Works	183
7	References	185

List of figures

Chapter 1

Figure 1.2.1 A; stages of the cell cycle.....	3
Figure 1.2.1 B; the structure of Cisplatin.....	7
Figure 1.2.2; the structure of methotrexate.....	8
Figure 1.2.3; the structure of Doxorubicin.....	10
Figure 1.2.4; the structure of Etoposide.....	12
Figure 1.3.2 A; morphological changes observed in apoptotic cell death.....	15
Figure 1.3.2 B; summary of the two main apoptotic pathways.....	17
Figure 1.3.2 C; the perforin/granzyme cell death pathway in cytotoxic T cells...	21
Figure 1.3.3; Necrosis cell death.....	22
Figure 1.3.5A; macroautophagy formation process in mammalian cells.....	25
Figure 1.3.5B; the Beclin-1-Vps34 complex.....	26
Figure 1.4; the solved crystal structure of RGN (SMP30).....	28
Figure 1.4.2.1; the suppressive effect of Regucalcin on cell death and apoptosis.	31
Figure 1.6; mechanisms of calcium signalling.....	35
Figure 1.6.1; Ca^{2+} Channels, Exchangers and Pumps in a typical Cell.....	37
Figure 1.6.2; structure of the Ca^{2+} -ATPase in conformationl state E1	40
Figure 1.6.2.1.1; scheme of Ca^{2+} transport cycle of SERCA.....	42

Chapter 2

Figure 2.2.8.4: western and blotting sandwich assembly.....	56
---	----

Chapter 3

Figure 3.2.1; the correlation between absorbance at 590 nm using an MTT assay and cells number.....	62
Figure 3.2.2; shows the percentage of cell viability of COS-7 cells.....	63
Figure 3.3.1; shows the cell viability using MTT assay with different concentrations of DMSO (0-0.15% v/v) in HepG2 cells.....	64
Figure 3.3.1.1 A-D; shows the effects of MTX on the viability of COS-7 (A), HK2 (B) HepG2 (C), and Huh7.5 (D) cells.....	65
Figure 3.3.1.2 A and B; shows the effect of MTX (200 μ M) on COS-7 (A) and Huh7.5 (B) on cell viability.....	66
Figure 3.3.1.3 A-C; shows the inhibition effects of MTX on COS-7 (A), HK2 (B) and HepG2 (C) on cells proliferation.....	68
Figure 3.3.2 A-D; shows the effect of Etoposide on the viability of COS7 (A), HK2 (B) HepG2 (C), and Huh7.5 (D), cell lines.....	70
Figure 3.3.3 A-D; shows the effects of Cisplatin on the viability of COS-7 (A), HK2 (B), HepG2 (C), and Huh7.5 (D).....	72
Figure 3.3.4 A-D; shows that DOX reduces viability of COS-7 (A), HK2 (B) HepG2 (C), and Huh7.5 (D).....	73
Figure 3.4.1.1 A-D; the effects of caspase inhibitor-3 on Etoposide induced cell death.....	78
Figure 3.4.1.2 A-D; the effects of Cisplatin-induced death by caspase inhibitor-3.....	81
Figure 3.4.1.3 A-D; effect of caspase inhibitors -3 on DOX-induced cell death...	84
Figure 3.4.2; Illustrates light and fluorescence field of COS-7 cells pre-treated with fluorogenic substrate (488 Nuc caspase-3) and then treated with doxorubicin	85
Figure 3.4.2.1A; shows the effect of MTX on apoptotic cells.....	86
Figure 3.4.2.1B; shows the effect of MTX on apoptotic cells.....	86
Figure 3.4.2.2 A-D; shows the effect of Etoposide on apoptotic kidney and liver cell lines.....	89

Figure 3.4.2.3 A-D; shows the effect of Cisplatin on apoptosis cell in different kidney and liver cell lines COS-7 (A), HK2 (B), HepG2 (C), and Huh7.5 (D).....	90
Figure 3.4.2.4 A-D; shows the effect of Doxorubicin on inducing apoptotic cells in different kidney and liver cell lines.....	92
Figure 3.5.1.1 A-D; shows the effects of Etoposide with and without necrostatin in liver and kidney cells.....	95
Figure 3.5.1.2 A-D; shows the effects of Cisplatin with and without necrostatin on liver and kidney cell lines.....	97
Figure 3.5.1.3 A-D; the effects of DOX with and without necrostatin pre-treatment in liver and kidney cell lines.....	100
Figure 3.5.2.1A and B; the effect of Etoposide on lactate dehydrogenases (LDH) release in COS-7 cells (A) and HepG2 cells (B).	101
Figure 3.5.2.2A and B; the effect of Cisplatin on lactate dehydrogenases (LDH) release in kidney cells COS-7(A) and liver cells HepG2 (B).....	102
Figure 3.5.2.3 A and B; the effect of DOX on lactate dehydrogenases (LDH) release in COS-7 cells (A) and HepG2 cells (B).....	103
Figure 3.6.1; the percentage of LC3-GFP punta transfected cells treated with Etoposide.....	105
Figure 3.6.2; the percentage of LC3-GFP punta in transfected cells treated with Cisplatin.....	106
Figure 3.6.3; the percentage of punta in LC3-GFP transfected cells treated with DOX.....	108
Figure 3.7.1 A; images from Comet IV software, showing COS-7 intact nuclei and a damaged nuclei after DOX treatment.....	109
Figure 3.7.1 B and C; shows the tail intensity of control, H ₂ O ₂ , and DOX treated cells with one comet assay.....	110
Figure 3.7.2 A; images from Comet IV software, showing HepG2 intact nuclei and a damaged nuclei after DOX treatment.....	111
Figure 3.7.2 B and C; shows the tail intensity of control, H ₂ O ₂ , and DOX treated HepG2 cells with one comet assay.....	111

Chapter 4

Figure 4.2A and B; the restriction map for PCDNA and SMP30-PcDNA plasmids.....	122
Figure 4.2.1 A and B; western blots of cell lysates overexpressing SMP30 in COS-7 (A) and HepG2 (B).....	123
Figure 4.2.2.1; the effects of Etoposide (A), Cisplatin (B) and DOX (C) on cell viability of COS-7 cells.....	126
Figure 4.2.2.2; the effect of DOX on cell viability of HepG2 cells in the presence of empty vector-PCDNA and SMP30.....	128
Figure 4.2.3.1; the effect of SMP30 plasmid on COS-7 cell viability.....	129
Figure 4.2.3.2; the effect of SMP30 overexpression on COS-7 cell proliferation.	130
Figure 4.3.1A: shows the Origene vector with RGN-C-tagged Human Variant 1	132
Figure 4.3.1B; COS-7 cells transfected using three conditions of plasmid and turbofect transfection reagent.....	131
Figure 4.3.1C; illustrates the optimal condition of RGN-GFP transfection with (1:2) (1 µg Plasmid RGN-GFP:2 µl transfection reagent) in COS-7 cells.....	133
Figure 4.3.2; western blot to detect RGN detection in cell lysates of kidney and liver cell lines.....	134
Figure 4.3.3; effect of DOX on COS-7 cell viability in the present or absence of RGN-GFP expression.....	135
Figure 4.3.4; the effect of RGN-GFP and PCDNA on COS-7 cell number.....	136
Figure 4.3.5.1; time-lapse of RGN-GFP transfected COS-7 cells treated with 7 µM DOX.....	137
Figure 4.3.5.2.1A; fluorescence images with confocal microscopy of untreated COS-7 cells.....	139
Figure 4.3.5.2.1B; colocalization data analyzed with JACOps plugin for COS-7 cells of red and green channels.....	140
Figure 4.3.5.2.1C; colocalization data with JACOps plugin for COS-7 cells of blue and green channels.....	141

Figure 4.3.5.2.1D; fluorescence images of late apoptotic COS-7 treated with DOX.....	142
Figure 4.3.5.2.1E; colocalization data analysed with JACOPs plugin.....	143
Figure 4.3.5.2.1F; colocalization data analysed with JACOPs plugin.....	143
Figure 4.3.5.2.2A; treated COS-7 cells with Etoposide (150 μ M).....	145
Figure 4.3.5.2.2 B; colocalization data analysed with JACOps plugin for Etoposide (150 μ M) treated COS-7 cells in the red and green channels.....	146
Figure 4.3.5.2.2 C; colocalization data with JACOps plugin for Etoposide (150 μ M) treated COS-7 cells in the blue and green channels.....	146
Figure 4.3.5.2.3A; merged image of fluorescence images obtained by confocal microscopy.....	147
Figure 4.3.5.2.3B; fixed Fluorescence emerge images taken by confocal microscope for DOX treated COS-7 cells at early stage of apoptosis.....	148
Figure 4.3.5.2.3C and D; colocalization analysis of RGN-GFP transfected COS-7 cells treated with DOX for a short time of period.....	149
Figure 4.3.6.1; western blotts of RGN expression in HepG2 cells.....	150

Chapter 5

Figure 5.2; shows the effects of Doxycubicin with and without BAPTA-AM pre- treatment in COS-7 cells.....	156
Figure 5.3; shows the effects of Cisplatin with and without BAPTA-AM pre-treatment in COS-7 cells.....	157
Figure 5.4.1; western blot of HepG2 (1) and COS-7 (2) cell lysate for SERCA...	159
Figure 5.4.2; transfected of COS-7 cells with the two different condition of SERCA1-GFP plasmid.....	160
Figure 5.4.3; fluorescence images showing the localisation of SERCA1-GFP and SERCA2b-GFP in COS-7 cells.....	162

Figure 5.4.4.1A; the effect of DOX on COS-7 cell viability in the present of (SERCA1-GFP and PCDNA).....	163
Figure 5.4.4.1B; the effect of Cisplatin on COS-7 cell viability in the presence of (SERCA1-GFP and PCDNA alone).....	164
Figure 5.4.4.2A; the effect of DOX on cell viability of COS-7 cells in the present of SERCA2b.....	165
Figure 5.4.4.2B; shows COS-7 cell viability in the presence of SERCA2b-GFP or PCDNA and treated with Cisplatin.....	166
Figure 5.5.2; fluorescence images shows the localisation of SPCA1a-GFP and SPCA2-GFP in COS-7 cells.....	168
Figure 5.5.3.1A and B; the effects of DOX and Cisplatin on cell viability of COS-7 cells overexpressing SPCA1a-GFP or PCDNA alone.....	170
Figure 5.5.3.2A and B; the effects of Doxorubicin and Cisplatin on COS-7 cell viability, in cells overexpressing SPCA2-GFP.....	171
Figure 5.6; detection of SERCA in COS-7 cells incubated in media with different calcium concentrations.....	173
Figure 5.7; the effect of Cisplatin on ER.....	176
 Chapter 6	
Figure 6.1C; schematic showing summary of this study.....	182

List of tables

Table 2.2.4;	the number of cells and the volumes of growth media used in this study.....	51
Table 3.3;	comparison of lethal concentration 50 (LC ₅₀) values of different anti- cancer drugs	74
Table 3.8.4;	summary of the different cell death pathways using various assays.....	118
Table 4.2.2.1;	summarizes the LC ₅₀ in μ M values of COS-7 cells with the different drugs.....	127
Table 5.4.2;	the transfection efficiency of the two different conditions of SERCA plasmid.....	160
Table 5.5.1;	the transfection efficiency of SPCA plasmids after 24 hrs.....	167
Table 6.1A;	summary of the different cell death pathways and different chemotherapeutic drugs used in this study.....	179
Table 6.1B;	summarized the different Ca ²⁺ binding proteins and their protection, against chemotherapy drugs in COS-7 cells.....	182

List of Abbreviations

ATP: adenosine triphosphate

APP: amyloid precursor protein

Apaf-1: Apoptotic protease activating factor-1

AIF: apoptosis-inducing factor

Bcl-2: B-cell lymphoma 2

BPA: Bis-phenol A

Ca²⁺: calcium ions

cAMP: 3',5'-cyclic AMP

cGMP: 3',5'-cyclic GMP

[Ca²⁺]_i: intracellular concentration of calcium

CaM: calmodulin

Cisp: Cisplatin

COS-7: fibroblast-like cell line from monkey kidney tissue

DISC: death-inducing signal complex

DOX: Doxorubicin

DNA: deoxyribonucleic acid

DMSO: dimethyl sulfoxide

DR: death receptors

ER: endoplasmic reticulum

Etop: Etoposide

FADD: Fas associated death domain

GFP: green fluorescent protein

GPCRs: G protein-coupled receptors

HepG2: human liver cancer cell line

HK2: tubule epithelial cell line from human kidney

hrs: hours

HCX: Ca^{2+} exchanger

Huh7.5: human hepatoma cell line

IP3: inositol 1,4,5-triphosphate

IP3Rs: inositol-1,4,5-trisphosphate receptors

KDa: kilodalton

LC₅₀: concentration causing 50% lethal

LC3: microtubule-associated protein 1 light chain 3

LDH: lactate dehydrogenase hormone

MCU: mitochondrial Ca^{2+} uniporter

MOMP: mitochondrial outer membrane permeabilization

min: minutes

MTT: 3-(4,5-dimethylthiazol-2-yl)-2,5-diphenyltetrazolium bromide

MTX: methotrexate

NCX: $\text{Na}^+ / \text{Ca}^{2+}$ exchanger

NAADP: Nicotinic acid–adenine dinucleotide phosphate

PI: propidium iodide

PLC: phosolipase c

PMCAs: plasma membrane Ca^{2+} -ATPase

PTP: permeability transition pore

MPTP: mitochondria permeability transition pore

PKC: protein kinase C

PMSF: phenylmethanesulphonyl fluoride

PMCA: plasma membrane Ca^{2+} ATPase

PKA: protein kinase A

PKC: protein kinase C

PARP: poly (ADP-ribose) polymerase

RGN: regucalcin protein

RyRs: ryanodine receptors

ROS: reactive oxygen species

SERCA: sarco/endo plasmic reticulum Ca^{2+} ATPase

SERCA1a: sarco/endo plasmic reticulum Ca^{2+} ATPase, variant 1 a

SERCA2b: sarco/endo plasmic reticulum Ca^{2+} ATPase, variant 2 b

SMOC: secondary messenger operated ion channel

SMP30: senescence marker protein 30

SOCs: store-operated Ca^{2+} channels

SPCAs: secretory pathway Ca^{2+} ATPase

SPCA1: secretory pathway Ca^{2+} ATPase, isoform 1

SPCA2b: secretory pathway Ca^{2+} ATPase, variant 2 b

SDS: sodium dodecyl sulphate

TNF: tumor necrosis factor

TNF- α : tumor necrosis factor- α

TRADD: TNFR associated death domain

TRAIL: TNF related apoptosis inducing ligand

VOX: voltage-operated Ca^{2+} channels

CHAPTER 1

Introduction

1 Introduction

1.1 Chemotherapy

It is now known that cancer is one of the major health problems of the developed world and causes one of the most deaths in the human population (Ma and Yu, 2006). Cancer can be simply defined as uncontrolled cell division; many abnormal cells that undergo division can lead to tumor formation in the body. Some tumor cancer cells can easily spread to distance locations within the body through the vascular system and consequently lead to secondary tumor growths or metastasis (Lodish et al., 2000).

In spite of the different causes of cancer, i.e. genetic inheritance, environmental factors, age, lifestyle and nutrition, medical research over many years has developed a variety of different treatments. These include treatments such as radiation therapy, surgery, targeted therapy, immunotherapy and chemotherapy (Baskar et al., 2012). Surgery is usually considered the most effective option compared to other types, and if possibly is applied in the early stages of cancer development and diagnosis, while radiation therapy can be applied before or after surgery to damage / kill cancer cells. On the other hand, when cancers cells have spread in the body through metastasis, chemotherapy treatment is usually considered the main option (Baskar et al., 2012).

Chemotherapy is a type of cancer treatment that uses medicines and drugs in order to prevent, slow and/or stop tumor cancer cells multiplying. Chemotherapy drugs are also commonly given to patients (orally or intravenously), in order to destroy any remaining cancer cells following surgery (Skeel and Khelif, 2011). This form of therapy mainly acts either by interacting with the cell cycle or inhibiting DNA replication (Payne and Miles, 2008).

Approximately 60% of the commonly used anti-cancer agents are derived from natural resources (Cragg et al., 2005). These potential anti-cancer agents have been derived from plants, microorganisms, and marine organisms (Butler, 2004). The biochemical diversity of the natural world has in the past been a great source for developing of new anti-cancer agents compounds. In fact about 100 naturally derived drugs have been

discovered for the treatment of various cancers during the last five decades (Wagner et al., 2002).

As an ideal way to improve a patients' prognosis and life expectancy, some chemotherapy treatments are given in combination. This enhances the potential of such drugs to cause remission (Frei and Eder, 2003, Yardley, 2013). However, on the other hand, the toxicity of these drugs is increased. Chemotherapeutic drugs either singly or in combination have the ability to damage blood cells which causes by anemia, fatigue and immuno-suppression (Groopman and Itri, 1999). Other common side effects of chemotherapy drugs are mouth sores, diarrhea that is the result of mucous membrane damage, and hair loss, which is caused by destruction of hair root and follicles (Raji, 2005, Lenz, 2012). Some chemotherapeutic drugs can also specifically damage some organs.

The toxic effects of some of these drugs to healthy cells will induce severe side-effects (Kuo, 2008). Therefore, with chemotherapy treatment, unfortunately about 8% of cancer patients exhibit some degree of liver damage (Ramadori and Cameron, 2010). Some chemotherapy drugs can cause severe liver injury and even liver failure (Moar and Malnickls, 2013). Furthermore, some of these drugs can also affect kidney and heart function and causes nephrotoxicity and cardiotoxicity (Cornelison and Reed, 1993, Christenson, 2015). This may mean that the patients are not able to continue their chemotherapy treatment due to serious damage caused by these hepatotoxic and nephrotoxic drugs that prohibit cells from performing their normal metabolic functions (King and Perry, 2001, Lawrence et al., 1973).

1.2 Classes of Chemotherapy drugs

Chemotherapy Agents are classified in several ways; they can be classified according to their biochemical mechanisms, chemical structures, and their interaction with each other. Hence, according to their mechanism of action, chemotherapy drugs can be divided in to some of the following types; alkylating agents, antimetabolites, anti-tumor antibiotics and topoisomerase inhibitors.

1.2.1 Alkylating Agents

Common alkylating agents include Nitrogen mustards, Triazines, Nitrosoarenes, Ethylenimines and Alkyl sulfonates. These kinds of drugs mainly attack cancer cells through binding covalently to DNA. Unlike other chemotherapeutic agents, alkylating agents are not 'phase- specific' and have the ability to modify the DNA throughout their cell cycle (Warwick, 1963, Swift and Golsteyn 2014) (Figure 1.2.1A).

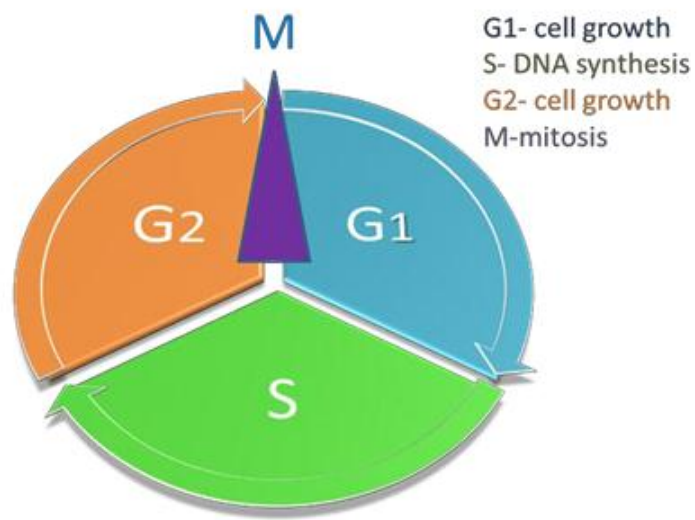


Figure 1.2.1 A; stages of the cell cycle. Where G1 means cell growth and protein synthesis takes place (time periods, 18-30 hrs). S, is where DNA replication takes place (time period, 18-20 hrs). G2, is where secondary cell development and genetic code checking take place before M phase (time period, 2-10 hrs), and M is where all Mitosis stages taken places (i.e. prophase, metaphase, anaphase and telophase, etc.) and formation of 2 new cells (times period, 30-6- hrs) (Adapted from Cooper, 2000).

Nitrogen mustards alkylating agents consist of Mechlorethamine, Ifosfamide, Melphalan, Cyclophosphamide and Chlorambucil. Mechlorethamine was the first to be used as an anti-cancer agent (Gilman and Philips, 1946). This radiomimetic chemical drug is used to treat Hodgkin's disease and other lymphomas (De Alencar et al., 2014). Ifosfamide is also a nitrogen mustard derivative, which is used to treat solid tumors. This anti-agent is most often used in combination with other drugs such as Cisplatin, Etoposide, and Doxorubicin (Kawasaki et al., 2014). Furthermore this anticancer-drug is commonly used to treat sarcoma and lung cancer, but it has been known to cause damage to nervous system (Brunello et al., 2007) and is therefore neurotoxic (Imtiaz and Muzaffer, 2010).

Melphalan has been mainly used in the treatment of multiple myeloma and ovarian cancer (Falco et al., 2007). But Cyclophosphamide is highly recommended for treating various types of lymphomas in combination with other drugs (Yu, 2015), Leukemia (Assouline et al., 2015) and many other types of cancer. Like many other chemotherapy drugs, Cyclophosphamide has many side-effects and is known to cause pulmonary damage (Bhattacharjee et al., 2015) and is hepatotoxic (Koler and Forgren, 1958). On the other hand, Chlorambucil is used to treat follicular lymphoma (Herold et al., 2015). Besides that, this anti-cancer agent is the standard drug of choice for chronic lymphocytic leukemia (Goede et al., 2014) when a proportion of the lymphocytes are in the bone marrow. Unfortunately, many patients who have taken this drug are often diagnosed with liver damage as well as damage to the spleen and lymph nodes (Kolar and Forgren 1958).

Triazines drugs include Decarbazine and Temozolomide. Temozolomide has been used in combination with other anti-cancer agents to treat Hodgkin lymphoma (Gandikota et al., 2015) and melanomas (Ferrucci et al., 2015, Hill and Hill, 1979). However, patients can suffer from hepatic failure during Temozolomide-treatment (Frosch et al, 1979). Decarbazine is widely used to treat brain tumors such as gliomas (Van Rijn, 2000).

Nitrosoureas is another class of alkylating agent and consist of three main drugs: Carmustin, Lomustin and Streptozotcin. Carmustin has been used for a long time for treating metastatic brain tumors (Ewend et al., 2007) and for lymphomas when used in

combination with Etoposide, Cytarabin and Melphalan (Martin et al., 2015). Lomustin is used for treating Glioblastomas and relapsed lymphoma (Harvey et al., 2015, Moore, 1999). Recently this drug has also shown to cause hepatotoxicity (Musser et al., 2012). Streptozotcin is a diabetagenic compound that induces beta cell cytotoxicity when injected into mice and causes insulinitis (Rossini et al., 1977). This drug was originally discovered as an antibiotic in 1959 (Vavra et al., 1959). Recently this drug has been used in many research studies as a diabetes inducer (Oztürk et al., 2015, Zhu et al, 2011). Streptozotcin and Carmustin can both cause irreversible changes to liver and kidney cells after only a few doses of treatment and changes to liver and kidney function have occurred in 15% to 67% of patients, respectively, given these drugs (Schein et al., 1974).

The Ethylenimines class of chemotherapeutic drugs include; Thiotepa and Hexamethylmelamine. Thiotepa is a known human carcinogen (Proctor et al., 2007) and is used in bone marrow and stem cell transplantation. This agent can be used to treat a range of different cancers including; lymphoma, leukemia, and other soft and solid-tumors (Davies, 2001). However, there have been reports of a direct correlation between Thiotepa and toxicity, such as mucositis, hepatitis and brain toxicity (Nieto and Vaughan, 2004). Hexamethylmelamine has replaced cisplatin as a better anti-cancer agents drug for the treatment of ovarian cancer (Rosen et al, 1987). Furthermore, Hexamethylmelamine has been successfully used to treat metastatic breast cancer (Henderson and Shapino., 1991).

Busulfan is the only alkylating sulfonate drug. In spite of the lung changes it causes during therapy (Brittig et al., 1993), busulfan is still useful to treat leukaemia (Underwood et al., 1971, Nagler et al., 2014).

The platinum anticancer- drugs (e.g. Cisplatin, Carboplatin and Oxaliptin) are most often used with alkylating agents as they work in the same way but they are likely to be less immunosuppressive than the other alkylating agents (Kufe et al., 2003). Many researchers have suggested that the cytotoxicity of platinum drugs are different. Oxaliptin has less toxic side effects, while carboplatin is more myelotoxic than the others. Cisplatin appears to be the most neurotoxic and nephrotoxic of the platinum drugs (Cavaletti, 2008). Cisplatin is known as cis- diamminedichloroplatinum (CDDP)

and considered the first metal complex that has been used as a chemotherapy drug. It consists of platinum ion and is surrounded by four ligands arranged in a square; two are amines and two chlorides (Figure 1.2.1 B). Once cisplatin enters the cell, it loses these two chloride ions and binds to DNA bases (Goodsell, 2006). Cisplatin is commonly used in testicular cancer as well as many other epithelial malignances such as ovary, bladder, cervix, head, neck, prostate, lymphoma, and carcinomas of esophageal (Oyanagi, et al., 2015, Rozencweig et al., 1977). Cisplatin and other anticancer- agents for instance Etoposide, Doxorubicin, Vinblastine etc., has shown a potential advance in the 5 year survival rate for non-small-cell lung carcinoma (Molina et al., 2008). Drug distribution studies suggest that about 10% of Cisplatin dose can pass into the blood serum then interact with the cancer cells, while 90% of the drug binds to plasma proteins and therefore has no effect on cancer cells (Michael et al, 1990, Deconti, et al., 1973). It has strongly been suggested that platinum drugs can accumulate in primary sensory neurons and are therefore neurotoxic, although the mechanism is not fully understood (Shord et al., 2002, Cavaletti et al., 2001, 1998, 1992). Furthermore, Cisplatin also causes liver toxicity as a side effect (Waseem et al., 2015).

As mentioned previously, the mechanism of toxicity for this drug is complicated because Cisplatin has the ability to bind to various biomolecules (DNA, RNA, protein, and phospholipids). However, its interaction with DNA could be the most critical factor for inducing toxicity inside the cells (Zamble and Lippared, 1995), and apoptosis could be the major mechanism for this due to DNA-cross linking (Goodsell, 2006, Zhen et al., 1992).

As research continues, efforts have been taken to determine whether cell death by Cisplatin is specifically by apoptosis (Victor et al., 2001). Based on several research studies, cell populations treated with Cisplatin shows both pathways of cell death ie apoptosis and necrosis are involved (Pestell et al. 2000). Many other hypotheses of cell death have been suggested since for instance some leukemia cells showing apoptotic cell death lacked many of the morphological and biochemical features that are distinctive of apoptosis (Segal-Bendirdjian and Jacquemia- Sablon, 1995). Therefore, necrosis cell death has been suggested the main form of cell death induced by Cisplatin,

However, this depends on Cisplatin concentration, cellular condition and energy availability (Victor et al., 2001).

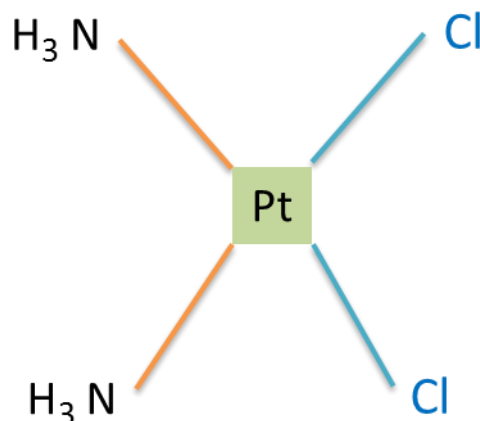


Figure 1.2.1 B: the structure of Cisplatin

(Adapted from Messori and Merlino, 2016)

1.2.2 Antimetabolites

Antimetabolites drugs generally work by affecting DNA and RNA, either by incorporating into these genetic materials or by inhibiting their biosynthesis. These types of drugs damage cells during S phase and are widely used to treat variety of cancers (Von Hoff et al., 2003).

Some common examples of Antimetabolites drugs include; Methotrexate, 5-fluorouracil, 6- mercaptopurine, Capecitabine, Cladribine, Gemcitabine, Hydroxyurea Clofarabine, Floxuridine, Fludarabine, Pemetrexed, Pentostatin, Thioguanine and Cytarabine.

Both 5-fluorouracil and Capecitabine are commonly used in treating breast cancer (Asara et al., 2012, Mrozek-Orlowski et al., 1999), colorectal cancer (Twelves et al., 2012), gastric cancer (Kang et al., 2014, He et al., 2015), pancreatic cancer (Short et al., 2013, Kruger et al., 2015) and colorectal cancer (Petrelli et al., 2012). Unfortunately, these two drugs are still considered as substantially toxic because of their cardiotoxicity affects (Segalini et al., 1987, Tutkun et al., 2001 and Fontanella et al., 2014).

Methotrexate (MTX) (Figure 1.2.2) is an antimetabolite agent and acts as an inhibitor of tetrahydrofolate reductase, which blocks tetrahydrofolate formation, a necessary component for nucleotide biosynthesis and thus inhibits cell division (Warlick et al., 2000).

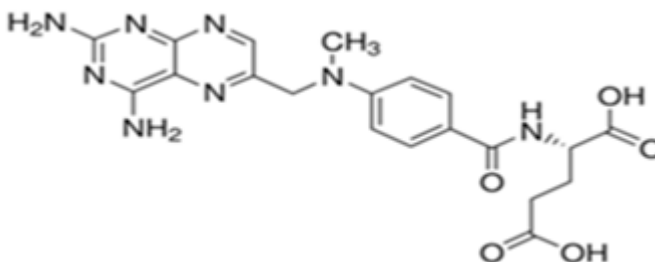


Figure 1.2.2; the structure of methotrexate (Alcántara, et al., 2010)

MTX was the first antimetabolites discovered in the 1940'S (Cuellar and Espinoza, 1997). It is also one of the most commonly used anti-rheumatic drugs and has also been used for decades for treatment of Psoriasis, Spondyloarthropathy, and Vasculitis, etc. (Laohapand,et al., 2015). This anticancer-agent has attracted physician's attention for many different reasons. For instance, rheumatoid arthritis requires long term therapy, however, there are also many factors which increase MTX toxicity such as age, diabetes, obesity, hepatitis B or C virus infection, alcohol consumption, etc. (Malatjalian, et al.,1996, Rheumatol 1995, sotoudehmanesh, 2010 and Bath et al., 2014). Although MTX is widely used as anti-cancer agent, it should be used with monitoring due to its hepatotoxicity and haematological toxicities that it could exert (Gilani et al., 2012). MTX hepatotoxicity might be related to its effects on the retinoid receptor (Ewees et al., 2015). MTX leads to necrosis when directly applied to hepatocytes (Lee, 2003). Other reports have suggested that MTX can also cause liver fibrosis (Jaskiewicz et al., 1996). In addition, others body organs have been shown to be affected during MTX therapy. Some examples are acute renal failure (Isoda et al., 2007), lung toxicity (Kaplan, 2014), neurotoxicity (Taylor et al., 2015) Myelosuppresion (Hayashi, 2010), skin disorders or alopecia (Weiss et al., 1986), ocular irritation (Doroshow et al., 1981), men and women fertility problems (Shamberger

et al., 1981, Elise and Durham, 1991). For this reason, MTX therapy is closely monitored and avoiding daily MTX dosage (Jones and Patel, 2000).

1.2.3 Anti-tumor Antibiotics

This chemotherapy drug group can be divided into anthracyclines, (eg Daunorubicin, Doxorubicin (Adriamycin®), Epirubicin, Idarubicin) and non-anthracyclines groups, (Actinomycin-D, Bleomycin, Mitomycin-Co).

Anthracyclines antibiotics were considered one of the most effective anticancer drugs ever developed when first used (Weiss, 1992). In the 1960s, the first anthracyclines, Daunorubicin and Doxorubicin were isolated from *Streptomyces peucetius* (Lomovskaya et al., 1999).

The anti-cancer mechanisms of these anthracyclines is still controversial, as numerous papers have been published that indicate different modes of action. These includes, inhibition of DNA function after DNA intercalation, damaging of DNA as a result of free radical formation, causing alkylation, inhibiting topoisomerases II (involved in DNA replication), inducing apoptotic cell death and unwinding of DNA by affecting helicase activity (Gewirtz, 1999).

In terms of structure there is not much difference between Daunorubicin and Doxorubicin, Daunorubicin terminates with methyl while Doxorubicin, terminates with primary alcohol.

Doxorubicin (DOX) is a throcyclin antibiotic anti-cancer drug. Chemically, it consists of an amino-sugar daunosamine which is bound to C7 of the tetracycline ring structure (Carvalho, 2009) (Figure 1.2.3). Biochemically, DOX reacts and interferes with DNA and the other nucleic acids, DNA polymerases at phase G1 and G2 of the cell cycle (Lal et al., 2010). This interaction inhibits topoisomerase II and stops nucleic acid replication and transcription (Tan et al., 2009). DOX is considered one of the most potent chemotherapeutic drugs that is used (Carvalho, 2009), because this drug has the ability to damage DNA by alkalation and also inhibit enzymes that produce DNA and RNA by free-radical damage (Minotti et al., 2004).

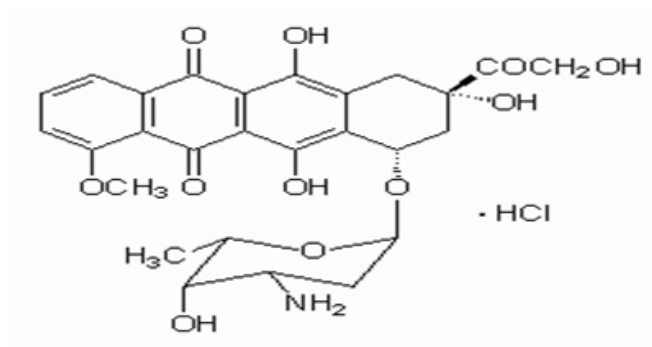


Figure 1.2.3; the structure of Doxorubicin (Arcamone, 1981)

Furthermore, DOX interacts with plasma membrane proteins and electron transfer process to causes highly reactive hydroxyl free radical formation (Cardosol et al., 2008). In spite of these side effects, DOX is a powerful anticancer drug, either in isolation or in combination, for treating ovary, haematological malignance, breast, stomach, liver, and prostate cancers (Tacer and Dass 2013).

In addition to what has been previously mentioned, DOX has effects on many biological molecules either directly or indirectly, which can lead to cell death. Cyclic Adenosine monophosphate (cAMP) -activated protein kinase can be activated via DOX in embryonic ventricular myocardial Hac₂ rat cells as well causing reactive oxygen species accumulation (Chen 2011). DOX has been shown to affect mitochondrial function which might cause elevation of reactive oxygen species (Armstrong and Dass, 2015). The suppressor tumor protein p53 is known to be a cell cycle regulator and activate DNA repair mechanisms, as well as being involved in angiogenesis (Sionov et al., 2000). Under certain forms of cellular stress p53 induces apoptosis to stop uncontrolled cell growth (Lee et al., 2002, Brooks and Gu, 2010). Several studies have shown that DOX induces p53 activation leading to apoptosis in both normal and tumor cells (Wang et al., 2004). Cell death via apoptosis during DOX therapy is not limited to p53 activation but also includes decreasing Bcl2 and increasing Bax, which leads to cytochrome c release from the mitochondria and which ultimately, leads apoptosis via caspase 3 activation (Leung and Wany, 1999). Once caspase-3 is activated it leads to the activation of caspase-6 and -7 which can also contribute to apoptosis cell death (Ueno et al., 2006). However, other research has

shown that DOX can additionally induce caspase-independent cell death (Youn et al., 2005), by an unknown mechanism.

1.2.4 Topoisomerase inhibitors

Topoisomerases are a group of enzymes that play a crucial role in DNA synthesis and replication (Andersen et al., 1996). These enzymes help in DNA strands separation during mitosis and cell division. As Topoisomerase II has different roles and modes of action compared to topoisomerase I, a number of clinical chemotherapy drugs have been developed, which inhibit the different types of Topoisomerases. These drugs include Topotecan and Irinotecan, which are Topoisomerase I inhibitors, while Etoposide, Teniposide and Mitoxantrone are Topoisomerase II inhibitors (Sinha, 1995). Although, both Etoposide and Teniposide are podophyllotoxin derivatives, the mechanism of action of these two drugs are different from the parent compound. Etoposide and Teniposide arrest cells in late S and G2 phase and have no influence on tubulin assembly, while podophyllotoxin affect cells during mitosis by disorganizing tubulin polymerisation (Wozniak and Ross 1983, Loik and Horwitz 1976, Chen et al., 2013). Generally, Topotecan has been used to treat a number of cancers such as ovarian cancer (Wei et al., 2015), cervical cancer (Musa et al., 2013) and lung cancer (Tiseo et al., 2014). Mitoxantrone has also been prescribed to treat breast cancer (Stuart-Harries et al., 1984) and lymphomas (Zinzani et al., 2013).

Etoposide inhibits topoisomerases II and causes DNA breakage (Baldwin and Osheroff, 2005), however, once Etoposide treatment has stopped the DNA damage is quickly repaired (Teixeira et al., 2009). Etoposide is a plant-derived natural product; it is a podophyllotoxin derivative and is considered to be one of the most important and commonly used anticancer drugs (Figure 1.2.4).

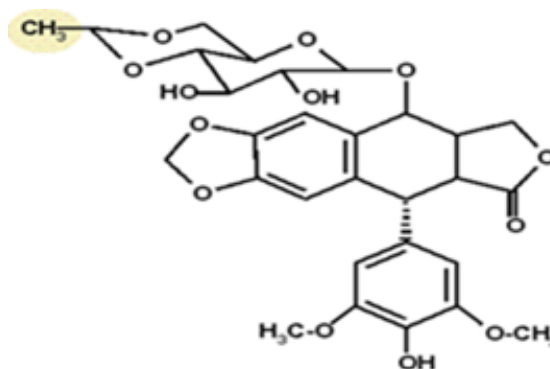


Figure 1.2.4; the structure of Etoposide (Minev, 2011)

In the early 1940s podophyllatoxins were shown to have effects on benign tumours. Later acyclic acetate derivative which is prepared from 4'-demethylepipodophyllotoxin P-D-glucopyranoside and acetaldehyde and was synthesised and tested which led to the development of Etoposide. This drug arrests cells on G2 phase and leads to apoptosis (Walker et al., 1991). Many factors are involved in apoptosis induced by etoposide, such as presence of certain oncogene products, growth factors, and p53, (Lowe et al., 1993, Kamesaki et al., 1993). The cytotoxic effects of Etoposide have been demonstrated in many different cell lines (Hartwell and Checker, 1985). Etoposide therapy requires careful supervision, when administered to patients, as some reports have shown that patients exposure to 10 µg/ml for 1 hour showed 100-fold less cytotoxicity compared to 1 µg/ml Etoposide given in one go (Hande, 1996). At standard doses, this anti-cancer drug has no hepatotoxic effects, while at higher doses it has been shown to cause hyperbilirubinemia, elevated blood aminotransferases and alkaline phosphatase during a three week period of treatment indicating of liver damage (Tran et al., 1991). Etoposide has been shown to have proven efficiency in treating various cancers, ovarian cancer (Thavaramara et al., 2009, lung cancer (Souhami et al., 1997), testicular cancer (Lehrer, 1991), Leukaemia (Papiez, 2013), Kaposi's sarcoma (Chagaluka et al., 2014) and lymphomas (Toyoda et al., 2014).

1.2.5 Other Types of chemotherapy drugs

Numerous anti-cancer drugs are being developed using a personalized/targeted therapy approach. Some of these drugs are classified as chemotherapy drugs such as, L-asparaginase treatment (Yeh et al., 2004), Corticosteroid (such as Prednisone) (Liu et al., 2013) and mitotic inhibitors (such as Taxanes, Etoposides, Vinca alkaloids and Estramustine) (Carvaja et al., 2005). Non-chemotherapeutic drugs are considered to be less toxic and mainly target cancer cells and not normal healthy cells (Torrissi et al., 2011).

These new non typical-chemotherapeutic drugs can be divided into Targeted therapies (Shore, 2014), hormonal therapy (Shore, 2014), immunotherapy (Van der Most et al., 2005). Targeted therapies are used for attacking cells with mutant versions of specific oncogene, or cells that are expressing too many copies of certain genes. Imatinib, gefitinib, erlotinib and bortezomib can be listed as targeted therapy (Ciavarella et al., 2010). Hormone therapy is a category of drugs that attacks cancer cells which are usually grown in response to natural hormones, such as some breast, prostate, endometrial cancers (Liu et al., 2004). However, these drugs are sex hormones and influence the production of female or male hormones or prevent cancer cells from using specific hormones that are necessary for growth (Henderson and Feigelson, 2000) (e.g. Anti-estrogen, Aromatase inhibitors, Progestins, Estrogen, Anti-androgens and Gonadotropin-releasing hormone). Finally, Immunotherapy is a group of drugs used to increase the natural immune-system in order to recognize and fight cancer cells (Liu et al., 2004). Some of these drugs are called 'Active' immunotherapies, which boost or increase the body's own immune-system to attack cancer cells, whilst 'Passive' immunotherapy provides the body with synthetic antibodies. Some examples of this immunotherapy agents include; Rituximab, alemtuzumab, and Herceptin (which are themselves antibodies) as well as BCG, thalidomide and interferon- Alfa which boost the immune-system (Neves and Kwok, 2015).

1.3 Cell Death

Vogt in 1842 observed and described a first form of cell death, ie the destruction of notochord cells, although at that time the term cell death was not used. A more rigorous approach to experimentally investigating cell death really started in the middle of twentieth century, where other researchers reported morphological changes associated with the death of individual cells (Saunders, 1966, Ellis and Horvitz 1986). The most published studies of cell death at that time were histological studies, where commonly noted specific morphological features of cell death were observed and later identified as hallmarks of apoptosis (a term coined by Andrew Wyllie in the 1972) (Clark and Clark 1995). As this field developed, cell death, under certain circumstances, was viewed more as a biological control process and the term “programmed cell death” began to be used. Subsequently, John Kerr, was the first researcher who clarified the complete characteristic features of programmed cell death starting with cell rounding, shrinkage, blebbing, and other cytoplasmic changing, leading to nuclear component alterations (Kerr, 1971, Kerr and Harman, 1991).

1.3.1 Major Forms of cell death

Histologically and according to the morphological observations, cell death has been categorized to three major types, Apoptosis, Necrosis, and Autophagy (Green, 2011).

1.3.2 Apoptosis

The term “apoptosis” was first coined in 1972 by Kerr, Wyllie and Currie to characterize the morphological and biochemical feature of programmed cell death (Kerr et al., 1972). These morphological features can be summarized by; Plasma membrane blebbing, chromatin condensation, DNA laddering, and formation of apoptotic bodies (Wyllie et al, 1980) (Figure 1.3.2A). Whilst, the biochemical changes can include, increases in mitochondrial permeability, phosphatidylserine externalisation, and DNA degradation (Martin et al., 1995, Hengartner, 2000). Once these features occur, neighbouring cells or macrophages can distinguish these plasma membrane changes and engulf the apoptotic cells without any inflammatory response taking place (Jacobson et al., 1997). More recently, a number of other forms of programmed cell death have been described, which differ in some of these features and there could also be some others still to be elucidated (Formigli et al., 2000, Debnath et al., 2005).

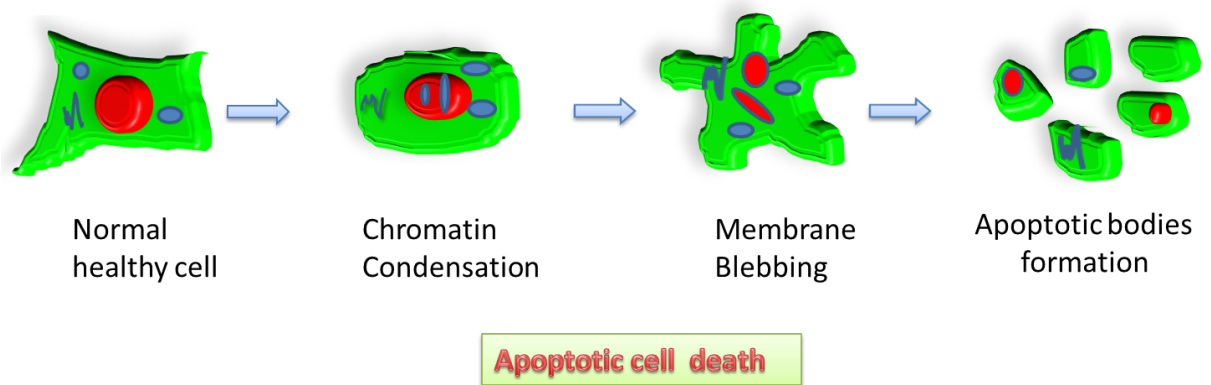


Figure 1.3.2 A; morphological changes observed in apoptotic cell death. Cell death starts with the cell becoming rounded and chromatin condensation. This is followed by membrane blebbing and finally, fragmentation of cell into small bodies called apoptotic bodies (Imajoh et al., 2004).

Apoptosis can be defined as programmed cell death involving specific gene expression to remove all unwanted (damaged) cells under internal or external responses (Savill and Fadok, 2000). Apart from removing damaged cells, apoptosis cell death maintains homeostasis, and plays a role in development and in the pathogenesis of some diseases such as cancer, human immunodeficiency virus infection, cardiovascular disorder, and acute neurodegeneration (Stroke, Alzheimer's diseases) (Raffray and Coher, 1997). Genetic control of programmed cell death was initially identified in 1986 in the nematode *c. elegans* with the finding that *ced-3*, *ced-4*, *ced-9* genes, being essential for the death of the cell (Ellis and Hovavitz, 1986). Several factors have now been reported for cell death activation including; steroid hormone activation, DNA damage, growth factor withdrawal, stress (both physically and chemically induced) and death receptor activation (Zhou et al., 1995, Baehrecke 2002, Nowsheen and Yang 2013).

Upon studying the molecular mechanism of programmed cell death. It was identified that a number of *ced* homologues were also identified in mammals and were found to belong to a family of cysteine-aspartate proteases which were named “caspases” and which specially cleaves protein substrates after an aspartic acid residue (Alnemri et al., 1996).

According to their function, these caspases can be categorized as “initiator” caspases such as caspase-8, and -9, which activate the “effectors” caspase, and effector the caspases such as caspase-3,-6 and -7, which directly activates apoptosis (Chang and Yang, 2000). These caspases work together to form a caspases cascade (Cohen, 1997).

Apoptosis has been shown to be a major cell death pathway induced by toxicological and chemotherapeutic drugs, a huge number of chemicals have been described which induce apoptotic cell death either directly or indirectly (Kerr et al., 1994).

Mechanisms of cell death

Cells to undergo apoptosis, through intrinsic and extrinsic pathways (Figure 1.3.2B).

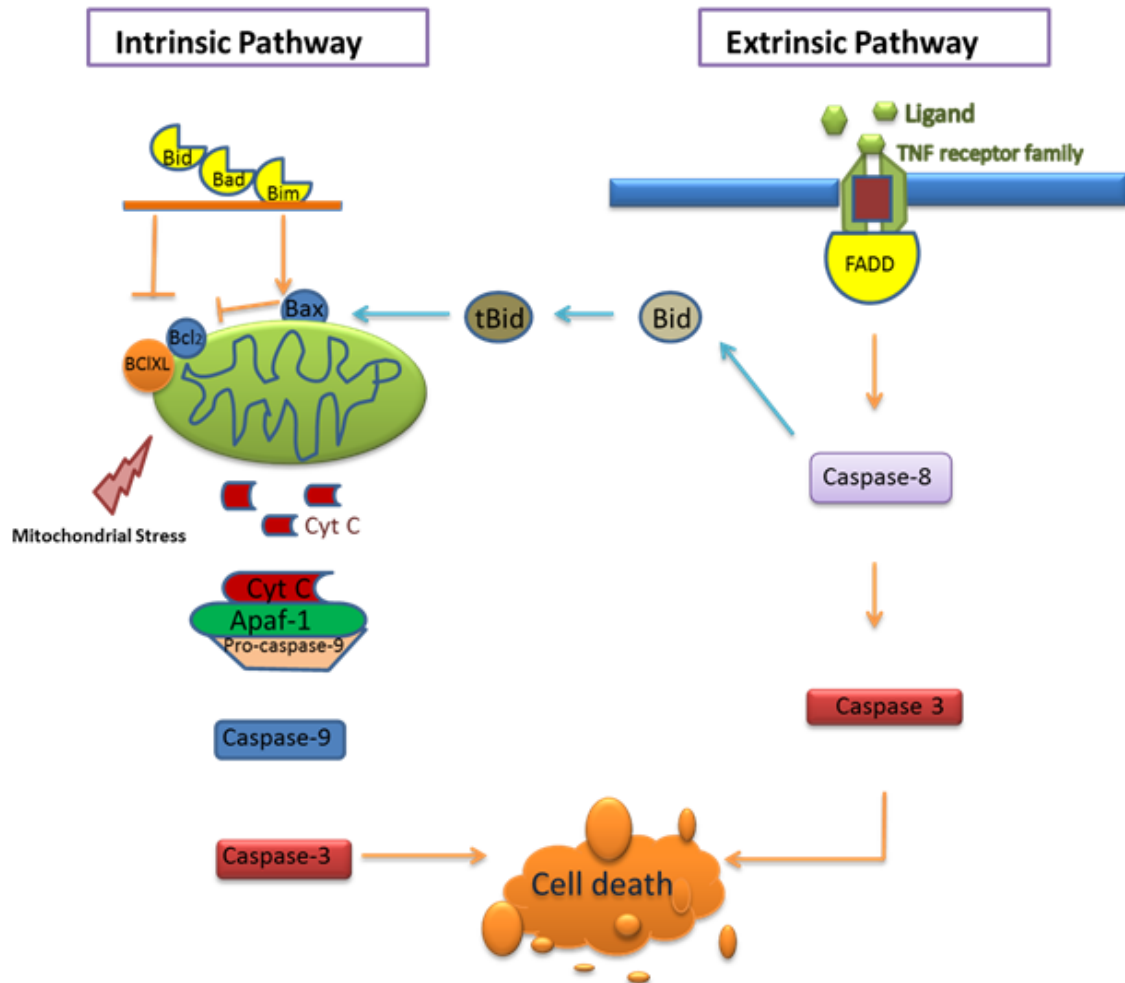


Figure 1.3.2 B; summary of the two main apoptotic pathways. Both extrinsic and intrinsic pathways, the extrinsic pathway starts with the ligand binding to the TNF receptor (a death receptor), which then activates FADD. This then activates caspase-8 and subsequently, caspase-3. In the intrinsic pathway, the mitochondria release cytochrome c through the MPTP probably as a result of Bax activity or Ca^{2+} overload. Cytochrome c is then released and in association with Apaf1 and procaspase-9 forms the apoptosome which activates caspase-9 and then promotes procaspase-3 cleavage, leading eventually to cell death. However, caspase-8 can activate Bid to tBid, which connects the two pathways (Adapted from Woo et al., 2000).

1.3.2.1 Extrinsic apoptotic pathway

The extrinsic apoptotic pathway is usually initiated by a specific transmembrane receptor interaction, which are known as death receptors, these include; Fas receptor (FasR), tumor necrosis factor receptor (TNFR), death receptors (DR3, DR4 and DR5), which are activated by FasL, TNF- α and TRAIL ligands, respectively (Locksley et al., 2001). When Fas receptors bind the Fas Ligand, the FasR cytoplasmic domain reorganizes and recruits a complex involved in propagating the death inducing signalling pathway called fas associated death domain (FADD). FADD activates caspase-8, which then activates other initiator caspases such as caspase-2 and 10. These caspases in turn cleave the effector caspase, procaspase-3 to caspase 3 (Chang and Yang, 2000).

Calcium channels may also participate in the apoptotic pathway, since calcium ion plays a major role in the signal transduction regulation in both cell proliferation and cell death (Yang et al., 2010). It is clear that the extrinsic apoptotic pathway plays an essential role in homeostasis and responding to external signals. Other factors also have the ability to trigger the extrinsic apoptotic pathway, such as bacteria, virus, RNA fragmentation and DNA damage (Obregón-Henao et al., 2012), However, it is still unclear how.

1.3.2.2 Intrinsic apoptotic pathway

The intrinsic pathway, is also commonly referred to the mitochondrial pathway. This pathway is controlled via mitochondria through a family of regulator proteins known as Bcl2, which regulate the permeability of mitochondria membrane pores (Cory and Adams, 2002). Bcl2 family proteins can regulate mitochondria permeability and can either be pro-apoptotic or anti-apoptotic (Tsujimoto, 1998). To date, some of the Bcl2 family proteins can be controlled by the tumour suppressor p53 (Chipuk et al., 2003). Generally, Bcl2 family proteins can be classified to three categories, the first category includes anti-apoptotic family includes Bcl2, Bcl-xl, Bcl-w and Mcl-1 proteins. The second category includes the pro- apoptotic proteins such as Bax, Bak and Bok. The third category includes BH3-domain proteins and includes a number of pro-apoptotic proteins such as Bid, Bim, Bik, Bad, Baf, and others (Tzifi, et al., 2012). Bax and Bak are essential for mitochondrial pore formation, whilst, Bid and Bad are apoptotic promoters since they bind to the active Bax and Bak. However, the anti-apoptotic Bcl2

family proteins have a role in mitochondrial permeabilization protection (Green, 2006). Therefore, all these proteins participate together and control mitochondrial cytochrome c release (Donovan and Cotter 2004, Lukovic et al., 2003). Furthermore, mitochondrial release of Smac/DIABLO proteins, can control this cascade by reversing inactivated caspases (Laken and Leonard, 2001). Beside these proteins, reactive oxygen species (ROS) also contributes to this pathway. Increasing level of ROS also increases mitochondria membrane permeability. ROS also elevates polyADP ribose polymerase (PARP-1), an essential apoptosis-inducing factor (AIF) (Kang et al., 2004). Subsequently, cytochrome c, Apaf-1 and ATP enhance apoptosome formation, which then leads to caspase- 9 activation and apoptotic cell death. Although these pathways have different caspase cascades, they are not independent from each other, as caspase 8 can cleave Bid to tBid which can then activate Bax and lead to the release of cytochrome c (Candè et al., 2002).

Furthermore, mitochondria plays an vital role in intracellular Ca^{2+} homeostasis, signalling and intracellular Ca^{2+} communication as well as cell survival (Cerella et al., 2010). Mitochondria matrix, is a Ca^{2+} reservoir, which is helps in the accumulation of large amounts of Ca^{2+} (Csordas et al., 2006, Kass and Orrenius, 1999). The mitochondria allows the removal of excessive Ca^{2+} ions from cytosol, and therefore maintains Ca^{2+} cell homeostasis and signalling functions (Walsh et al., 2010). However, Ca^{2+} overload of the mitochondria when exceeding capacity, can lead to the Mitochondrial Permeability Transition Pores (MPTP) opening (Qian et al., 1999, Michelangli and East, 2011). Once MPTP is opened, it increases mitochondrial inner membrane permeability and then causes cytochrome c release. This apoptotic pathway is Bax translocation independent (Qian et al., 1999, Zorov et al., 2000, Mullauer et al., 2009). Subsequently, cytochrome c activates caspase and leads to apoptotic cell death (Richter, 1993).

More recently another apoptosis pathway has been identified which is called Perforin/ Granzymes pathway. Granzymes (granule enzymes) belong to the serine protease family and that are present in cytotoxic T cells. Perforin is a pore forming protein, and initiates rapid granzymes endocytosis, which can begin apoptosis either directly or indirectly (Lieberman, 2003). Perforin possibly with the help of the Ca^{2+} binding

protein calreticulin creates pores in the surface of the target cells, which then allow the granzymes to enter the cell membrane. This then allows granzyme release from endocytic vesicles (Figure 1.3.2 C) (Fraser et al., 2000, Shi et al., 1997). Granzyme A can also induce caspase-independent apoptosis via targeting the endoplasmic reticulum-associated complex (SET complex), which consists of p53, pp32 and NM23-H, the nucleosome-assembly protein SET (DNA-binding protein HMG2) and APE1 repair enzyme (Fan et al., 2002). This type of cell death induction does not involve mitochondria or cytochrome c activity. In contrast, Granzyme B, can induce caspase-dependent apoptosis via caspase3/CPP32 activation (Wang et al., 1996), as well as the possible involvement of caspase-6,-7,-8,-9 and -10 as determined from in vitro studies (Preedy, 2015). Once caspase-3 becomes activated, it can cleave other pro-apoptotic substrates, such as poly (ADP-ribose) polymerase (PARP) and causes activation of caspase activated DNase, followed by morphological alteration and DNA degradation. For activation of both Granzyme A and B, selective proteolysis takes place, carried by cathepsin C/dipeptidyl peptidase I (DPPI), which is a part of pro dipeptide domine serine protease complex (Mc Guire, 1992, Mc Guire et al., 1993).

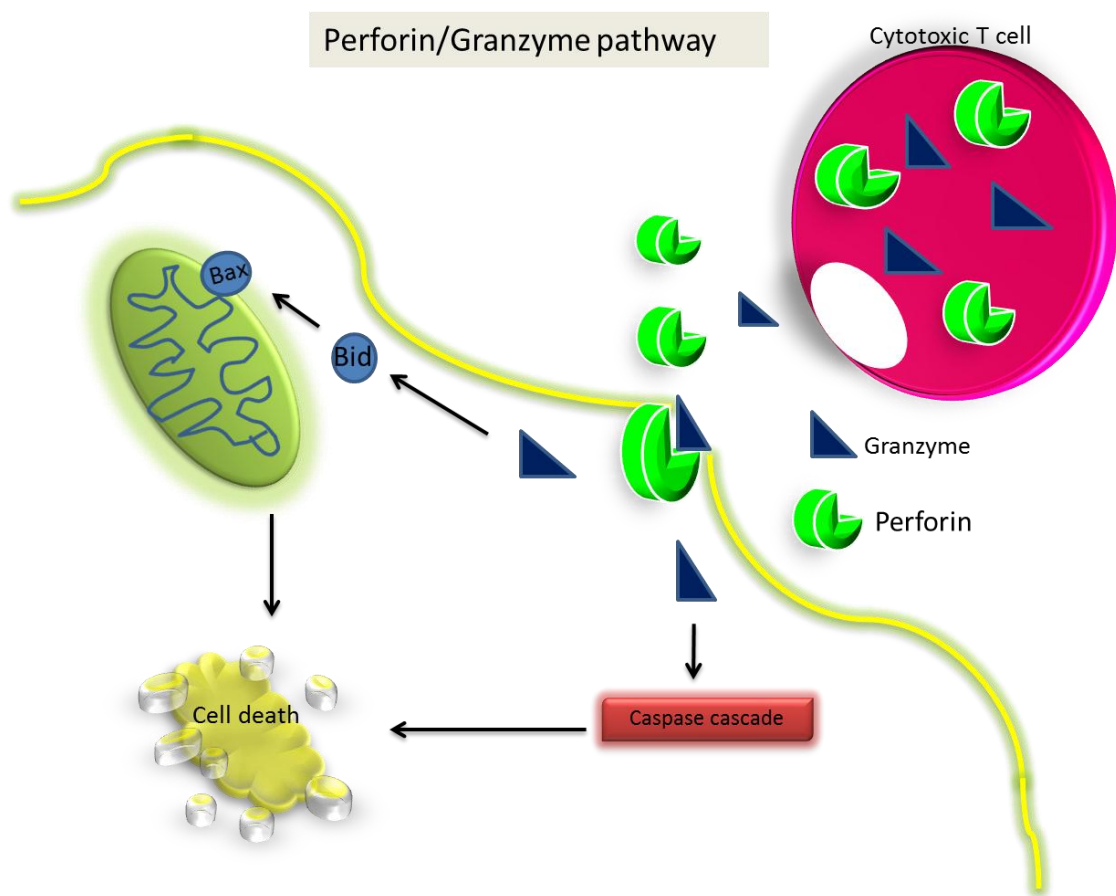


Figure 1.3.2 C; the perforin/granzyme cell death pathway in cytotoxic T cells. Perforin and granzyme bind to the cell surface and perforin permit granzymes to enter the target cell. The granzymes then induce cell death either by the extrinsic caspase cascade or through mitochondrial induced apoptosis (Adapted from DeFranco et al., 2007).

1.3.3 Necrosis cell death

Originally necrosis was viewed as an “accidental” form of cell death and refers to extreme structural modifications such as cell membrane damage, which are easily visible under a microscope (Major and Joris, 1995). Various factors can initiate necrosis, which are most likely to be physical factors such as heat, diseases, Ischemia, oxidative stress etc. (Rani and Yadav, 2014). Necrosis is characterized by cell swelling, impairment of the cell membrane, cytoplasmic enzyme release, and inflammation of the surrounding cells and tissues (Figure 1.3.3) (Proskyuryakov et al., 2003). Once necrosis begins, the cells secrete a variety of pro-inflammatory factors,

which activate the immune effector cells via the pathogen recognition receptors (PRRs) to initiate the inflammatory reaction this is then followed by phagocytosis via macrophage cells. These pro- inflammatory factors include; histone proteins, heat-shock proteins (e.g. HSP27, HSP60, HSP70 and HPS90) and high mobility group box proteins (Zitvogel et al., 2010).

Biochemically, the most notable hallmark of necrotic cell death is karyolysis (ie chromatin dissolution and nuclear fading), pyknosis (chromatin condenses and clumping), karyorrhexis (pyknotic nuclei membrane and nuclear fragmentation) and also phosphatidylserine (PS) exposure on the external side of the plasma membrane (Hammill et al., 1999).

There has been some dispute regarding necrosis as Major and Joris (1995), suggested that necrosis is not a specific type of cell death but rather the end phase of any forms of cell death, since both necrosis and apoptosis have several similarities in their features especially in the advanced phase (Leist and Jaattela, 2001). Nevertheless, as apoptotic cells are not always recognized by phagocytes cells, this consequently led to the term of secondary or apoptotic necrosis (Sanders and Wide, 1995).

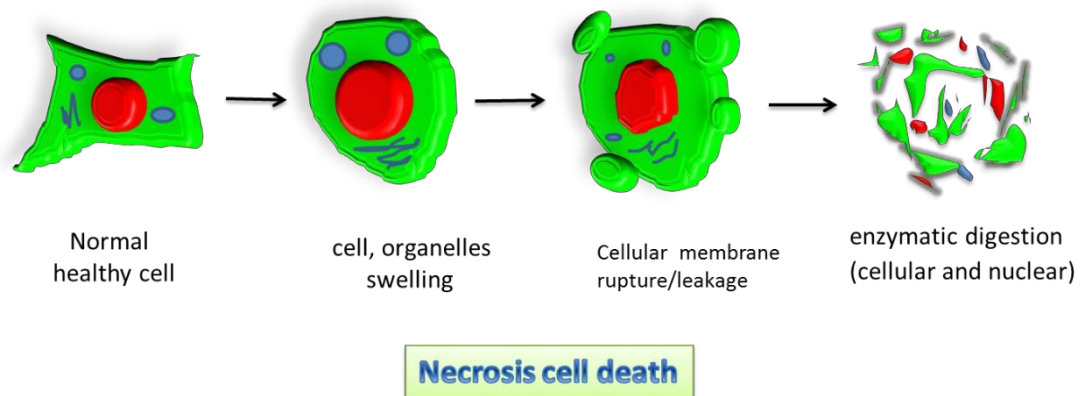


Figure 1.3.3; Necrosis cell death. Necrosis starts with swelling of cell and organelles, cellular membrane rupturing and some blebbing and then ends with total cell digestion via cellular enzymes that releases pro-inflammatory factors into the surrounding tissues (Fink and Cook, 2005).

1.3.4 Necroptosis

Necroptosis can be generally defined as a regulated form of necrosis, and therefore shares many of the same morphological characteristics of necrosis (cellular organelle swelling, cellular leakage, etc.) (Hirosova and Gores, 2015).

Cytokine tumour factors, such as TNF, play a vital role in the necroptosis pathway, triggering cell death and involved in immune system function (Kawasaki et al., 2002). Induction of regulated necrosis occurs through many different receptor families, in addition to TNF there are many others, such as cluster differentiation (CD 95 L) (which includes FASL and apoptotic antigen receptors APO-1L), receptor induction protein kinases (TRAIL) such as APO-2L (Holler et al., 2000), TWEAK receptor (Wilso and Browning 2002), T cell receptor (Chen et al., 2008). Cell inflammation can also be induced by genetic stress (Huang, 2013), anticancer drugs (Tenev et al., 2011) and DNA- dependent activator of TNF-regulator factors. Once necroptosis is activated, the necrosome complex is formed, which consists of the receptor-inducing protein kinases (RIPK1), RIPK2, and caspase -8 (Berghe et al., 2014), The Fas-associated death domain (FADD) can also be involved in necrosome activation. Inside the cells, caspase -8 then recruits a series of other caspases that results in cell death. Alternatively, the mixed lineage kinases domain-like (MLKL) mediates events that ultimately leads to necroptosis without caspase -8 activation (Degterev, et al., 2005). Furthermore, the chemical inhibitor Necrostatin (NEC1) plays a role in blocking RIPK activation thereby stopping regulated necrosis (Degterev, et al., 2012).

1.3.5 Autophagy

Autophagy can be defined as a catabolic process involving the removal and degradation of unused or long lived cellular components with a view to maintaining cellular energy levels (Levine and Kroemer 2008). Although this process was identified in 1950's, it has still not been fully elucidated (Tooze, 2012). Autophagy plays an important role in cell homoeostasis because it recycles unwanted amino acid, metal ions and sugars, thereby it helps to maintain the cells energy (Paglin et al., 2001). Furthermore, autophagy (which is sometimes referred to as type II programmed cell death) is initiated as a result of nutrient starvation, therefore the deficiency of any essential nutrient can trigger autophagy (Levine and Kroemer, 2008). However, autophagy, has also been

shown to be involved in development since it is demonstrated to cause inter-segmental muscle formation during embryogenesis (Daniel and Korsmeyer, 2004). According to its physiological roles and its removal mechanisms, autophagy can be divided in to three subdivisions: macroautophagy, chaperone-mediated autophagy and microautophagy (Kurz and Terman, 2008). Macroautophagy (commonly referred as classical autophagy) starts with the degradation of a portion of cytoplasm (cargo) by forming a double membrane organelle (autophagosome), which then fuses with lysosomal vesicles to form an autolysosome (Figure 1.3.5A). In chaperone-mediated autophagy, the cargo delivery performs by a specific sequences signal starting from cytoplasm, towered lysosomal membrane (Cuervo and Dice1996). However, in microautophagy the lysosomal membrane itself pinches off a portion of the cytoplasm and then digests it via the action of lysosomal hydrolases (Ahlberg et al., 1982).

Autophagy is initiated through activation of a series of proteins such as phosphoinositide 3- kinses (PI3K), Beclin 1 complex, ATGs 1, 3, 5, 7, 10, 12 and 16 as well as microtubule associated protein 1 light chain 3 (LC3) and phosphatidylethanolamine conjugation. These interactions lead to the formation of the phagophore which then matures into the autophagosome. The mature autophagosome then fuses with the lysosome to form the autolysosome and cytoplasmic material encapsulated within it is subjected to digestion and degradation (Kando et al., 2005), and finally peptide units and energy produce from this process shift back to cytoplasm to be reused (Mizushima, 2007).

Many studies on yeast have helped clarify the molecular mechanisms of autophagy (Klionsky, 2004) and approximately 30 autophagy genes have so far been discovered (commonly abbreviated as ATGs). Atg1 or ULK2 (the mammalian Homologue) induces autophagy by binding to Atg13 controlled via phosphorylation which causes the Atg1-Atg13 complex to increase (Kamada et al., 2000). Furthermore, Beclin 1 activates the autophagy signal pathway by binding to class III phosphatidylinositol-3 kinases VPS34 (Kamada et al., 2000). VPS34 is associated with VPS15, and bind to Beclin1, which can be inhibited by the anti-apoptotic proteins Bcl2/Bcl-XL (Tassa et al., 2003). Beclin1 is activated to form the autophagosome by additionally binding the Ambra protease as well, two other proteins UVRAG and

endophilin B1 (Bif-1) to promote VPS34 activity, (Figure 1.3.5B) (Takahashi et al., 2007).

One of the biggest debates amongst scientists in the field is whether autophagy is a cell death mechanism as well as a cell surviving mechanism. However, some studies have reported that some cytotoxic agents can trigger autophagy cell death in such cells treated with caspases inhibitors, or expressing high levels of Bcl2 or Bcl-XL (Shimizu et al., 2004, Yu et al., 2004), or with caspases genetically knocked out (Wong et al, 2013). This mechanism may also be regulated by Ca^{2+} (Wang et al, 2009).

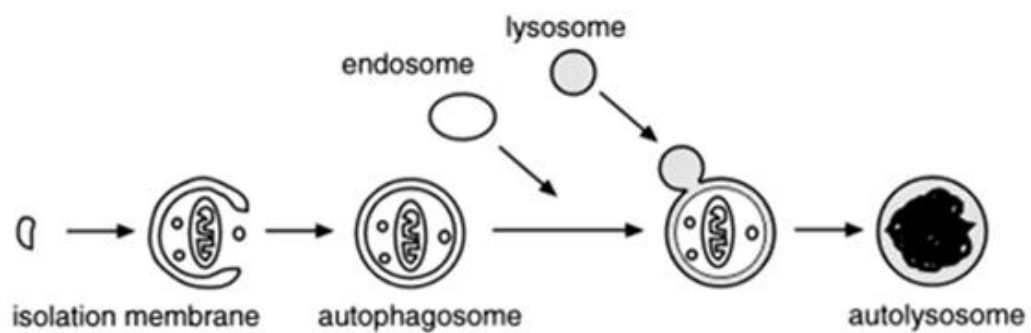


Figure 1.3.5A; macroautophagy formation process in mammalian cells. Autophagic isolation membrane (phagophore) encloses a portion of cytoplasm forming autophagosome and then the lysosome fuses with autophagosome to form autolysosome (Mizushima et al., 2002).

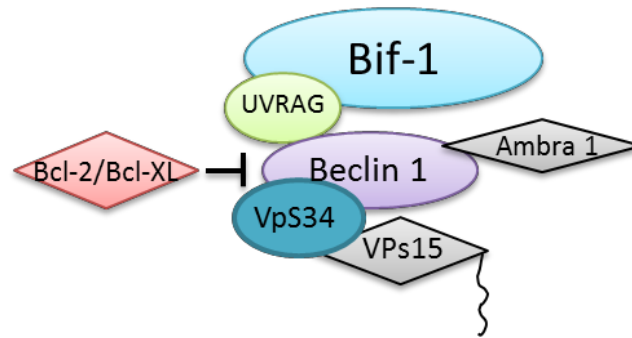


Figure 1.3.5 B; the Beclin-1-Vps34 complex. Beclin-1, UVRAG, Bif-1 and Ambra activate VPS34 lipid kinase, while Bcl2 and Bcl-XL inhibit autophagy when it binds to Beclin-1. The lipid tail attached to VPS15 helps the complex to anchor the autophagosome membrane (Adapted from Funderburk et al., 2010).

1.4 Regucalcin

In 1978, regucalcin (RGN/SMP30) was discovered as an abundant liver cytosolic Ca^{2+} binding protein (Yamaguchi and Yamamoto, 1978). The name, regucalcin, was proposed for this protein because it has the ability to regulate various liver Ca^{2+} dependent enzymes. Although RGN is able to bind Ca^{2+} it does not have an EF hand which might be expected to form a part of protein in order to bind Ca^{2+} (Figure 1.4) (Yamaguchi, 2000). RGN is a 299 amino acid polypeptide which has a 33 MW of kDa and has an intracellular location in both the cytoplasm and nucleus (Omura and Yamaguchi, 1999, Yamaguchi and Yamamoto, 1978). RGN is a multifunctional protein that is involved in number of cellular processes including; calcium homeostasis by regulating Ca^{2+} binding protein activity such as Ca^{2+} ATPases, calmodulin kinase and PKC (Karota and Yamaguchi, 1997). Furthermore, RGN has an established defence role in Ca^{2+} mediated stress protection. RGN has been shown to be an important ageing marker protein in many organisms, as it increases its expression through the neonate stage into early adulthood and then drops significantly in old age (Ishigami, 2010, Maruyama et al., 2010). Therefore, RGN is also refers to as senescence marker protein - 30 (SMP30) (Fujita et al., 1996). Overexpression of RGN can inhibit L-type Ca^{2+} channels (Nakagawa and Yamaguchi, 2005) and the Ca^{2+} sensing receptor in NRK52E cells (Yamaguchi, 2013). While the low levels of RGN in mice has been shown to be linked with X-linked muscular dystrophy (Doran et al., 2006). Besides its effects on Ca^{2+} signalling it also has other functions such as in the synthesis of vitamin C in some

mammals as it acts as a gluconolactonase enzyme as well as acting as a detoxifying enzyme in liver cells (Kondo et al., 2004). Moreover, RGN depletion can increase the oxidative stress within brain cells (Son et al., 2006).

Subcellular localisation of RGN has to be found in the cytosol, nucleus (Nakagawa and Yamaguchi, 2008) and to a much lower levels in mitochondria (Yamaguchi et al., 2008) and is predominately found in tissues such as kidney, liver and brain (Yamaguchi, 2000a). The expression level of RGN protein in the liver appears to be age-dependent (Hong et al., 2012). Moreover, mRNA of this protein has been reported in cerebrum and lung, testis and heart (Mori et al., and Doran et al., 2006). More recently RGN mRNA has also been detected in both mammary and prostate gland of rats, as well as pancreas (Maia et al., 2008, 2009, Yamaguchi, 2015).

Therefore it is very likely that RGN, which is a multifunctional and multi-locational protein, could be associated with many pathological conditions, such as cancer, osteoporosis and Alzheimer's disease (Sun et al., 2006). Other age-related disorder such as hearing loss (Kashio et al., 2009), liver lipid accumulation (Yamaguchi, 2010) and decreases intolerance to glucose have also been identified in the RGN knockout mouse (Hasegawa et al., 2010). Moreover, RGN may play a role as in reducing oxidative stress and apoptosis (cell death) within cells (Misaka et al., 2013).

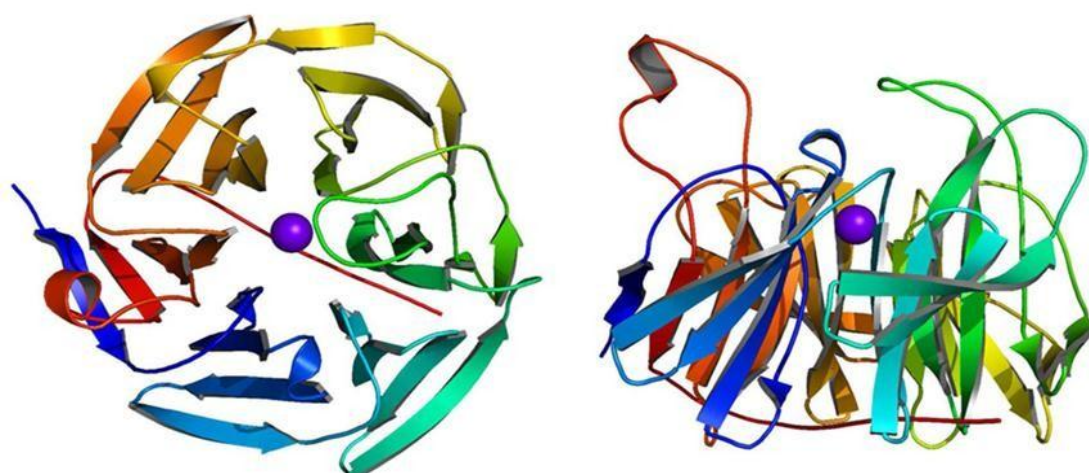


Figure 1.4; the solved crystal structure of RGN (SMP30). The ribbon structure of RGN with Ca^{2+} (purple sphere) is the binding position, in the centre of six- β -propeller barrel fold (Chakraborti and Bahnson, 2010).

1.4.1 Transcription Regulation of Regucalcin expression

Principally, NF1-A1 and AP-1 nuclear transcription factors, predominantly influence RGN expression level (Yamaguchi, 2005), along with, a novel transcription protein factor known as RGPR-p117, regucalcin gene promoter region related protein, which binds to TTGGC(N)6CC sequences and participates in regucalcin mRNA expression in NRK52E cells (Misawa and Yamaguchi, 2001). The RGPR-p117 gene product has been shown to be expressed in human, fish and yeast, as well as various animals, for instance bovine, rabbit, cow, dog and others (Misawa and Yamaguchi, 2002). Moreover, the RP11-6501 sequence has been used to confirm RGPR-p117 gene structure, thus the results shows that RGPR-p117 transcription factor consist of 26 exons spanning approximately 4.1 kbp (Misawa and Yamaguchi, 2001). Overexpression studies in liver and kidney cells, demonstrated the RGPR-p117 is sensitive to $[\text{Ca}^{2+}]$ levels within liver cells (Misawa and Yamaguchi, 2002), and this study also described the essential role of RGPR-p117 in regulating the expression of regucalcin in kidney cells and on inhibiting DNA and protein synthesis. Some studies have also shown that, RGPR-p117 over-expression alone cannot significantly alter RGN mRNA levels and that hormonal control is also required (Yamaguchi, 2009).

A significant increase in RGPR-p117 mRNA expression has been noticed after calcium elevation in rat liver (Yamaguchi, 2009), therefore some studies have suggested that this change is mediated through a Ca^{2+} elevation-induced secondary factor, but not related directly to Ca^{2+} , during gene expression. A related study also reported the stability level of RGPR-p117 to different physiological changes such as aging, Fasting or re-feeding (Yamaguchi, 2009). However, RGPR-p117 has been shown to have suppressor effects on many cell death factors including, tumour necrosis factors- α (TNF- α), lipopolysaccharide (LPS) and cell death induced by Bay k 8644 in NRK52E cells (Yamaguchi, 2007). RGPR-p117 also reduces death in NRK52E cells in the presence of apoptosis stimulation factors such as caspase-3,-9,-8 and Fas-associated death domain protein (FADD) (Yamaguchi, 2007).

1.4.2 Regucalcin and apoptosis

Regucalcin has been shown to have an effect on cell function via suppressing intracellular Ca^{2+} homeostasis as well as Ca^{2+} - dependent and independent enzyme activity, cell signalling, protein production and nuclear signalling (Yamaguchi, 2012).

1.4.2.1 Regucalcin role in suppressing cell death and apoptosis in liver cells

Many studies have reported the apoptotic effect of TNF- α and Nitric oxide on hepatocytes rat cells (Abou-Elella et al., 2002, Belloma et al., 1992). Furthermore, TNF- α induced cell death in mammalian adenocarcinoma cells has been shown to be by increasing cytoplasmic [Ca^{2+}] concentration level and DNA fragmentation (Belloma et al., 1992). TNF- α also causes significant cell death in the hepatoma cell line H4-II-E by apoptosis, however overexpression of regucalcin in these cells was shown to protect against apoptosis even with high concentrations of TNF- α (Izumi and Yamaguchi, 2004). Likewise, the regucalcin anti-apoptotic properties has been reported in RGN-transfected H4-II-E cells, after treating cells with lipopolysaccharide (LPS), caspase-8 modulator and an apoptotic inducer.

Further studies have indicated the suppressive role of regucalcin on apoptosis cell death. It is known that, apoptosis induction is correlated to protein kinases, since both dibucaine, Ca^{2+} dependent kinases protein inhibitor, and PD98059, an inhibitor of extracellular signal-regulated kinases, causes H4-II-E cell death. However, such an effect was not detected when H4-II-E cells transfected with regucalcin (Izumi and

Yamaguchi, 2004). Regucalcin may affect Bcl2 stimulation or caspase inhibition, since dibucaine acts on various caspases, including caspase-3,-6,-8 and -9 and has the ability to change membrane depolarization and release cytochrome c (Arita et al., 2000). PD89059 is known to activate Bcl2 and increases Bcl2 phosphorylation in human prostate cancer cells (Zelivianshi et al., 2003). Over expression of regucalcin decreases liver cell death when cells are treated with both PD89059 and dibucaine (Yamaguchi, 2005). Furthermore, regucalcin has been shown in NRK52E kidney cells to cause a rise in Bcl2 mRNA expression (Nakagawa and Yamaguchi, 2005). Additionally, a high Ca^{2+} concentrations might causes cell death through apoptosis (Cohen and Duke, 1984), and the calcium pump inhibitor such as thapsigargin causes apoptosis in many different cells by causing DNA fragmentation (Izumi and Yamaguchi, 2004). Likewise, there is evidence to demonstrate the suppressor effect of regucalcin on cell death and apoptosis caused by nitric oxide (Izumi and Yamaguchi, 2004, Izumi et al., 2003) (see figure 1.4.2.1).

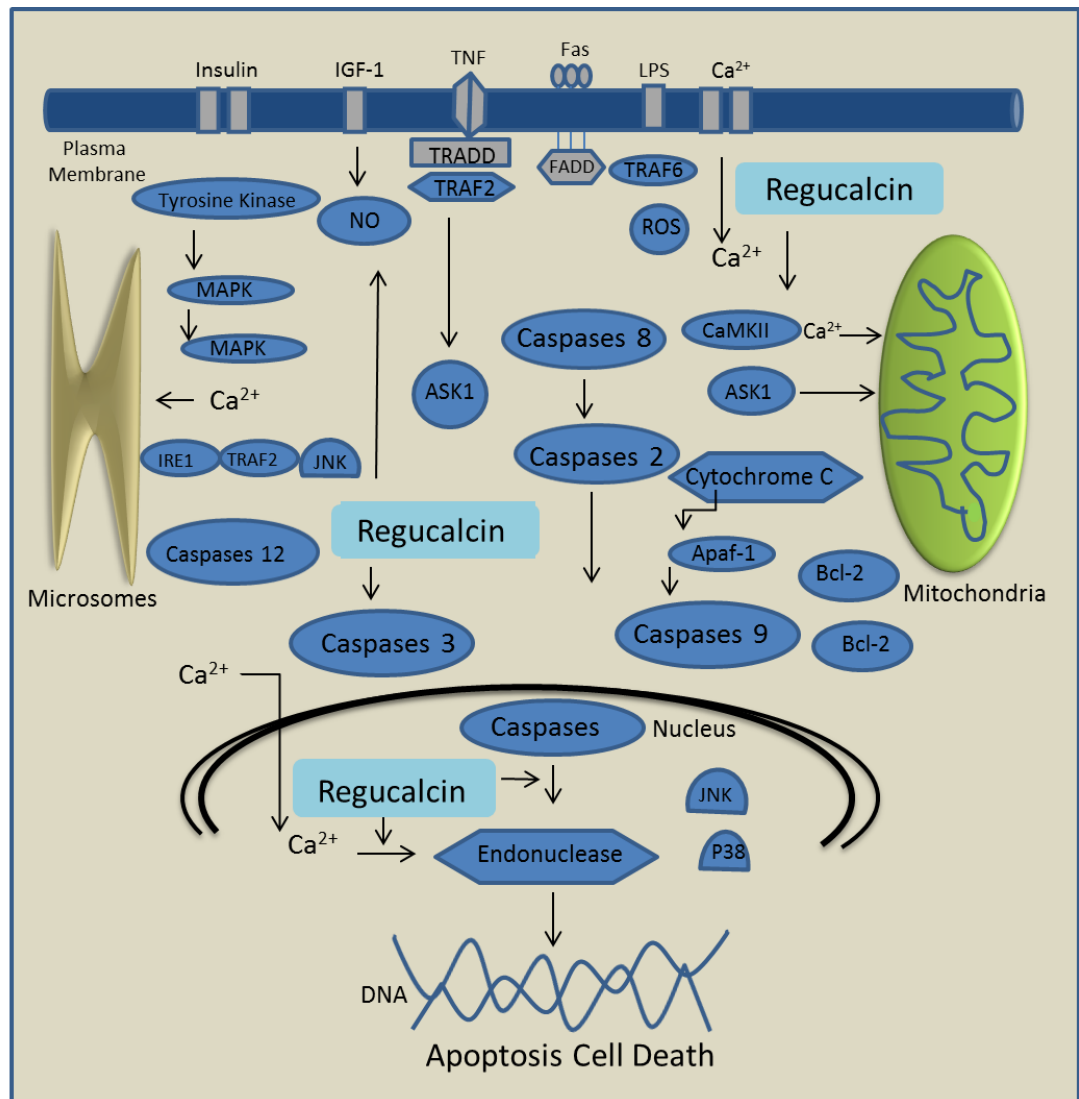


Figure 1.4.2.1; the suppressive effect of Regucalcin on cell death and apoptosis. This is mediated by the inhibition of NO synthase, caspase-3 or Ca^{2+} -dependent endonuclease, and activation of Bcl2. This cell death is induced by many factors (Bay K866, dibucaine, IGF-1, Insulin, LPS, PD89059, Thapsigargin, $\text{TNF-}\alpha$ or Sulforaphane (Adapted from Yamaguchi, 2012).

1.4.3 Regucalcin protein and Ca^{2+} Homeostasis

Calcium ion plays a significant role in a variety of critical cellular functions, such as cell divisions and gene expression, as well as hormonal secretion and muscle contraction. Calcium ions are also fundamental to neurotransmission and metabolism (Berridge et al, 2000). Regucalcin is a calcium- binding protein, which can binds Ca^{2+} as

well as other divalent metal ions such as Mn^{2+} (Chakraborti and Bahnson, 2010). Regucalcin can affect a number of different Ca^{2+} or Ca^{2+} /Calmodulin-dependent enzymes in liver cells (Yamaguchi and Mori, 1988, Yamaguchi and Shibano, 1987). Fujita and his colleagues reported that regucalcin could decrease intracellular $[Ca^{2+}]$ levels and modulate plasma membrane Ca^{2+} pumping activities in Hepatic cells (Fujita et al., 1998). Regucalcin was also found to control Ca^{2+} ATPase activity in renal cortex of rat kidneys and also helps re-absorption of Ca^{2+} in the nephron kidney cortex (Agus et al., 1997). Regucalcin has been shown to regulate ER Ca^{2+} pumps (Yamaguchi, 2000) through an as yet unknown mechanism and to increase SERCA Ca^{2+} pump expression in kidney cells (Lai et al., 2011). Ca^{2+} homeostasis role of regucalcin has also been studied on both heart and brain cells (Akhter et al., 2006).

1.5 Cytoprotection

Chemotherapy drugs are defined as a toxicant, natural or synthetic, chemicals that generate harmful side effects on the living organism. These can be toxic at specific doses and most of these drugs are also carcinogens such as antitumor antibiotic, antibiotic antimetabolites and nitrogen mustards. Some drugs can have epigenetic effects such as Diethylstilbestrol which has shown to cause a cervix and vagina cancer in the offspring of women treated with it (Hodgson, 2004).

Once drugs affect the body, a variety of defence mechanisms and barriers can be initiated to reduce their toxic effects. Chemotherapy drugs can easily enter the blood stream, because these drugs are usually administered by intravenous, intra-muscular injection, subcutaneous injection or orally, which are then easily distributed via vascular system (Hodgson, 2004). Cancer chemotherapy drugs have been specially designed to kill cells, both cancerous and normal cells, by affecting cellular activity such as proliferation, differentiation and cell death. Genes called proto-oncogenes, have a powerful association with tumor formation and cell transformation. Once these genes are activated (sometimes, through the action of toxicants), the oncoproteins produced influence signal transduction pathways and an example of that is the reactive oxygen species (ROS) gene and tumor suppressor genes (Hodgson, 2004), to minimize cell death.

Reactive oxygen species (ROS) contribute to many cell functions for instance cell growth, differentiation and cell signalling. ROS at high levels is also a mediator of cell death. Therefore, the ROS levels are controlled by different proteins such as catalase and superoxide dismutase (SOD). The high levels of ROS have been correlated to neurodegenerative disorder, DNA damage and cancer (Loft et al., 2008).

The most noted forms of ROS are hydroxyl radicals, peroxides and superoxides. Antioxidants such as vitamin E, C and K, dietary flavonoids, polyphenols, e.g. resveratrol, quercetin etc., can neutralize ROS directly or indirectly (Thompson and Van Bel, 2012).

The tumor suppressor p53 plays an important role in the prevention of mutation and inhibition of abnormal cell growth. p53 activation occurs during cellular stress, and affects cell cycle progress. During such circumstances, p53 acts by blocking the cell cycle or inducing cell death. Furthermore, p53 contribute to both DNA repair and angiogenesis inhibition (Thoreen, 2009). Poly (ADP-ribose) polymerase (PARP) has been shown to be involved in p53 activation and regulation. This polymerase plays a positive role in DNA damage detection and DNA repair (Serpi, 1999). p53 has the ability to activate cell death autonomously via sub-cellular translocation as well as stimulation of pro-apoptotic Bcl2-2 family members. Different factors can trigger p53 activation for example, DNA damage, and radiation, hypoxia, as well as chemotherapy drugs.

Cytoprotective heat shock proteins such as Hsp60 and Hsp70 (Morimoto and Santoros, 1998), also plays a vital role in protein folding, blocking caspase activation and protecting against oxidative stress (Bellmann et al., 1996), inflammation (Klosterhalfen et al., 1996) and ischemia (Mestril et al., 1994). Apart from this role, changes in Ca^{2+} concentration levels have on many biochemical and biophysical processes, large increases in $[\text{Ca}^{2+}]$ levels can also contributed to ischemia and therefore affect survival. Hence, some drugs have been developed which have the ability to alter cellular Ca^{2+} concentrations inside cells such as Dantrolene and Ursodeoxycholic acid (Thompson and Van Bel, 2012). As mentioned before, regucalcin has also been shown to affect Ca^{2+} homeostasis, by possibly affecting Ca^{2+} levels. Therefore, we hypothesize that

regucalcin, can act as a cytoprotector protein which helps reduce abnormality of high $[Ca^{2+}]$ levels caused by cell stress and then prevents or reduces cell death.

1.6 Calcium

It is now widely recognized that Ca^{2+} ions and Ca^{2+} homeostasis have a crucial role to play in most biological systems (Berridge et al., 2000). The importance of Ca^{2+} ions was first identified as playing a key physiological role in the 19th century (Ringer, 1882). Ca^{2+} is essential to many cellular functions in all prokaryotic and eukaryotic cells. In higher organisms Ca^{2+} are involved muscle contraction, fertilization, cell division, proliferation, development, learning and memory, secretion, metabolism, and cell death (Brini and Carafoli, 2009).

Ca^{2+} concentration inside the cytoplasm needs to be strongly controlled. In cells, resting cytosolic Ca^{2+} concentration is kept very low, roughly 100 nM and approximately 10,000 fold less than outside the cell. When stimulated to undertake normal cellular function this concentration could increase to 10-100 fold which can then be utilised a variety of Ca^{2+} dependent enzymes and proteins to initiate biochemical changes (Michelangli et al, 2005). Very high concentrations of Ca^{2+} in some cells, like hippocampal neurons cells can causes cell death instead of carrying out normal stimulation (Randal and Thayer, 1992) by causing both apoptosis and necrosis to take place (Berridge et al., 2000; Carafoli et al., 2001). Inhibition of Ca^{2+} channels can also reversibly inhibit proliferation in some cancer cells (Kohn et al, 1996). The highly regulated Ca^{2+} homeostasis is controlled by the cooperation of many Ca^{2+} channels and pumps activity in both plasma membrane and other intracellular Ca^{2+} stores membrane (Berridge et al., 2000, Michelangeli et al., 1999)(figure 1.6).

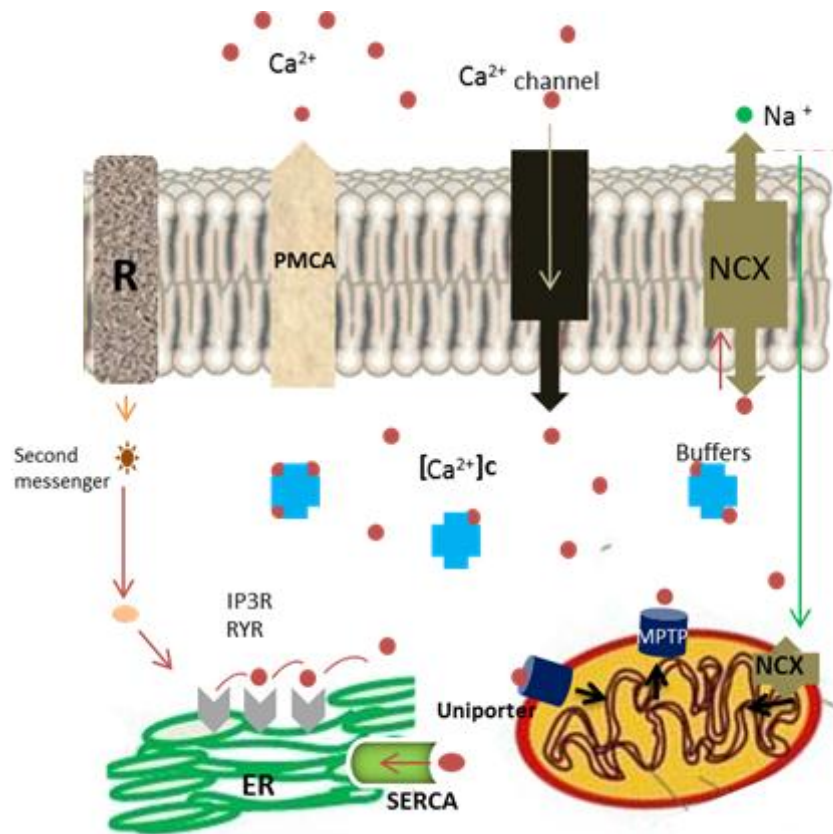


Figure 1.6; mechanisms of calcium signalling. Agonists stimulate cells to form second messengers which induce the Ca^{2+} release from the ER through the IP3R. In addition; some agonists can activate the extracellular Ca^{2+} entrance through plasma membrane channels. A high percentage of cytosolic Ca^{2+} is bound to Ca^{2+} binding proteins which can causes biochemical changes inside the cell. Various pumps and exchangers act to remove Ca^{2+} , including NCX and plasma membrane Ca^{2+} -ATPase (PMCA) that remove the Ca^{2+} from the cell and the SERCA which pumps take Ca^{2+} back to the ER. The Ca^{2+} release to cytoplasm by mitochondria can occur through the mitochondrial permeability transition pore (MPTP) (Adapted from Rosado et al., 2004).

1.6.1 Ca^{2+} channels and pumps

There are three main types of Ca^{2+} channels which regulate intracellular $[\text{Ca}^{2+}]$ level and control Ca^{2+} influx on the cell; these are Voltage-operated Ca^{2+} channel (VOX), store-operated Ca^{2+} channel (SOCs) and receptor-operated Ca^{2+} channel (ROCs) (Bootman et al., 2001). The cell membrane also contains several more protein transporters that move Ca^{2+} to the outside the cells, such as $\text{Na}^{2+}/\text{Ca}^{2+}$ exchanger (NCX), and plasma membrane Ca^{2+} -ATPase (PMCA) (Michelangli et al, 2005). Inside cells are Ca^{2+} storage organelles, such as ER, mitochondria, nucleus, lysosome etc. (see figure 1.6.1). These organelles contain number of Ca^{2+} channels such as, inositol-1,4,5-triphosphate receptor (IP3R), nicotinic acid adenine dinucleotide phosphate receptor (NAADPR) and ryanodine receptors RyR, which are the second messenger-operated Ca^{2+} channels (SMOCs) (Calcraft et al., 2009). These organelles are involves in decreasing intracellular $[\text{Ca}^{2+}]$ level also promoting Ca^{2+} movement in the opposite direction by the activation of transporters, namely (Sarco) endoplasmic reticulum (SR/ER) Ca^{2+} -ATPase (SERCA), mitochondrial Ca^{2+} uniporter (MCU) and H^{+}/Ca exchanger (HCX) (Michelangli et al, 2005).

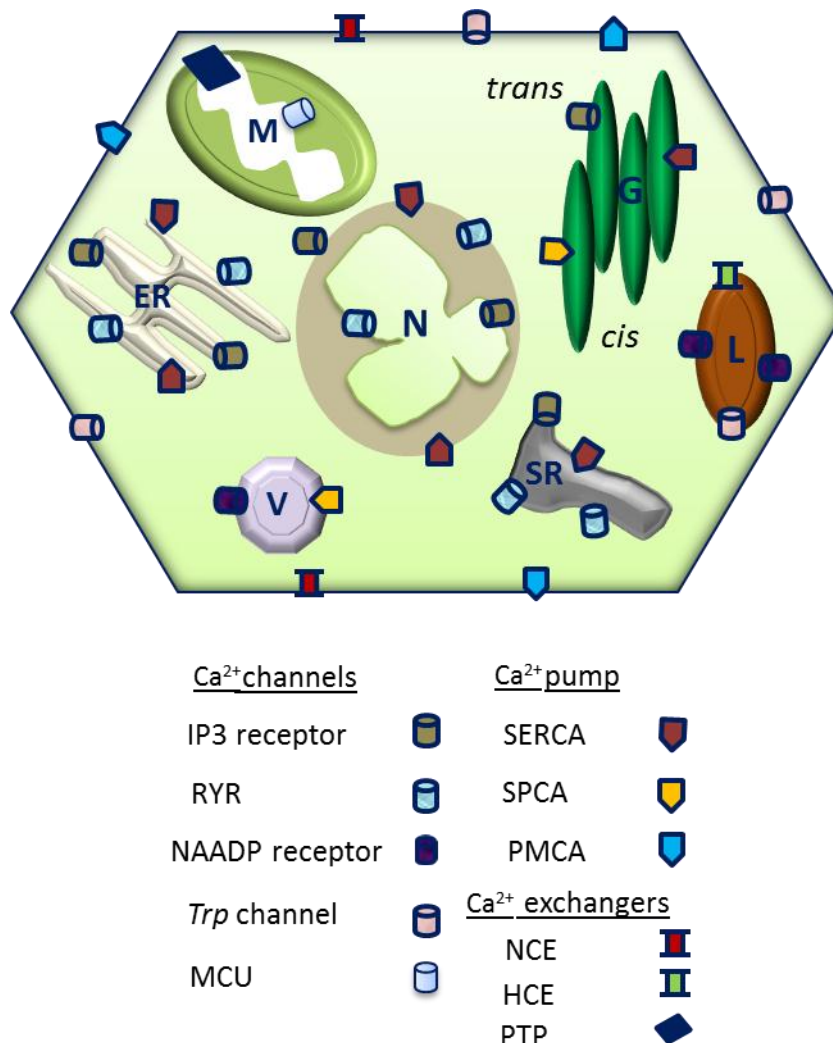


Figure 1.6.1; Ca²⁺ Channels, Exchangers and Pumps in a typical Cell. The diagram shows the organelles that act as a Ca²⁺ stores inside the cell and the associated Ca²⁺ transport (ER- Endoplasmic Reticulum, G- Golgi Apparatus, L- Lysosomes, M- Mitochondria, N-Nucleus, SR-Sarcoplasmic Reticulum, V-Vacuoles). Also listed are some Ca²⁺ transporters associated with the various organelles (Adapted from Michelangeli et al., 2005).

1.6.1.1 Inositol 1, 4, 5-triphosphate receptors (IP3Rs)

IP3Rs consist of four subunits, have a molecular mass of about 1200KDa, and are located on the ER membrane and belong to the family of second-messenger operated ion channels (SMOC) (Berridge et al., 2000). There are three isoforms of IP3Rs, namely type 1 (IP3R1), type 2 (IP3R2) and IP3R type 3 (IP3R3) (Patel et al., 1999, Dyer and

Michelangeli, 2001). These receptors are activated by inositol, 1, 4, 5-trisphosphate (IP₃).

The IP₃R can be opened typically by activating the cell through the binding of an agonist to a G protein couple receptor (GPCR) which in turn activates a membrane G protein. This then activates an enzyme phospholipase C (PLC) and the enzyme cleaves the bond phospholipids of phosphatidyl inositol, 4,5-bisphosphate (PIP₂) in to both diacylglycerol (DAG) and IP₃ (Berridge et al., 2000). Once IP₃ binds to IP₃R it affect its Ca²⁺ sensitivity and opens to produces higher Ca²⁺ concentration in the cytoplasm of a normal cell (Kasri et al., 2004). Phosphorylation or dephosphorylating of IP₃ to IP₄ or IP₂ then takes place to remove the second messenger. An inactivation process on the channel can also take place to restore IP₃R to its unstimulated state (Dyer and Michelangeli, 2001).

Many protein kinases can causes in IP₃R phosphorylation such as PKG, PKA and CaMKII (Ferris et al., 1992; Wojcikiewicz and Luo, 1998; Szado et al., 2008, Dyer and Michelangeli, 2003), and regulate its activity.

1.6.1.2 Ryanodine receptors (RyRs)

RyRs is one of the largest heterotetrameric Ca²⁺ channels, which is located in the endo(sarco) plasmic reticulum of different types of cells (Fill and Cappello, 2002). RyRs are made up of four subunits (monomers) each one being 565 KDa in size. In Mammals, there are three different isoforms and each one encoded by a different gene. This Ca²⁺ channels plays a central role in muscle excitation-contraction coupling through regulating Ca²⁺ mobilization from the sarcoplasmic reticulum (Fleischer, 2008). RyR1 is found in skeleton muscle, RyR2 is highly expressed in cardiac muscle, while low levels of expression of RyR3 is present in neuronal and other tissues (Fill and Cappello, 2002). These different RyRs isoforms have different properties that may allow them to perform different functions (Fill and Cappello, 2002). Isolated hepatocytes express RyR1 receptors, but not type 2 or type 3 (Pietrobon et al., 2006). While RyR2 has been detected in rabbit kidney (Tunwell and Lai, 1996). The sequence analysis shows two functional domains of RyR proteins, a large N-terminal cytoplasmic domain and C-terminal domain, which forms part of the channel. The N-domian includes a variety of

proteins binding sites for various ligands such as Calmodulin (CaM), FK-506 Binding proteins, as well as kinase-dependent phosphorylation sites (Williams et al., 2001).

1.6.1.3 Mitochondrial permeability transition pore channels (MPTP)

MPTP is a channel located on the inner mitochondrial membrane, this pore are very sensitive to many physiological conditions such as calcium concentration, and ROS formation as well as in the regulation of physiological pH (Lapidus and Sokolove, 1994). Once these pores open it becomes highly permeable to solutes and under some circumstances the osmotic gradient between cytosol and matrix causes the mitochondria to swell and then release cytochrome c (Zoratti and Szabo, 1995). Cytochrome c is an apoptosis regulator, associated with caspase-9 which activates caspase-3 and then leads to apoptosis (Gustafsson and Gottlieb, 2003, Halestrap et al., 1997). The MPTPs are usually regulated by pro-apoptotic members of Bcl2 (BAK and Bax), which also contributed to apoptotic cell death (Gustafsson and Gottlieb, 2003, Tsujimoto and Shimizu, 2009).

1.6.2 Ca²⁺ Pumps

P-type ATPase pumps are ion transport pumps which form as a large family of membrane protein. Within mammalian biological membranes there are three types of Ca²⁺ ATPase pumps; Plasma membrane Ca²⁺-ATPase (PMCA) (Niggli, et al., 1982, Shull and Greb, 1988, Carafoli, 1994). Sarco (endo) plasmic Ca²⁺-ATPase (SERCAs) (MacLennan 1970; Burk et al., 1989, Rossi and Dirksen, 2006) and secretory pathway Ca²⁺-ATPase (SPCAs) (Gunter-Hamblin et al., 1992; Ton et al., 2002; Wuytack et al., 2003; Shull et al., 2003; Van Baelen et al., 2001; Wootton et al., 2004). These pumps are characterized by their ability to undertake ATP-dependent phosphorylation during the reaction cycle and Ca²⁺ transport (Palmgren and Axelsen, 1998). Ca²⁺ ATPase pumps are composed of a single polypeptide chain and consist of 10 transmembrane helices and 3 cytosolic domains (nucleotide-binding (N), actuator (A), and phosphorylation (P) domain) (see figure 1.6.2) (Dileve et al., 2008).

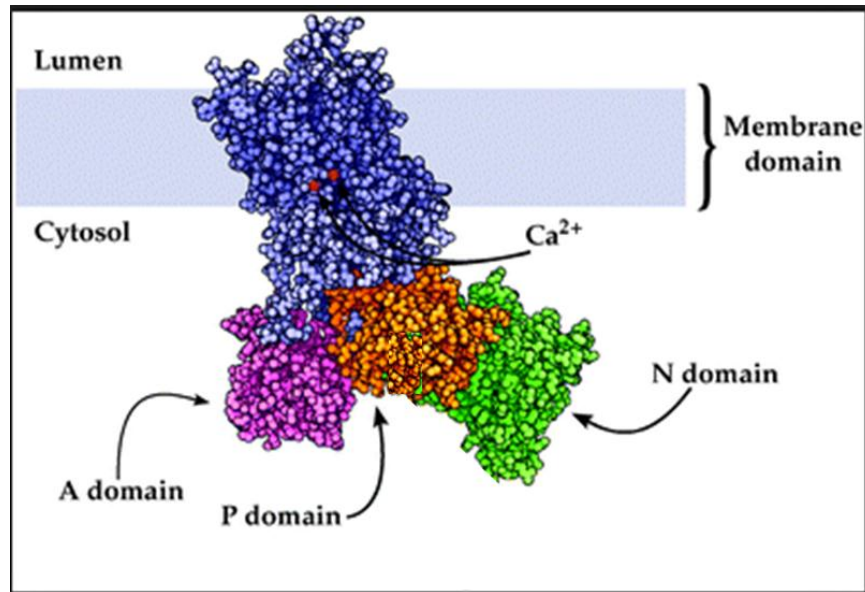


Figure 1.6.2; structure of the Ca^{2+} -ATPase in the conformational state, E1. Show the three domains, nucleotide-binding (N), actuator (A), and phosphorylation (P) domain. Ca^{2+} binding occurs close to the membrane region (Adapted from Lervik et al., 2012).

1.6.2.1 Overview of the Sarco (endo) plasmic reticulum Ca^{2+} -ATPase (SERCAs)

SERCAs belong to the P-ATPase family (Toyoshima et al., 2000 and Moller et al., 1996) which serve as the main Ca^{2+} pumps in the ER. SERCAs are single poly-peptide with molecular mass 110 KDa (MacLenran, 1985) consist of three cytoplasmic domains, actuator (A) domain, phosphorylation (P) domain and nucleotide or ATP-binding (N) domain and 10 α -helices transmembrane domain. Both, phospho Lamban and sarcolipin are protein modulators of SERCA (Lytton et al., 1991; Periansamy and Kalyanasundaram, 2007). In mammals, three separate genes encode SERCA pumps (SERCA1, SERCA2, and SERCA3) with more 10 spliced variants. SERCAs can transport two Ca^{2+} ions which bind co-operatively to the transmembrane region per one ATP hydrolysed (Moller et al., 2005, Lee, 2002). The main expression of SERCA1 is in skeleton muscles, which has two spliced variants; SERCA1a is expressed in adult tissue and SERCA 1 b is exclusively expressed on foetal tissue (Brandle et al., 1986). SERCA 2 exists in three different spliced variants with different expression locations, SERCA2a is mainly expressed in mammalian heart cells, whereas SERCA2b is located in most other tissues at least at low levels. SERCA2c is expressed in cardiac and skeletal muscle

tissues (Lompre et al., 1994). SERCA3 has up to six spliced variants found in both smooth muscle and non-muscle tissues (Bobe et al., 2004; Hovnanian, 2007; Periansamy and Kalyanasundaram, 2007, Chemaly et al., 2013).

1.6.2.1.1 SERCA kinetic cycle

Many intermediate conformations are involved during catalysis and transport of Ca^{2+} through the transmembrane region of SERCA Ca^{2+} pumps with the main ones being the E1 and E2 conformations (Post et al., 1972; Toyoshima et al., 2000; Danko et al., 2004, Michelangli and East, 2011). Initially, the catalytic cycle involves, the Ca^{2+} -ATPase being in a high affinity Ca^{2+} binding E1 state, which binds to Ca^{2+} and ATP ($\text{Ca}_2\text{E1-ATP}$) (Sorensen et al., 2004; Toyoshima et al., 2004), This then activates the N and P domains, to come together and transfer P from ATP to the P domain (ASP351) and also causes the occlusion of Ca^{2+} ions ($\text{Ca}_2\text{E1-P-ADP}$) (Jensen, 2006; Sorensen et al., 2004). At this stage, this triggers the conformation to the low affinity Ca^{2+} E2 state. Upon this, Ca^{2+} is then released from the binding site and passes through the ATPase in to the SR lumen as a result of the decreased Ca^{2+} affinity (Inesi, 1985; Toyoshima and Inesi 2004) (See figure 1.6.2.1.1).

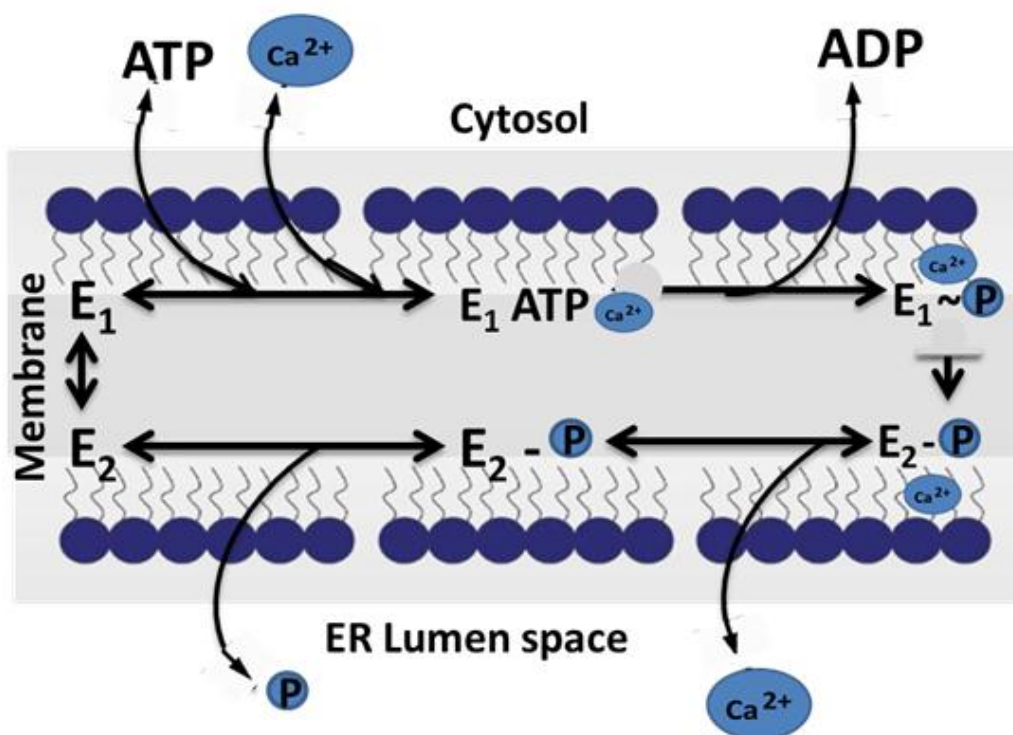


Figure 1.6.2.1.1; scheme of Ca^{2+} transport cycle of SERCA.

1.6.2.1.2 SERCA Ca^{2+} pumps inhibitors

Several chemical agents have been used as a SERCA Ca^{2+} pumps regulators in mammalian cells (Michelangeli and East, 2011). These inhibitors helped elucidate the mechanism of Ca^{2+} entry to ER (Wictome et al., 1992b; Wotton and Michelangeli, 2006). The most well-known inhibitors are, thapsigargin (Tg) (Layton et al., 1991, Estrogen agents, such as bis-phenol A (BPA), butylated hydroxyanisole (BHA), 3,5-dibutyl-4-hydroxytoluene (BHT), 4-n-nonylphenol (NP), 1,1,3,3-tetramethylbutylphenol, diethystibestrol (DES) (Khan, 2001), quercetin, as well as many others (Sokolove et al., 1986; Shoshan and MacLennan, 1981). Thapsigargin (Tg), however, is a highly lipophilic compound and has good penetration of the cell membrane. Tg is an extremely potent inhibitor with an LC_{50} of less than nanomolar (Wotton and Michelangeli, 2005). The inhibition controlled by Tg cause changes in Ca^{2+} ATPase binding affinity to Ca^{2+} , which locks the ATPase in to the low affinity rather than high affinity state (Sagara and Inesi et al., 1991; Wictome et al., 1995).

Furthermore, inhibitory effects of SERCA have dramatic effects on cells and can cause cell death (Michelangeli 2008).

1.6.2.2 Overview of secretory pathway Ca^{2+} –ATPase (SPCAs)

SPCAs also belong to the P-ATPase family and consist of two isoforms (SPCA1 and SPCA2). These are encoded by two genes (ATP2C1 and ATP2C2) in mammals (Van Baelen et al., 2004). As mentioned earlier, PMCAs remove excess Ca^{2+} from the cytosol to the extracellular space, while SERCA and SPCA transfer Ca^{2+} back to sarco (endo) plasmic reticulum and Golgi complex, respectively (Reinhardt et al., 2009). The similarity of amino acid sequence between human SERCAs and SPCAs are more similar than PMCAs. Early studies on SPCA were undertaken in yeast *Saccharomyces cerevisiae*, where it was first identified (Rudolph et al., 1989). Later, SPCA was also identified in rat brain, testes and stomach tissue and most other tissue which suggest that SPCA likely has housekeeping roles in most cell types (Guteski-Hamblin et al., 1992). Furthermore, SPCA pumps are present only in Golgi apparatus, but not in ER. Differently to SERCA, SPCAs also have a very affinity for Ca^{2+} or Mn^{2+} and only translocate one Ca^{2+} (or Mn^{2+}) ion per each hydrolysed ATP, compared to SERCA pumps which bind to two Ca^{2+} ions. Moreover, SPCA has less potential charged residues in Ca^{2+} binding site to bind protons (Van Baelen et al., 2004). As, SPCA has no specific inhibitor, this has prevented our understanding of the specific role of SPCA in cellular homeostasis (Lai and Michelangeli, 2012). Many biochemical studies on this protein have been dependent on the overexpression experiments or studies on keratinocytes obtained from Hailey-Hailey skin diseases patients (Hu et al., 2000, Sudbrak et al., 2000) since they have mutation in SPCA1 (Behne et al., 2003). Generally, three different splice variants SPCA1a, SPCA b, and 1c have been found. These spliced variants, except SPCA1c, are functional (Dode et al., 2006).

1.6.2.2.1 The multifunctions of SPCA in Eukaryotic cells

SPCA1 can be involved in many cellular processes. In the studies with HeLa cells, SPCA1 showed it could affect cytosolic Ca^{2+} signalling due to the reduction of histamine-induced baseline Ca^{2+} -oscillations in SPCA knockdown cells (Van Baelen et al., 2004). A similar effect of SPCA was also seen in insulin secreting cells (Mitchell et al., 2004). The decreased resistance to oxidative stress was observed in *c.elegans* with SPCA1 knockdown (Cho et al., 2005). Furthermore, the role of SPCA1 in affecting Ca^{2+} uptake within vascular smooth muscle has been suggested in the diabetic state (Lai and Michelangeli, 2009). More recently, SPCA has been shown to be involved in protein synthesis, ER stress, lactation, brain development, and other Ca^{2+} homeostasis functions (Vandecaetsbeek, 2011). SPCA₂ has also recently been implicated to play a role in breast cancer by regulating Ca^{2+} entry into the cell (Fengre et al, 2010).

1.7 Aims of this study

1. To determine which chemotherapeutic drugs are most toxic to a range of human liver and kidney cell lines. To determine their mechanisms of cell death, i.e. whether this involves apoptosis, necrosis or autophagy.
2. Determine the level of RGN in some human liver and kidney cell lines and then transfecting these cells with a RGN plasmid to increase its expression, followed by testing these cells for toxicity with known hepatotoxic and nephrotoxicity chemotherapeutic drugs. This will help us to determine whether human liver and kidney cells manipulated to increase their expression of RGN can afford cytoprotection against these chemotherapeutic drugs.
3. Transfecting cells with SERCA and SPCA plasmids followed by testing cell toxicity with known hepatotoxic and nephrotoxicity drugs. This will help us to investigate whether human liver and kidney cells manipulated to increase their expression of SERCA and SPCA and can give some protection against these chemotherapeutic drugs.

CHAPTER 2

Materials and Methods

2 Materials and Methods

2.1 Materials

- Etoposide; (Calbiochem)
- Cis-Diammineplatinum II dichloride; (Sigma- Aldrich)
- Methotrexate; (Sigma- Aldrich)
- Doxorubicin hydrate; (Sigma-Aldrich)
- Dulbecco's Modified Eagle Media (DMEM).high glucose(4,5g/l)with L-glutamine (with and without phenol red); (PAA)
- Foetal bovine serum (FBS); (PAA)
- Penicillin Streptomycin; (PAA)
- Non-essential amino acids; (PAA)
- Dulbecco's phosphate buffered saline (DPBS); (Lonza)
- Trypsin +5% EDTA; (PAA)
- Absolute ethanol; (Fisher Chemicals)
- Absolute Methanol; (Fisher Chemicals)
- Dimethyl Sulfoxide (DMSO); (Sigma-Aldrich and Fisher Scientific)
- 3-(4,5-Dimethylthiazol-2-yl)-2,5-diphenyl tetrazolium bromide (MTT); (Calbiochem)
- Hexabromocyclododecane (HBCD); (Sigma-Aldrich)
- Caspase-3 Inhibitor III; (Sigma-Aldrich)
- BAPTA/AM; (Calbiochem)
- Necrosis inhibitor; (Calbiochem)
- Hydrogen peroxide (H₂O₂); (Fisher Chemicals)

- Precept; (Jounson)
- LB agar; (Sigma-Aldrich)
- LB Broth; (Sigma-Aldrich)
- Ampicillin; (Sigma-Aldrich)
- Miniprep Kits; (Qiagen)
- Maxiprep Kits; (Qiagen)
- Fast Digest SfaAI restriction enzyme; (Thermo Scientific)
- DNA ladder; (New England Biolabs[®])
- Transfection reagent; Turbofect (Thermo Scientific)
- RGN plasmid cDNA; (OriGene)
- PCDNA3.1; (Thermo Scientific)
- pEGFP-LC3 (Gift from Prof. Tamotsu Yoshimori) (Addgene plasmid 21073)
- SERCA1-EGFP (Gift from Prof. J.M. East, University of Southampton) in PCDNA3.1
- SERCA2b-EGFP (Gift from Belgium, Loven University) in PCDNA6.2
- SPCA1-EGFP (Gift from Belgium, Loven University) in PCDNA6.2
- SPCA2-EGFP (Gift from Belgium, Loven University) in PCDNA6.2
- N-Acetyl-Asp-Glu-Val-Asp-p (Sigma-Aldrich)
- Nucview 488 Caspase-3 substrate (Biotium)
- DH5 α TM Competent Cells (InvitrogenTM)
- SYBR[®] Safe DNA Gel stain (InvitrogenTM)
- MitoTracker[®] Deep Red FM (Cell Signalling)
- Kanamycin (Sigma-Aldrich)

- Propidium Iodine (Sigma-Aldrich)
- Hoechst 33258 pentahydrate stain (Invitrogen™)
- Hypomount agar (National Diagnostics)
- RGN 045 antibody (Previously made in Prof. Frank Michelangeli group)
- Y1F4 pan SERCA (Gift from Prof. J.M. East, University of Southampton)
- Donkey anti-mouse IR DYE 800 - LiCOR
- LMPA agar (Promega)
- NMPA (Sigma-Aldrich)

2.2 Methods

2.2.1 Cell culture technique

All cells culturing was completed in an aseptic environment, using a lamina flow hood, and Ethanol (70% v/v) was used to sterilize all materials in the hood. Cells were incubated in CO₂ incubator at 5% v/v CO₂ and 37 °C. Finally waste solutions were treated with precept before being discarded. All materials were sterilized either as purchased or autoclaved at 110-120 °C for 20 min.

2.2.2 Mammalian cells culture and subculturing

All four types cell lines (two livers cell lines; HepG2, Huh7.5, and two kidney cell lines; HK2, COS-7) were grown in sterile 25 cm² and 75 cm² cell culture flasks, with DMEM supplemented with 10% FBS, 1% v/v Essential amino acid, 1% Penicillin/streptomycin and 2 mM glutamine. The media was changed every 2 days. When cells reached 70-80% confluency, the cells were sub cultured, by removing the old media and washing the cells with DPBS three times, then 2 ml Trypsin –EDTA (for 75 cm³) was added. The cells were incubated in the CO₂ incubator for about 2-4 min, then gently agitated to fully detach the cells, the cell suspension was split to 1 in 2 (COS-7, HK2 and Huh7.5) to 4 (HepG2) in new culture flasks for re-culturing. The cells were usually grown in 10 ml media, when seeded in a 75 cm² culture flask.

2.2.3 Mammalian cells freezing and thawing

At +80% confluent, some cells were trypsinized and frozen for the future work. The suspension of cells was centrifuged for about 5 min at 1000 rpm, the media removed followed by adding 10% DMSO in full culture medium to the pelleted cells at approximately 1/10 of original volume. After gentle re-suspension the cells were aliquoted in 1ml fractions in to cryovials and stored at -80 °C in an isopropanol container for 24 hrs. Next day, all the frozen cryovials were moved to be store on -196 °C on the liquid nitrogen storage tank. Thawing procedure starts with thawing cells in a water bath at 37 °C, and then cells diluted with fresh new media and centrifuged at 1000 rpm for 5 min, after removing the media the cell re-suspended and cultured in 25 cm² flasks containing 5 ml full culture medium. Dependent upon the cell line, the cells reached the full confluency after 2-4 days.

2.2.4 Mammalian cells counting Via a Haemocytometer

A haemocytometer was used to estimate cell number, a 10 μ l of suspended cells was added to the slide and sealed with cover slip. Under X100 magnification light microscope the number of cells were counted within the grid and repeated three times. Then the averages were taken to calculate the number of cell in 1 ml, based on the number of cells within the 0.1 μ l grid. The number of cells required (depends on the type of well plates used). The number of cells and the volumes of growth media used in the different plates are given in Table 2.2.4 (www.invitrogen.com). Cells were left for attachment for about 24 hrs, and then the experiments were undertaken.

Table 2.2.4, the number of cells and the volumes of growth media used in this study.

Culture plates (ml)	Surface Area (cm ²)	Seeding Density	Growth media
6-well	9	0.3x10 ⁶	3-5
12-well	4	0.1x10 ⁶	1-2
24-well	2	0.05x10 ⁶	0.5-1
48-well	1	9.5x10 ⁴	0.2-0.5

2.2.5 Cell viability assay (MTT Assay)

Cells were seeded in (12, 24) well-plates and allowed to grow and reach 80-90% confluency at 37 °C. Drug treatment was applied with different concentrations and periods (24-48, 72 hrs). The cells viability was measured by using MTT solution made in Hank's and/or PBS buffer (0.5 mg/ml, final concentration). The MTT assay is a metabolic assay that measures the mitochondria activity by following formazan formation in live cells. Cells were incubated for about 40-60 min and after removing the MTT solution the cells were dissolved in 1 ml DMSO. The cells suspension was placed into 96 well plates and the cells viability were measured using spectrophotometers using an ELISA plate reader at 590 nm and subtracting light scattering if necessary at 650 nm

(Hughes et al., 2000). The percentage of cell viability was calculated dependent on the following equation:

$$\% \text{ viable cells} = \frac{\text{Absorbance difference of treated cells (A590 - A650)}}{\text{Absorbance difference of untreated cells (A590 - A650)}} * 100$$

In most experiments the cells were mostly near-confluent (70-80%), however, in proliferation experiments with MTX, sub-confluent cell cultures of about 20 to 30% was used.

2.2.6 Stock solution preparation

Both, Doxorubicin and Cisplatin were dissolved in 0.9% w/v saline and made as 10 mM stock solution. In contrast, DMSO was used as the solvent for Etoposide and MTX, and made in 0.25 M, 20 mM, 10 mM stocks. Because of the slight toxicity with DMSO the final concentration of DMSO used was as low as possible and tested on the cells in order to minimize its effect on cell viability, hence the concentration of DMSO was always less than 0.4% v/v. DMSO was also used to dissolve caspase inhibitor, necrosis Inhibitor and BAPTA-AM.

2.2.7 Caspase activity assay

Caspase enzyme activity was tested with caspase inhibitor Caspase -3 inhibitor (N-Acetyl-Asp-Glu-Val-Asp-p). Cells were seeded in 48 well plates and incubated at 37 °C overnight. The day after the media was replaced with 0.5 ml of serum-free DMEM and the cells treated with 60 µM of the caspase -3 inhibitor and incubated for 5-4 hrs. Cells were then treated with different drugs and incubated for 48 hrs. MTT assays were performed to measure the cell viability using a Multiskan[®] Microplate spectrophotometer at 570 nm and 650 nm.

2.2.8 Caspase-3 substrate activity

Apoptotic cell death was assayed with Nucview 488 caspase-3. Cells were incubated in the presence of DMEM media in 24 well plates and left to attach for 24 hrs. After 24 hrs, cells were treated with the different drugs for 24 hrs in 0.5 ml serum free DMEM media at 37 °C. 2 µM of caspase substrate in PBS was prepared and 170 µl of the substrate added to the cells after serum-free was removed. The cells were then incubated for 40 min at 37 °C. The number of cells that appeared green using the fluorescence

microscope (Nikon Eclipse TS100) with FITC cube were counted and the % of fluorescence vs non-fluorescence cells (under white light) were calculated.

2.2.9 Necrosis inhibitor

Necrosis cell death was detected with the use of the necrostatin inhibitor. Cells were seeded in 48 well plates and incubated at 37 °C overnight. The day after, 10 μ M of necrostatin was added to the cells in free serum media and incubated for 4-5 hrs. Cells were then treated with the different drugs and incubated for up to 48 hrs. MTT assays performed to measure the cell viability of control and treated cells.

2.2.10 Lactate Dehydrogenase (LDH) activity

Cells were seeded in to 6 well plates overnight, the following day, the drugs were added to several wells and left for 24 hrs. 10% Triton alone was also added to some of the wells and incubated for 30 min (100%, positive control), cells media were collected and centrifuged at 1,500 rpm for 5 min, then 50 μ l of each was added to the cocktail buffer (1 ml) (100 mM potassium phosphate, 0.66 mM sodium pyruvate, 0.25 M NADH pH 7) and the rate of oxidation of NADH was followed at 340 nm in spectrophotometer pharmacia ultraspes 1000.

2.2.11 LC3-GFP Autophagy transfection

Cells were seeded in 12 well plates and incubated at 37 °C to allow for attachment. The next day cells were transfected with a plasmid for Autophagosome marker LC3 with a green fluorescence protein (GFP), in different conditions (1 μ g plasmid/2 μ l TR, 1 μ g plasmid/4 μ g TR, and 2 μ l plasmid/4 μ g TR) in 1000 μ l of serum-free media. The cells were left for upto 48 hrs to increase transfection efficiency. After LC3-GFP transfection for 48 hrs the cells were treated with the drugs for about 3-4 hrs. Images were taken using the Nikon TS 100 fluorescence microscope (with FITC-Cube) and the numbers of fluorescent cells with and without distinct punta were calculated for both control and treated cells and converted to percentages.

2.2.12 Flow cytometry and cell viability

COS-7 Cells were plated into 48 well plates, and then cells were treated with Etoposide for 48 hrs. Cells were then washed with PBS twice and then incubated with 0.05% trypsin-EDTA for 4-5 min. Once the cells detached, complete media was added and

cells then centrifuged for 2 min at 1000 rpm. The cell pellet was again washed with PBS and suspended in 2% Propidium Iodine (PI) in PBS and incubated in room temperature for 40-50 min. FACS Calibur was used and set at 488 nm to detect PI. Cells suspensions were transferred to FACS tube and run directly through the machine without any others additions. Data collected and analysed with the Weasel (FACS dedicated) software.

2.2.13 Comet Aassay

Cells (200,000/well) were seeded in 6- well plates, and incubated overnight at 37 °C.

Cells were then treated with the drugs for 6 and 24 hrs in 2 ml of free-serum media.

-slide preparation

Slides were prepared 48 hrs prior to the start of the comet assay. Clean slide were coated with normal melting point agarose (NMPA), and left to dry at room temperature for 48 hrs. Serum-free media was replaced with PBS and the cells were washed again with PBS and trypsinized with 1 ml Trypsin-EDTA and centrifuged for about 1 min at 1000 rpm. The cells were re-suspended in 150 µl of PBS and 150 µl of pre-warmed low melting point agarose (LMPA) mixed with 15 µl of the cell sample and then added to the NMPA-coated slide. The slides were covered with coverslips and left over an iced-metal tray for 20 min tray to allow solidification to occur.

-Lysis

Once solidified, the cover slips were removed carefully and the slides placed in Coplin jars containing lysis buffer (146.4 g NaCl, 37.2 g Na₂EDTA, 1.21 g Tris-Base, 33.3 ml sodium laurylsarcosinate, in 1liter of dH₂O pH 10). The jars were covered and foiled and stored for 1 hr in the cold room.

-Electrophoresis and Staining

Cells were transferred to a large electrophoresis tank containing buffer (NaOH, 9 M, Na₂ EDTA, 20 mM in dH₂O) and left for 20 min in the tank, then the slides electrophoresed at 32 V (~300 mA) for an additional 20 mins. For staining, slides were washed for 5 min with neutralisation buffer (Tris Base, 0.4 M in dH₂O pH 7.5) 3 times and then washed with dH₂O one min each time. Slides were stained with 50 µl SYBR

gold solution followed by adding the coverslips, slides were placed in a moist box and stored overnight in cold room.

-Counting

Cells were scored (100 cells/slide) and comet assay IV software used to analyse the data.

2.2.14 Protein estimation

2.2.14.1 Preparation of Cell lysates

HepG2, Huh7.5, COS7 and HK2 were grown to 80-90% confluency in 6 well plates, then the media removed and 400 µl of lysis buffer (50 mM Tris-HCl, 1 mM EDTA, 1 mM PMSF, 150 mM, NaCl, 1% w/v sodium deoxycholate, 0.1% w/v SDS and 1% v/v Triton X100, pH 7.4) was added to each well for 10 min at room temperature. Homogenisation was performed by passing the cell suspension through a narrow gauge needle (25 G) and 1 ml syringe about 10 times, followed by centrifugation at 2400 g for 5 min. The supernatant was collected and aliquoted into eppendorf tubes and stored at -20 °C, until required.

2.2.14.2 Bradford protein concentration determination assay

The amount of protein in the cell lysates was estimated using the Bradford assay (Bradford, 1976). Standard calibration curve was constructed from three replicate, with 950 µl Bradford reagent (Sigma) and using 1mg /ml of Bovine Serum Albumin (BSA) as the protein standard stock and varying in amounts between 0-50 µg BSA to give a final volume 1 ml by adding the relevant volume of deionised water. The absorbance of the samples was read at 590 nm using spectrophotometer in order to estimate the protein concentration values.

2.2.14.3 SDS_PAGE

BIORAD miniPROTEAN^{®3} system was used according to the manufacturer's instructions. The pre-made (Biorad) gel was added to the tank and the Running Buffer (192 mM glycine, 25 mM Tris and 0.1 % w/v SDS) was used to fill the electrophoresis tank. The protein samples (typically at 2 mg/ml) were mixed with an equal volume of

the loading solubilizing buffer, (125 mM Tris, 4.6% w/v SDS and 20% w/v glycerol, pH 6.8) and to this buffer was added 2-mercaptoethanol mixed at a ratio 20:1 (5%) and a trace amount of bromophenol blue. Each sample was heated at 100 °C for 5 min before being loaded into the wells of the gel. The gel was electrophoresed for about 45 min at 120 Volts and then the plates carefully separated and the gel either stained with EZBlue™ staining reagent for protein visualization, or directly used for transfer onto nitrocellulose membranes for Western blotting.

2.2.14.4 Western blotting

The gel was transferred onto nitrocellulose membranes using a sandwich assembly (Figure 2.2.8.4) and the Biorad Semidry transfer apparatus manufacturer's instructions followed. Once transferred, the membrane was washed with dH₂O and the membrane was marked on right face with a pencil. The membrane was blocked for the non-specific protein binding sites using milk solution (5% w/v semi-skimmed milk powder in TTBS buffer (25 mM Tris-HCl (pH 8.0), 150 mM NaCl and 0.05% v/v tween 20)). The membrane was left at -4 °C overnight with gently agitation. ATBS (20 mM Tris and 137 mM NaCl at pH 7.6) was prepared to dilute the primary and secondary antibodies. After 1.5–2.0 hrs of incubation of the nitrocellulose with the primary antibody, the membrane was washed 3 times for 5 min with dH₂O, followed by another blocking step for 30 min and incubation with a fluorescently tagged secondary antibody for 1.5–2 hrs (IRDye). After washing the membrane 3 times with TBST high salt and dried on filter paper, the membrane was viewed using the Odyssey LiCor infrared scanner (Li-Biosciences) to detect the fluorescent antibody labelled bands.

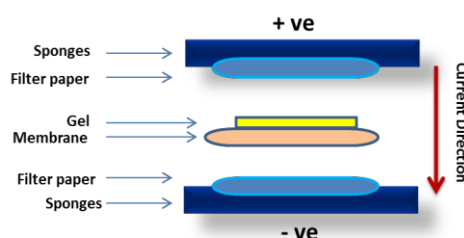


Figure 2.2.8.4, western and blotting sandwich assembly. The transfer is done using an electric field oriented perpendicular to the surface of the gel. The sandwich from cathode to anode includes sponges, Filter papers, gel, nitrocellulose membrane, filter paper and sponges.

2.2.15 Transfection

2.2.15.1 Making Luria-Bertani (LB) and Agar Plates

A septic conditions were used throughout. 20 ml of 2% LB media and 1.5% Agar were made and autoclaved, then heated on microwave for 3 min (medium power). The LB agar was allowed to cool down, followed by addition of 10 µl of Ampicillin (100 mg/ml), avoiding any bubbles. The LB agar was poured in to 10 cm diameter petri dishes and allowed to set.

2.2.15.2 DH5α cells transformation and RGN plasmid preparation

50 µl of DH5α cells were thawed on ice for 10 minutes and 1 µl of 0.1 µg/µl of Human RGN cDNA clone (Pcmv6 AC-GFP-RGN with C-terminal GFP tag) added to cells, the mixture placed on ice for 30 min. After that, cells heat shocked at 42 °C for 30 seconds. Cells were then placed on ice for 5 min, and then 950 µl of LB media added to the mixture at room temperature, and cells incubated for 60 min at 37 °C. A serial of 10-fold dilutions were made and 50 µl of each dilution used to spread the plates and incubate cells at 37 °C overnight. Next day, three single colonies were transferred to three LB media tubes (5 ml) and grown overnight in an orbital shaker at 37 °C. Following the manufacturer's instruction, RGN plasmid DNA was isolated using QIAprep[®] Spin Miniprep. In order to possess a high DNA plasmid amount, QIAfilter Plasmid Midi and Maxi Kits was used, after overnight grown of 500 ml bacterial cell cultures.

2.2.15.3 Estimation of plasmid RGN DNA quantity

Measurement of the DNA plasmid concentration and purity were performed by NanoDrop (ND-1000) spectrophotometer. The 260/280 (A_{260}/A_{280}) absorbance ratio was also measured to assess DNA purity.

2.2.15.4 Transfection of COS-7 cells

COS-7 cells were seeded in 24 well plates at 37 °C, with 1ml of DMEM media, supplemented with glutamine, Non-essential amino acids, 10% FBS and 1% penicillin/streptomycin. Three transfection conditions were used to optimize the transfection efficiency each done in triplicate. The transfection reagent used was Turbofect as used following the manufacturer's recommended instructions. After

24 hrs and when cells reached 40-50% confluence, DMEM media without FCS with the solution of plasmid (SERCA1-GFP, SERCA2b-GFP, RGN-GFP, SPCA1a-GFP, SPCA2-GFP and PCDNA 3.1) and transfection reagent was added to cells and incubated for 24, 48, 72 hrs, after 24 hrs the media was removed and new DMEM media with FCS was added to the cells and the fluorescent microscopy images (20x magnification power) was used after each 24 hrs to estimate the transfection efficiency for the GFP-tagged expressed proteins for each condition. White light and fluorescence images for the same field were taken and routine cell counting was performed to calculate the total cell transfection percentage.

The mammalian expression plasmids for the Ca^{2+} ATPases used were as follows:

pcDNA3.1 Rabbit SERCA1b-N-GFP (Newton et al., 2003, Wotton, PhD thesis 2005, Al-Mousa, PhD thesis, 2010)

pcDNA6.2 Human SERCA2b-N-GFP (Baron et al., 2010)

pcDNA6.2 Human SPCA1a-N-GFP (Baron et al., 2010)

pcDNA6.2 Human SPCA2-N-GFP (Baron et al., 2010)

The plasmid identities were confirmed through diagnostic restriction enzyme analysis.

2.2.15.5 Co-Localization of RGN

COS-7 cells were seeded on to sterilized coverslips in 6 well plates overnight at 37 °C for attachment to occur. Cells were then transfected with RGN-GFP in 2ml media (serum free DMEM) and viewed under the fluorescence microscope after 48 hrs to determine that the expression level was at least 35-45%. Cells were then treated with DOX (20 μM) in 2 ml serum free media for 2 hrs. Cells were washed with PBS 3 times and treated with (0.5 μM) Mitotracker® Deep RedFM in 2ml DMEM media and incubated for 30-40 min. Cells then were washed with PBS, 2 times and then the DMEM media replaced by 4% paraformaldehyde (PFA) in PBS pH 7.4 to allow the cells to be fixed. After 20 min, cells were washed with PBS twice and 1 $\mu\text{g/ml}$ of Hoechst 33258 was added to the cells, covered in foil and then incubated for 30 mins. Finally cells were washed again with PBS twice more. The coverslips were removed from the slide gently and 70 μl of Hypomount agar was added to the side and left in the

dark to allow air drying to occur. Then the cells were viewed with transmission, Red, Blue, Green channels of Leica SP2 or Nikon Eclipse Ti microscope.

2.2.15.6 Cell proliferation and crystal violet assay

100 µl of cells were seeded on to 96 well plates and the cell allowed to attach overnight. Next day the cells were transfected with the plasmids and the cells were incubated for 24 hrs. The media was changed and cells were left for more 24 hrs. The day of assay, cells were washed with PBS (PH 7.4) after media aspiration, then cells were fixed with 100 µl of 4% paraformaldehyde in PBS for 15 min. After that, paraformaldehyde was replaced with 100 µl of 0.5% crystal violet (in 10% ethanol, 90% dH₂O) for 20 min. The cells were again washed three times with dH₂O to remove any access dye and cells left to dry, 100 µl of 10% acetic acid was added for 20 min to allow the dissolution. An additional dilution of 1:2 with 10% acetic acid was used and then absorbance measured at 595 nm with the plate reader.

2.3 Statistical Analysis

The data taken from chapter 1 and 5 have been analyzed using sigma plot version 12.5, mean and standard division (SD) were calculated with Microsoft Excel. *p* values, two tailed equal variation t-test were applied. Weasel.Jar software used to analyze flow cytometry data.

2.4 Image analysis

LI-COR Odyssey used to detect the western blot bands, ImagJ was used to measure the bands intensities on chapter 4 and 5, ImagJ JACOP's plugin used for colocalization analysis (Bolte & Cordelières, 2006).

CHAPTER 3

Mechanisms of cell death by chemotherapeutic drug

3 Mechanisms of cell death by chemotherapeutic drug

3.1 Introduction

As cancer is considered one of the major causes of death, research over many years have developed a variety of different treatments, such as radiation therapy, surgery and chemotherapy. Although, chemotherapy can be an effective treatment for killing cancer cells, chemotherapy can affect normal dividing cell as well (Debatin, 1997), due to their cytotoxic nature. Therefore, with chemotherapy treatment, unfortunately 85% of cancer patients exhibit some degree of liver damage (Ramadori and Cameron, 2010), furthermore, these drugs can affect kidney function and causes nephrotoxicity (Cornelison and Reed, 1993). This may mean that they are not being able to continue their chemotherapy treatment due to serious damage caused by these hepatotoxic and nephrotoxic drugs that prohibit cells from performing their normal functions (King and Perry, 2001 & Lawerence et al., 1973).

The work presented in this chapter investigates the molecular mechanisms of cell death of four chemotherapy drugs (Methotrexate, Etoposide, Cisplatin, and Doxorubicin), which are often used in clinical treatment of some forms of cancer. Furthermore, four various cell lines were used from kidney and liver cells (COS-7, HK2, HepG2 and Huh7.5) to investigate the effect of these drugs on cells derived from these particular susceptible organs. An investigation of apoptosis, necrosis and autophagy cell death mechanisms was the main focus in this chapter.

3.2 Cell viability and DMSO concentration

3.2.1 Cell viability with MTT assay

MTT cell viability experiments were performed to show that the absorbance measured is directly correlated to cell number. Different numbers of HepG2 cells were plated in 24 cell culture plates. Cells were incubated 24 hrs in CO₂ incubator at 37 °C, then the MTT protocol performed, as described in section 2.2.5 and the results presented in figure 3.2.1. As can be seen a linear correlation between the cell number (or cell viability) and the absorbance values is observed.

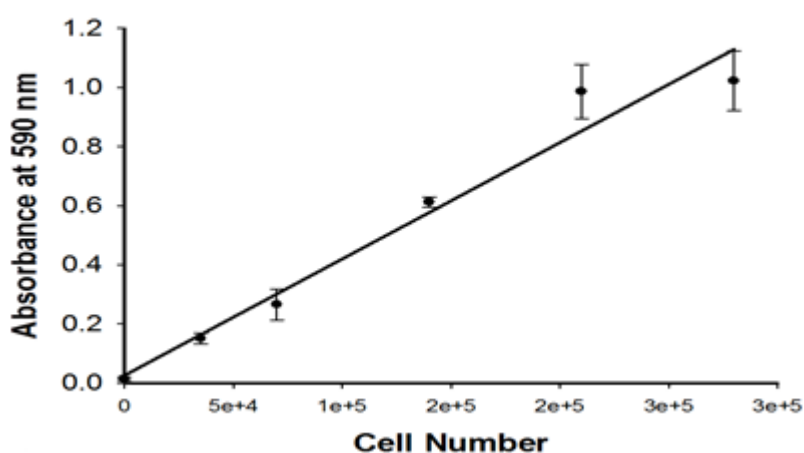


Figure 3.2.1; the correlation between absorbance at 590 nm using an MTT assay and cells number. The data represented is mean \pm SD of between 3-4 determinations.

3.2.2 Cell Viability with Flow Cytometry

COS-7 cells were treated with trypsin/EDTA and cells were stained with PI, used in order to measure the viability of these cells using flow cytometry. As shown in figure 3.2.2, 95% of cells were considered live cells (i.e. having lower levels of PI fluorescence), while only 5% were labelled cells which were considered dying cells (As they showed high levels of PI fluorescence).

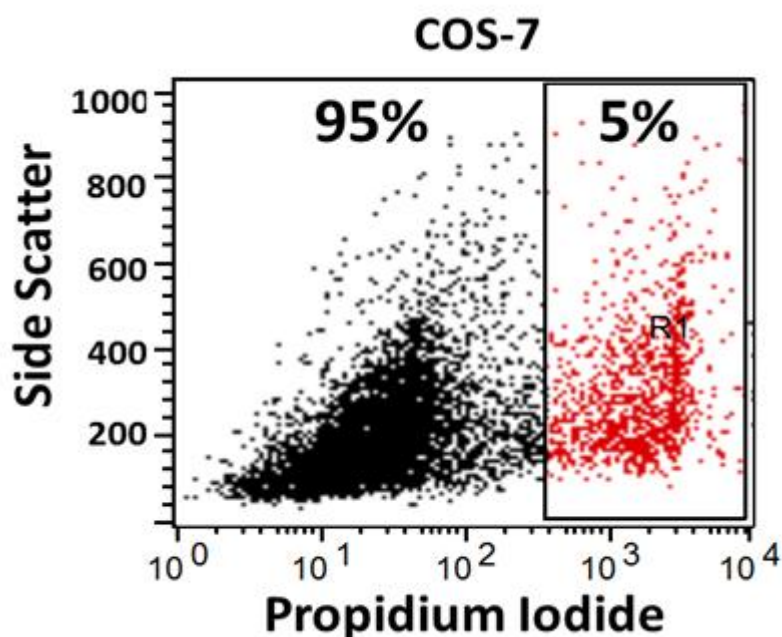


Figure 3.2.2; shows the percentage of cell viability of COS-7 cells. Cells were labelled with propidium iodide and run through a flow cytometry (Calibure16). Dead cells with very low side scatter were excluded prior to analysis. The results showed two populations of cells with the required cell size, with one population considered positive for PI staining (therefore indicating dying cells). This plot is typical of at least three experiments.

3.3 The effect of chemotherapy drugs on the viability of liver (HepG2, Huh7.5) and kidney cells (COS-7, HK2)

3.3.1 The effect of chemotherapy drug Methotrexate on the viability of kidney cells (COS-7, HK2) and liver cells (HepG2, Huh7.5) using the MTT assay

A number of liver and kidney cells were monitored with different concentrations of Methotrexate (MTX) drug to determine the nephrotoxicity and hepatotoxicity, by measuring cell viability. As DMSO was used as a solvent for MTX and Etoposide drugs, the effects of DMSO on cell viability was first determined. As shown in figure 3.3.1 the total concentration for DMSO should be kept to less than 0.4% (v/v) in HepG2

cells. As this causes no significant effect on cell death. This was also similar for the other cell lines tested.

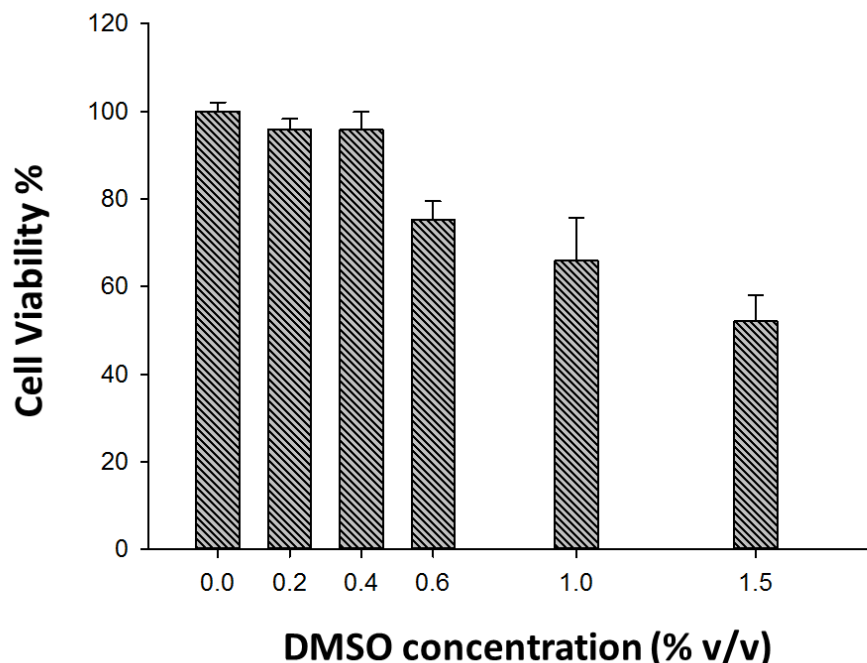


Figure 3.3.1; shows the cell viability using MTT assay with different concentrations of DMSO (0-1.5% v/v) in HepG2 cells. The data represented is mean \pm SD of between 3-4 determinations.

Figure 3.3.1.1 A-D; shows the dose-dependent effects of a range of concentrations of MTX (0 to 200 μ M) on kidney cells COS-7 (A), HK2 (B) and liver cells HepG2 (C), Huh7.5 (D). The cells were incubated for 48 hrs with the drug at 37 $^{\circ}$ C and the cell viability was measured via MTT assays and compared with control DMSO alone treated cells. All data represented the mean and the standard deviation (mean \pm SD) of 3-4 replicates. It can be seen that this chemotherapy drug shows the little toxicity with the liver cell lines compared to the kidney cells. Both kidney cell lines showed that about 50% of the cells were very sensitive to low μ M concentration of MTX, while about 50% were relatively in-sensitive to MTX. In contrast, both HepG2 and Huh7.5 cells show little or no effect on cell viability even with high concentrations of MTX (100 to 200 μ M). As a result, COS-7 and Huh7.5 cells at low confluency (20%) were treated with high concentrations of MTX (200 μ M) and the cells were left for 96 hrs in

order to determine whether MTX drug reduced the rate of cell proliferation. Figure 3.3.1.2 shows the effect of MTX on COS-7 (A) and Huh7.5 (B) cell proliferation, compare to DMSO treated cells which were used as a control. The MTT assay was carried out after 4 days. COS-7 cells showed a reduction of about 40% in the rate of cell proliferation as compared with DMSO control, while Huh7.5 cells showed a 30% reduction in cell proliferation compared to DMSO.

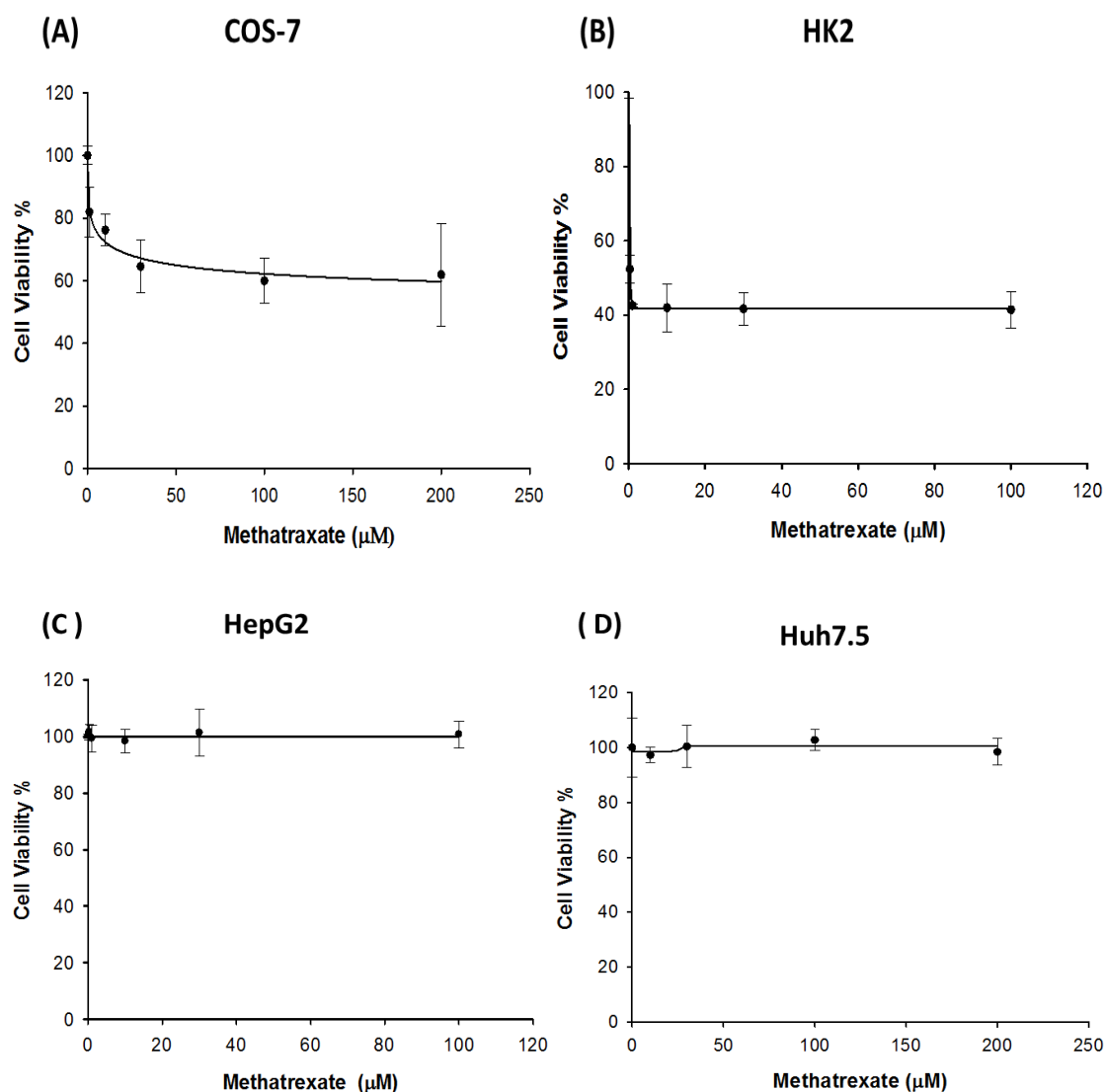


Figure 3.3.1.1 A-D; shows the effects of MTX on the viability of COS-7 (A), HK2 (B) HepG2 (C), and Huh7.5 (D) cells. The cells incubated with MTX over a range of concentrations for 48 hrs at 37 °C and then cell viability measured using the MTT

assay. The data represented is mean \pm SD of between 3-4 determinations.

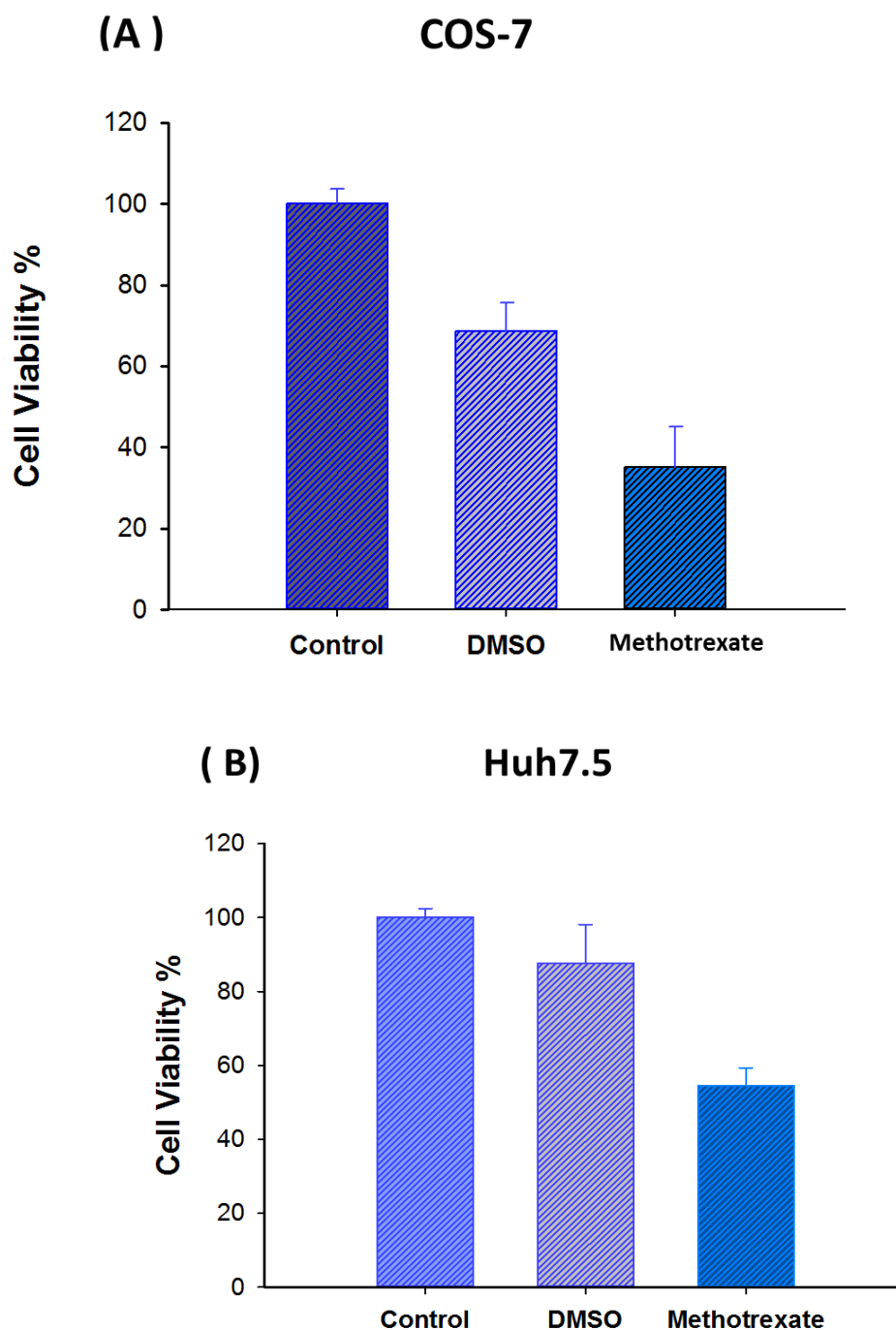
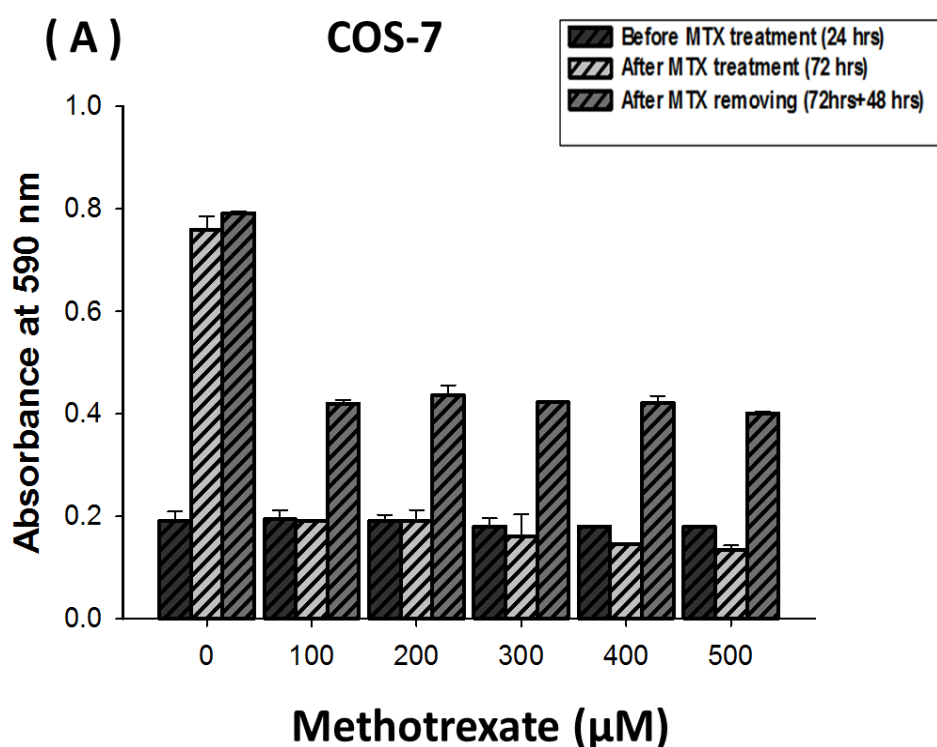


Figure 3.3.1.2A and B; shows the effect of MTX (200 μ M) on COS-7 (A) and Huh7.5 (B) on cell viability. As +/- DMSO treated cells were used as a control, COS-7 and Huh7.5 cells were incubated with MTX on 37 $^{\circ}$ C for 96 hrs and the MTT assay was performed. All data represent the mean \pm SD of between 3-4 determinations.

The results suggested that MTX plays a role in reducing cell proliferation and therefore a range of MTX concentrations (0, 50, 100, 200, 300, 400, 500 μM) were used to treat (COS-7, HK2 and HepG2) cells at low 20% confluency (9 replicates). Cells were incubated in 5% CO_2 and 37 $^\circ\text{C}$, then MTT assays were performed for 3 replicates after 24 hrs, the other 6 replicates were treated with MTX, and after 72 hrs three replicates were used to measure the cell viability. Again after then the MTX drug was removed and cells incubated for a further 48 hrs to investigate the effect of MTX removal on cell proliferation. Figure 3.3.1.3 shows the effects of different concentrations of MTX drug on the different cells lines. COS-7 cells showed no cell growth at < 100 μM or higher, while HK2 cells showed some slight cell growth, which decreased with increasing drug concentrations. In contrast, HepG2 cells showed clear cell proliferation even at 500 μM MTX concentration. Once the MTT assays were performed, after 48 hrs of removing the MTX, all cell lines showed some restoration of cell growth.



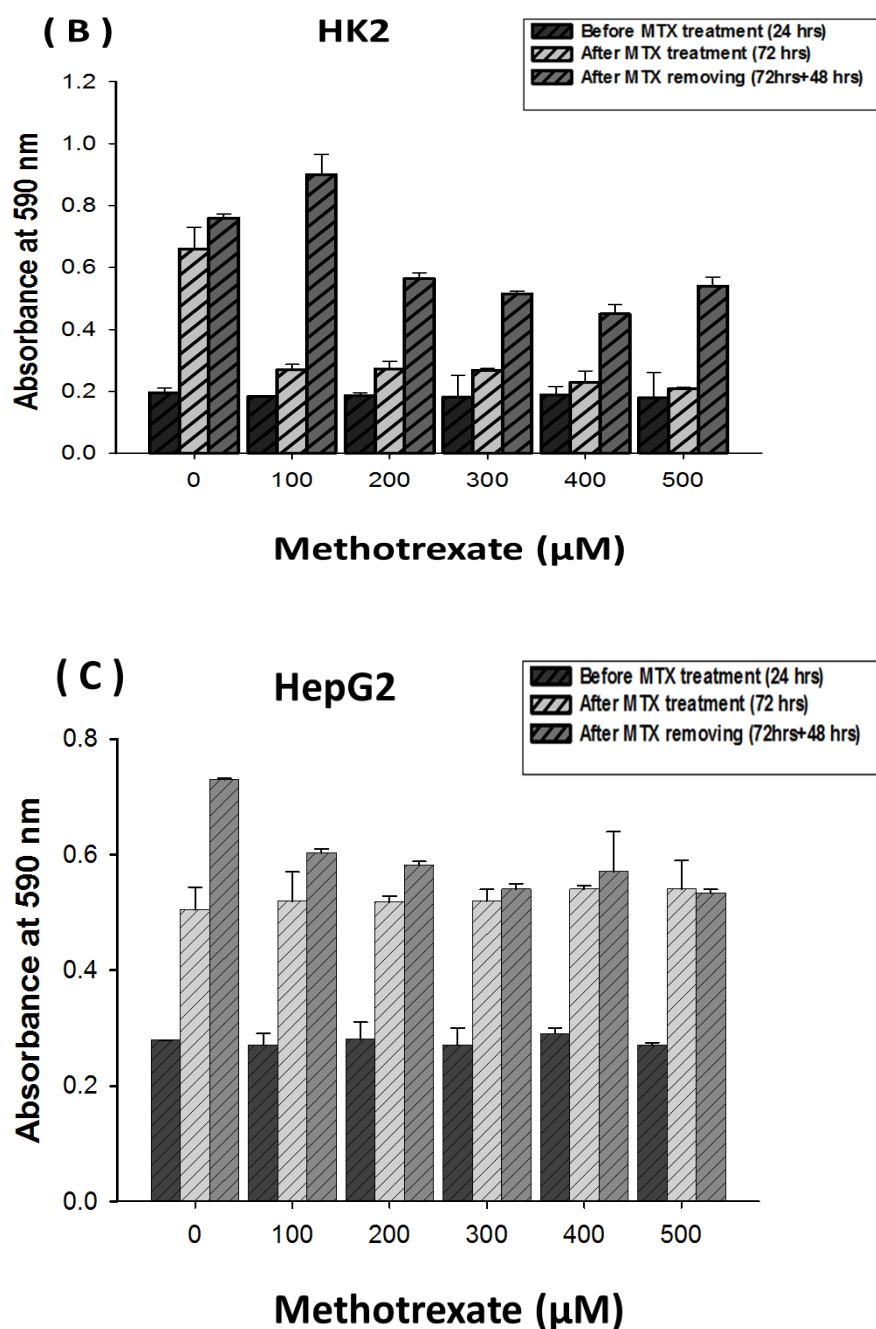
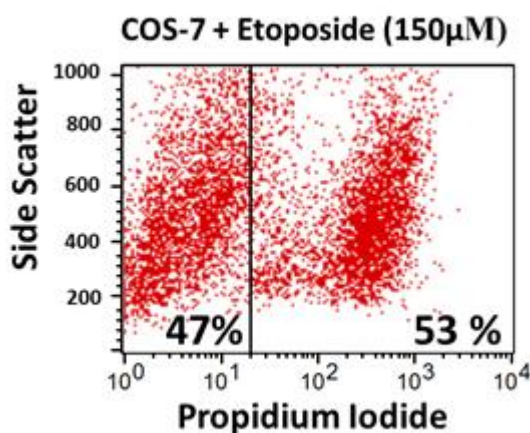


Figure 3.3.1.3 A-C; shows the inhibition effects of MTX on COS-7 (A), HK2 (B) and HepG2 (C) on cells proliferation. The MTT assay was carried out, before and after drug administration as well as after removing MTX after 72 hrs. Cells were incubated at 37 °C and MTT assay carried out after 24 hrs of cell seeding, 72 hrs after drug exposure, and 48 hrs after removing the drug. All data represent the mean \pm SD of up to 9 determinations.

3.3.2 The effect of chemotherapy drug Etoposide on the viability of kidney (COS-7, HK2) and liver cell lines (HepG2, Huh7.5) as performed using the MTT assay

A series of liver and kidney cell lines viability measurements were monitored at different concentrations of etoposide to determine its nephrotoxicity and hepatotoxicity. Figure 3.3.2 A-D; shows the dose-dependent effects of a range of concentrations of Etoposide (0 to 2000 μM) on kidney cell lines (COS-7 (A), HK2 (B)) and liver cell lines (HepG2 (C), Huh7.5 (D)). The cells were incubated for 48 hrs with the drug at 37 °C and cell viability was measured via the MTT assay and compared with control, (DMSO alone), all data represents the mean and the standard deviation ($\text{mean} \pm \text{SD}$) of 3-4 replicates. In figure 3.3.2 it can be seen that both kidney and liver cell lines are sensitive to Etoposide drug with LC_{50} values of 50 ± 6 , 120 ± 6.4 and 150 ± 9.1 μM for HK2, HepG2, and COS-7 cells, respectively. While Huh7.5 shows a much higher LC_{50} (1000 ± 11.1 μM). Figure 3.3.2 the insert confirmed that 150 μM Etoposide also causes about 50% cell death in COS-7 cells as measured using PI and flow cytometry (Figure 3.3.2 inset) (BD FACS caliber).



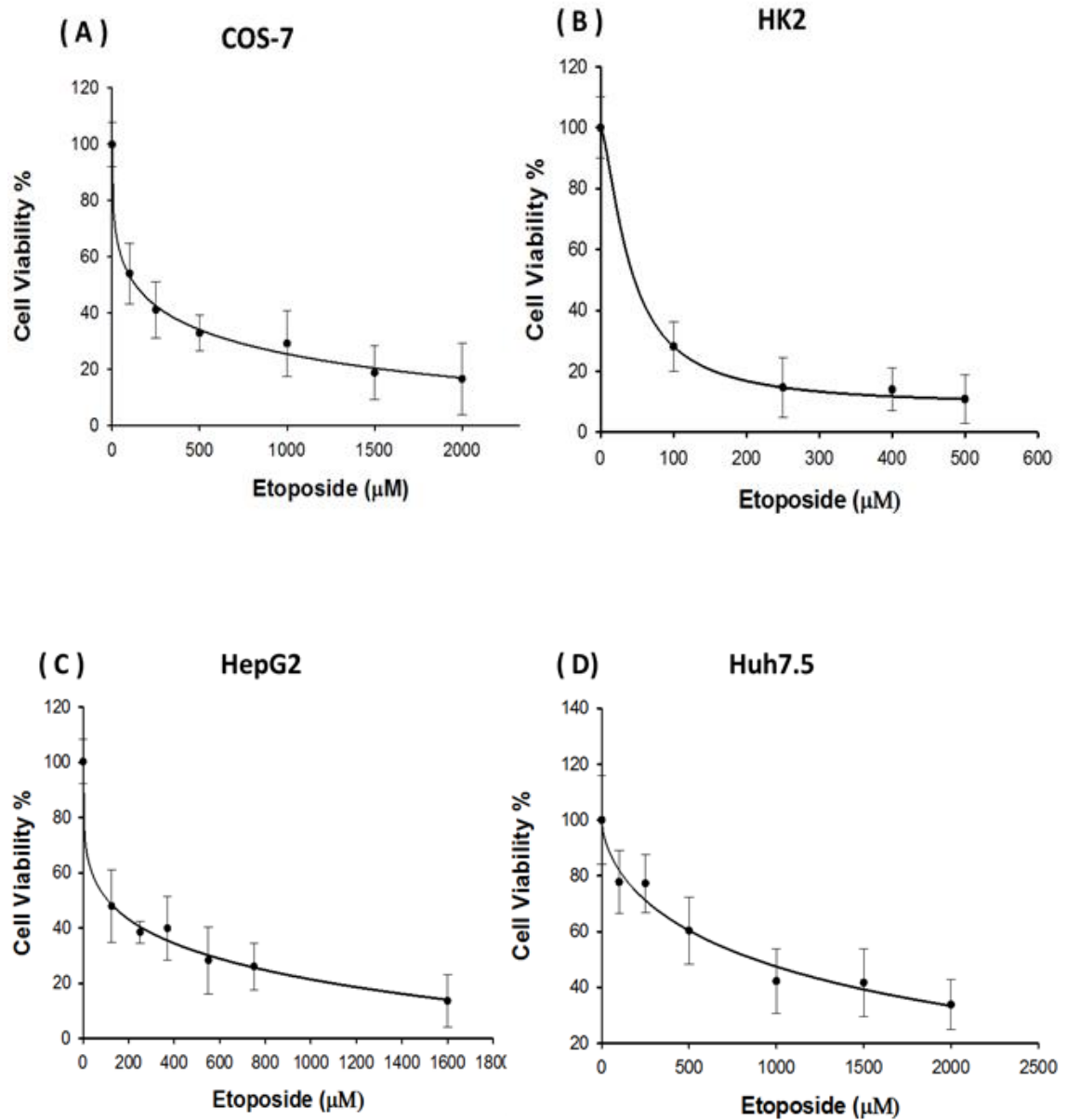


Figure 3.3.2 A-D; shows the effect of Etoposide on the viability of COS7 (A), HK2 (B), HepG2 (C), and Huh7.5 (D), cell lines. Cells were incubated for 48 hrs at 37 °C. The data represents the mean \pm SD of between 3-4 determinations. The flow cytometry graph (inset) above that shows COS-7 cells (47% live cells and 53% dead cells) after cell treated with 150 μM etoposide for 48 hrs. For control compare this with figure 3.2.2.

3.3.3 The effect of chemotherapy drug Cisplatin on the viability of kidney cell lines (COS-7, HK2) and liver cell lines (HepG2, Huh7.5), as performed using the MTT assay

Figure 3.3.3 A-D; shows the dose-dependent effects of a range of concentrations of Cisplatin (0, 0.1, 10, 100, 1000 μM) on kidney COS-7 (A), HK2 (B) and liver cells HepG2 (C), Huh7.5 (D)). The cells were incubated for 48 hrs with drug at 37 °C and the cell viability was measured via MTT assay and compared with control, all data represents the mean and the standard deviation (mean \pm SD) of 3-4 replicates. Figure 3.3.3 shows differences between the different cell lines used. HK2 cells is the most sensitive cell lines for cisplatin (LC_{50} was $20 \pm 7 \mu\text{M}$) compared to other cell lines HepG2, COS-7 and Huh7.5 (with LC_{50} were 35, 46, 90 μM), respectively.

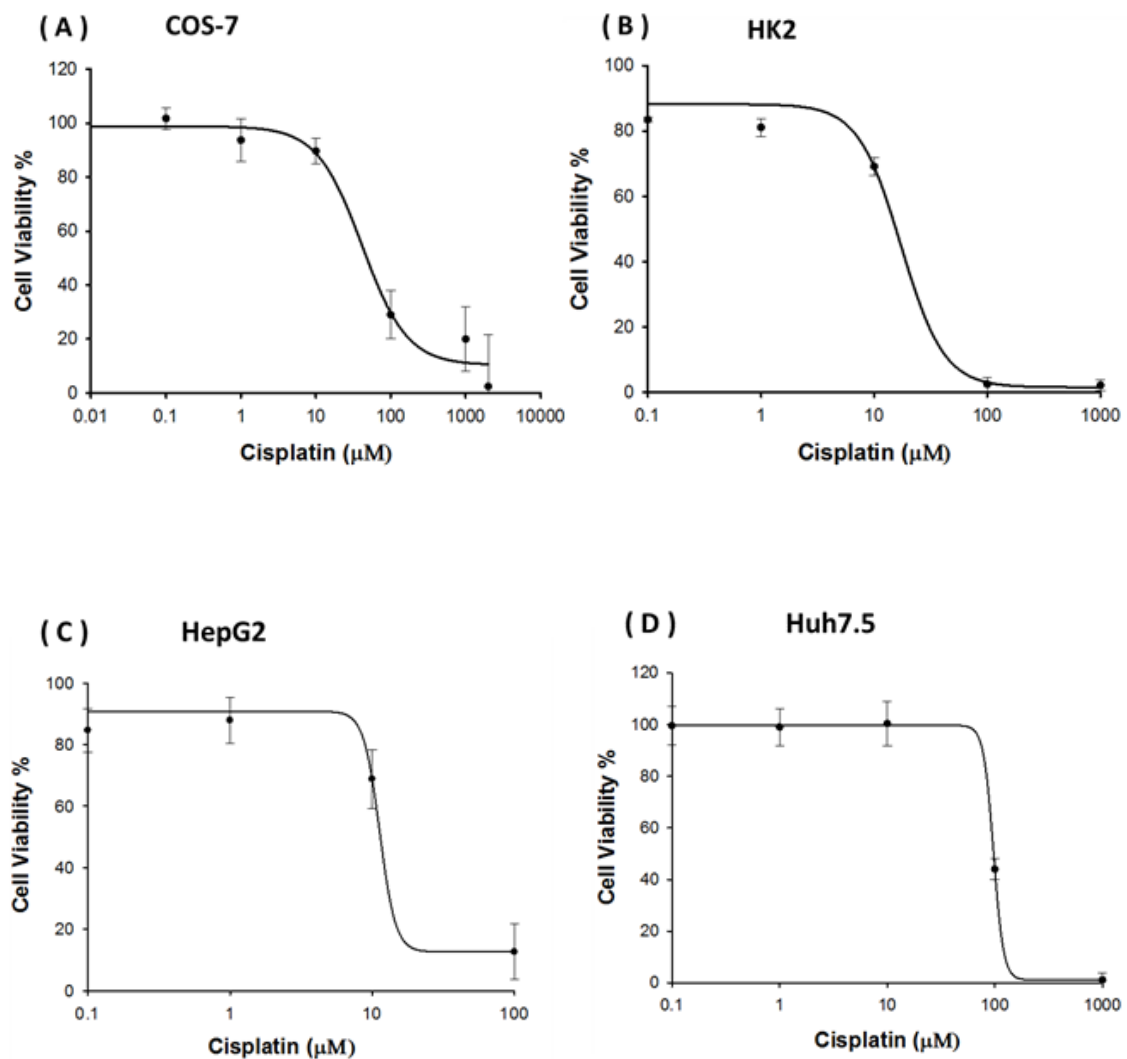


Figure 3.3.3 A-D; shows the effects of Cisplatin on the viability of COS-7 (A), HK2 (B) (HepG2 (C), and Huh7.5 (D). Cells were incubated for 48 hrs at 37 °C with drug. The data represented is mean \pm SD of between 3-4 determinations.

3.3.4 The effect of chemotherapy drug Doxorubicin (DOX) on the viability of kidney (COS-7, HK2) and liver cells (HepG2, Huh7.5) as performed using the MTT assay

Figure 3.3.4 A-D; shows the dose-dependent effect of a range of concentrations of DOX (0, 0.01, 0.1, 10, 100 μM) on kidney cell lines COS-7 (A), HK2 (B) and liver cell lines HepG2 (C), Huh7.5 (D). The cells were incubated for 48 hrs with the drug at 37 °C and the cell viability was measured via MTT assay and compared with control,

all data represent the mean and the standard deviation (mean \pm SD) of 3-4 replicates. Dox causes cell death in all the cell lines used with similar LC₅₀ values, in low μ M concentration (See table 3.3).

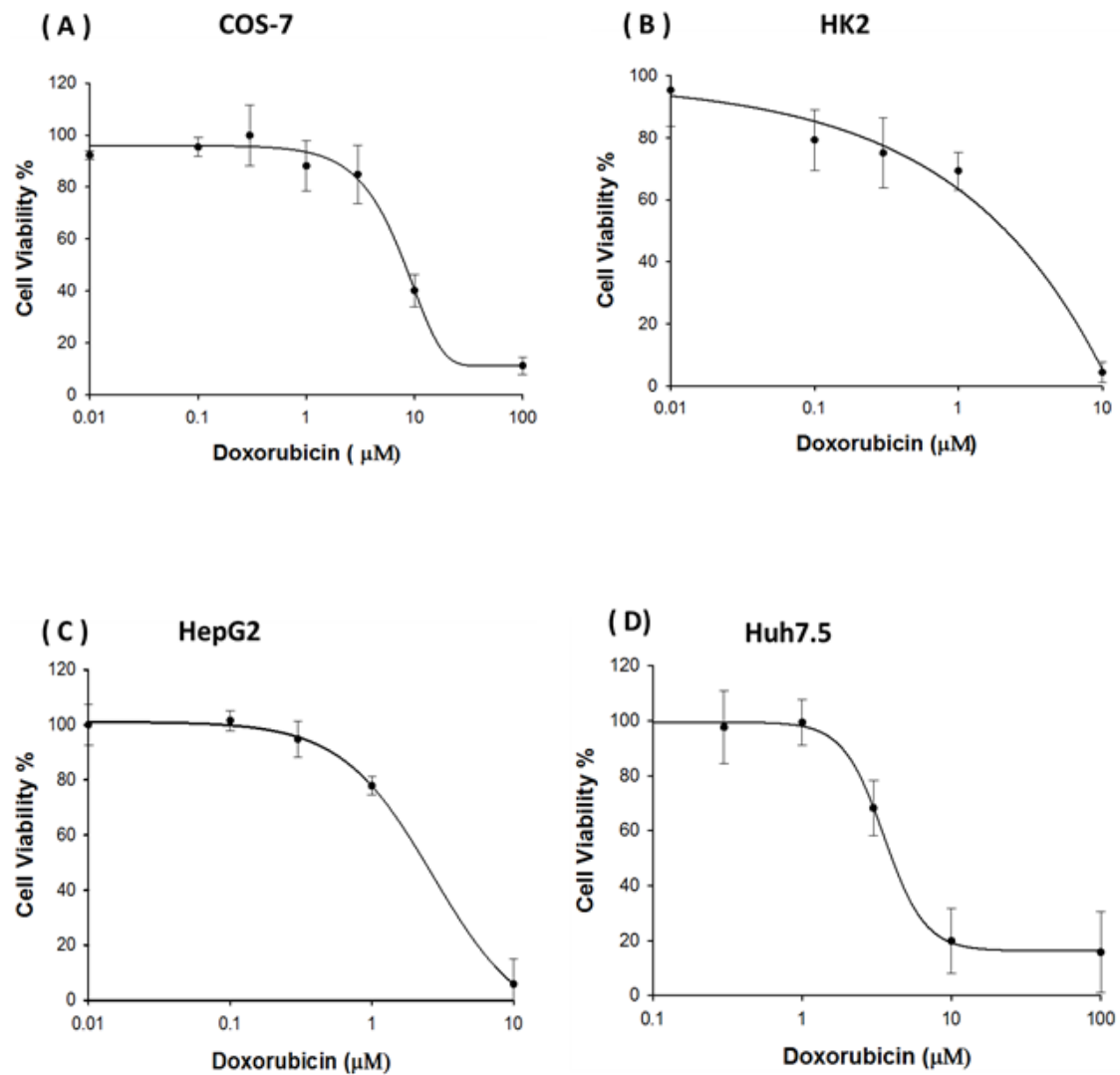


Figure 3.3.4 A-D; shows that DOX reduces viability of COS-7 (A), HK2 (B), HepG2 (C), and Huh7.5 (D). Cells were incubated for 48 hrs at 37 °C. The data represented is mean \pm SD of between 3-4 determinations.

Table 3.3 summarizes concentration that causes 50% cell death (LC_{50}) for cell viability of these chemotherapy drugs, it is clear that DOX is the most potent anti-cancer drug compared to other drugs test here. In contrast, MTX showed its little effect on rate of cell proliferation, and Etoposide was only weakly toxic with an LC_{50} $1000 \pm 11.2 \mu M$ on Huh7.5 cell.

Table 3.3; comparison of lethal concentration 50 (LC_{50}) values of different anti-cancer drugs. All data represent the mean \pm SD of between 3-4 determinations.

Cell line	50% cell death [LC_{50}](μM)			
	DOX	Cisplatin	MTX	Etoposide
HepG2	$\sim 4 \pm 5$	35 ± 3	No effect	120 ± 6.4
Huh7.5	6 ± 7	90 ± 10.5	No effect	1000 ± 11.2
HK2	3 ± 5	20 ± 7	At $200 \mu M$ still cell viability 60%	50 ± 6
COS7	7 ± 8	$\sim 46 \pm 8.7$	At $200 \mu M$ still cell viability 60%	150 ± 9.1

3.4 Detection of apoptosis induced by MTX, Etoposide, Cisplatin, and Doxorubicin using caspase 3 inhibitors and the fluorogenic substrate (488 Nuc caspase-3) on kidney and liver cell lines

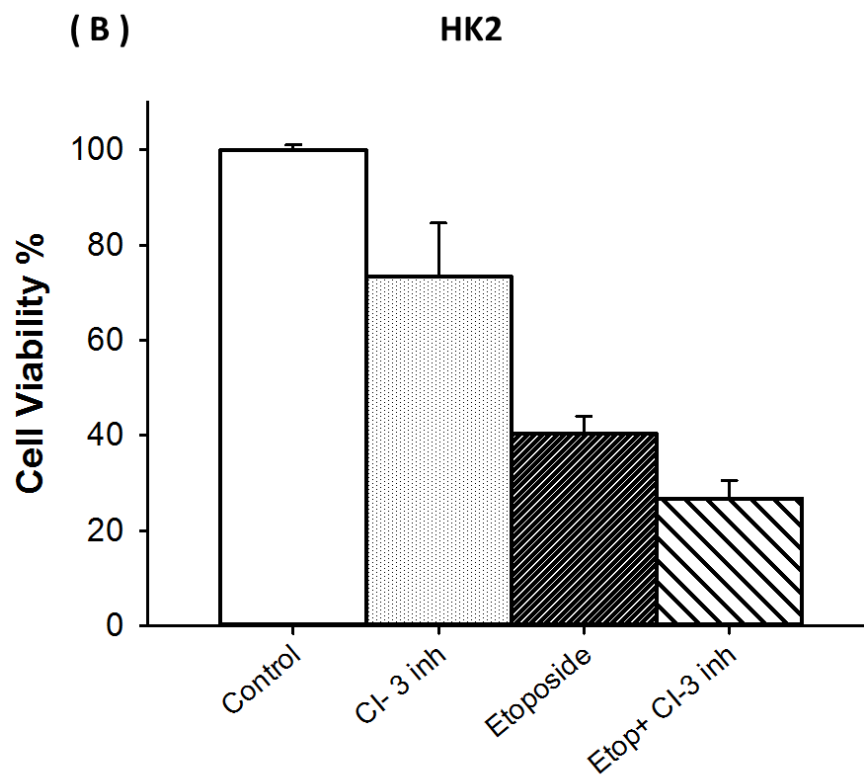
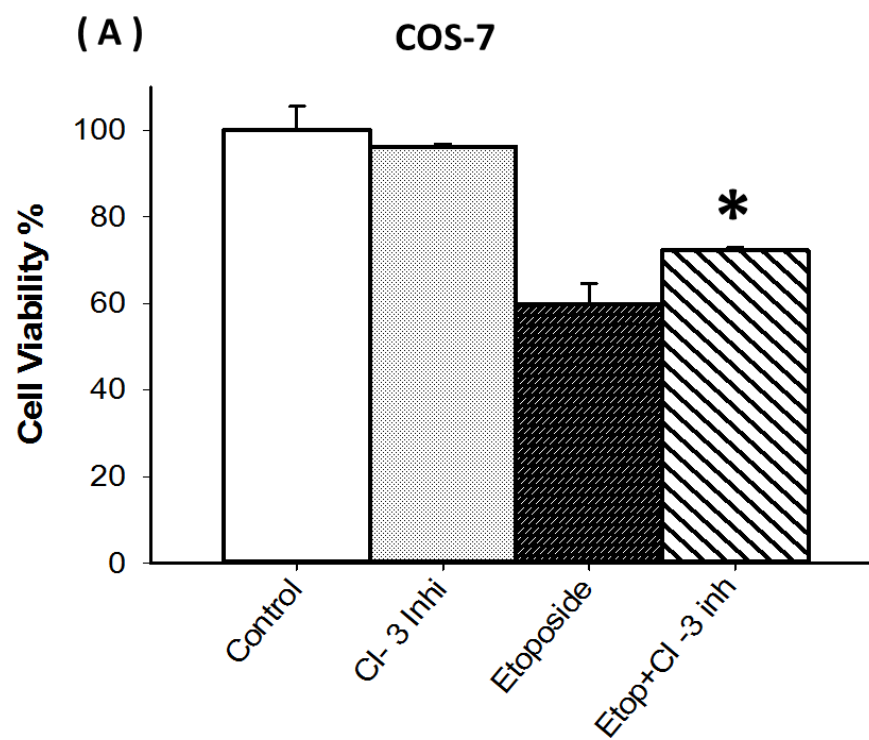
These experiments were carried out to determine whether cell death by these anti-cancer drugs, at least in part, involved the apoptosis pathway. Therefore, a caspase inhibitor was used to see if they affected cell viability in the presence of these drugs. The fluorogenic substrate (488 Nuc caspase-3) was also used to determine if caspase activity was directly affected, within intact cells.

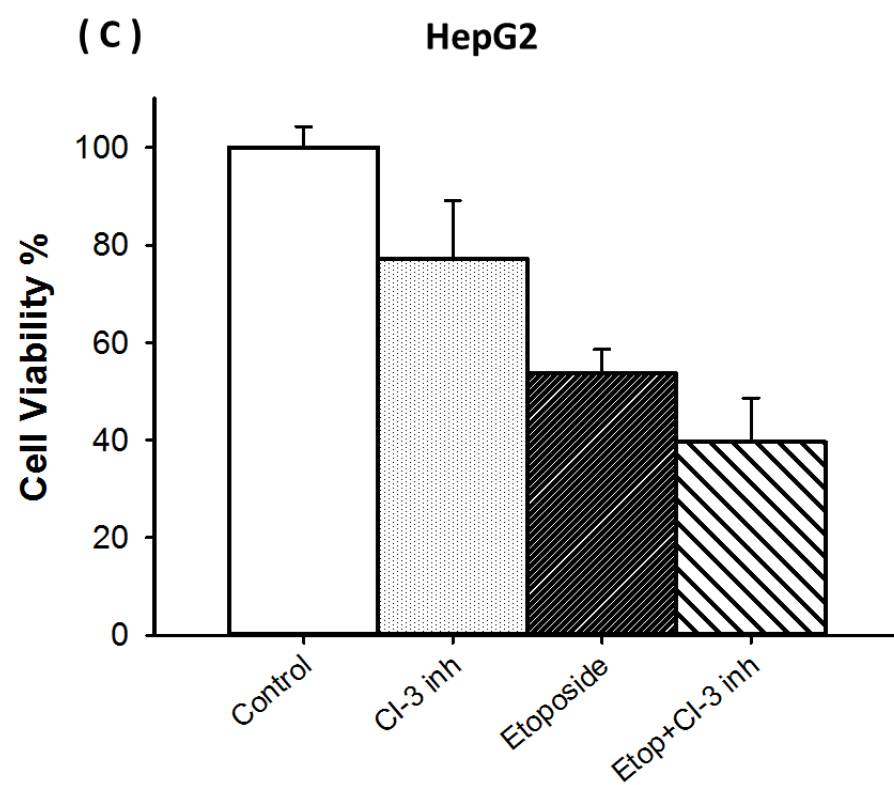
3.4.1 Detection of apoptosis by caspases caused by Etoposide, Cisplatin, and Doxorubicin using a caspase 3 inhibitor to detect the effects on cell viability

3.4.1.1 Effect of caspases inhibitor on Etoposide induced cell death

From the figure 3.4.1.1 A-D; it can be seen the caspase -3 is involved in kidney and liver cell death, where the cells were treated with 60 μ M of caspases inhibitor for 4 hrs before adding the etoposide (at LC₅₀ concentration for each of the cell lines). Cells were incubated with the drug at 37 °C for 48 hrs and MTT was performed.

In figure 3.4.1.1A and 3.4.1.1B, COS-7 and HK2 cells were treated with Etoposide (at the following concentration 150, 50 μ M, respectively). COS-7 cells showed a significant difference in the presence of caspase 3 inhibitor, where significantly less cells died compared to Etoposide alone. However, none of the other cell lines were protected from etoposide-induced cell death. These results would suggest that caspases dependent apoptosis only occurs in COS-7 cells and not the other cell tested.





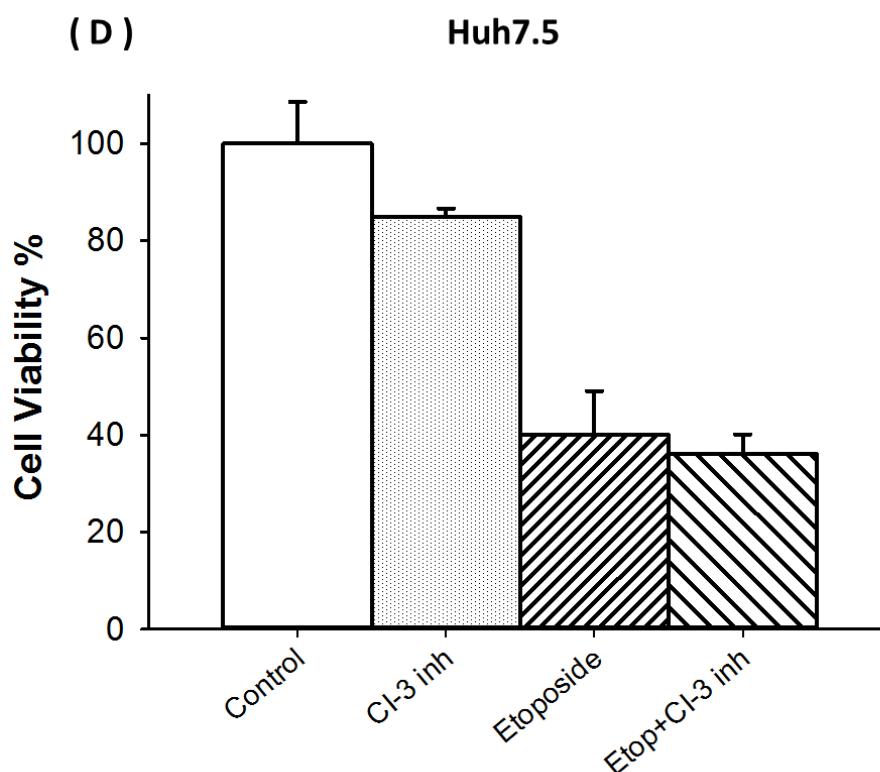


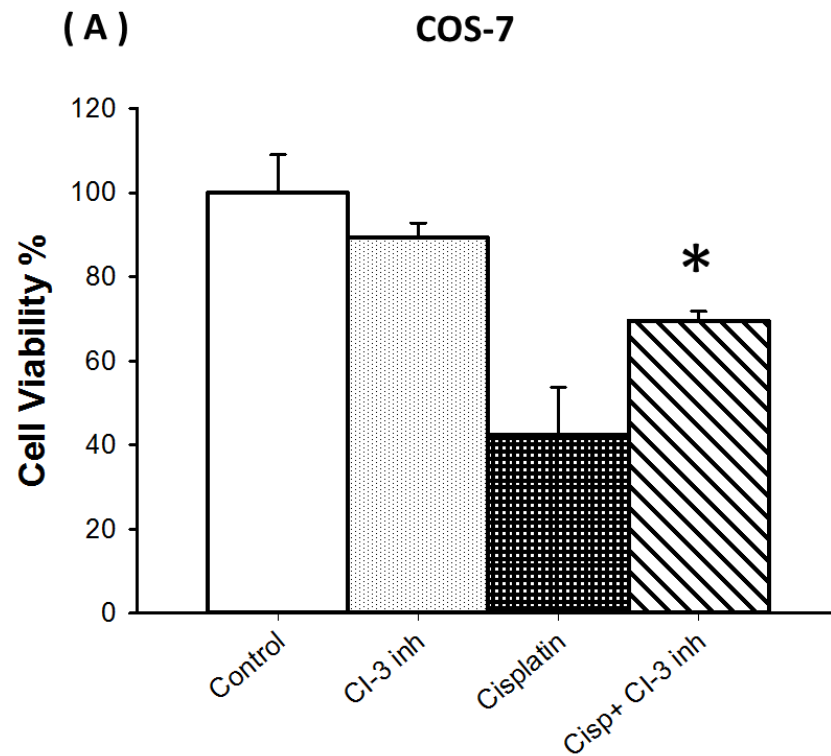
Figure 3.4.1.1A-D; the effects of caspase 3 inhibitor on Etoposide induced cell death. (A) shows COS-7 cells with caspase 3 inhibitor and Etoposide (150 μ M), (B) shows HK2 cells with caspase 3 inhibitor and Etoposide (50 μ M). (C) Shows HepG2 cells with caspase 3 inhibitor with Etoposide (120 μ M), (D) shows Huh7.5 cells with caspase 3 inhibitor and Etoposide (1000 μ M). Confluent (70-80%) cells were incubated for 48 hrs with the drug. Values are presented as mean \pm SD of 3-4 determinations. (* value points were significant different from the Etoposide, $p \leq 0.05$), using t-test.

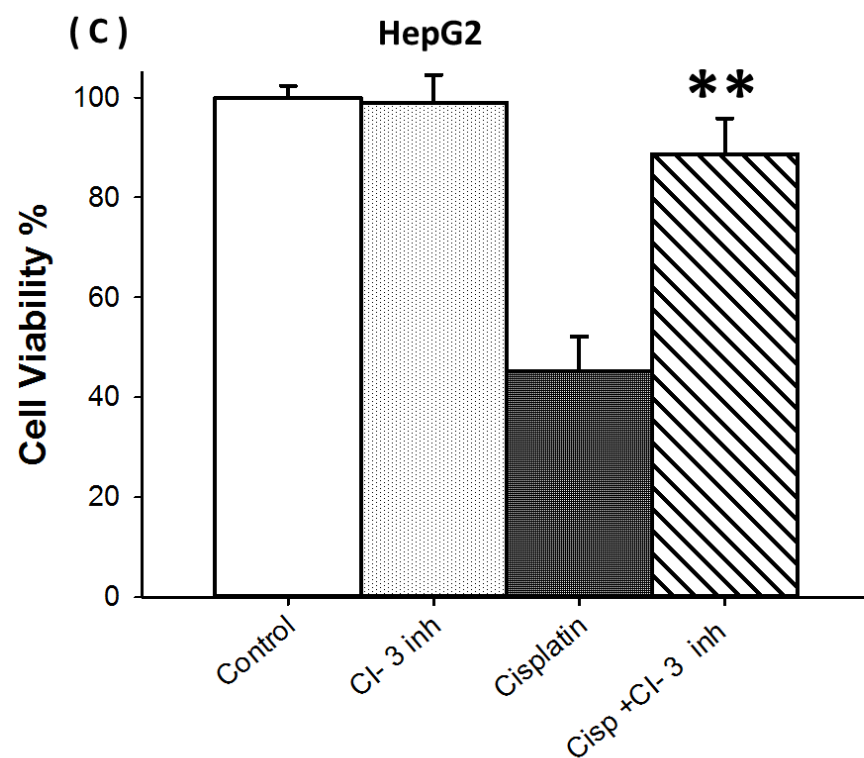
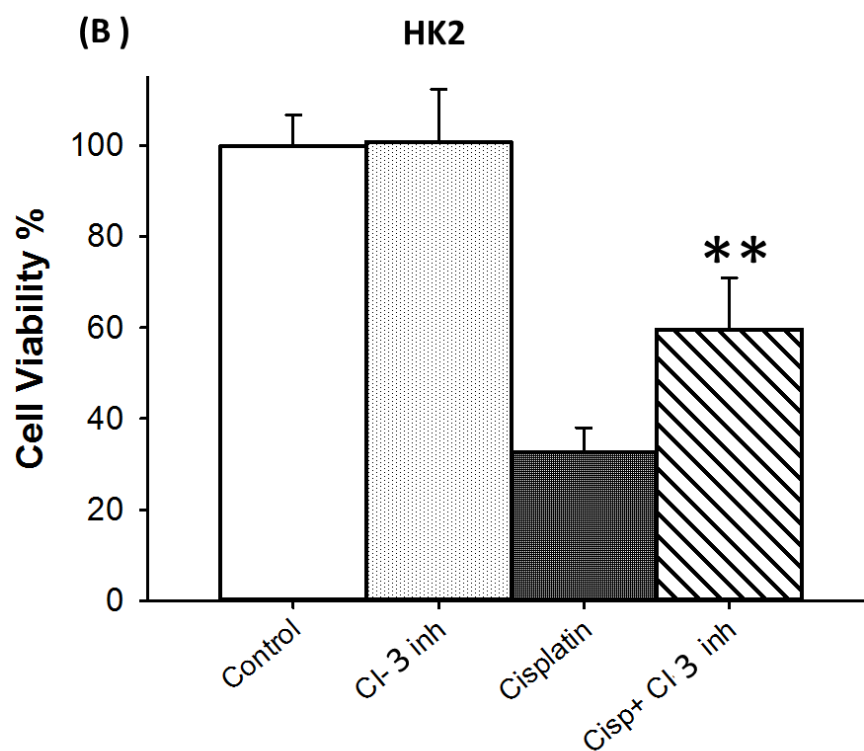
3.4.1.2 The effect of caspase inhibitor -3 on Cisplatin induced cell death

Figure 3.4.1.2A-D; shows the effect of caspase -3 on kidney and liver cells. Cells were pretreated with 60 μ M of caspase inhibitor for 4 hrs before adding Cisplatin (at the LC_{50} of each type of cell). Cells were incubated at 37 $^{\circ}$ C for 48 hrs and then MTT assays performed.

In figure 3.4.1.2A and 3.4.1.2B, COS-7 and HK2 cells were treated with Cisplatin at 46, 20 μ M, respectively. The cells showed significant protection from cell death induced by Cisplatin. COS-7 and HK2 cells showed increased cell viability of about 30%, while figure 3.4.1.2C and 3.4.1.2D shows HepG2 and Huh7.5 treated with Cisplatin (35,

90 μ M), respectively. The results showed a significant effect of caspases 3 inhibitor on cell viability for both liver and kidney cells. The cell viability of Huh7.5 and HepG2 cells increased to almost control levels using caspase 3 inhibitor .





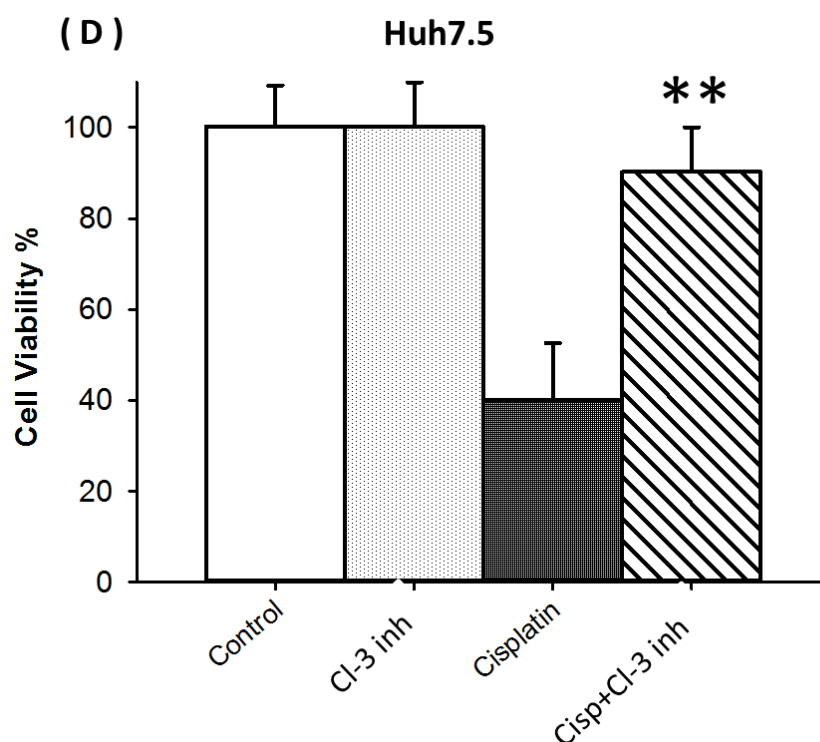


Figure 3.4.1.2A-D; the effects of Cisplatin-induced death by caspase 3 inhibitor.

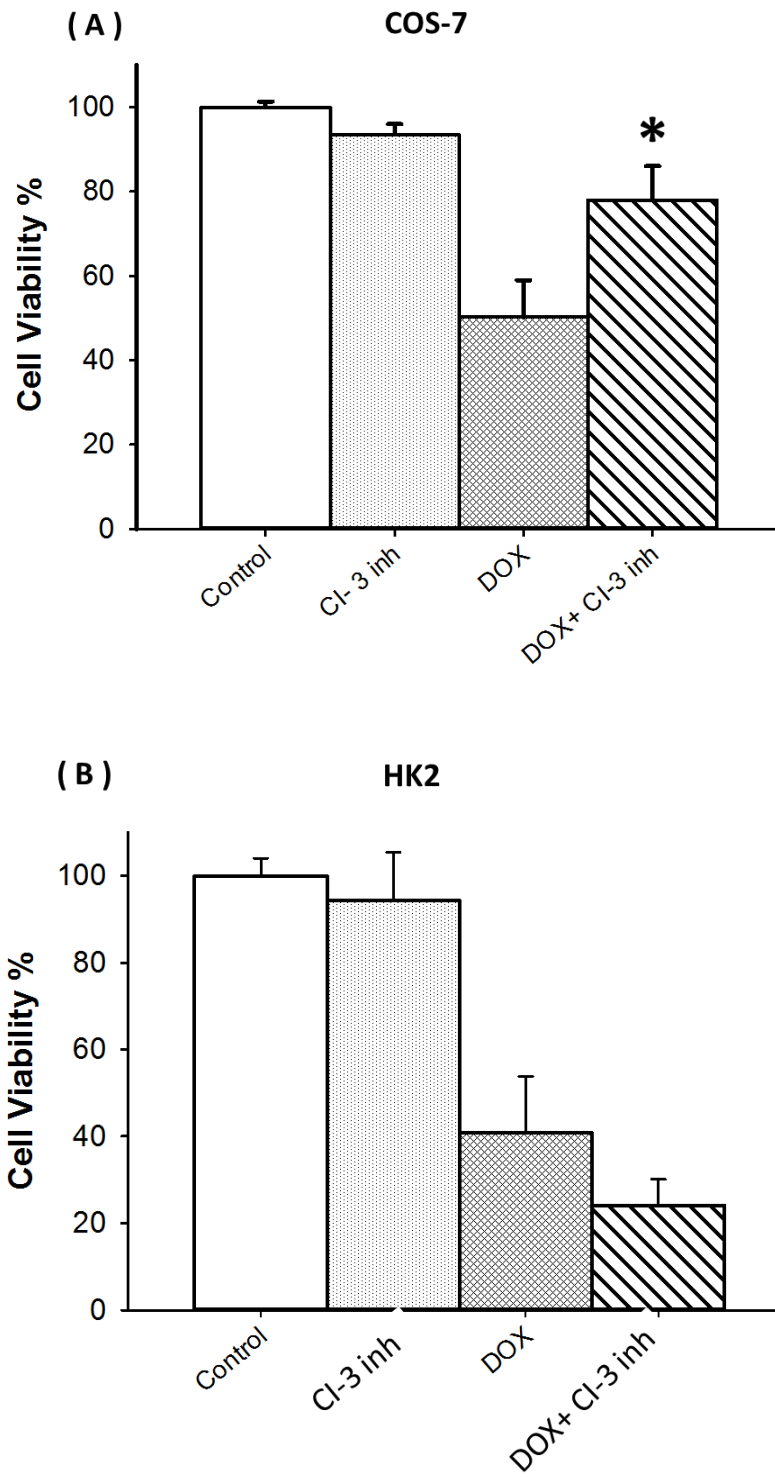
(A) Shows COS-7 cells pretreated with caspase 3 inhibitor and then Cisplatin (46 μ M), (B) shows HK2 and Cisplatin (20 μ M). (C) Shows HepG2 cells with Cisplatin (35 μ M), (D) shows Huh7.5 cells with Cisplatin (90 μ M). Cells incubated for 48 hrs with the drug. Values are presented as mean \pm SD of 3-4 determinations. *p* values were presented with caspase inhibitor followed by Cisplatin compared to Cisplatin treatment alone are indicated by (* $p \leq 0.05$, ** $p \leq 0.01$), using t-test.

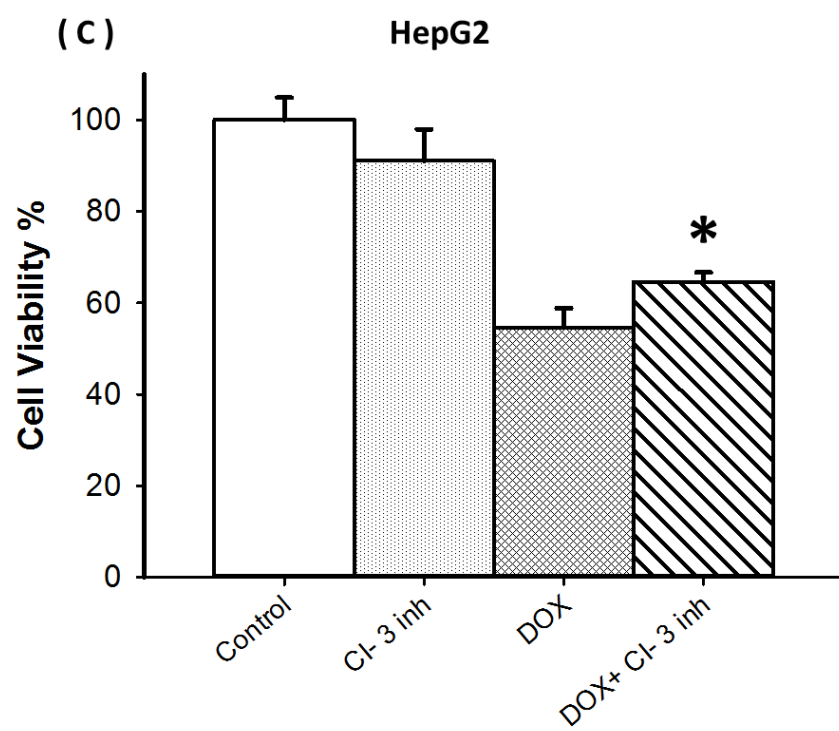
3.4.1.3 The effect of caspase inhibitor -3 on Doxorubicin induced cell death.

Figure 3.4.1.3A-D; shows the effects of caspases 3 inhibitor on kidney and liver cell viability. The cells were treated with 60 μ M of the caspases inhibitor for 4 hrs before adding DOX (at LC_{50} of each cell type). Cells were incubated at 37 °C with the drug for 48 hrs and then MTT assays were performed.

In figure 3.4.1.3A and 3.4.1.3B, COS-7 and HK2 cells were treated with DOX (7, 3 μ M respectively). The cell viability was significant increased using caspase 3 inhibitor with COS-7, but not in HK2 cells. Figure 3.4.1.3C and 3.4.1.3D, shows HepG2 and Huh7.5 were treated with DOX (4, 6 μ M respectively). Results showed a small but significant

effect of caspase inhibitor on cell viability for HepG2 cells, but on the Huh7.5 cell viability was not, however, affected.





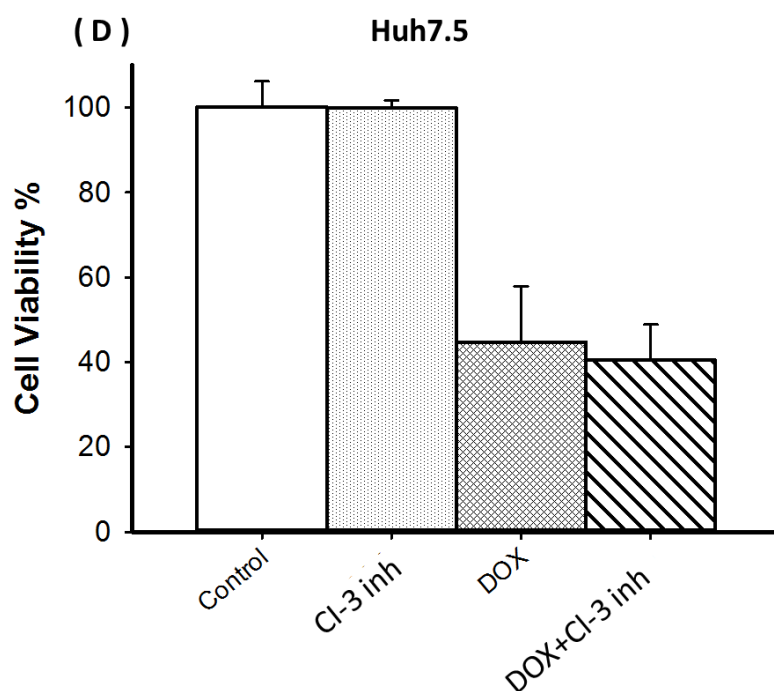


Figure 3.4.1.3A-D; the effect of caspase 3 inhibitors on DOX-induced cell death.

(A) shows COS-7 cells pretreated with caspase 3 inhibitors and then DOX (7 μ M), (B) showed HK2 cells pretreated with caspase 3 inhibitors and then DOX (3 μ M). (C) showed HepG2 cells pretreated with caspase 3 inhibitors and then with DOX (4 μ M), (D) shows Huh7.5 cells pretreated with caspase inhibitor and then with DOX (6 μ M). Cells were incubated for 48 hrs after exposure to the drug. Values are presented as mean \pm SD of 3-4 determinations (* $p \leq 0.05$).

3.4.2 Detection of apoptosis by caspase activation induced by MTX, Etoposide, Cisplatin, and Doxorubicin using a fluorogenic substrate (488 Nuc caspase-3)

In order to confirm apoptotic cell death induced by these drugs on liver and kidney cell lines, a second technique was used, which is fluorogenic substrate (488 Nuc caspase-3 kit). This generates green fluorescent product inside cells if caspase 3 become activated within the cells (see figure 3.4.2). This method has greater sensitivity than the use of caspase inhibitors, because it is fluorescence based.

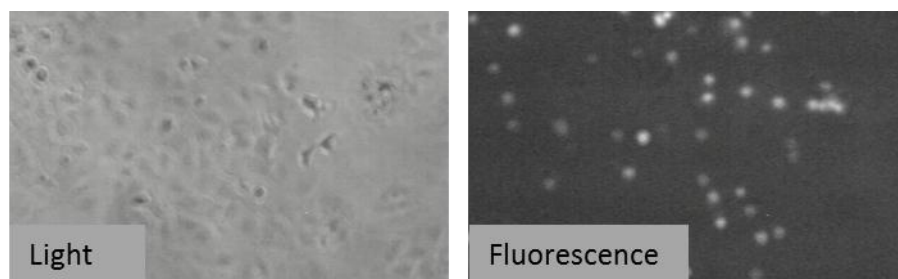


Figure 3.4.2; Illustrates light and fluorescence field of COS-7 cells pre-treated with fluorogenic substrate (488 Nuc caspase-3) and then treated with doxorubicin.

3.4.2.1 Detection of apoptosis by caspase activation induced by MTX, using a fluorogenic substrate (488 Nuc caspase-3) on kidney and liver cell lines

As MTX was shown previously to have a little or no effect on cell death but mainly affected cell proliferation, in order to confirm this, *in vivo* caspase-3 substrate was used. Figure 3.4.2.1(A) COS-7 cells and figure 3.4.2.1(B) Huh7.5 cells, were treated with MTX 100 μ M for 24 hrs, then cells were treated with 2 μ M of caspase substrate-3 and incubated for a further 30-40 min. Fluorescence microscopy images were taken of the cells under white light and fluorescence conditions for the same field. Fluorescent and total numbers of cells were counted and the apoptotic cell death percentage was calculated for each group. As MTX was dissolved in DMSO, two controls were used (i.e. controls with and without DMSO). Figure 3.4.2.1(A) shows only about 10% of cells are fluorescence and therefore undergo apoptosis upon MTX treatment, while about 12% of Huh7.5 cells undergo apoptotic cell death.

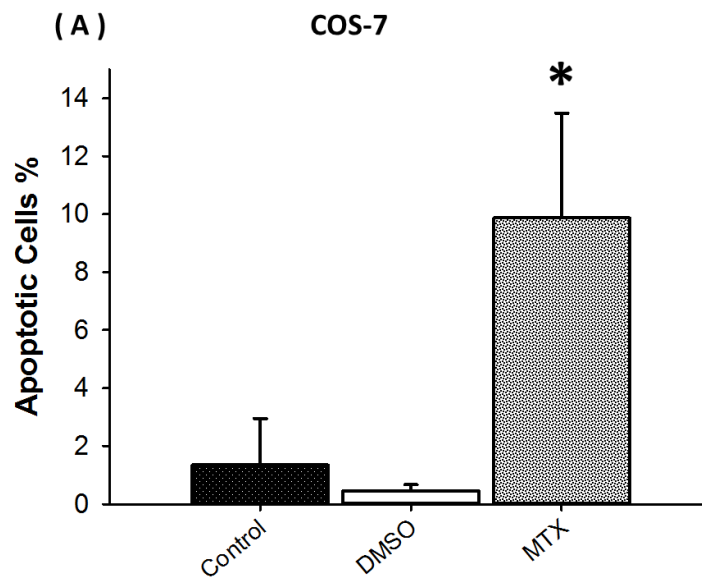


Figure 3.4.2.1A; shows the effect of MTX on apoptotic cells. COS-7 cells were exposed to the drug for 24 hrs. The caspase-3 substrate was monitored after 30 min of incubation at 37 °C. Data represents the mean \pm S.D of 3-4 determinations (* value points were significantly different from the DMSO control, $p \leq 0.05$, ** $p \leq 0.01$), using the t-test.

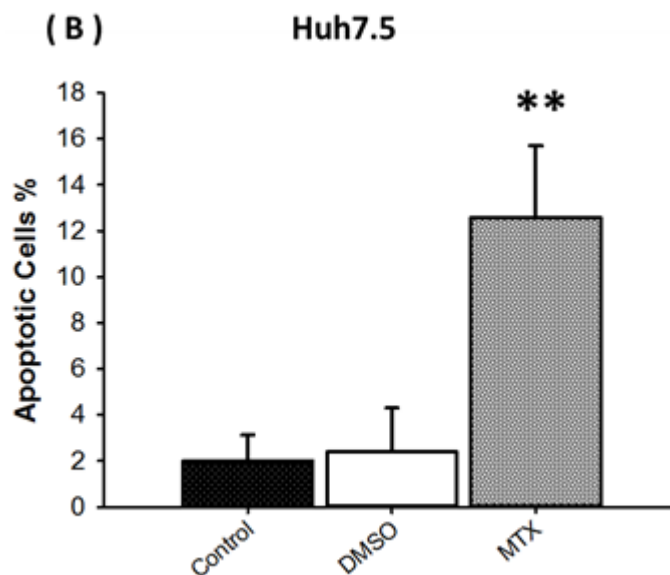
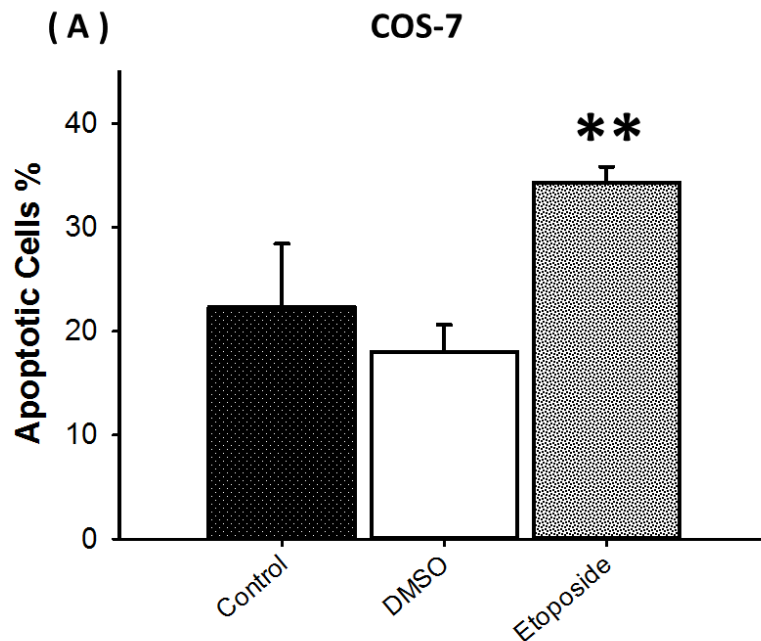


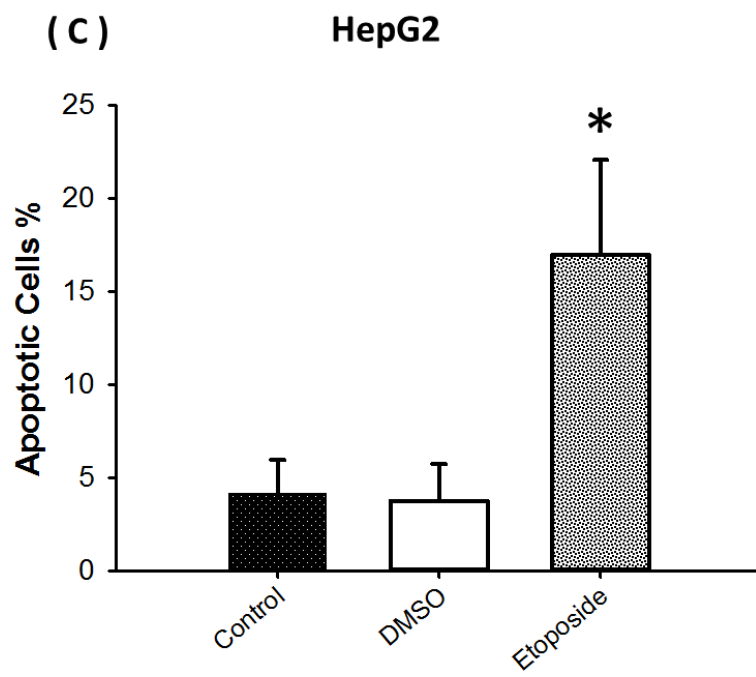
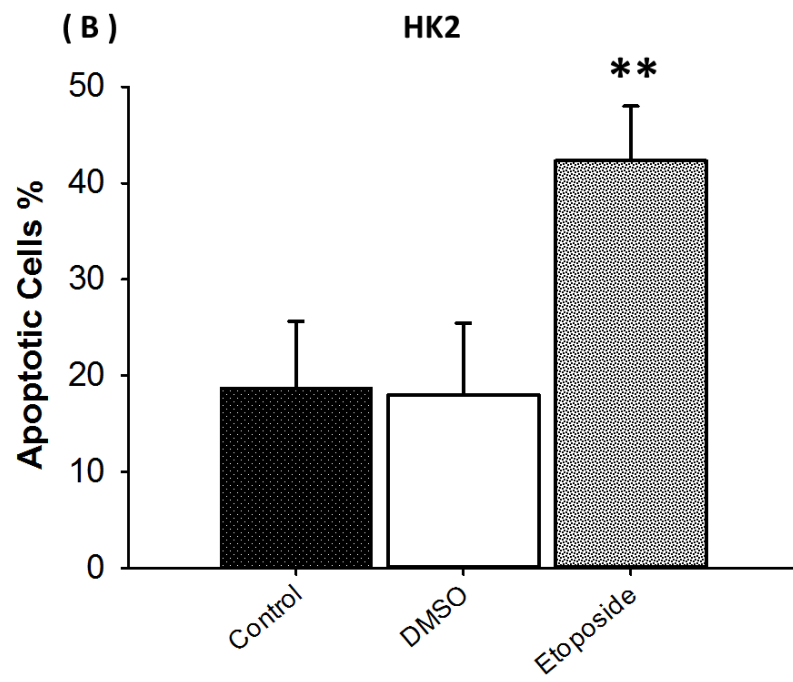
Figure 3.4.2.1B; shows the effect of MTX on apoptotic cells. Huh7.5 cells were exposed to the drug for 24 hrs. The caspase-3 substrate was monitored after 30 min of

incubation at 37 °C. Values are presented as mean \pm SD of 3-4 determinations (* value points were significant different from the DMSO, $p \leq 0.05$, ** $p \leq 0.01$), using the t-test.

3.4.2.2 Detection of apoptosis by caspase activation induced by Etoposide, using the fluorogenic substrate (488 Nuc caspase-3) on kidney and liver cell lines

In order to confirm that cell death was induced by apoptosis, the fluorogenic caspase-3 substrate was used. Figure 3.4.2.2 shows the effect on COS-7 (A), HK2 (B), HepG2 (C), and Huh7.5 (D), when treated with Etoposide (150,50,120,1000 μ M), respectively, for 24 hrs, then cells were treated with 2 μ M of caspase substrate-3 and incubated for about 30-40 min. Fluorescence microscopy was used and the cells imaged under light and fluorescence conditions for the same field of view. Fluorescence and total number of cells were counted and the apoptotic cell death percentage was calculated for each group. As etoposide was dissolved in DMSO, two control groups have taken, controls with and without DMSO. A significant difference of the % of apoptotic cells between control and treated cells, in all the four cell lines was observed. Both kidney cell lines showed increases in apoptotic cell numbers cell with HK2 and Huh7.5 showing that 40-60% of the cells were apoptotic.





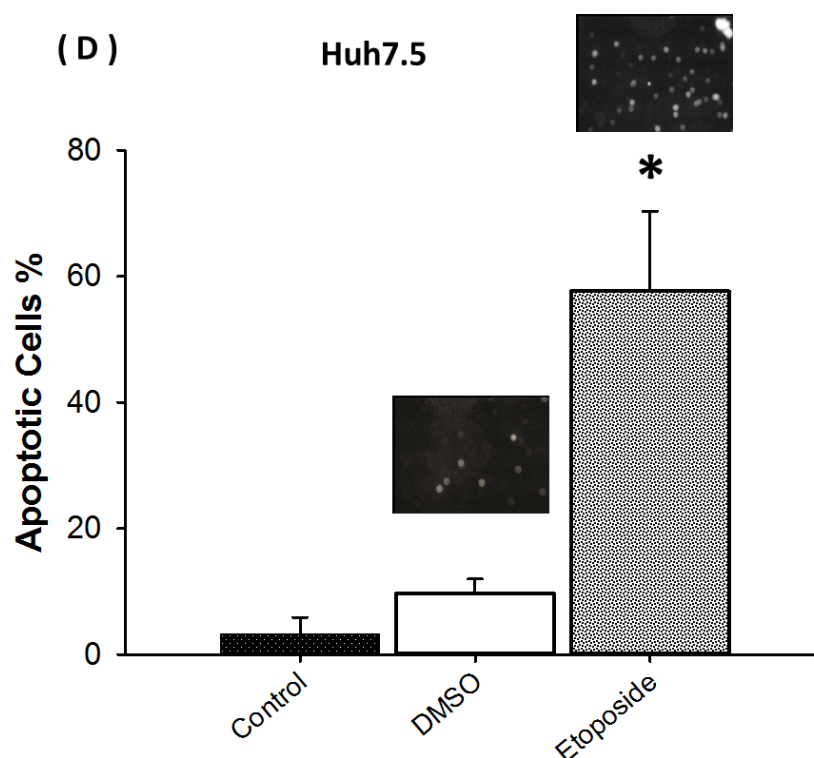


Figure 3.4.2.2A-D; shows the effect of Etoposide on apoptotic kidney and liver cell lines. COS-7 (A), HK2 (B) HepG2 (C), and Huh7.5 (D), cells were exposed to Etoposide drug for 24 hrs. The caspase-3 substrate added and the cells monitored after 30 min of incubation at 37 °C. Data represents the mean \pm SD of 3-4 determinations. (* value points were significant different from the DMSO control, $p \leq 0.05$, ** $p \leq 0.01$), using the t-test.

3.4.2.3 Detection of apoptosis by caspase activation induced by Cisplatin, using the fluorogenic substrate (488 Nuc caspase-3) on kidney and liver cell lines

In order to determine whether apoptosis was induced by Cisplatin, the fluorogenic caspase-3 substrate was used. Figure 3.4.2.3 shows COS-7 (A), HK2 (B), HepG2 (C), and Huh7.5 (D), were treated with Cisplatin (at the LC_{50} concentration 35, 20, 35, 90 μ M, respectively), for 24 hrs, followed by incubation with 2 μ M of caspase substrate- for about 30-40 min. Images were then taken of the cells under white light and fluorescence conditions for the same field, and the number of fluorescence cells and total number of cells were counted such that the apoptotic cells percentage could be calculated for each group. All cells showed significant increases in apoptotic cell

numbers compared to control. COS-7 and HK2 were more sensitive to Cisplatin than HepG2 and Huh7.5.

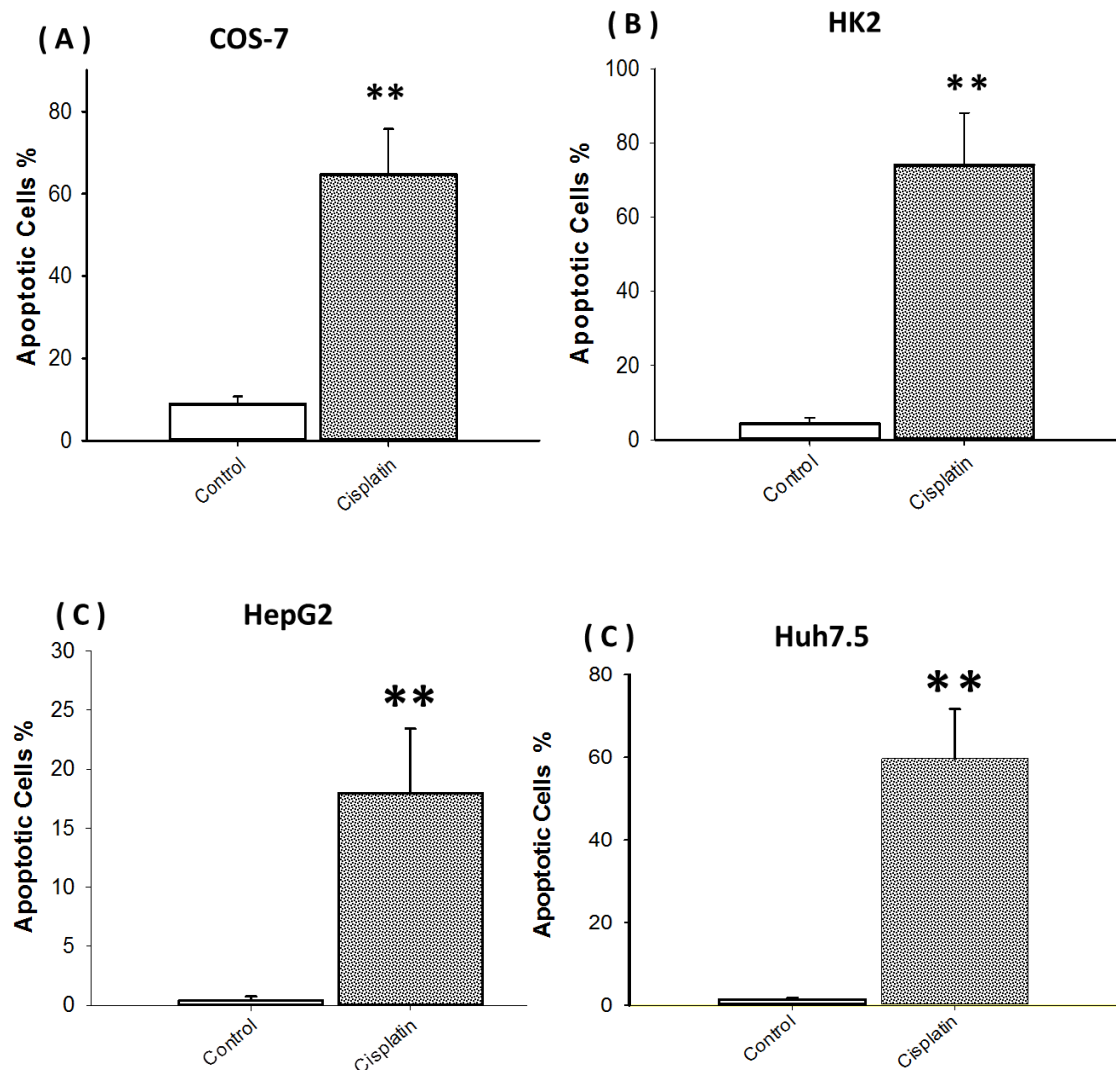
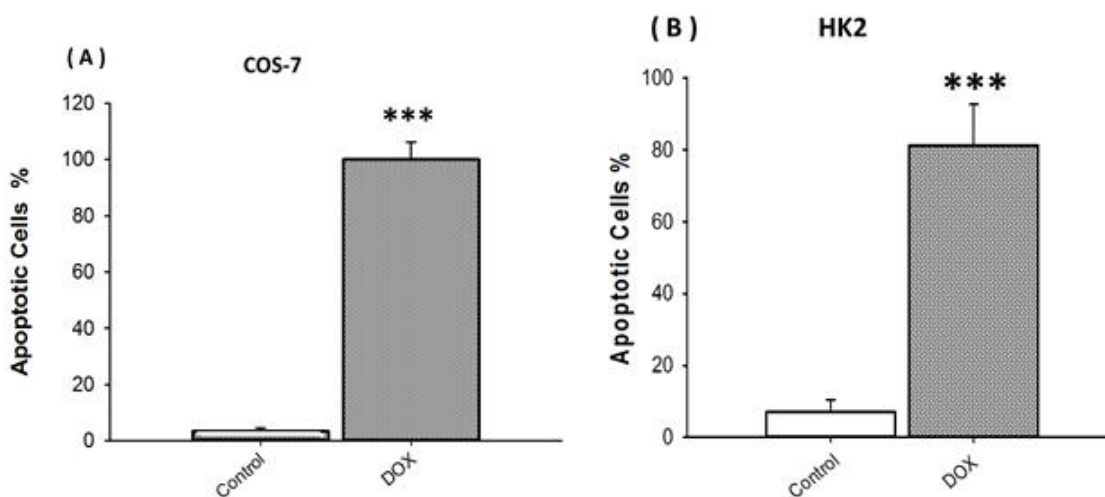


Figure 3.4.2.3 A-D; shows the effect of Cisplatin on apoptosis cell in different kidney and liver cell lines COS-7 (A), HK2 (B), HepG2 (C), and Huh7.5 (D). Cells were exposed to the drug for 24 hrs and the caspase-3 substrate for 30 min at 37 °C. Data represents the mean \pm S.D of 3-4 determinations. Value that were significant with Cisplatin (** $p \leq 0.01$), using the t-test.

3.4.2.4 Detection of apoptosis by caspase activation induced by Doxorubicin, using a fluorogenic substrate (488 Nuc caspase-3) on kidney and liver cell lines

Apoptotic cells induced by DOX was monitored using the caspase substrate 488 Nuc caspase-3. Figure 3.4.2.4 shows COS-7 (A), HK2 (B), HepG2 (C), and Huh7.5 (D), treated with doxorubicin at the LC_{50} concentration i.e. (7, 3, 4, 6 μ M, respectively), for 24 hrs, followed by treatment with 2 μ M of fluorogenic caspase substrate-3 then, images were taken of the cells under white light and fluorescence condition, for the same field. All cells exposed to DOX showed between 70-90% were apoptotic.



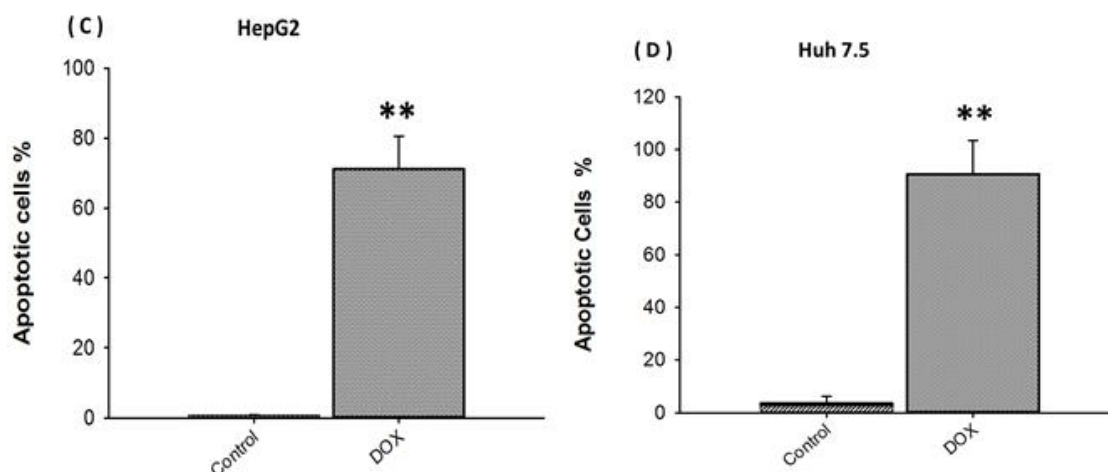


Figure 3.4.2.4A-D; shows the effect of Doxorubicin on inducing apoptotic cells in different kidney and liver cell lines. COS-7 (A), HK2 (B), HepG2 (C), and Huh7.5 (D) cell lines were exposed to the drug for 24 hrs. The fluorogenic caspase-3 substrate was incubated for 30 min at 37 °C. The data represents the % of apoptotic cells mean \pm S.D of 3-4 determinations. Value points were significant different from the DOX ($p \leq 0.05$, ** $p \leq 0.01$, *** $p \leq 0.001$), using the t-test.

3.5 Determination of Necrosis involved in the cell death process induced by the chemotherapy drugs

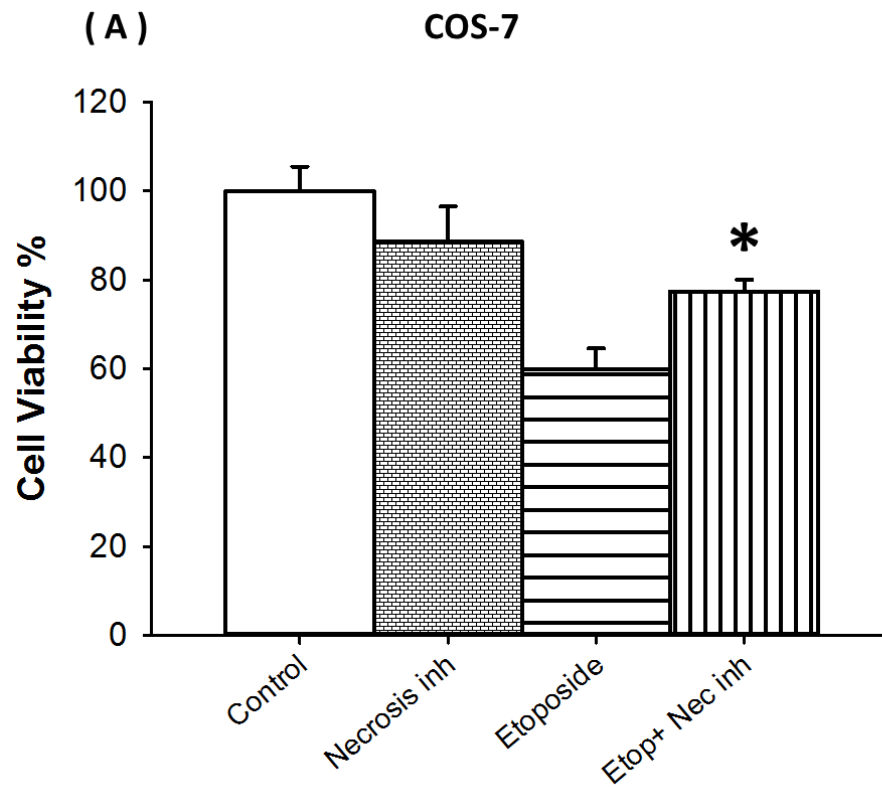
In order to determine whether cell death by these chemotherapy agents was, at least in part, due to regulated necrosis, necrostatin (an inhibitor of regulated necrosis), or normal necrosis leakage of cytosolic lactate dehydrogenases enzyme in to the media, was undertaken.

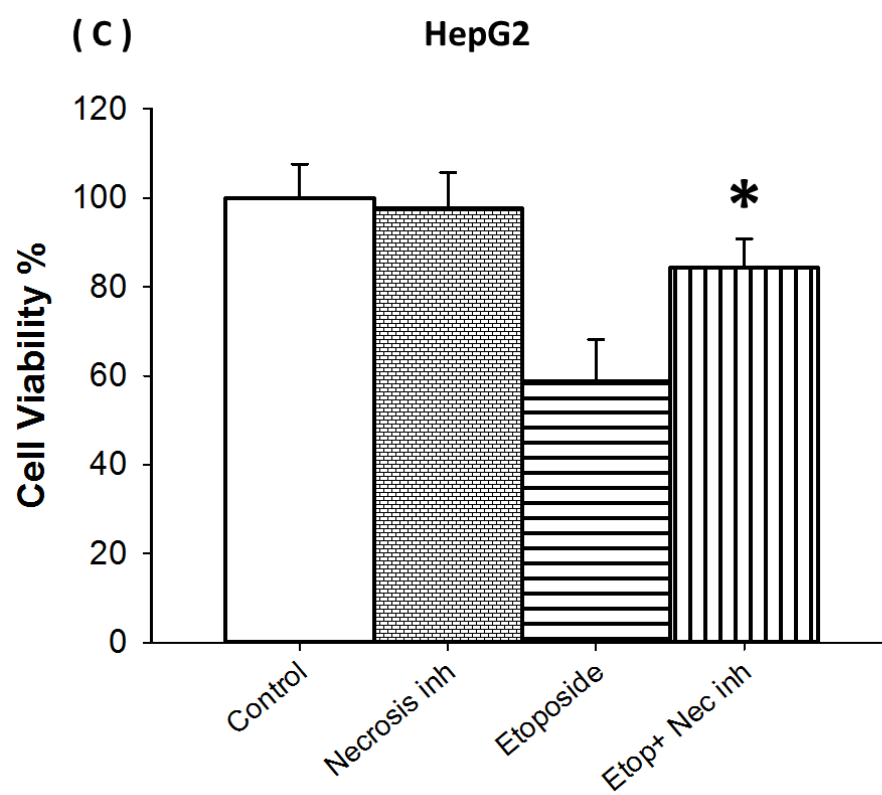
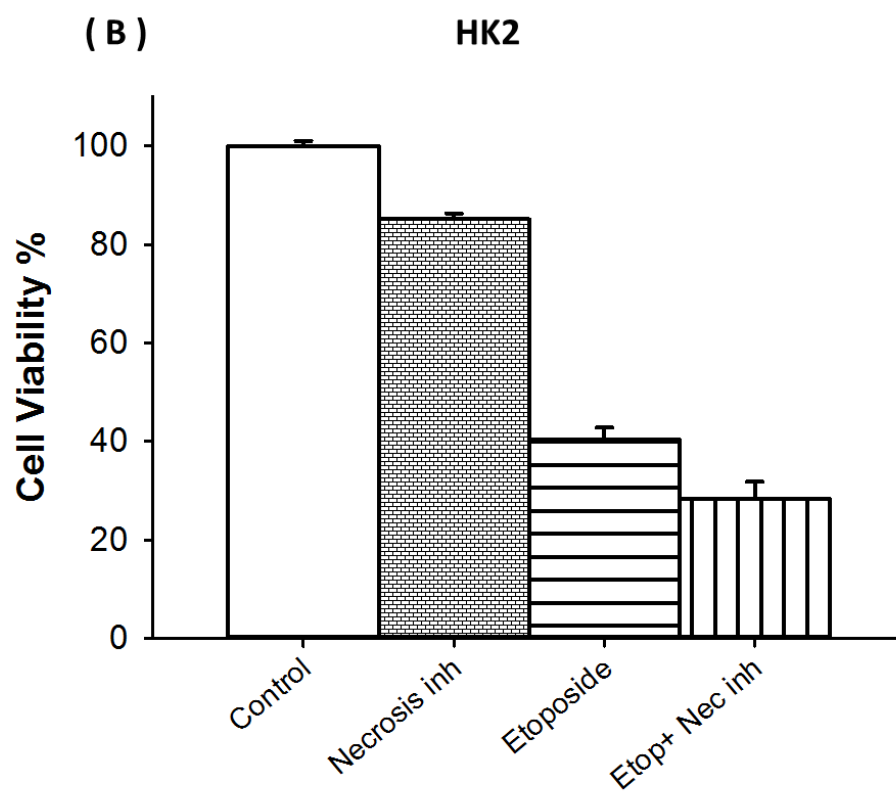
3.5.1 Determination of necrosis using necrosis inhibitor (necrostatin by Etoposide, Cisplatin and doxorubicin) in kidney and liver cell lines

3.5.1.1 Detection of regulated necrosis using necrostatin by Etoposide in kidney and liver cells

Necrosis inhibitor necrostatin (10 μ M) was pre-incubated with the cells, for 4 hrs, and then cells were exposed to Etoposide (i.e. for COS-7, 120 μ M; HK2, 50 μ M; HepG2, 120 μ M; and Huh7.5, 1000 μ M). Cells were incubated at 37 °C for 48 hrs then the

MTT assays were performed. Figure 3.5.1.1A, 3.5.1.1B, 3.5.1.1C, and 3.5.1.1C represents COS-7, HK2, HepG2, and Huh7.5 cells, respectively. The results show that the necrosis inhibitor does affect the viability of both COS-7 and HepG2 cells to a significant extent, but had either no effect with HK2 and Huh7 cells.





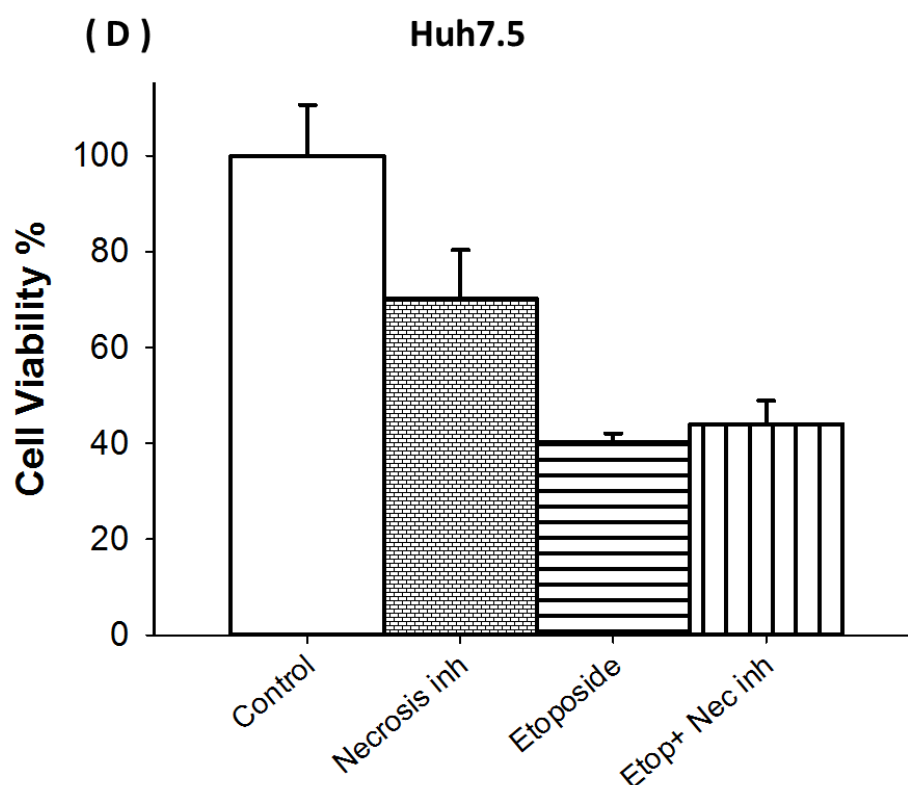
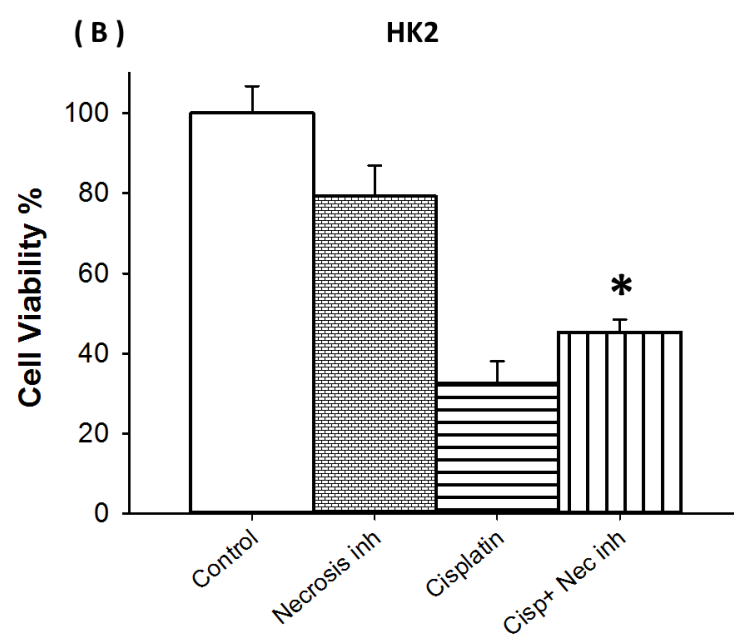
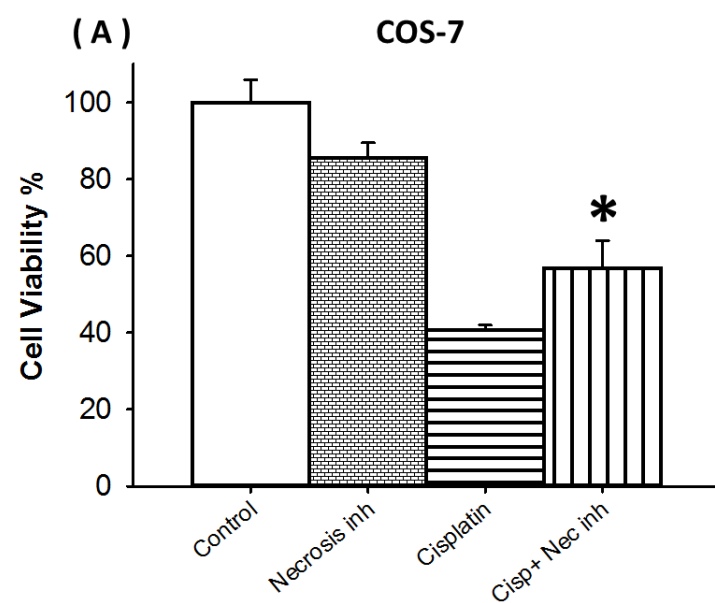


Figure 3.5.1.1 A-D; shows the effects of Etoposide with and without necrostatin in liver and kidney cells. COS-7(A), HK2 (B), HepG2 (C) and Huh7.5 (D) cells were pretreated with necrostatin (10 μ M) and then exposed to the Etoposide for 48 hrs at 37 °C. Data represents the mean \pm SD of 3-4 determinations. Values were significantly different from the Etoposide ($p \leq 0.05$, ** $p \leq 0.01$), using the t-test.

3.5.1.2 Determination of regulated necrosis induced by Cisplatin in kidney and liver cell lines

Necrosis inhibitor (necrostatin) (10 μ M) was pre-incubated with the cells used for 4 hrs, and then the cells were exposed to Cisplatin (COS-7, 46 μ M; HK2, 20 μ M; HepG2, 35 μ M; Huh7.5, 90 μ M, respectively) at 37 °C for 48 hrs and then MTT assays were undertaken. Figure 3.5.1.2A, 3.5.1.2B, 3.5.1.2C, and 3.5.1.2D represents COS-7, Hk2, HepG2, and Huh7.5 cells, respectively. The results showed that the necrosis inhibitor does affect cell viability significantly, compared to cisplatin treatment alone in all cells tested.



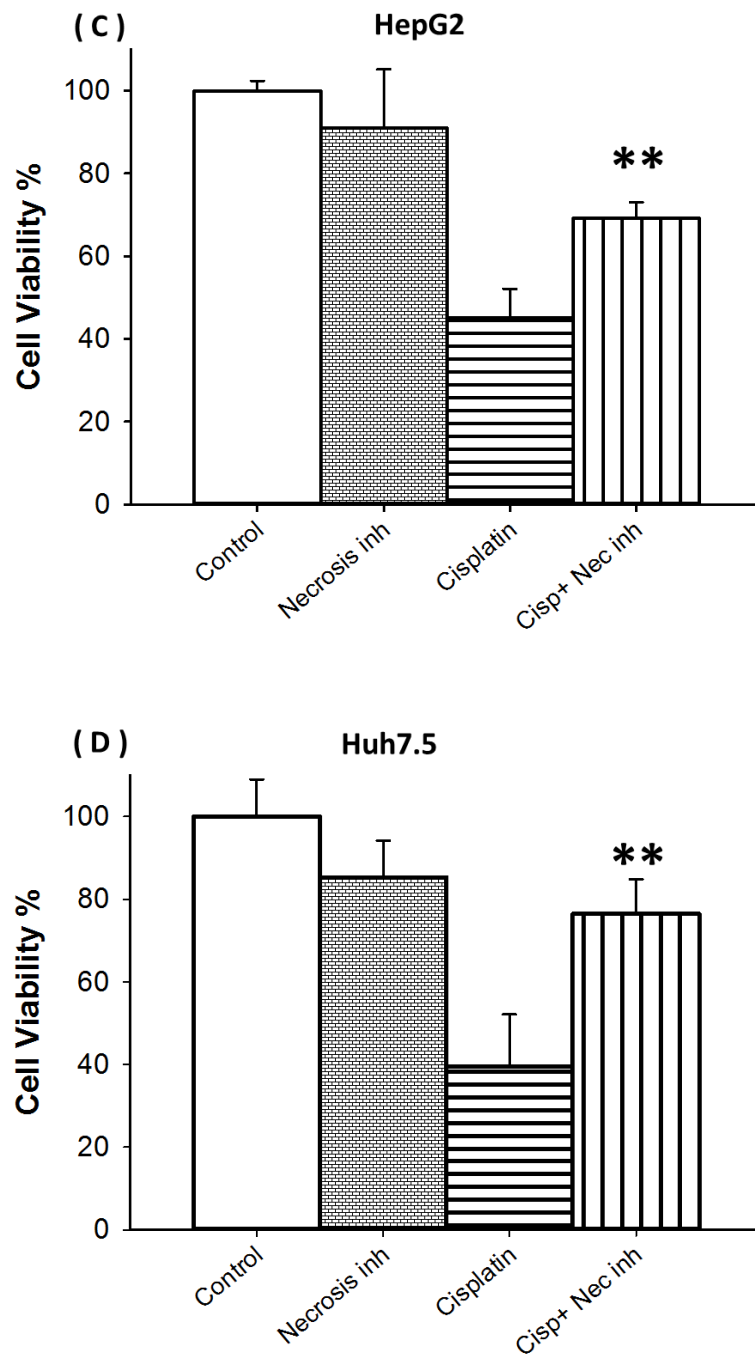
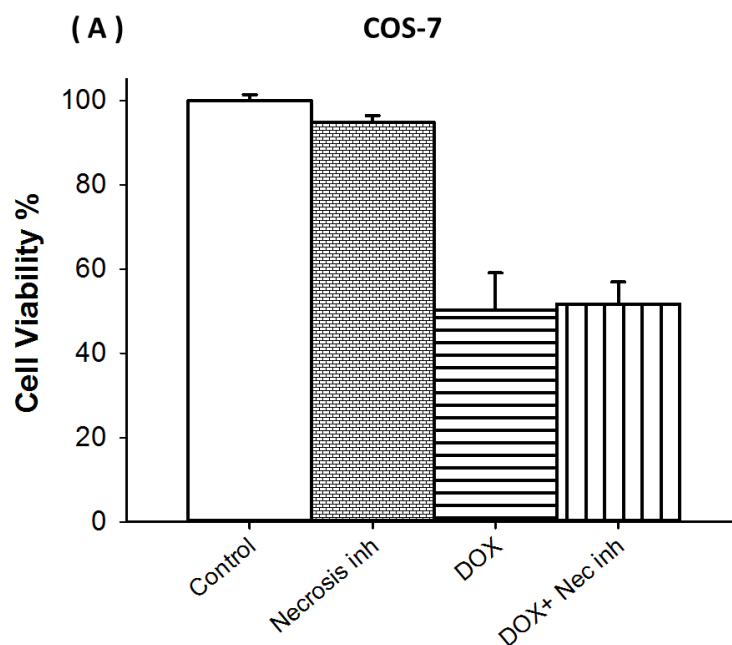
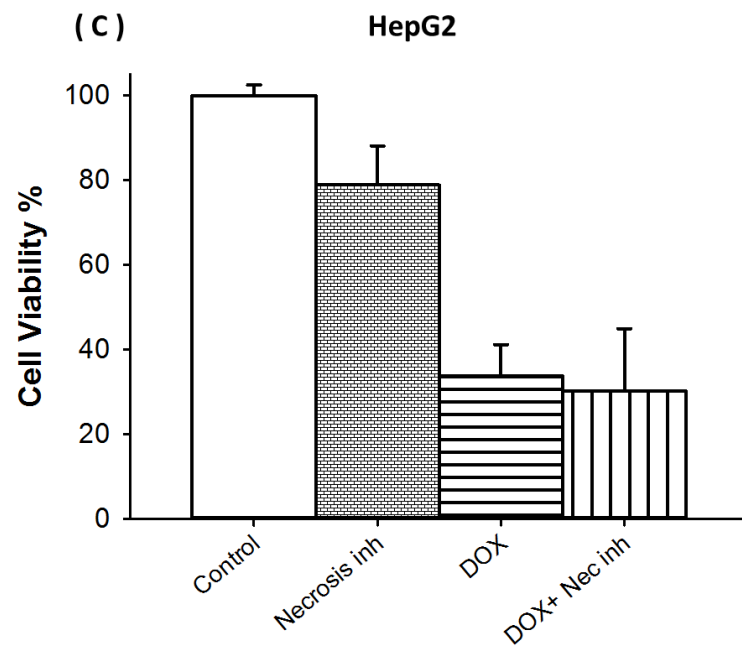
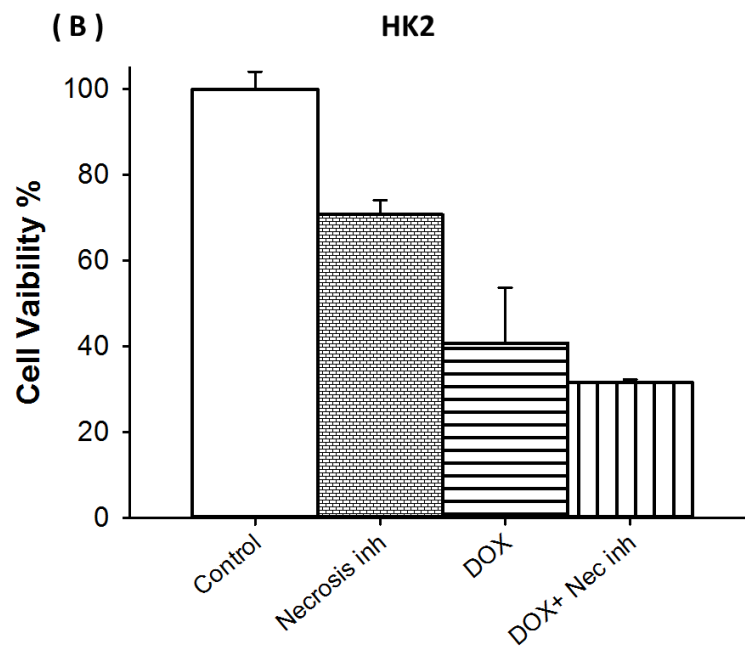


Figure 3.5.1.2A-D; shows the effects of Cisplatin with and without necrostatin on liver and kidney cell lines. COS-7(A), HK2 (B), HepG2 (C) and Huh7.5 (D), cells were pretreated with necrostatin and then exposed to Cisplatin for 48 hrs at 37 °C. The data represents the mean \pm SD of 3-4 determinations. (* where value points were significantly different from the controls, $p \leq 0.05$, $**p \leq 0.01$), using t-test.

3.5.1.3 Using necrostatin to determine whether regulated necrosis is involved in cell death induced by Doxorubicin in kidney and liver lines

The necrostatin (10 μ M) was incubated with the cells for 4 hrs, and then the cells; COS-7, HK2, HepG2 and Huh7.5 were exposed to DOX (7, 3, 4, and 6 μ M, respectively), at 37 °C for 48 hrs. MTT assays were then performed. Figure 3.5.1.3A, 3.5.1.3B, 3.5.1.3C, and 3.5.1.3D represents COS-7, HK2, HepG2, and Huh7.5 cells, respectively. Necrostatin did not affect the cell viability compared to drug alone for all the cells tested.





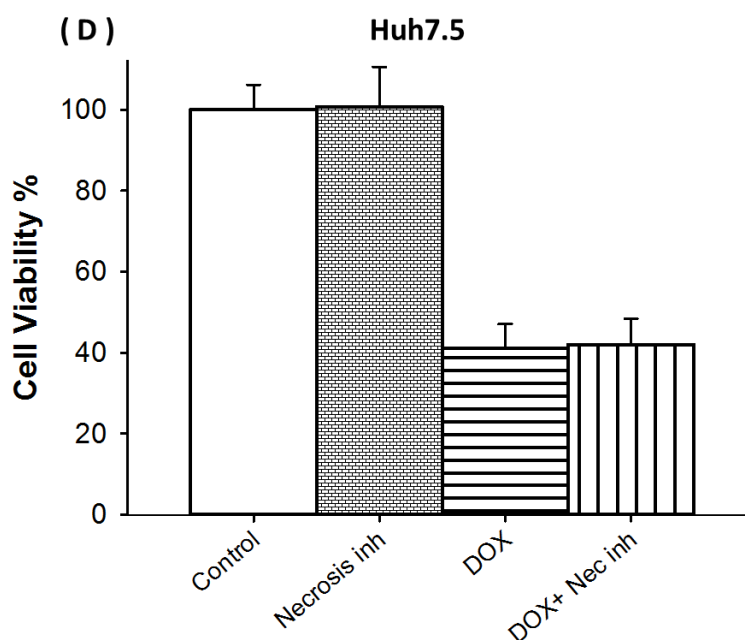


Figure 3.5.1.3A-D; the effects of DOX with and without necrostatin pre-treatment in liver and kidney cell lines. COS-7(A), HK2 (B), HepG2 (C) and Huh7.5 (D) cells were pretreated with necrostatin and then exposed to the DOX for 48 hrs and incubated at 37 °C. Data represents the mean \pm SD of 3-4 determinations.

3.5.2 Lactate dehydrogenases release assay to determine necrosis through plasma membrane leakage when kidney and liver cell lines are exposed to chemotherapy agents

The current experiments were designed to determine whether cell deaths caused by these chemotherapy drugs are related to release of lactate dehydrogenases (LDH) enzymes from the cytoplasm in to the surrounding media, as a part of necrostatic cell death, due to increase of plasma membrane permeability.

3.5.2.1 Detection of necrosis induced by Etoposide in kidney and liver cell lines using the lactate dehydrogenases release assay

As the necrosis inhibitor studies specifically investigate regulated necrosis as a means of cell death, it was important to determine whether classical necrosis was also involved by measuring LDH release. Cells were treated with Etoposide (150 and 120 μ M) for both (COS-7 and HepG2, respectively) and after 24 hrs, the LDH assay was performed. The data in figure 3.5.2.1A and B shows COS-7 and HepG2

cells treated with the drug and incubated at 37 °C for 24 hrs. Figure 3.5.2.1A show a small significant effect on increasing LDH releases. However, HepG2 cells show no significant effect compared to control.

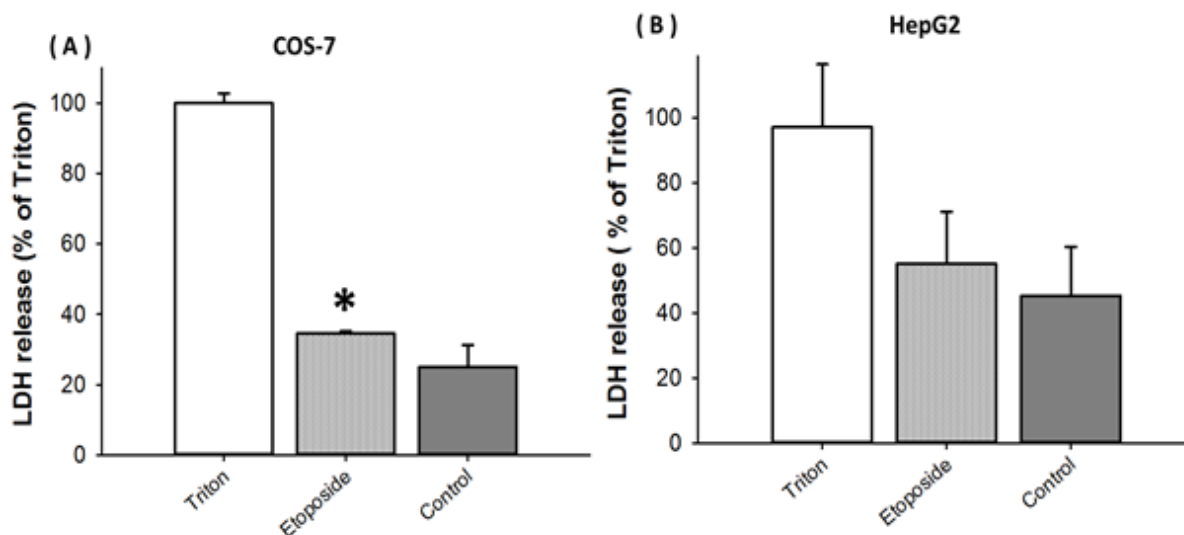


Figure 3.5.2.1A and B; the effect of Etoposide on lactate dehydrogenases (LDH) release in COS-7 cells (A) and HepG2 cells (B). Cell were treated and incubated for 24 hrs and then LDH release assayed. Data represents the mean \pm SD of 3-4 determinations. (* values were significantly different from the controls, $p \leq 0.05$), using the t-test.

3.5.2.2 Determination of necrosis induced by Cisplatin in kidney and liver cells using the lactate dehydrogenases assay

Cells were treated with cisplatin (46 μ M, COS-7; 35 μ M, HepG2) and after 24 hrs, the LDH assays were performed. The data in figure 3.5.2.2A and B show COS-7 and HepG2 cells treated with drugs and incubate at 37 °C. Figure 3.5.2.2A and B shows a significant effect on LDH releases similar to that of the positive control (Triton). However, other cell lines showed a high control background (data not shown).

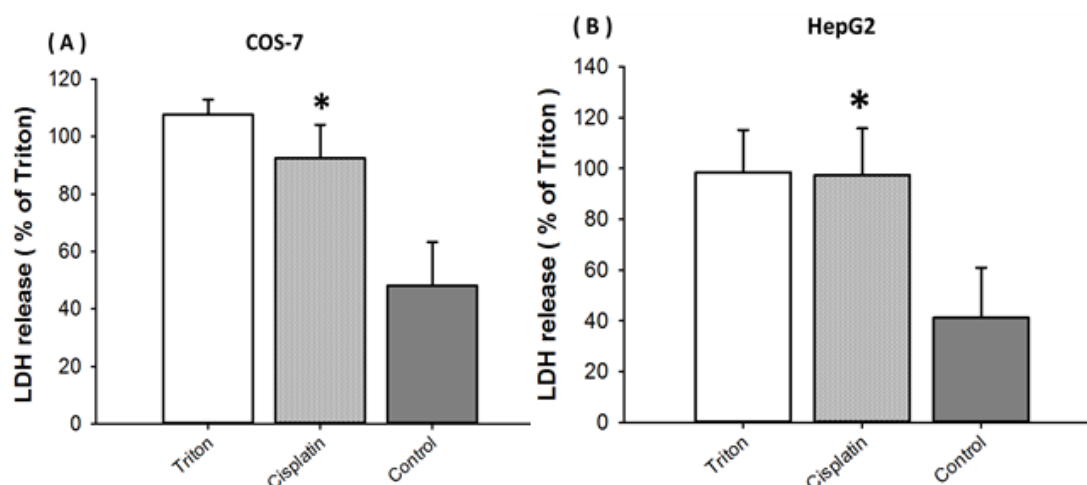


Figure 3.5.2.2A; the effect of Cisplatin on lactate dehydrogenases (LDH) release in kidney cells COS-7 (A) and liver cells HepG2 (B). Cells were treated with Cisplatin and incubated for 24 hrs and then the LDH release assays performed. Data represents the mean \pm SD of 3-4 determinations. (* values were significantly different from the controls, $p \leq 0.05$), using the t-test.

3.5.2.3 Detection of necrosis induced by doxorubicin in kidney and liver cell lines using the lactate dehydrogenases assay

Cells were treated with DOX (7 COS-7, 4 μ M HepG2) and after 24 hrs, the LDH assays were performed. Figure 3.5.2.3A and B shows no significant effect on increasing LDH release.

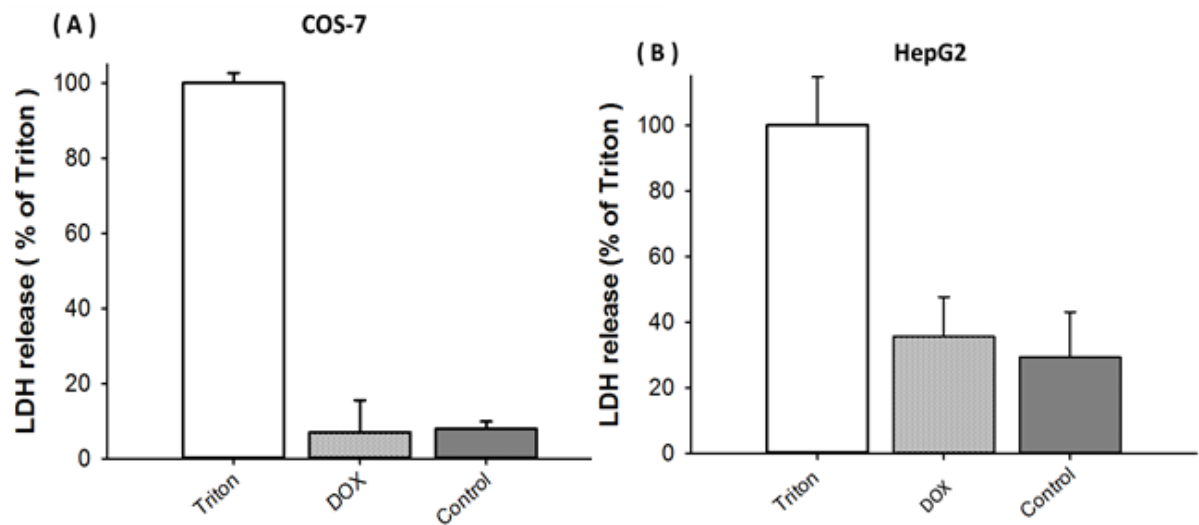


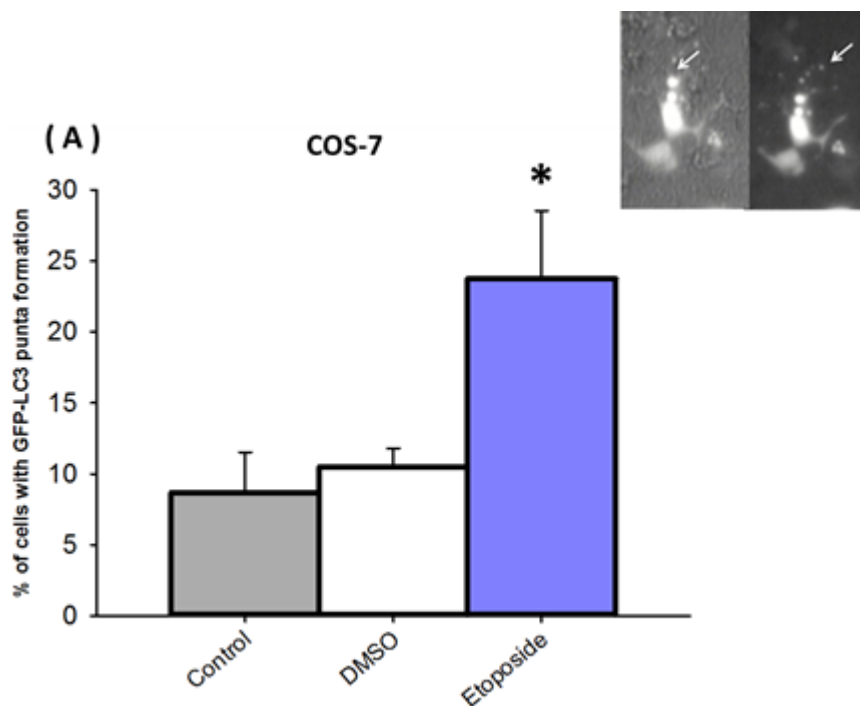
Figure 3.5.2.3A and B; the effect of DOX on lactate dehydrogenases (LDH) release in COS-7 cells (A) and HepG2 cells (B). Cells were treated with DOX and incubated for 24 hrs and then LDH release assays performed. Data represents the mean \pm SD of 3-4 determinations.

3.6 Autophagy detection using cytosolic LC3-GFP as a biomarker for autophagosome formation

As a part of autophagosome formation, during the autophagy, LC3 protein is involved. LC3 usually found diffused inside the cells, but under certain forms of cell stress it is converted to phosphatidylethanolamine (PE)- Linked form located on the phagophore. Therefore, LC3 was used as a biomarker protein to monitor the initiation of autophagy in COS-7 and HepG2 cells treated with different chemotherapy drugs (i.e. Etoposide, Cisplatin and DOX). LC3-GFP when recruited to the autophagosome gives the appearance of fluorescence hot spots or “punta” when visualized under the fluorescence microscope (Wong et al, 2013) (see figure 3.6.1, inset).

3.6.1 Monitoring autophagy using LC3- GFP by Etoposide in kidney and liver cells

Both COS-7 and HepG2 Cells were transiently transfected with GFP-LC3 plasmid for 48 hrs to allow the expression of this protein to be visualized under the fluorescence microscope and then cells were treated with etoposide [(150 and 120 μ M) for both COS-7 and HepG2 cells]. Figure 3.6.1, shows the percentage of punta formation on both control/DMSO and Etoposide COS-7 (A) and HepG2 (B) treated cells for 4 hrs post transfection. This figure shows that COS-7 cells shown no significance difference between DMSO and the Etoposide group. HepG2 cells also showed a clear difference between the both groups where approximately 25% of cells were showing punta formation.



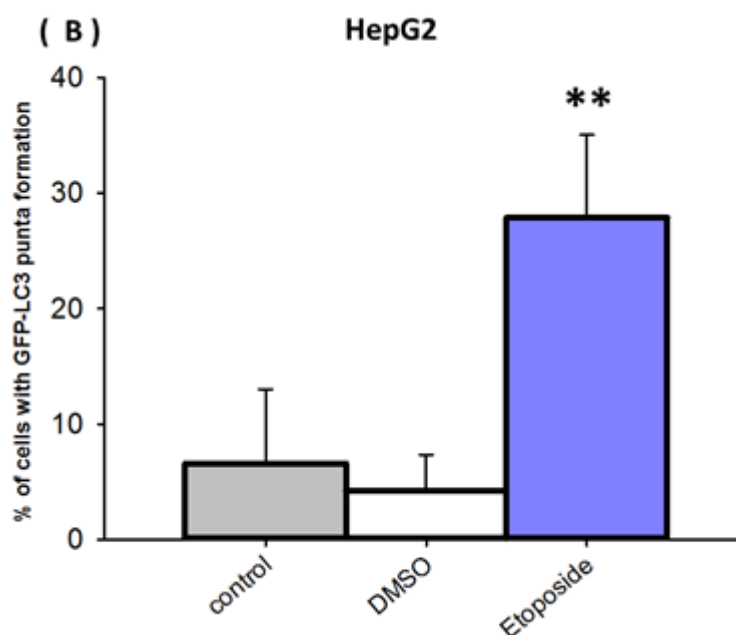


Figure 3.6.1; the percentage of LC3-GFP punta transfected cells treated with Etoposide. COS-7 (A) and HepG2 (B) cells were transfected with LC3- GFP plasmid for 48 hrs, then the cells were treated with Etoposide (150 and 120 μ M), respectively, for 4 hrs. Punta formation was calculated using fluorescence microscope. Data represents the mean \pm SD of 5-6 determinations. (* value points were significant different from the controls, $p \leq 0.05$, ** $p \leq 0.01$), using the t-test. (Inset) the micrograph above shows the punta formation in COS-7 cells under light and fluorescence field following Etoposide treatment.

3.6.2 Monitoring autophagy using LC3- GFP by Cisplatin in kidney and liver cells

COS-7 and HepG2 cells were transiently transfected for 48 hrs with LC3-GFP to allow expression to be visualized under the fluorescence microscope and then cells were treated with the LC_{50} of Cisplatin (46 and 35 μ M) in COS-7 and HepG2 cells, respectively. Figure 3.6.2 shows the percentage of punta formed on both control (i.e. water) and Etoposide. This figure shows that both COS-7 and HepG2 cells forms a high percentage of punta about 70% which is highly significance compare to control group with only 20% punta were observed.

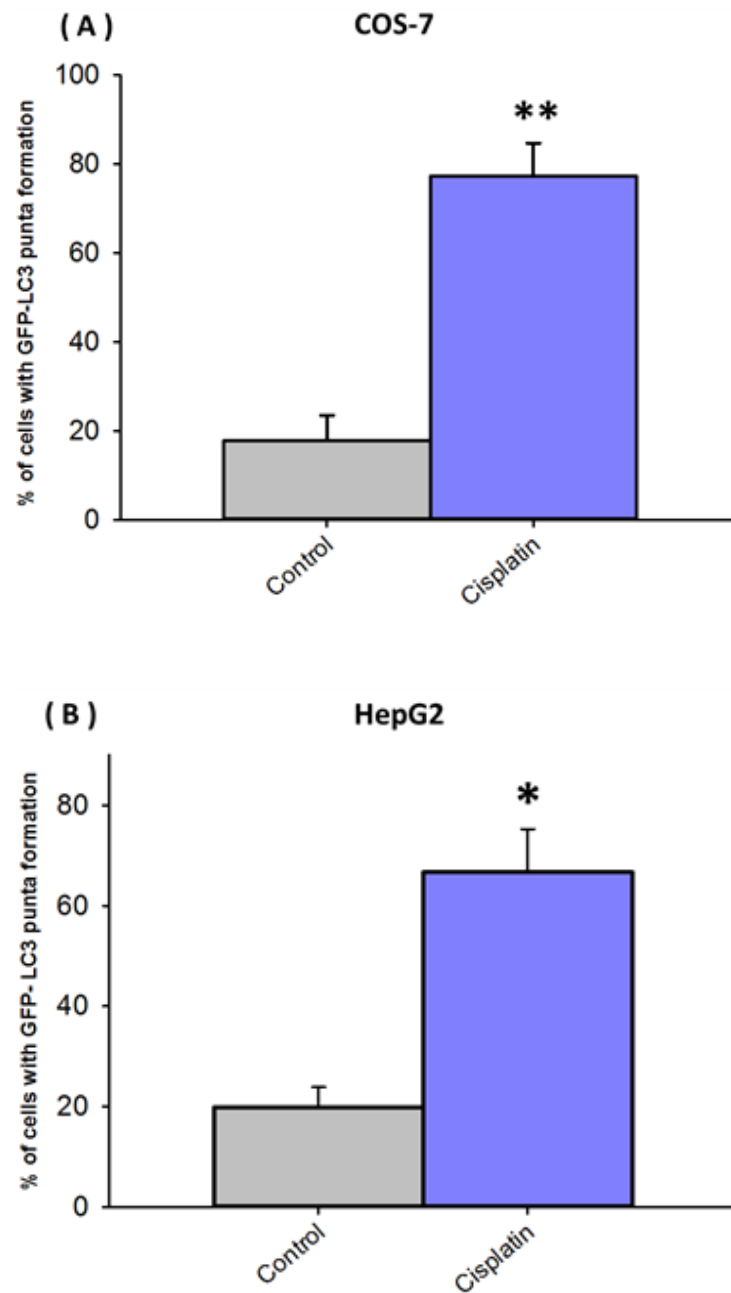
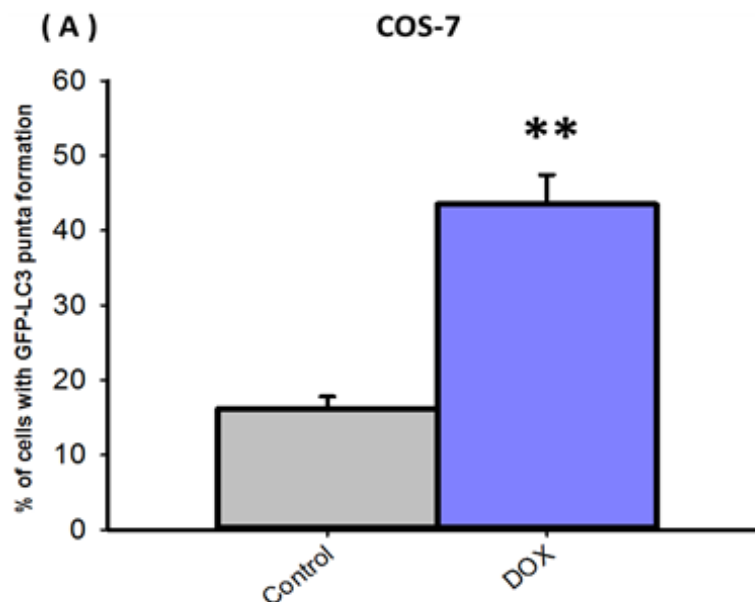


Figure 3.6.2; the percentage of LC3-GFP punta in transfected cells treated with Cisplatin. COS-7 (A) and HepG2 (B) cells were transfected with LC3-GFP plasmid for 48 hrs then the cells treated with Cisplatin (46 and 35 μ M) Respectively, for 4 hrs. Punta formation was determind using fluorescence microscopy. Data represents the mean \pm SD of 5-6 determinations. (* values were significant from the controls, $p \leq 0.05$, ** $p \leq 0.01$), using the t-test. The micrograph above shows the punta formation in COS-7 cells under white light and fluorescence field, during Cisplatin treatment.

3.6.3 Monitoring autophagy using GFP-LC3 by Doxorubicin in kidney and liver cells

Cells were transiently transfected for 48 hrs with LC3-GFP plasmid and then cells were treated with LC₅₀ of DOX (7 and 4 μ M) with COS-7 and HepG2 cells. Figure 3.6.3 shows the percentage of punta formation in both control and DOX, COS-7 (A) and HepG2 (B) treated cells for 4 hrs. Figure 3.6.3 shows that DOX causes about 45% and 60% punta formation in COS-7 and HepG2 cells, respectively. Treated cells showed a significant difference of autophagosomes formation compared to control cells (water).



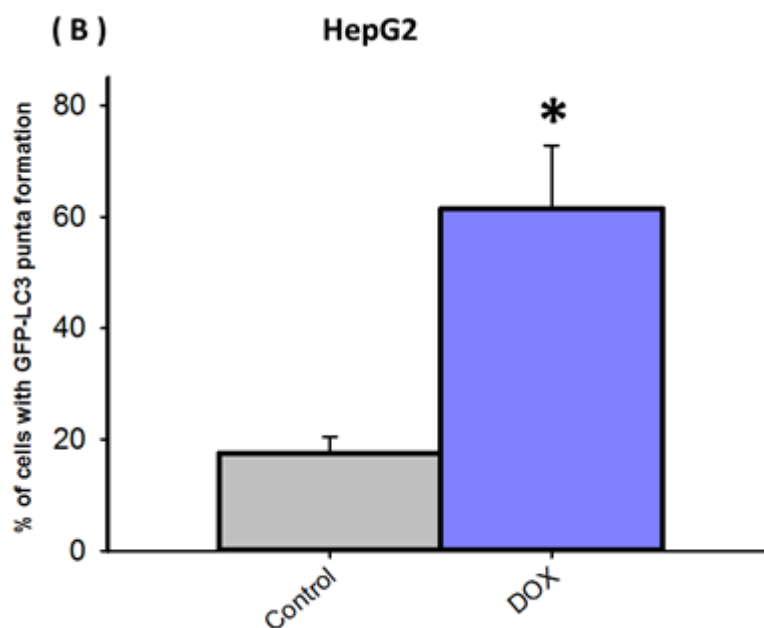


Figure 3.6.3; the percentage of punta in LC3-GFP transfected cells treated with DOX. COS-7 (A) and HepG2 (B) cells were transfected with LC3-GFP plasmid for 48 hrs then cells treated with DOX (7 and 4 μ M) Respectively, for 4hrs. Punta formation was calculated using fluorescence microscopy. Data represents the mean \pm SD of 5-6 determinations. (* values were significantly different from the controls, $p \leq 0.05$, ** $p \leq 0.01$), using the t-test.

3.7 Investigating DNA single strand breaks using comet assay

The comet assay is a sensitive assay for monitoring DNA single strand breaks inside cells. The head represents the undamaged part of the DNA in the cell while the tail represents the fragmented DNA electrophoresed out of the cell. Cells were treated with LC_{50} of DOX and after (4 and 24 hrs) comet assays performed to measure the extent of DNA damage. In this experiment, H_2O_2 was used as a positive control (100 mM for 60 min).

3.7.1 Comet assays for measuring DNA breaks in COS-7 cells treated cells with DOX

COS-7 cells were treated with 7 μ M of DOX for 4 and 24 hrs. H₂O₂ was added to some cells as a positive control. Comet assay IV software was used to calculate the tail intensity percentage for each group of 100 counted cells of 3 determinations. Figure 3.7.1A shows a section of a control cells slide with intact DNA and a section of a slide with cells treated with DOX. Figure 3.7.1B and C shows the percentage of total intensity that occurs in the tail of COS-7 cells treated with DOX (7 μ M) for 4 hrs (A) and 24 hrs (B), respectively. Comparing the control and DOX groups, a small but significant difference was observed after 4 hrs, while a more significant, about 25% tail intensity of single stand breaks, was observed after 24 hrs.

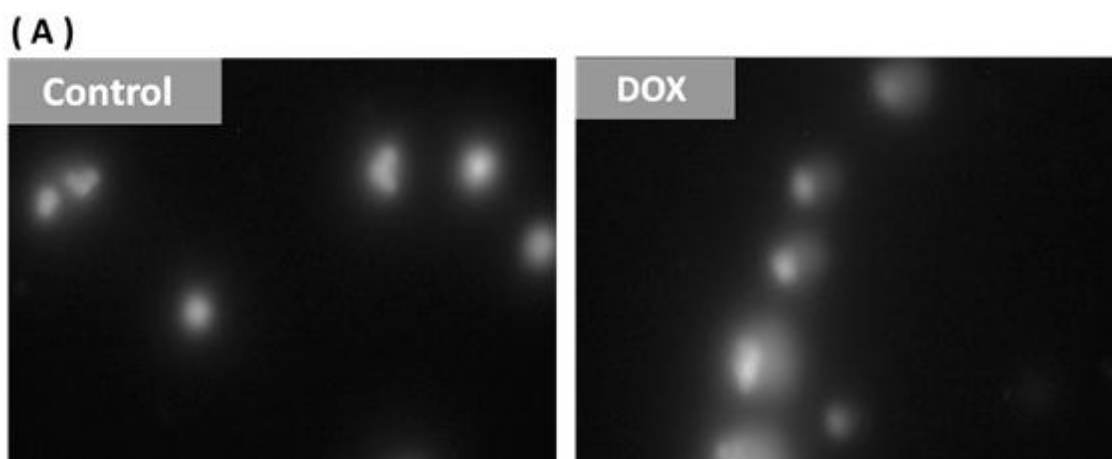


Figure 3.7.1A; images from Comet IV software, showing COS-7 intact nuclei and a damaged nuclei after DOX treatment.

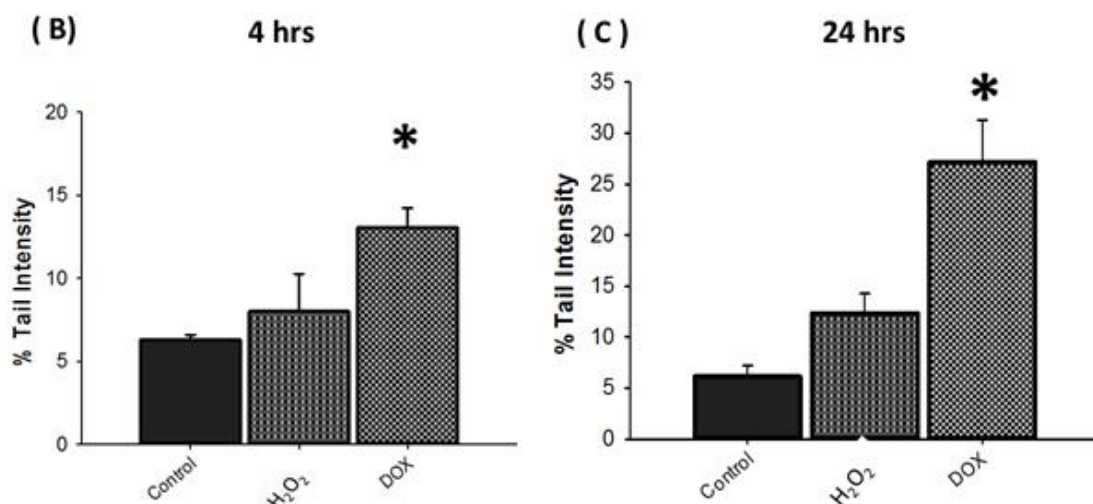


Figure 3.7.1B and C; shows the tail intensity of control, H₂O₂, and DOX treated cells with one comet assay. COS-7 cells were treated with 7 μ M of DOX and H₂O₂ for 4 and 24 hrs, then comet assay was performed and Comet IV software. (* values were significantly different from the controls, $p \leq 0.05$), using the t-test.

3.7.2 Comet assay for measuring DNA breaks in HepG2 cells treated cells

Cells were treated with (4 μ M) of DOX for 4 and 24 hrs. Comet assay IV software was used to calculate the tail intensity percentage for each group of 100 counted cells of 3 determinations. Figure 3.7.2A shows a section of a control cells with intact DNA and a section of cells treated with DOX. Figure 3.7.2B and C shows the percentage of tail intensity of HepG2 cells treated with DOX 4 μ M for 4 hrs and 24 hrs (B), respectively. Comparing both the control and DOX groups, a high significant difference was observed after 4 hrs, and after 24 hrs. DOX causes about 25% tail intensity of single strand breaks at both times, which suggest that DOX is highly damaging to HepG2 cells even after a short period of time.

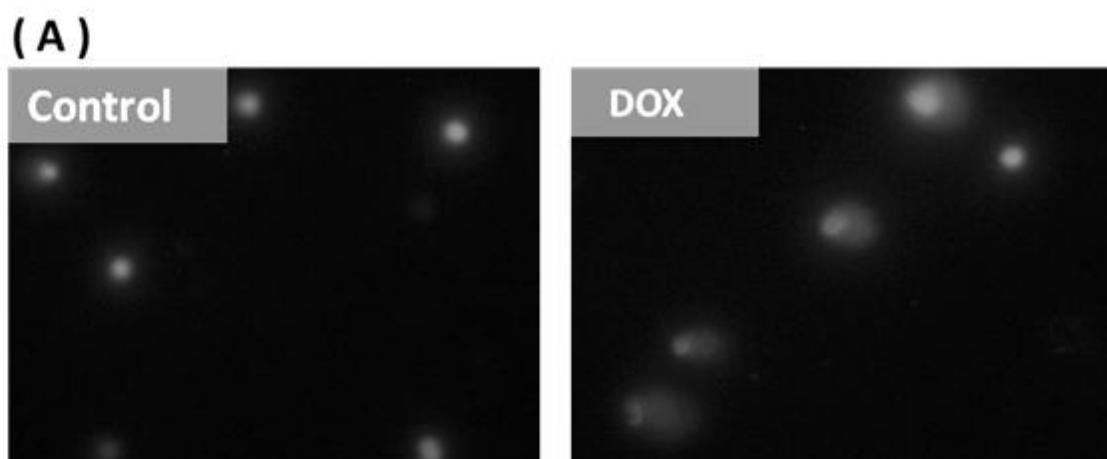


Figure 3.7.2A; images from Comet IV software, showing HepG2 intact nuclei and a damaged nuclei after DOX treatment.

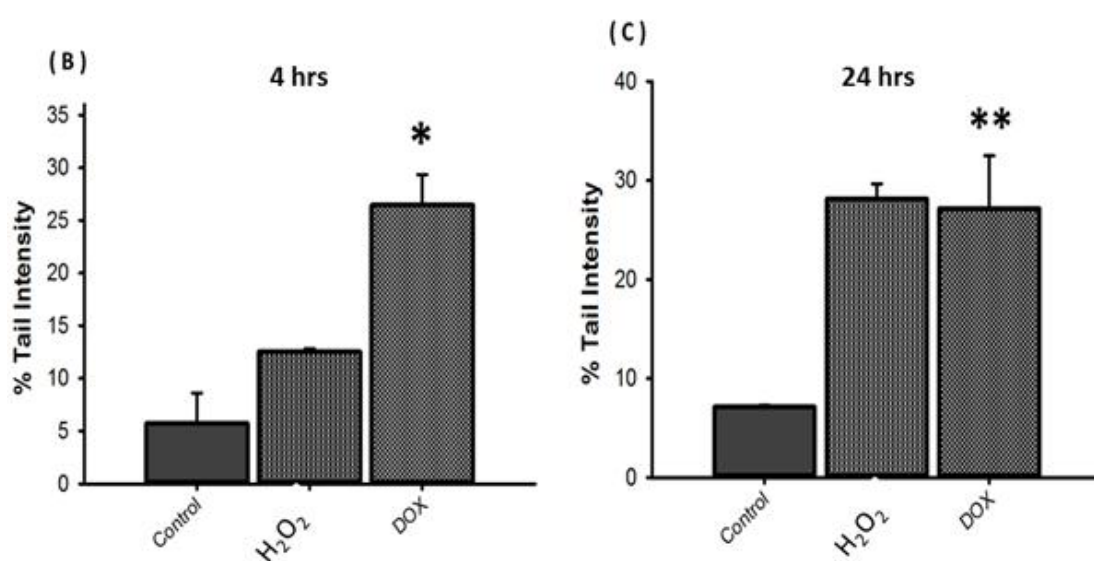


Figure 3.7.2B and C; shows the tail intensity of control, H₂O₂, and DOX treated HepG2 cells with one comet assay. HepG2 cells were treated with 4 μ M of DOX and H₂O₂ for 4 and 24 hrs, then comet assay was performed and Comet IV software. (* values were significantly different from the controls, $p \leq 0.05$, ** $p \leq 0.01$), using the t-test.

3.8 Discussion

Chemotherapy is a cancer treatment that uses medicines and drugs in order to kill and/or stop tumor cancer cells multiplying. Chemotherapeutic drugs are also used in order to destroy any remaining cancer cells following surgery (Skeel and Khelif, 2011). This form of therapy mainly acts either by interacting with the cell cycle, inhibiting DNA replication or activating cell death pathways (Payne and Miles, 2008). The effects of the drugs (MTX, Etoposide, Cisplatin and DOX) on cell viability of kidney (COS-7, HK2) and liver (HepG2, Huh7.5) cancer cell lines were studied in detail.

3.8.1 The effect of Methotrexate (MTX) in Kidney (COS-7, HK2) and liver (HepG2, Huh7.5) cancer cell lines

Methotrexate is an antimetabolite agent and acts as an inhibitor of tetrahydrofolate reductase, which blocks tetrahydrofolate formation, and which is necessary for nucleotide biosynthesis and therefore cell division (Warlick et al., 2000). Many studies have been undertaken to understand the mechanism of MTX toxicity. In order to investigate the cytotoxicity of MTX on kidney and liver cell lines, MTT assays were performed. As shown in figure 3.2.1.1 both kidney (COS-7, HK2) cell lines showed more sensitivity to toxicity by MTX than liver (HepG2, Huh7.5) cell lines and noticeably, HK2 cells were more sensitivity to MTX than COS-7 cells, with a LC_{50} of low μM . Therefore, this may indicate that different kidney cell lines are not similarly affected by this drug. Furthermore, the results with liver cells demonstrate that the toxicity of MTX has a limited effect on cell viability of liver cells even at high MTX concentrations (200 μM). The results are in agreement with other studies by Keefe et al., (1982), where murine leukaemia cells (L5178Y) exposed with $\geq 10 \mu M$ MTX for 42 hrs did not result in any further toxicity as compared to treatment with 0.1 μM MTX.

High MTX concentrations are usually used to treat tumours compared to the concentrations used for other diseases such as psoriasis and arthritis (Weinstein et al., 1990). In this study concentrations up to 500 μM MTX was used and showed only limited effects with confluent cells. However, at a density of about 20% cell confluency, treatment with high concentrations of MTX showed suppression of cell proliferation (see figure 3.3.1.3 A and B). These results are consistent with other studies which have

shown that MTX inhibits cell growth in a variety of cell lines (Mazor et al., 2015, Seigers et al., 2010 and Jeffes et al., 2005). Furthermore, when MTX drug was removed from the cells, they began to show more normal cell division and growth. Therefore, these results could be explained by MTX mainly affecting cell proliferation rather than cell death, this is consistent with the fact that MTX inhibits tetrahydrofolate reductase preventing the synthesis of an important nucleotide metabolites for DNA synthesis (Weinstern, 1990).

3.8.2 The effect of Etoposide in Kidney (COS-7, HK2) and liver (HepG2, Huh7.5) cell lines

Etoposide is one of the most commonly used anti-cancer drugs, which inhibits topoisomerases II and causes DNA breakage (Baldwin and Osheroff, 2005). Etoposide is a plant-derived natural product; it is a podophyllotoxin derivative and is considered to be one of the most important anticancer drugs. However, Etoposide has toxic side effects at the cellular and organ level (Minev, 2011). In order to examine the cytotoxicity of etoposide on kidney and liver cell lines; MTT assays, caspase inhibitor, caspase substrates, necrosis inhibitors, LDH assays and GFP-LC3 punta biomarker were used. Figure 3.3.2 A-D showed that HK2 cells are the most sensitive to Etoposide, with an LC_{50} of $50 \pm 6 \mu M$ as compared to the other cell lines which were much less sensitive i.e. HepG2, COS-7 and Huh7.5 with LC_{50} of $120 \pm 6.4 \mu M$, $150 \pm 9.1 \mu M$ and $1000 \pm 11.2 \mu M$, respectively. These data support other results which report a range of LC_{50} values with etoposide in different gastric cell lines (Yu, et al., 2007). Different methods were used to investigate the mechanism of cell death by Etoposide in this study. Our data suggested that Etoposide caused apoptotic cell death in COS-7 cells, when the cell viability, of pre-treated cells with caspase-3 inhibitor, increased about 10-25% of cell viability compared to Etoposide alone. However, caspase-3 substrate, which is much more sensitive could detect the involvement of caspase-3, more clearly in the other cell lines. This observation could be because caspase inhibitors are detecting cells that are either alive or dead, while, the caspase substrate method is assessing, all cells which are in the process of undergoing apoptosis and have not yet died. Dead cells in this methods are removed through the washing stages and so do not contribute to the cell number. Furthermore, the assay involves fluorescence detection is much more sensitive compared with the

absorbance based MTT assay. The observations presented here are in agreement with other studies that have shown that Etoposide specifically induces apoptosis in a range of different cell lines (Yu et al., 2007), Hep 3B hepatoma cells [(Yoo et al., 2012), HL60 cell (Barry et al., 1993), Male germ cell (Lizama et al., 2011) and HEK 293 kidney cells (Zhao et al., 2006)]. In this chapter other experiments were undertaken to determine whether other mechanisms of Etoposide- induced cell death were involved. Etoposide was also shown to causes necrosis cell death (using necrostatin and LDH assays) in COS-7 and HepG2 cells but not in HK2 and Huh7.5. This effect has also been found in another study (Litwiniec et al., 2013) where low concentrations of Etoposide on A549, a human lung epithelial cells line, showed early apoptosis, late apoptosis and necrosis using the annexin V-PI assay. More recently, another study has suggested that Etoposide can induce both necrosis in HK2 cells and apoptosis after inhibition of p53 (Kwon et al., 2015). However, our findings results shown little necrosis in HK2 cells exposed to Etoposide.

In addition, HepG2 and COS-7 cells shows statistically significant differences in LC3 punta formation when cells were exposed to Etoposide. Some studies showed not only apoptotic but autophagic phenotypes in Hep3B cells (Yoo, 2012), together the findings presented here indicate that, Etoposide induces a mixed type of cell death involving apoptosis, necrosis and autophagy, which appears to be cell line dependent.

3.8.3 The effect of Cisplatin in Kidney (COS-7, HK2) and liver (HepG2, Huh7.5) cell lines

Cisplatin is (cis- diamminedichloroplatinum (CDDP)), targets tumor cells of the testis as well as many other epithelial malignances such as ovary, bladder, cervix, head, neck, prostate, lymphoma, and carcinomas of esophageal (Oyanagi, et al., 2015, Rozenzweig et al., 1977). However, Cisplatin also causes acute nephrotoxicity and can accumulate in microsomes, nuclei, mitochondria and cytosol of these cells (Litterst, 1981). The data presented here showed the cytotoxicity of Cisplatin in kidney and liver cells, to be different in the cell lines. As mentioned previously with other drugs, HK2 cells seems to be the most sensitive cell line for Cisplatin a LC_{50} of $20 \pm 7 \mu M$ compared with LC_{50} values $35 \pm 3 \mu M$, $46 \pm 8.7 \mu M$ for HepG2 and COS-7 cells, respectively. Recent studies

of cell death induced by Cisplatin have suggested that both apoptosis and necrosis are involved (Karadeniz et al., 2011, Sand-Dejmek et al., 2011, Pestell et al., 2000).

The results presented here, also confirmed that Cisplatin significantly induces apoptosis via caspase 3 in both kidney (COS-7 and HK2) cells as well as liver cells (HepG2 and Huh7.5) (Figure 3.4.1.2 A-D). A recent study has shown that in HepG2 cells activation of caspase -3,-8,-9 in Cisplatin treated cells occurs (Chien, et al., 2015), which supports our finding. Our data are also consistent with the finding of activation of apoptosis in Cisplatin- treating cells is through caspases (Lu and Cederbaum, 2007, Barry, et al., 1990). The results presented here show that Cisplatin is also able to induce necrosis or regulated necrosis in all cell lines tested. These findings are consistent with that of Lim et al, (2010) that reported Oxaliplatin (Cisplatin analogue) caused necrosis in HepG2 hepatocellular carcinoma cells (Lim et al., 2010). Park et al. (2015) showed that Cisplatin could also induce necrosis cell death in HK2. Cisplatin at 50 μ M can also causes nuclei fragmentation, apoptosis and necrosis features (Lau, 1999). Interestingly, several studies have shown that Cisplatin can induced necrosis when inhibiting apoptosis pathway (Zhang et al., 2008, Gonzalez et al., 2001 and Sancho-Martinez et al., 2011). However, in COS-7 and HepG2 cell lines used in my study, I have shown necrosis cell death can occur without inhibiting of apoptosis pathway. In fact, Cisplatin inducing necrosis rather than apoptosis could be a concentration dependent process (Ganzalez at al., 2001).

The results presented here showed that Cisplatin also, causes autophagy in HepG2 and COS-7 cells (Figure 3.6.2 A and B). However, one study has suggested that the unfolded protein response (UPR) inhibits cisplatin-induced apoptosis in hepatocellular carcinoma cells, via heat shock protein mediated autophagy (Chen et al., 2011) indicating a cell survival process. This might suggest that these cells undergo autophagy within hours of Cisplatin exposure through a protective mechanism for cell survival prior to being overwhelmed and apoptosis then taking place (Periyasamy-Thandavan et al., 2008, Takahashi et al., 2012, Zou et al., 2012). To summarise, cisplatin has diverse effects on cell, causing cell death through types apoptosis, necrosis and autophagy.

3.8.4 The effect of Doxorubicin in Kidney (COS-7, HK2) and liver (HepG2, Huh7.5) cell lines

Doxorubicin (DOX) is a anthracycline antibiotic anti-cancer drug. DOX is also considered one of the most potent chemotherapeutic drugs that is currently used (Carvalho, 2009). This drug has the ability to damage DNA and inhibit DNA and RNA production by free-radicals damage (Minotti et al., 2004). It was very clear that DOX was the most toxic chemotherapy drug compared with the other chemotherapy drugs used in this study. All four cell lines showed low LC₅₀ values in contrast to Etoposide, Cisplatin and MTX. HK2 was the most sensitive cell line with LC₅₀ of 3±5µM followed by HepG2, Huh7.5 and COS-7 cells with LC50 of 4±5, 6±7, 7±8 µM, In this study, I showed that this drug is highly toxic and mediates a high level of apoptosis using the caspase-3 substrate in all four cell lines tested (Figure 3.4.2.4 A-D). However, the results were not as clear with HK2, HepG2 and Huh7.5 cells using caspase-3 inhibitor. This finding is consistent with other studies that showed that DOX could induce apoptosis in renal cells (Zhang et al., 1996), in hepatoma cell lines (Lee et al., 2002) and human neuroblastoma cell (Rebbaa, 2003, Jin et al., 2007). With regards to necrosis, little effect of DOX on this was observed (figure 3.5.2.3 A and B). This disagrees with the reports of DNA damaged-induced necrosis through a PARP1- dependent and p53- independent pathway by DOX in HK2 cells (Chin et al., 2015). As no effect were seen for either the necrostatin inhibitor or LDH release assay, we believe that different experimental conditions and treatments may account for these differences.

Autophagy, is a process involving lysosomal degradation and recycling of unwanted cytosolic proteins and other organelles. Activation of this might be either protective or destructive (i.e. causes cell death) depending on the specific pathological and physiological conditions (Mizushima, 2005, Levine and Yuan, 2005). DOX showed an increase in LC3-GFP punta with both COS-7 and HepG2 cells, indicating the potential for autophagy cell death. In support of this DOX has also been shown to exhibit autophagy in cardiomyocytes at low µM concentrations (Kabayashi, et al., 2010). The observation of autophagy cell death induced by DOX in both liver and kidney cells is a new finding and needs further study to be undertaken to determine whether this plays a major role in hepatotoxicity or nephrotoxicity in patients.

The alkaline single cell gel electrophoresis (comet assay) was used to quantitate the genotoxic effects of DOX in both HepG2 and COS-7. The results showed that DOX causes a substantial amount of DNA single strand breaks even after a short 4 hrs exposure to DOX. This degree of strand breaks only increased by a smaller amount after 24 hrs for HepG2 compare to COS-7 cells. Therefore, the early onset of DNA damage indicates that DOX is likely causing DNA damage directly rather than through apoptosis, which causes DNA damage over longer time periods. DOX also induces the production of reactive oxygen species in many different cells (Kim et al., 2006, Tsang, et al., 2003). When DOX binds to DNA it may cause oxidative damage at this site, therefore damaging DNA directly rather than through an indirect route (Cooke et al., 2003). It is obvious that the four cell lines investigated showed different sensitivities to these drugs with, in some cases, a big difference between similar types of cells. However, of all the cells tested, HK2 cells appeared to be the most sensitive cell line for the toxicity by the drugs used. In addition, these cell lines also undergo different forms of cell death (with different mechanisms) when treated with the same drug (see table 3.8.4 as a summary table), which underlines the complexity of the cell death. DOX was shown to be the most toxic drug compared to others used in this study. However, DOX showed no effect on the necrosis pathway in all four cell lines studied as compared to Cisplatin and Etoposide which did causes some necrosis. Finally, Caspase-3 substrate activity was found to be a much better method of detecting apoptosis in contrast with caspase inhibitors and cell viabilities, which has a limited sensitivity.

Table 3.8.4; summary of the different cell death pathways using various assay and different chemotherapeutic drugs used in this chapter.

Cell Death		Apoptosis						Necrosis						Autophagy		
Cell line	Drug	Etop		Cisp		DOX		Etop		Cisp		DOX		Etop	Cisp	DOX
		Caspase-3 inhibitor	Caspase-3 Substrate	Caspase-3 inhibitor	Caspase-3 Substrate	Caspase-3 inhibitor	Caspase-3 Substrate	Necrosis inhibitor	LDH	Necrosis inhibitor	LDH	Necrosis inhibitor	LDH			
COS-7		+	+	++	+++	+	+++	+	+	+	++	-	-	+	+++	++
HK2		-	++	++	+++	-	+++	-	-	+	++	-	-	ND	ND	ND
HepG2		-	+++	+++	+++	+	++	+	ND	++	ND	-	ND	+	+++	+++
Huh7.5		-	+++	+++	+++	-	++	-	ND	++	ND	-	ND	ND	ND	ND

- = Little or no effect

+ = A small but significant effect

+ + = A substantially significant effect

+ + + = A strong effect

ND = Not determined

CHAPTER 4

RGN over-expression in COS-7 and
HepG2 cells and drugs treatment

4 RGN over-expression in COS-7 and HepG2 cells and drugs treatment

4.1 Introduction

During acute cell inflammation the inflammatory cytokine, tumour necrosis factor alpha (TNF- α) is produced by macrophages and involved in various cellular signals, such as apoptosis or necrosis (Idriss and Naismith 2000). TNF- α mediates apoptosis in rat hepatocytes by activating D-galactosamine, increasing the intra-nuclear free $[Ca^{2+}]$ and causing DNA fragmentation (Abou-Elelle et al., 2002). Overexpression of RGN shows a protective effect on H4-II-E liver cells which were been treated with a high concentrations of TNF- α (10 ng/ml), and this suggested that RGN has exhibitory effects on cell death (Izumi and Yamaguchi, 2004). Since effect of TNF- α mediated cell death could be inhibited by caspase inhibitors. It was suggested that RGN might also have an inhibitory effect on the activation of caspases in cells (Yamaguchi, 2012). This effect was further investigated when cells treated with thapsigargin (SERCA Ca^{2+} pump inhibitor and an apoptosis inducer), caused a sustained increased in cytoplasmic $[Ca^{2+}]$ and caused apoptosis. Treating cells with either caspase inhibitors or overexpression of RGN, decreased this rise of intracellular Ca^{2+} (Yamaguchi 2005; Pereira et al., 2002) and also decreased the nuclear DNA fragmentation, again suggesting that RGN might have inhibitory effects on caspase activation during apoptosis cell death (Yamaguchi, 2012). RGN has been suggested to play a suppressor role in cell death and apoptosis in H4-II-E cells induced by sulforaphane, an isothiocyanate involved in cell cycle arrest (Gamet-Poyrastre et al., 2000). Since Sulforaphane mediates the pro-apoptotic protein Bax expression, increases cytochrome c release from mitochondria and proteolysis of polymerase Hi 29, these observations suggests that RGN protection may also have an effect on Bax, cytochrome c, caspase and Bcl2 proteins (Cohen and Cohen, 1989). The suppressor effects of RGN on apoptosis does not only apply to liver cells, but has also been observed in kidney cells as well (Nakagawa and Yamauchi 2005). In NRK52E kidney cells, hormones (parathyroid hormone, aldosterone, dexamethasone) stimulate an increase in expression of RGN (Nakagawa and Yamauchi 2005 a). The localization of RGN was also more highly expressed in nucleus following hormonal stimulation (Nakagawa and Yamauchi 2008). The Overexpression of RGN in NRK52E kidney cells

was also shown to have suppressive effects on apoptotic cell death, induced by TNF- α , LPS and thapsigargin (Nakagawa and Yamauchi 2005 b). Furthermore, the overexpression of RGN increased a number of key signalling pathway molecules, such as Apaf-1, Bcl-2 and Akt-1 (Zou et al., 1997; Vogelstein et al., 2000; Widmann et al., 1988). In addition, the NRK25E - RGN transfected cells showed a high increase in the expression of Bcl-2 mRNA and Akt-1 mRNA. However, Apaf-1 mRNA and caspase3 mRNA did not show any significant increase (Nakagawa and Yamaguchi, 2005). Therefore the main effect of RGN was to increase the expression of anti-apoptotic factors.

The main aim of this chapter is to investigate the effects of RGN overexpression in to COS-7 and HepG2 cells and to determine whether this protects the cells from cell death induced by the chemotherapeutic drugs used in the previous chapter.

N.B. Due to the origins of plasmids used in this chapter; SMP30 relates to the expression of human regucalcin, while RGN-GFP relates to the expression of human regucalcin that has a GFP attached to C-terminus.

4.2 SMP30, Over-expression, Detection, and Cytoprotection

As mentioned previously, some studies reported that regucalcin (RGN), known as senescence marker protein (SMP30) is able to protect the cells from cell death (Izumi and Yamaguchi, 2004 and Yamaguchi and Sakuria, 1991). As we have shown in the chapter 3 that some of the chemotherapy drugs causes cell death to occur by different pathways in different cell lines, the experiments described in this chapter were carried out in order to determine the protective role of RGN protecting cells against cell death. Furthermore, two versions of RGN plamid have been used to express SMP30 and RGN-GFP (see figure 4.2A and B), both RGN were overexpressed in COS-7 and HepG2 cells, for viability studies, while just RGN-GFP plamid was used in microscopy and localization experiments mainly for visualization purposes.

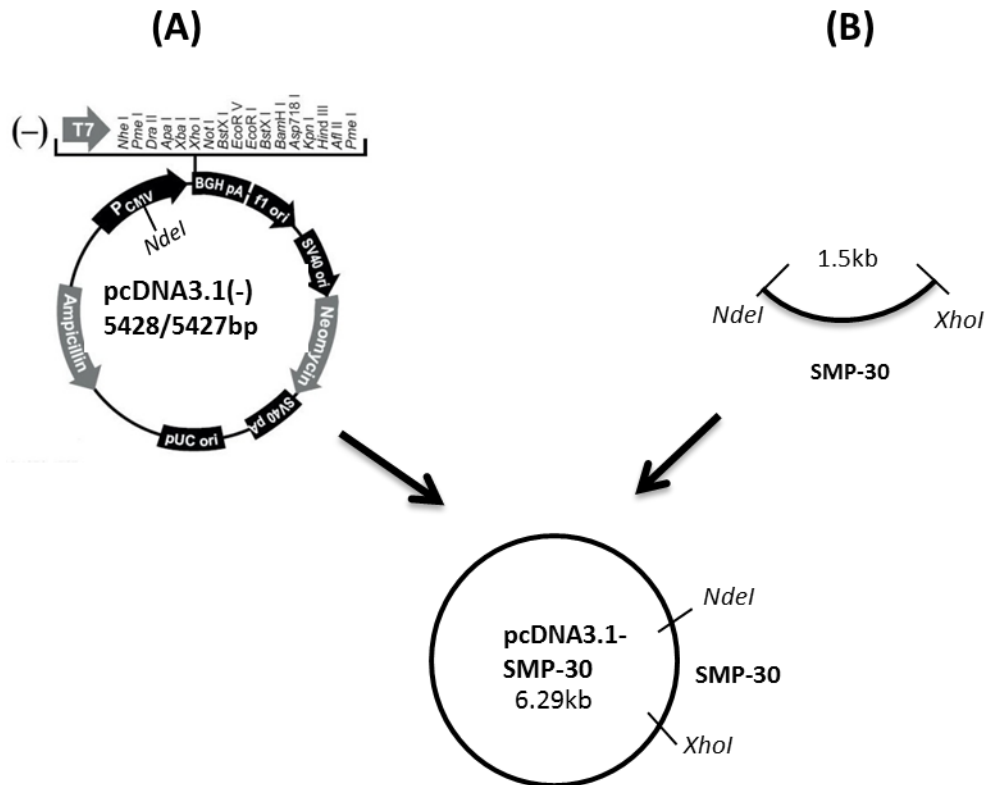


Figure 4.2A and B; the restriction map for PCDNA and SMP30-PCDNA3.1-plasmids. The plasmid human SMP30-PCDNA3.1- was constructed by Dr. Pei Lai (Lai, PhD thesis, 2009). The identity of the plasmid was confirmed by diagnostic restriction enzyme analysis.

4.2.1 Over-expression and Detection of SMP30

Cells were seeded into 6 well plates and transfected with the PCDNA 3.1 SMP30 plasmid with different plasmid and the Turbofect reagent (TR) concentrations, as illustrated on section 2.2.14. After 48 hrs cell lysis was performed and the cell lysate were separated by SDS-PAGE and transfected on to nitrocellulose and anti-Rabbit SMP30 antibody was used to detect it by Western blotting. Figure 4.2.1A and B show COS-7 and HepG2 cell lysates were overexpressed SMP30. Both Figures show that Condition 3 (1 μ g plasmid/2 μ l TR) is the best condition for COS-7 and HepG2 cells. In addition, it was also noticed that the untransfected cells also expressed a low level of SMP30 naturally. It had already been reported that these cells express low endogenous level of SMP30 (Lai et al., 2011).

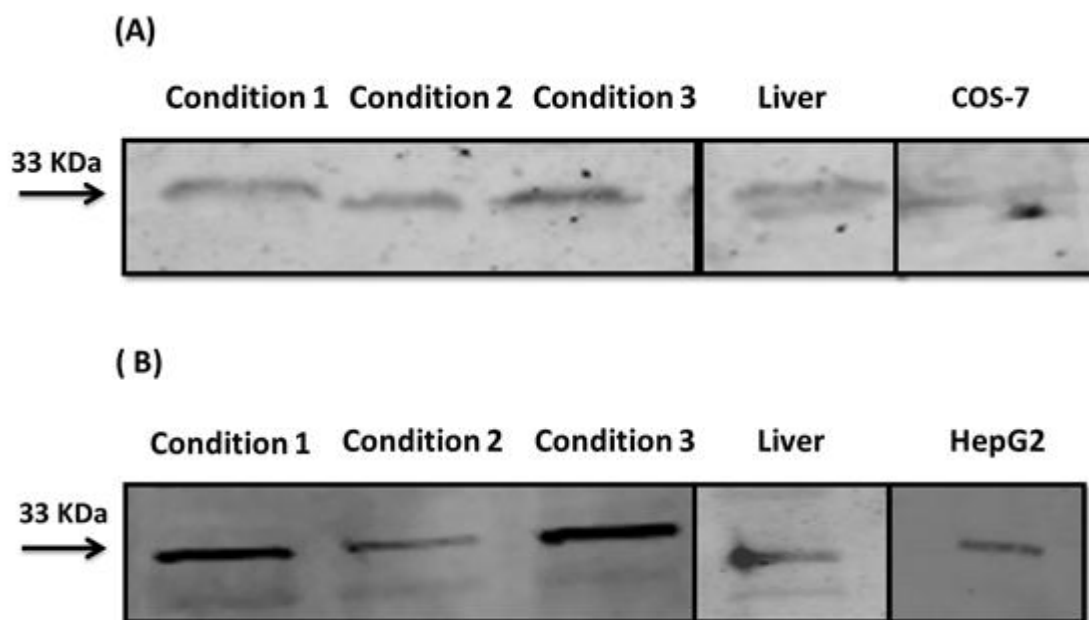
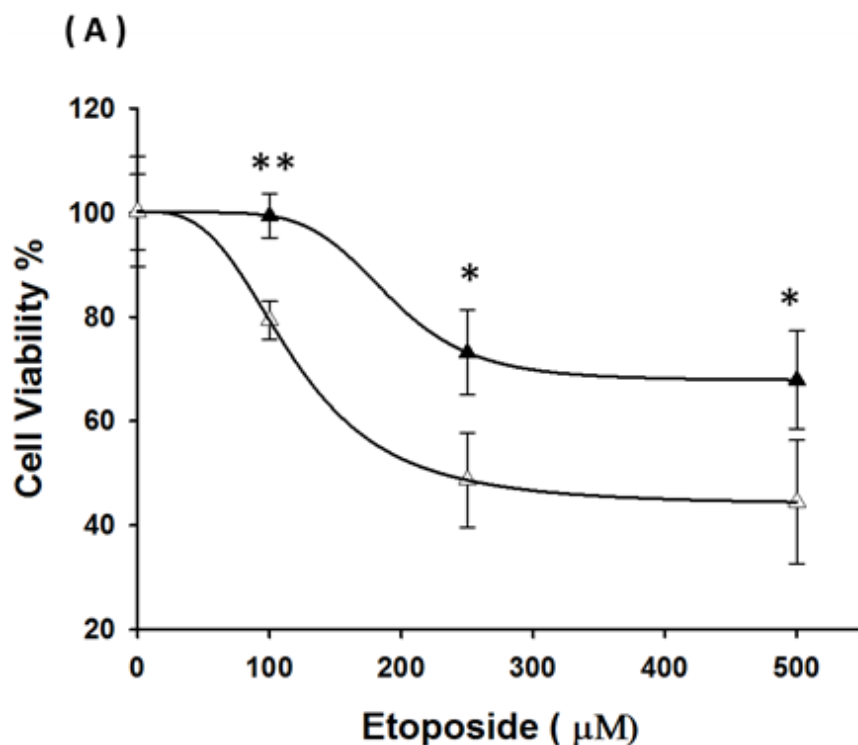


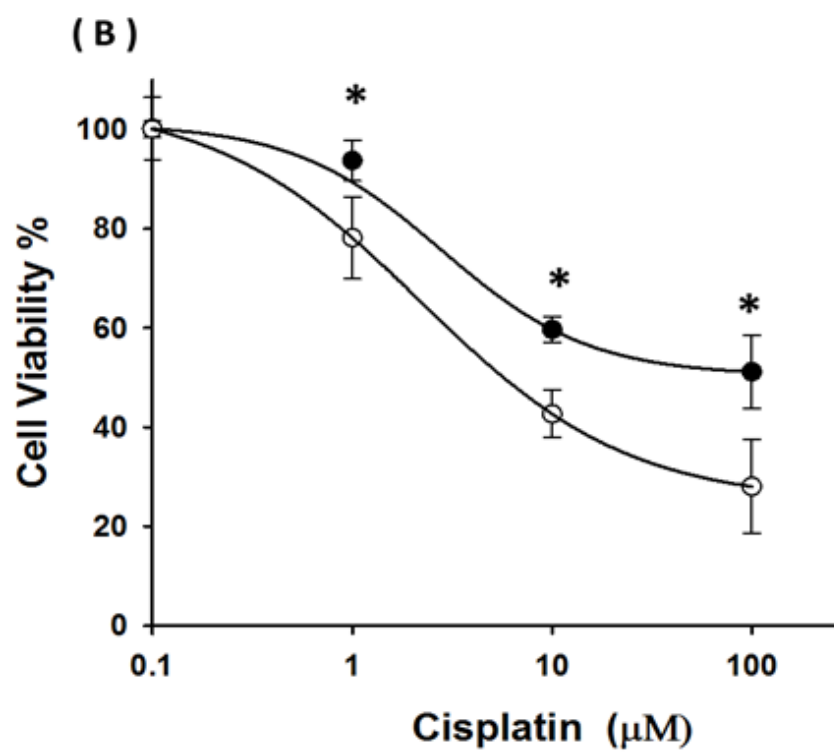
Figure 4.2.1A and B; western blots of cell lysates overexpressing SMP30 in COS-7 (A) and HepG2 (B). Cells were treated with different concentration of SMP30 and the transfection reagent. Condition 1 (2 μ g plasmid/4 μ l TR), condition 2 (1 μ g plasmid/4 μ l TR), condition 3 (1 μ g plasmid / 2 μ l TR), rat liver cytosolic fraction as a positive control and COS-7 and HepG2 cells alone as a ‘negative’ control. Total protein amounts loaded of each sample were 15 μ g (COS-7) and 30 μ g (HepG2) cells for each cells lysate condition in 6 well plates in 2 ml media. The 33 KDa SMP30 proteins were detected in all the lanes.

4.2.2 The cytoprotection of SMP30 overexpression in COS-7 and HepG2 cells exposed to chemotherapeutic drugs

4.2.2.1 The cytoprotection effect SMP30 overexpression in COS-7

COS-7 cells were transfected with either PCDNA or SMP30, 1 μg SMP30/2 μl TR and left for 48 hrs. Later, cells were treated with different drugs; Etoposide (A), Cisplatin (B) and DOX (C) at different concentrations and left for 48 hrs, then MTT assays were performed to measure the cell viability of each group. In COS-7 cells treated with etoposide the LC_{50} where shifted significantly. The LC_{50} was estimated to be more than 500 μM in SMP30 transfected cells compared to the empty vector PCDNA alone transfected cells which had a LC_{50} ~200 μM . SMP30 also shows a protection effect on cells treated with both Cisplatin and DOX, when the LC_{50} increased significantly with Cisplatin and DOX from 50 μM to > 300 μM and from 3 μM to 20 μM , respectively when comparing SMP30 transfected versus PCDNA alone-transfected cells (See table 4.2.2.1). Therefore, we could see the effect of SMP30 in protecting cells from death by a significant level.





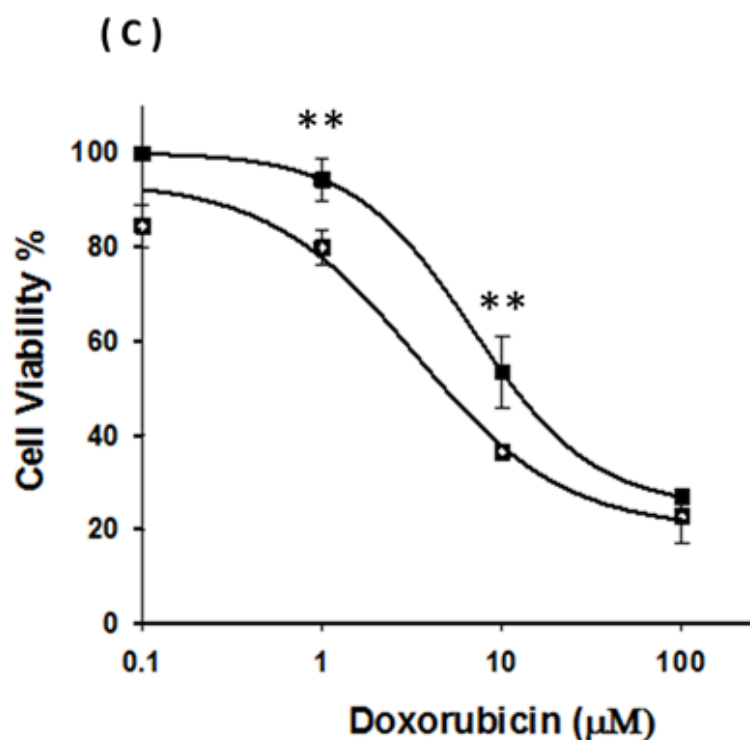


Figure 4.2.2.1; the effects of Etoposide (A), Cisplatin (B) and DOX (C) on cell viability of COS-7 cells. COS-7 transfected with empty vector (PCDNA) and SMP30. Cells were grown in 48 well plates in 1 ml media and then cells were transfected after 40-50% cell confluency, 1 μg of the plasmid and 2 μl of TR then left for 48 hrs. Cells were treated with Etoposide, Cisplatin and DOX, then MTT assay performed after 48 hrs. PCDNA alone transfected cells (\square), SMP30 transfected cells (\blacksquare). The data points represent the mean \pm SD of 3-5 determinations. (* $p \leq 0.05$, ** $p < 0.01$, compared to their corresponding values in empty plasmid group).

Table 4.2.2.1; summarizes the LC₅₀ in μ M values of COS-7 cells with the different drugs. When comparing SMP30-transfected and PCDNA-transfected cells and treated with Etoposide, Cisplatin and DOX.

Drug	LC ₅₀ (μ M)		
	PCDNA	SMP30	Fold Increase
Etoposide	200	> 500	> 2.5
Cisplatin	50	> 300	> 6
DOX	3	20	7

4.2.2.2 The cytoprotection effect of SMP30 overexpression in HepG2

To observe the effect of SMP30 overexpression on HepG2 cells, these cells (Figure 4.2.2.2) were transfected with 1 μ g PCDNA or 1 μ g SMP30 plasmid + 2 μ l TR in 1 ml and left for 48 hrs. Cells were then treated with DOX at different concentrations and left for 48 hrs, then MTT assays were performed to measure the cell viability. HepG2 cells shows less cell death with a LC₅₀ 40 μ M when transfected with SMP30, comparing with PCDNA transfected cells (LC₅₀ of 10 μ M).

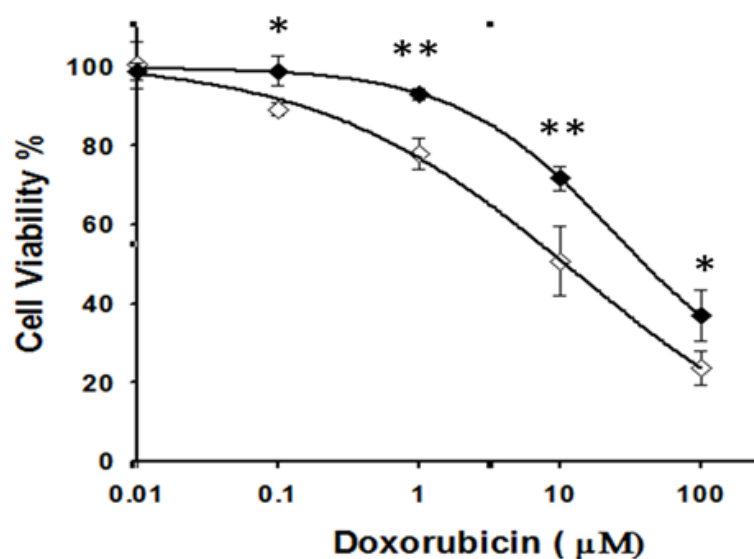


Figure 4.2.2.2; the effect of DOX on cell viability of HepG2 cells in the presence of empty vector-PCDNA and SMP30. HepG2 cells were grown in 48 well plates in 1 ml media and then cells were transfected after getting to 40-50% cell confluency, 1 μg of plasmid and 2 μl of TR were used to transfect cells with empty vector-PCDNA and SMP30 then cells were left for 48 hrs. Cells were treated with DOX (0.01, 0.1, 1, 10 and 100 μM) then MTT assays performed after 48 hrs. Empty vector- PCDNA transfected cells (◇), SMP30 transfected (◆). The data points represent the mean ± SD of 3-5 determinations. (* $p \leq 0.05$, ** $p < 0.01$, compared to their corresponding concentration values in the empty PCDNA plasmid group).

4.2.3 The effect of SMP30 on COS-7 cell viability and proliferation

4.2.3.1 The effect of SMP30 overexpression on COS-7 cells viability

COS-7 cells were plated on 24 well plates and incubated for 24 hrs, then cells were transfected with empty PCDNA or SMP30 (1 μg plasmid/2 μl TR), cells were left for 48 hrs before MTT assays were undertaken. As shown in figure 4.2.3.1, SMP30 expression cells decrease viability by 30 % compared to PCDNA which is significant ($p < 0.01$). This suggested the possibility of overexpressing SMP30 had a suppressor role in cell

proliferation. However it could also have effect on mitochondrial reductase which is what the MTT assay actually measures.

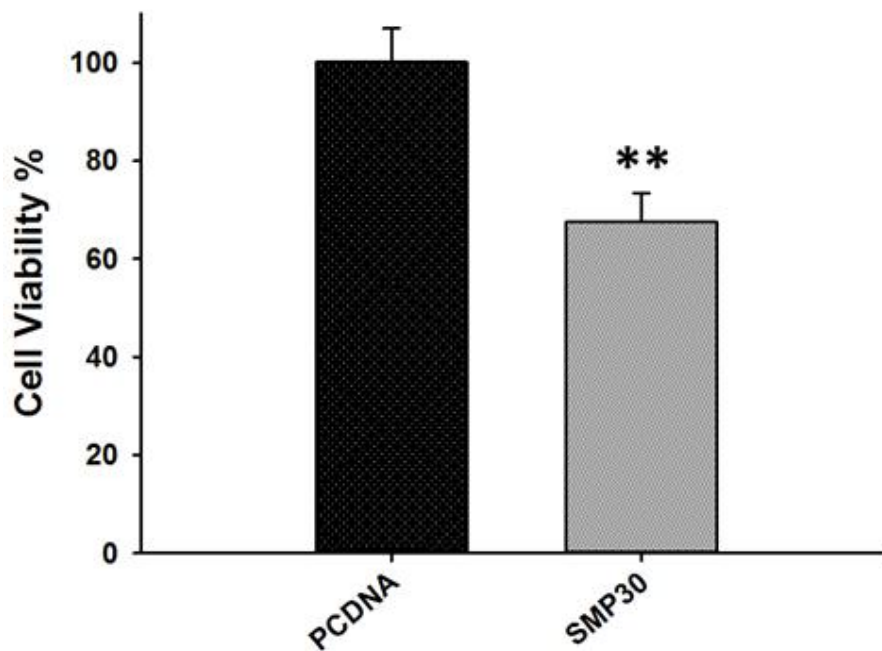


Figure 4.2.3.1; the effect of SMP30 plasmid on COS-7 cell viability. COS-7 seeded on 24 well plate, after 24 hrs cells were transfected with empty PCDNA or SMP30 (1 μ g plasmid/2 μ l TR). After 48 hrs of transfection, MTT assay was performed. The data points represent the mean \pm SD of 3-5 determinations. (** $p < 0.01$, compare to the empty PCDNA group).

4.2.3.2 The effect of SMP30 overexpression on COS-7 cell proliferation

As previous studies showed SMP30/RGN decreased cell proliferation. A series of experiments to test this were undertaken. Cells were plated in 48 well plates for 24 hrs at 37 °C, day after cells were transfected with SMP30 or empty PCDNA and left for 48 hrs. Crystal violet assays were performed to measure the number of cells in each group (a more direct measure of cell proliferation). Figure 4.2.3.2 shows the decrease in cell number with significance at $p < 0.05$ in the SMP30 group as compared to PCDNA

group. Therefore it is most likely that SMP30 decreased by 20% the proliferation of COS-7 cells.

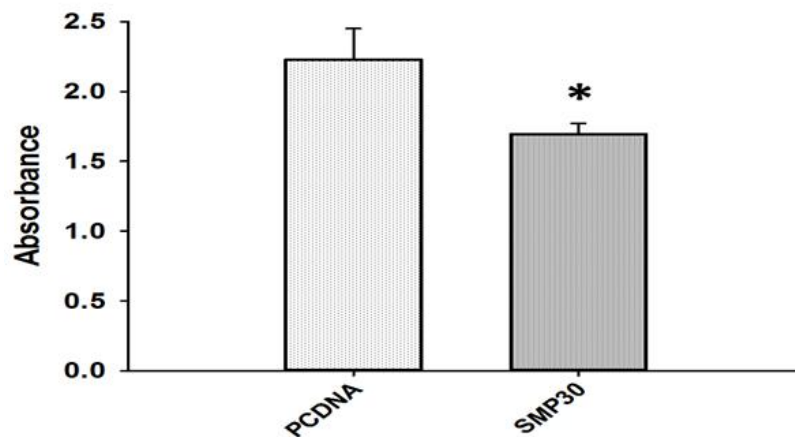


Figure 4.2.3.2; the effect of SMP30 overexpression on COS-7 cell proliferation. COS-7 cells were seeded on 48 well plates, after 24 hrs the cells were transfected with empty PCDNA or SMP30 (1 µg plasmid / 2 µl TR). After 48 hrs of transfection, crystal violet assays were performed. The data points represent the mean ± SD of 3-5 determinations. (* $p < 0.05$, compared to the PCDNA group).

4.3 RGN-GFP, Overexpression, Detection, Cytoprotection and Microscopy studies

4.3.1 Optimization of the transfection efficiency in COS-7 cells

COS-7 cells were seeded on 6-well tissue culture plates (to 50-60 % confluency). Three different concentration of turbofect transfection reagent (TR) and RGN-GFP plasmid (see figure 4.3.1A) were used to optimize the transfection efficiency. As shown in figure 4.3.1B and C after the cells were incubated for 48 hrs and at 72 hrs, the transfection efficiency was calculated according to the average percentage of the number of green fluorescent cells compared to total number of cells and three replicates for each condition was undertaken. Figure 4.3.1C illustrates the optimal condition for RGN-GFP transfection in COS-7 cells with condition 3 (1 μ g DNA: 2 μ l TR) for 72 hrs being the best.

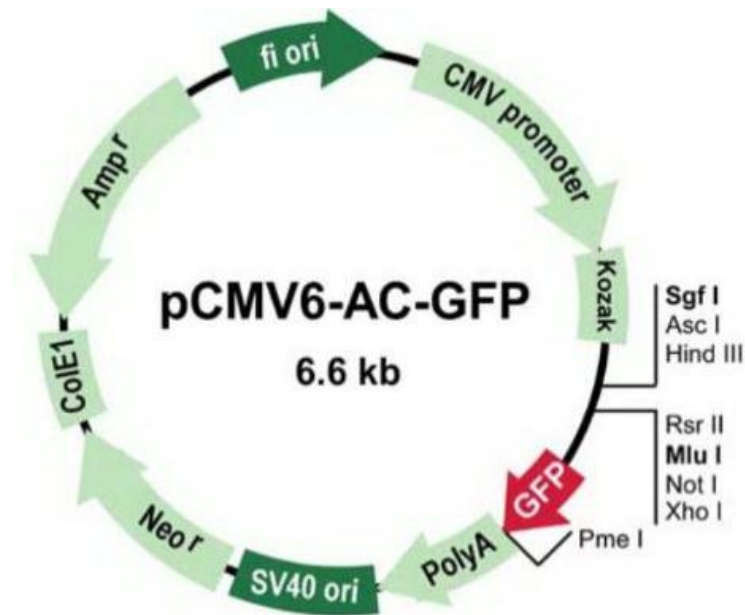


Figure 4.3.1A: shows the Origene vector with RGN-C-tagged Human Variant 1. Plus human RGN (RGN-GFP). The RGN gene was inserted within the multiple cloning site between the restriction site Sgf1 and Mlu 1.

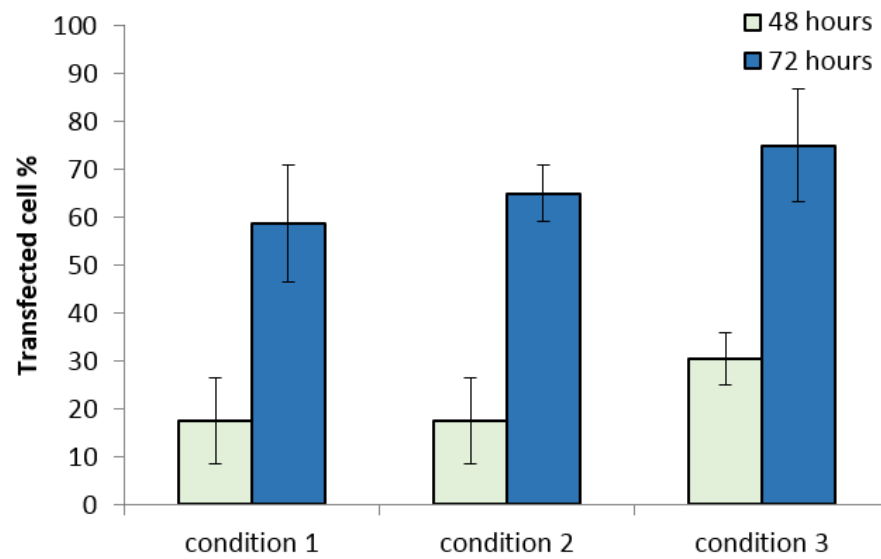


Figure 4.3.1B; COS-7 cells transfected using three conditions of plasmid and turbofect transfection reagent. Condition (1) refers to (2 μ g DNA:4 μ l TR), condition (2) refers to (1 μ g DNA:4 μ l TR) and condition (3) refers to (1 μ g DNA:2 μ l TR) ratio. The transfection efficiency was calculated after 48 and 72 hrs of transfection using fluorescence microscope.

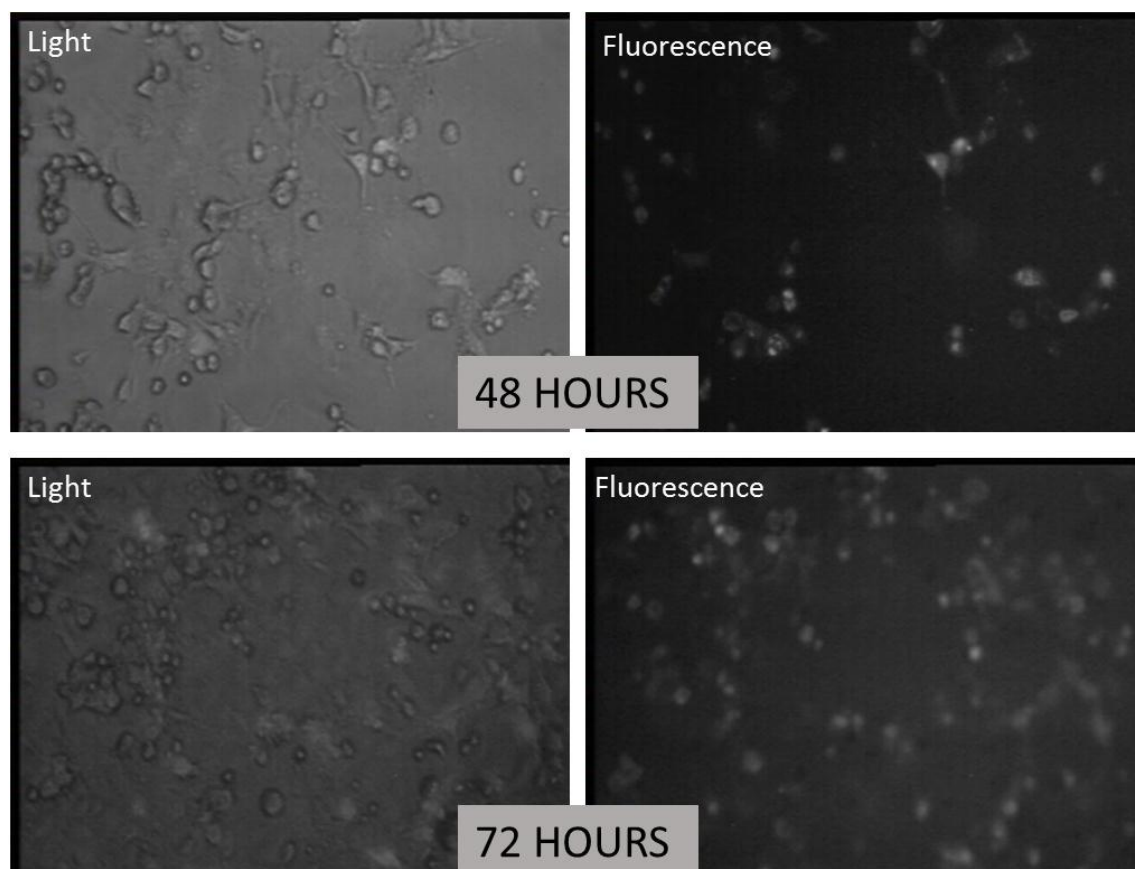


Figure 4.3.1C; illustrates the optimal condition of RGN-GFP transfection with (1:2) (1 μ g Plasmid RGN-GFP: 2 μ l transfection reagent) in COS-7 cells. COS-7 cells were cultured in 6-well plates and transfected 24 hrs later. Transfected cells were viewed with a fluorescence microscope at 200x magnification. Picture was taken using an Astrovid StellaCam-EX camera connected to the microscope at 48 and 72 hrs after transfection.

4.3.2 Detecting RGN at protein level in kidney and liver cell line

Figure 4.3.2 shows the presence of RGN protein in kidney (COS-7, HK2) and liver (HepG2) cell lines, using a primary rabbit anti-RGN antibody and anti-Rabbit 800 IR Dye secondary antibody. Cells (COS-7, HK2 and HepG2) were grown in 10 cm diameter Petri dish then lysed in 500 μ l of Lysis buffer. All three cell lines had shown low levels of endogenous RGN protein.

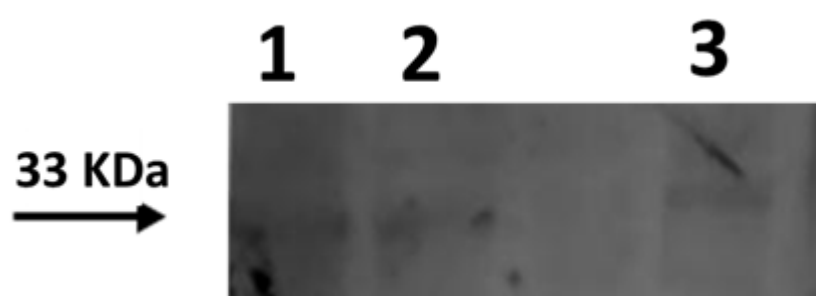


Figure 4.3.2; western blot to detect RGN detection in cell lysates of kidney and liver cell lines. A primary anti-RGN antibody was used. Lane 1, 2, 3 refers to HepG2, COS-7 and HK2 cells, respectively. All cell samples loaded at 200 μ g with 10 μ l of 250 KDa marker.

4.3.3 Effect of overexpression of RGN-GFP on COS-7 cell viability following treatment with Doxorubicin

To determine whether overexpression of RGN-GFP in COS-7 cells can protect against DOX-induced cell death, MTT assays were undertaken on the cells after transfection. As transfection efficiency reached 60%, cells were treated with DOX over a range of concentrations, as carried out previously. PCDNA was empty vector and used for the control group. Figure 4.3.3 shows the cell viability of COS-7 cells which were PCDNA-transfected compared to cells transfected with the RGN-GFP plasmid. The LC_{50} of PCDNA-transfected cells was $7 \pm 3 \mu$ M, while the LC_{50} for the RGN-GFP transfected cells was $20 \pm 2 \mu$ M. Therefore, RGN-GFP shows a protective role, which was statistically significant at 10 and 100 μ M ($p < 0.05$). This protection is similar to

that seen with SMP30 overexpression suggesting that the GFP part of the protein has only a little effect on the function of RGN.

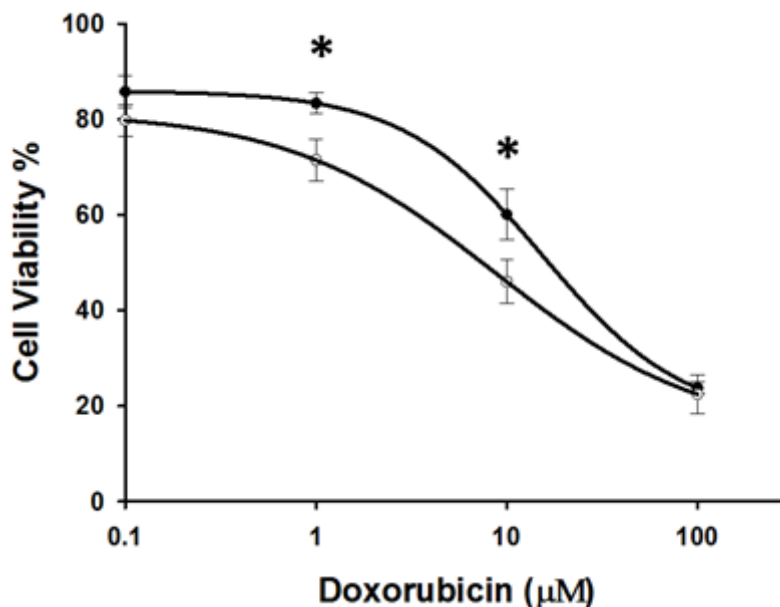


Figure 4.3.3; effect of DOX on COS-7 cell viability in the present or absence of RGN-GFP expression. Cells were transfected with RGN-GFP or PCDNA alone and then treated with the drug. MTT assays were carried out to determine the cell viability in both PCDNA-transfected (○) and RGN-GFP transfected cells (●). The data pointed represent mean \pm SD of 3-4 determines. (* $p < 0.05$, compared to PCDNA transfected cells).

4.3.4 The effect of RGN-GFP on COS-7 cell proliferation

In order to determine whether RGN-GFP also caused a reduction in cell proliferation, COS-7 cells were transfected with (PCDNA or RGN-GFP) to determine the effects of this protein on cell number using the crystal violet assay. Cells were seeded in 48 well plates, then after 24 hrs the cells were transfected with both plasmids (PCDNA and RGN-GFP), and then left for 48 hrs to express the protein, after which the crystal violet assays were performed. The results in figure 4.3.4 shows a significant difference in cell number at $p \leq 0.001$ in RGN-GFP transfected cells as compared with transfected with

empty PCDNA transfected cells, which suggests that RGN-GFP appears to maintain its suppressor effect on cell proliferation.

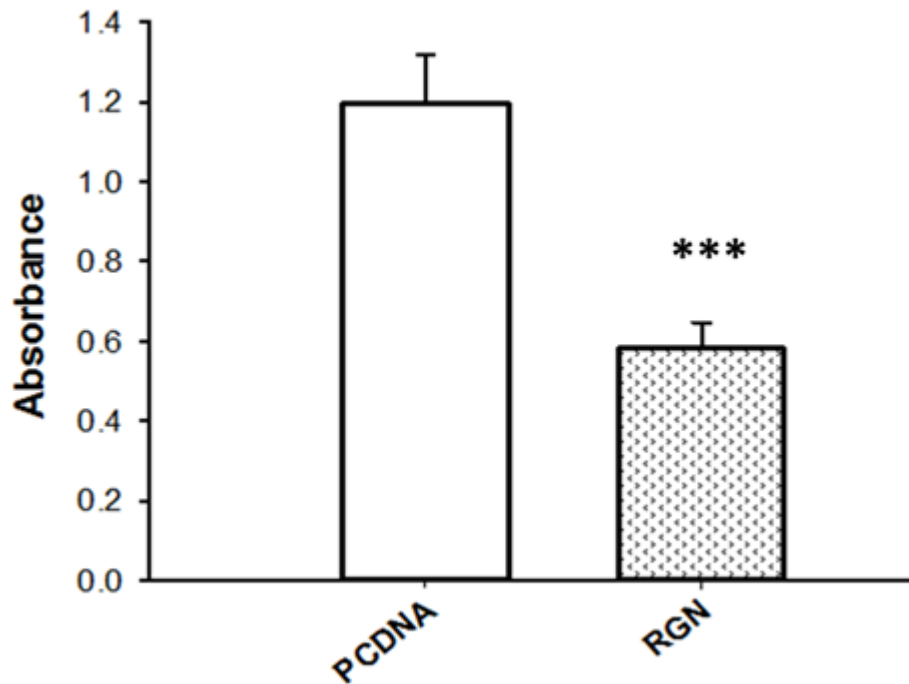


Figure 4.3.4; the effect of RGN-GFP and PCDNA on COS-7 cell number, Cells were transfected for 48 hrs with both plasmids. Crystal violet assays were used to measure cell numbers, where absorbance directly related to cell numbers. The data points represent the mean \pm SD of 3-5 determinations. (***) $p < 0.001$, compare to empty PCDNA group).

4.3.5 Microscopy studies of RGN-GFP treated with Doxorubicin

4.3.5.1 Time-lapse experiments with COS-7 and DOX

After exploring the protective function of RGN-GFP in COS-7 cells, it was interesting to visualize this protein under the fluorescence microscope, in order to determine its subcellular localization and whether this changes during cell stress caused by DOX.

Therefore, time-lapse experiments were undertaken. COS-7 cells transfected with RGN-GFP for 24 hrs, then cells were visualized under the fluorescence microscope. 7 μ M of DOX was added to the media and then the cells recorded for 30 min (a total 60 images). As shown in figure 4.3.5.1 is initially a widely distributed fluorescence location is observed, which then appears to focus around the cell body at the centre of the cells, following adding DOX. Therefore, this could suggest that RGN-GFP moves toward the nucleus under cell stress induced by DOX.

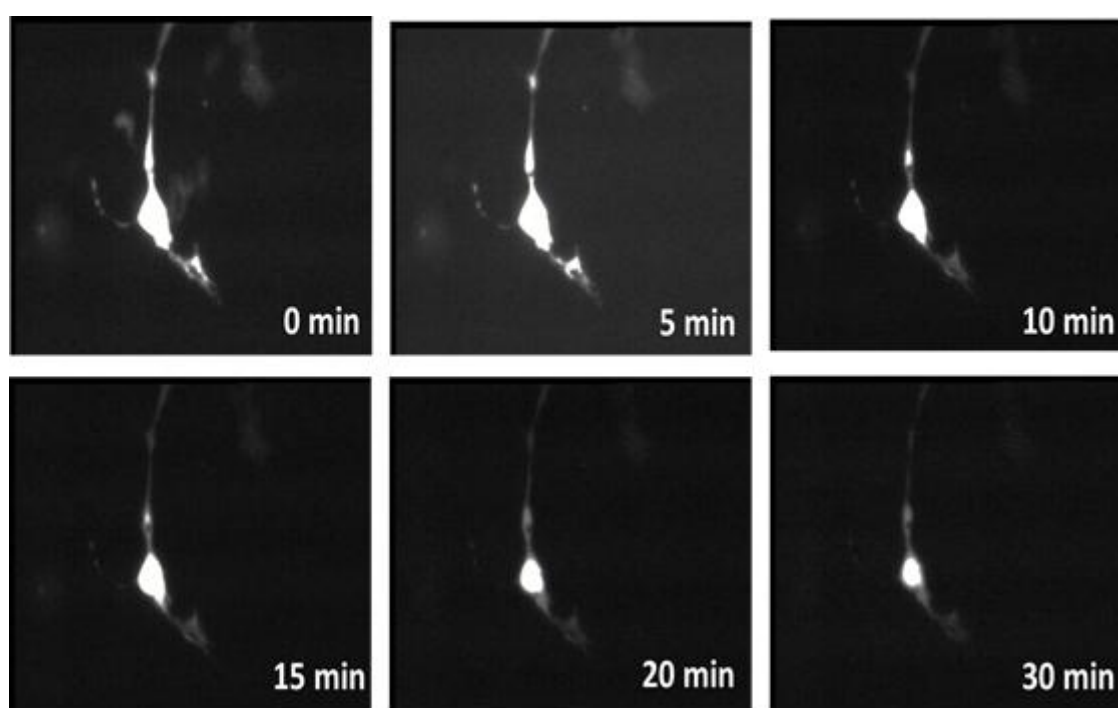


Figure 4.3.5.1; time-lapse of RGN-GFP transfected COS-7 cells treated with 7 μ M DOX. The figure shows the time points (in minutes) using 20X lenses power. A single cell is presented for clarify, but this was typical of some other cells observed.

4.3.5.2 Co-localization of RGN-GFP with COS-7 cells

4.3.5.2.1 Co-localization of RGN-GFP in COS-7 cells with mitochondria and nuclei and the effects of Doxorubicin

The co-localization of RGN-GFP with mitochondria and nuclei was undertaken further to understand the role of RGN. Confocal microscopy was used with the Hoechst dye for nucleic staining and Mitotracker-red for mitochondria staining. In addition, DOX was also added to determine whether RGN-GFP changed location within the cells.

Cells were seeded in coverslips of in 6 well plate overnight, cells were then transfected with RGN-GFP for 48 hrs, cells then stained with 0.5 μ M Mitotracker for 30- 40 min. PBS was used to wash the cells and the cells were fixed with 4% paraformaldehyde for 15 min, then 1 μ g/ml of the Hoechst stain was added to the cells for 30 min to stain the nucleus. The cells were examined under the confocal microscope, for treated cells, cells were initially treated with 5 μ M DOX for two hrs before staining.

Image statistical analysis were performed using ImageJ with the statistical plugin JACoP, this tool is used for localization analysis of two images and which calculates Pearson's coefficient, most common correlation coefficient-based tool used to assess the co-localization (Bolt and Cordelieres, 2006). In the analysis, Pearson's correlation coefficient was used to evaluate the correlation between the RGN-GFP (green channel) and mitochondria (red channel) or nuclei (blue channel). Based on the correlation coefficient estimation, values in the ~0.5-1 range indicate a significant overlaps and co-localization between two channels.

Figure 4.3.5.2.1A shows fluorescence images of control (non-treated) cells, transfected with RGN-GFP and then stained with Mitotracker and Hoechst, visualized with green, red and blue filters, respectively. The average Pearson's correlation coefficients was 0.192 (SD \pm 0.073) for the RGN-GFP co-localisation with the mitochondria (see figure 4.3.5.2.1B) and 0.564 (SD 0.036) for the RGN-GFP with the nuclei (see figure 4.3.5.2.1C). This analysis suggests, under control conditions RGN-GFP co-localises to some extent with the mitochondria (and probably the cytosol), but shows little co-

localisation with the mitochondria. Analysis of several other images showed similar results.

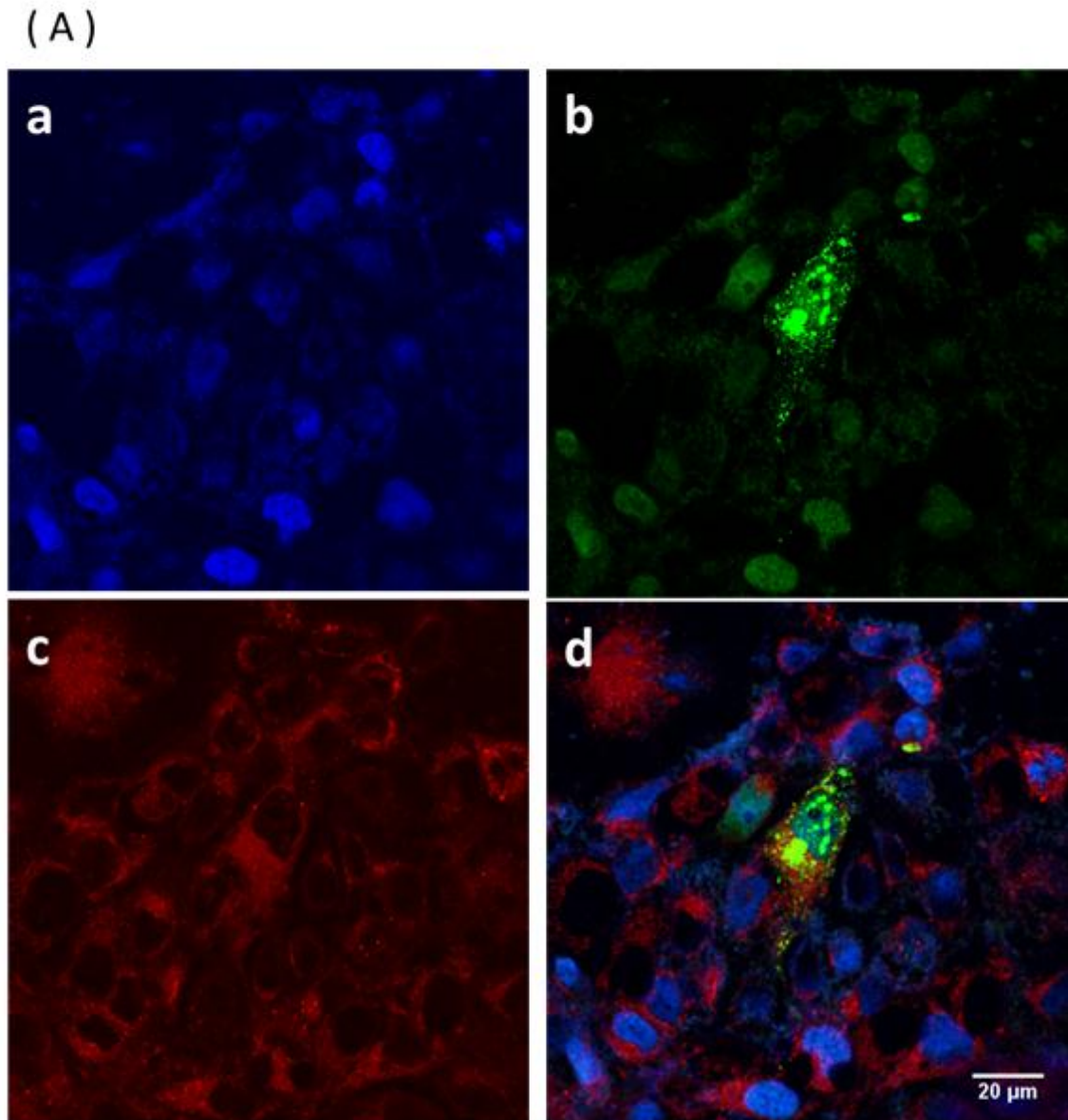


Figure 4.3.5.2.1A; fluorescence images with confocal microscopy of untreated COS-7 cells. (a) blue channels (for Hoechst i.e. nuclei), (b) green channels (for RGN-GFP); (c) red channels (for Mitotracker); (d) merged image of (a), (b) and (c).

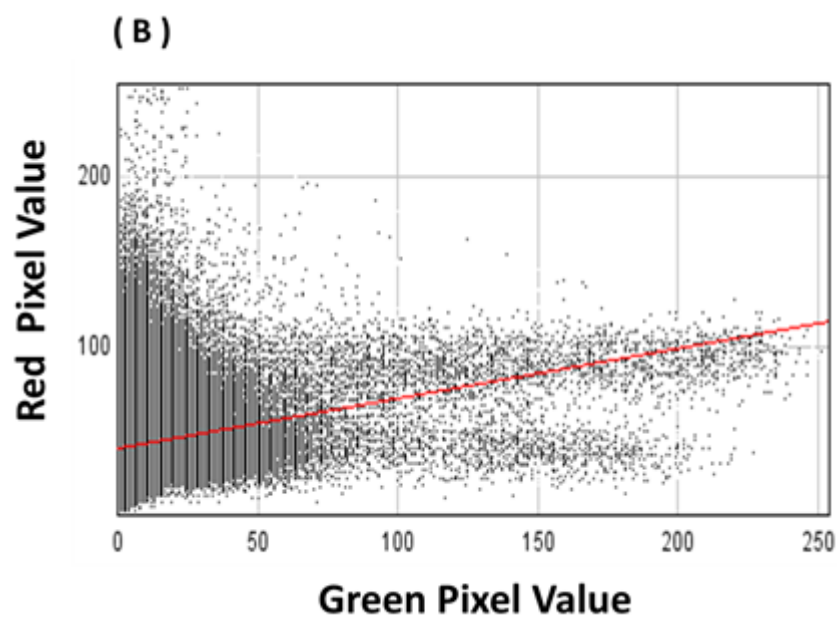


Figure 4.3.5.2.1B; colocalization data analyzed with JACOps plugin for COS-7 cells of red and green channels. Co-localisation with RGN-GFP and Mitotraker® Deep RedFM. Scatterplot of red and green pixel values gives a with Pearson's correlation coefficient value of 0.265 (For this specific image).

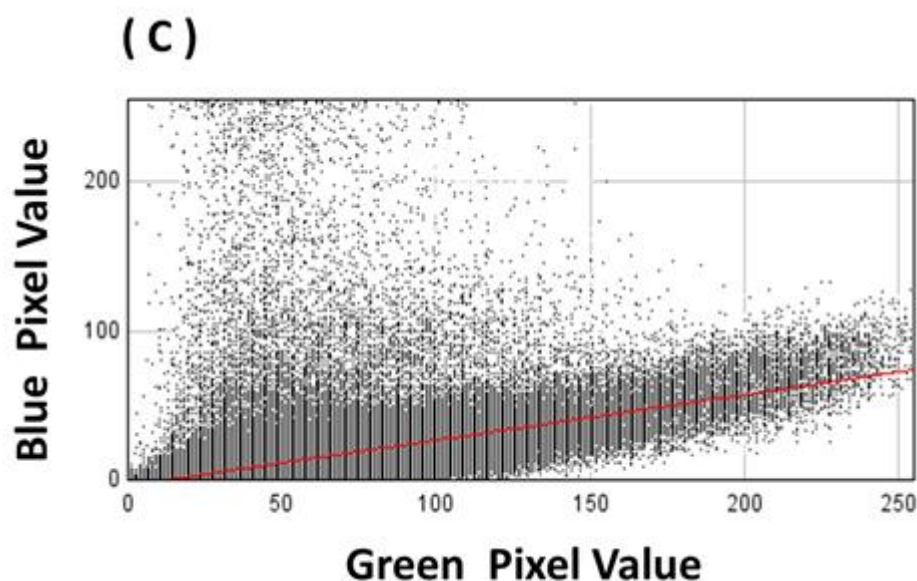


Figure 4.3.5.2.1C; colocalization data with JACOps plugin for COS-7 cells of blue and green channels. Co-localisation RGN-GFP and nuclei. Scatterplot of blue and green pixel values gives a Pearson's correlation coefficient value of 0.596 (For this specific image).

Figure 4.3.5.2.1D shows DOX treated COS-7 cells during late apoptosis (as the cells shows nuclear condensation, cell shrinkage and membrane blebbing). The cells were transfected with RGN-GFP and pretreated with DOX (3 hrs) then stained with Mitotracker and Hoechst and visualized with green, red and blue filters, respectively. The average Pearson's correlation coefficients was 0.8 ($SD \pm 0.0817$) for the RGN-GFP colocalisation with the mitochondria (see figure 4.3.5.2E) and 0.412 ($SD \pm 0.048$) for the RGN-GFP with the nuclei (see figure 4.3.5.2.1F). This analysis indicates that RGN-GFP were strongly co-localised with the mitochondria, and with possibly some colocalisation with nuclei.

(D)

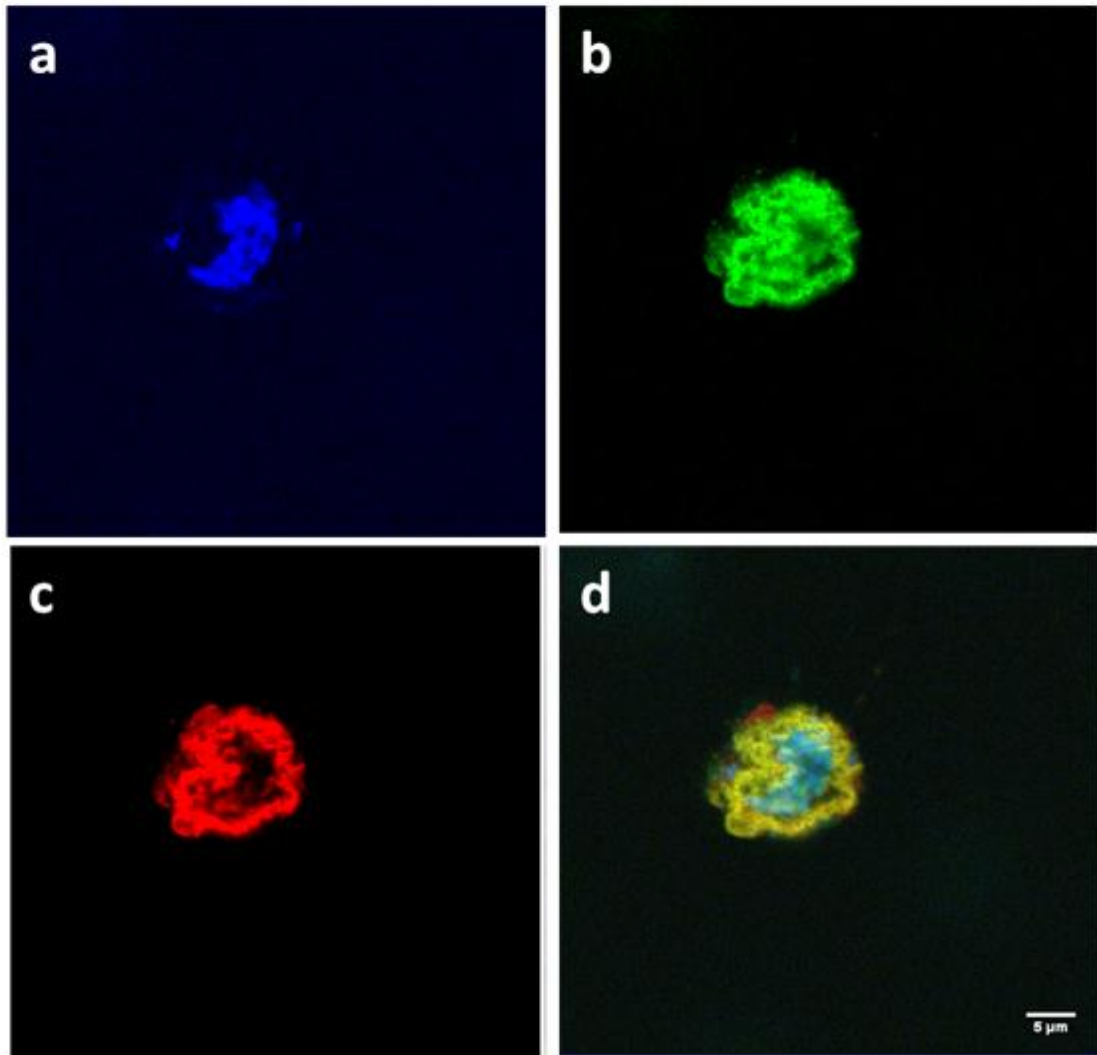


Figure 4.3.5.2.1D; fluorescence images of late apoptotic COS-7 treated with DOX. (a) blue channels (with Hoechst i.e. nuclei); (b) green channels (for RGN-GFP); (c) red channels (with Mitotracker), (d) merged image of (a), (b) and (c).Cells were first transfected with RGN-GFP then treated with 7 μ M DOX, and then followed by staining with Mitotracker and Hoechst before fixing the cells.

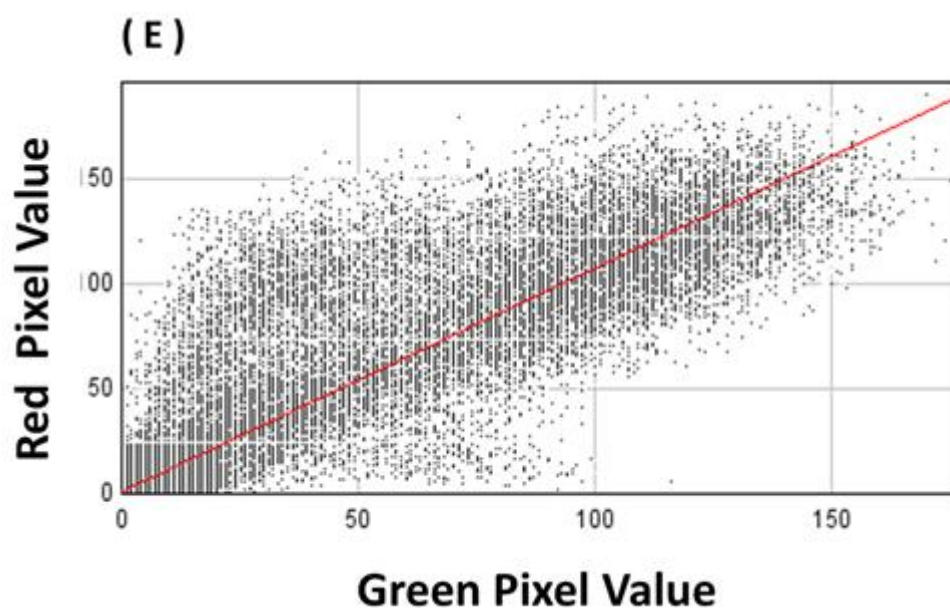


Figure 4.3.5.2.1E; colocalization data analysed with JACOPs plugin. Scatterplot of red and green pixel values of doxorubicin treated cells, Pearson's correlation coefficient value of 0.921 (For this specific image).

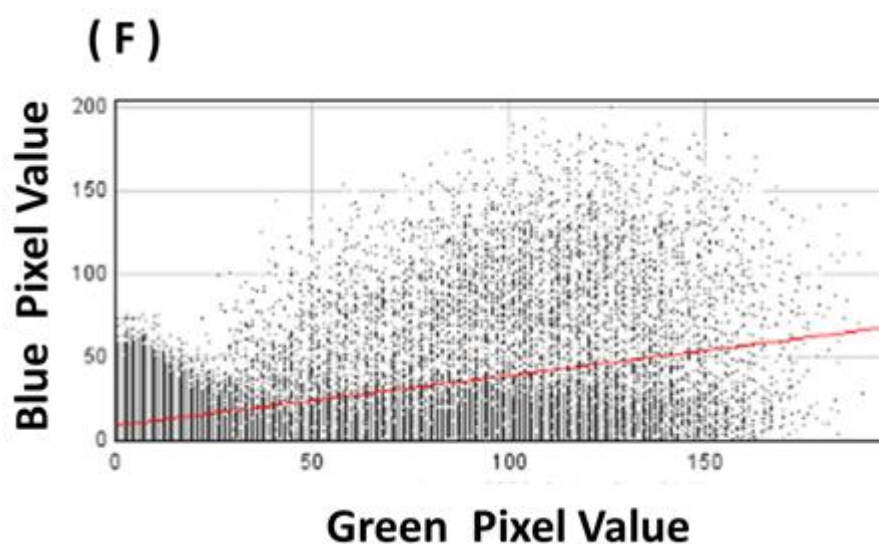


Figure 4.3.5.2.1F; colocalization data analysed with JACOPs plugin, scatterplot of blue and green pixel values of doxorubicin treated cells, Pearson's correlation coefficient value was 0.463 (For this specific image).

4.3.5.2.2 Co-localization of RGN-GFP with COS-7 cells and Etoposide

Once, the co-localization and the overlap of RGN has been demonstrated with DOX, similar experiments were done with etoposide to investigate whether a different drug causes a similar effect. 150 μ M as Etoposide was used to treat the cells. COS-7 cells were plated on 6 well plates with coverslips and attachment allowed over 24 hrs. Cells were transfected with RGN-GFP for 24 hrs. Next day, cells were treated with etoposide (150 μ M.) for 3 hrs then stained with Mitotracker and Hoechst stain. Images below in figure 4.3.5.2.2A shows apoptotic COS-7 cell with Hoechst nuclear staining (A), RGN-GFP staining (B), Mitro-traker staining (C) and the three merged images (D) of COS-7 cells treated with etoposide for 2hr.

The average Pearson's correlation coefficients (PCC) was 0.795 ($SD \pm 0.145$) for the RGN-GFP colocalisation with the mitochondria (see figure 4.3.5.2.2B) and 0.421 ($SD \pm 0.103$) for the RGN-GFP with the nuclei (see figure 4.3.5.2.2C). This analysis suggests that RGN-GFP strongly co-localised with the mitochondria, but not with the mitochondria. This suggested increased co-localization of RGN to the mitochondria during chemotherapy drugs treatment compared to untreated cells, which suggests that RGN might be involved in reducing apoptosis via the mitochondria.

(A)

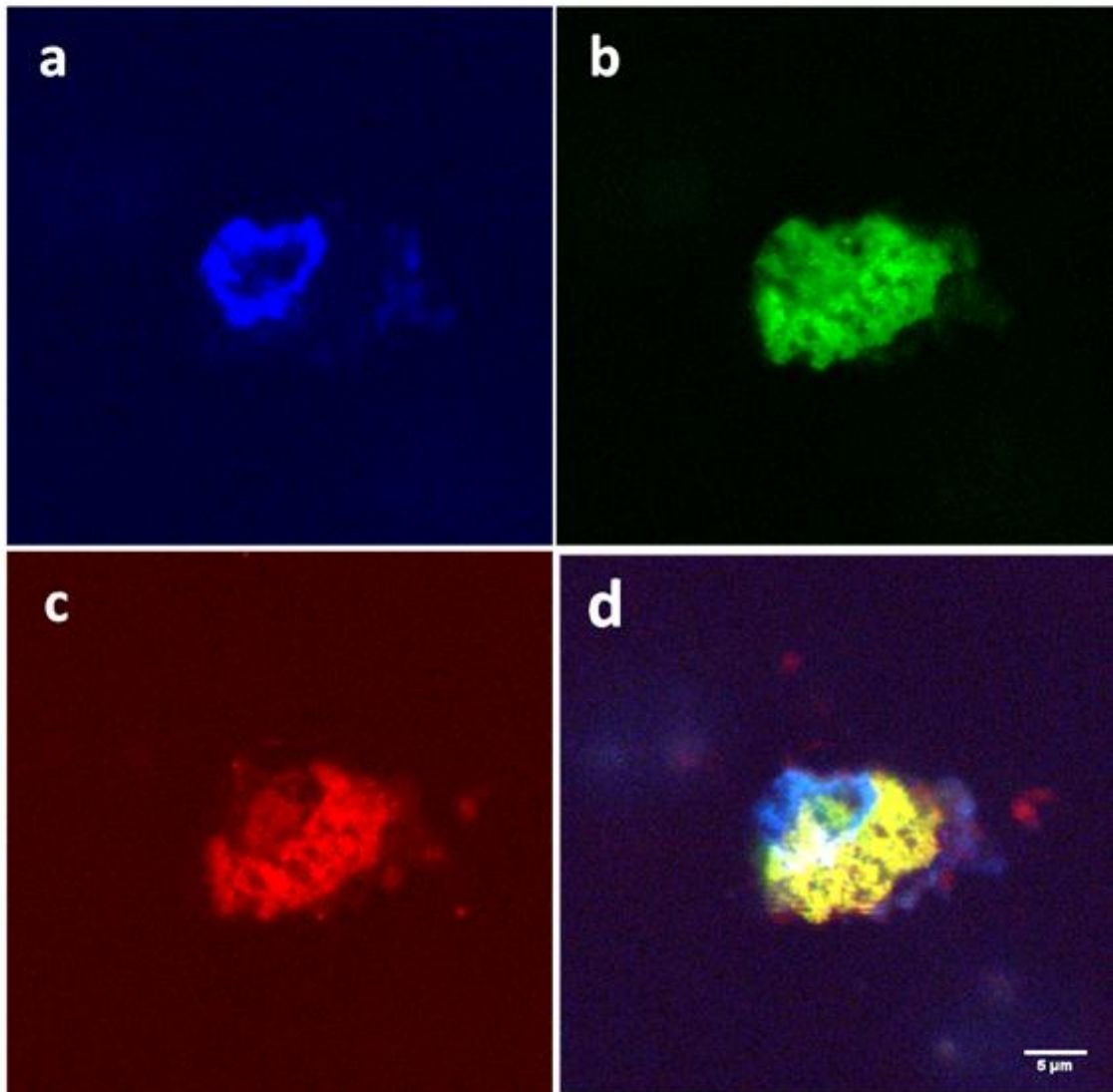


Figure 4.3.5.2.2A; treated COS-7 cells with Etoposide (150 μM). (A) Blue channels (for Hoechst ie nuclei), (B) green channels (for RGN-GFP); (C) red channels (for Mitotracker) and (D) overlay of the three channels.

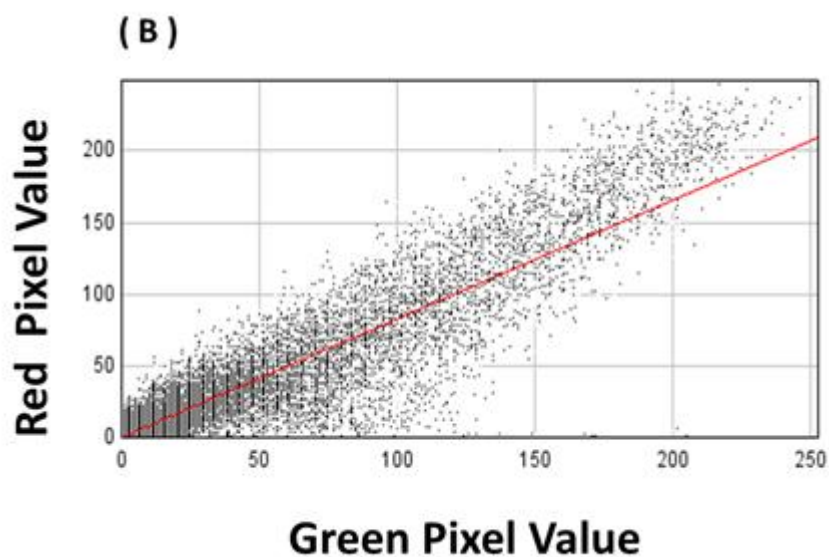


Figure 4.3.5.2.2B; colocalization data analysed with JACOps plugin for Etoposide (150 μ M) treated COS-7 cells in the red and green channels. RGN-GFP and Mitotracker® Deep RedFM (mitochondria) scatterplot of red and green pixel values, with average of Pearson's correlation coefficient value of 0.782 (For this specific image).

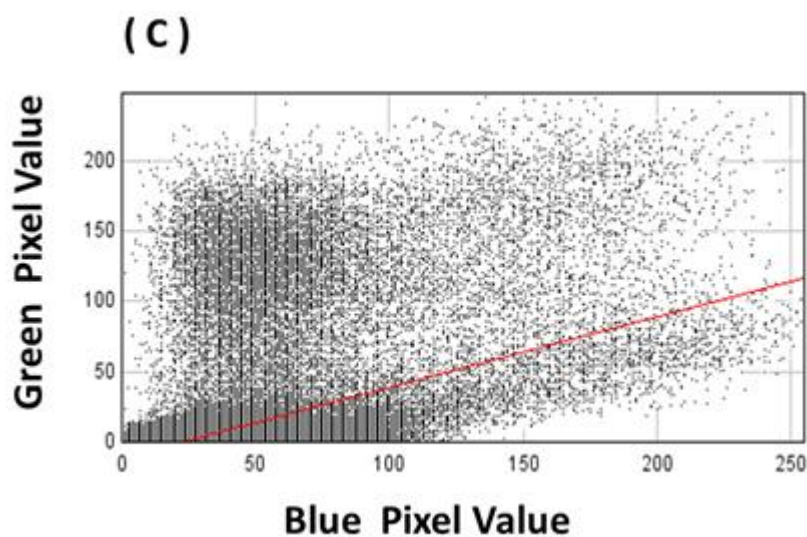


Figure 4.3.5.2.2C; colocalization data with JACOps plugin for Etoposide (150 μ M) treated COS-7 cells in the blue and green channels. RGN-GFP and Hoechst scatterplot of red and green pixel values with Average of Pearson's correlation coefficient value of 0.435.

4.3.5.2.3 Co-localization of RGN-GFP within COS-7 during the early stages of Doxorubicin treatment

Figure 4.3.5.2.3A shows control (non-treated) COS-7 cells. Cells were transfected with RGN-GFP and stained with both Hoechst and Mito-tracker before fixing. It is obvious, that the RGN-GFP location in control cells is distributed around the cell body and can be seen in nuclei, cytoplasm and mitochondria. As shown earlier, the average PCC values is 0.354 ($SD \pm 0.044$) for the RGN-GFP co-localisation with the mitochondria and 0.608 ($SD \pm 0.065$) for the RGN-GFP co-localisation with nuclei (which is similar to data presented in 4.3.5.2.1B and C).

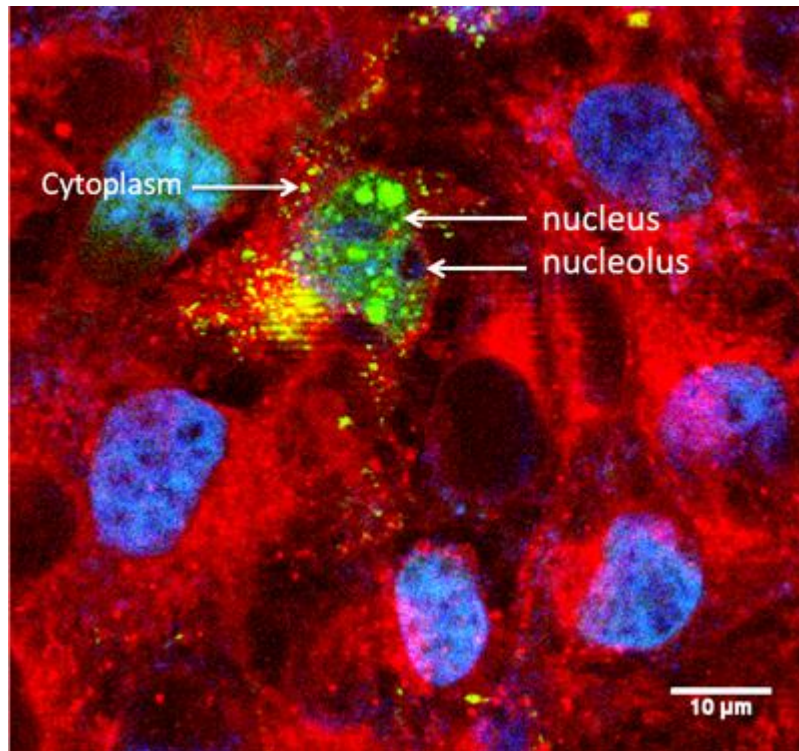


Figure 4.3.5.2.3A; merged image of fluorescence images obtained by confocal microscopy. COS-7 cells transfected with RGN-GFP but untreated with drug and fixed and then stained with Hoechst (Blue) and Mito-tracker (Red) at 1 µg/ml and 0.5 µM, respectively.

Figure 4.3.5.2.3B RGN-GFP transfected cells which were then treated with DOX (7 μ M) for approximately 1hrs and then stained with fluorescence dyes (Hoechst and Mito-tracker). These cells were considered at the early stage of cell death and no obvious morphological changes can see that the RGN-GFP is strongly localise to the nuclei and possibly accumulated around the nucleolus. The average of PCC values shows a limited correlation of 0.32 (SD \pm 0.016) of RGN-GFP with mitochondria and a very positive correlation OF PCC value 0.653 (SD \pm 0.06) for RGN-GFP with nuclei. Figure 4.3.5.2.3C and D plotted the overlap of green-red and green-blue pixels channels, respectively.

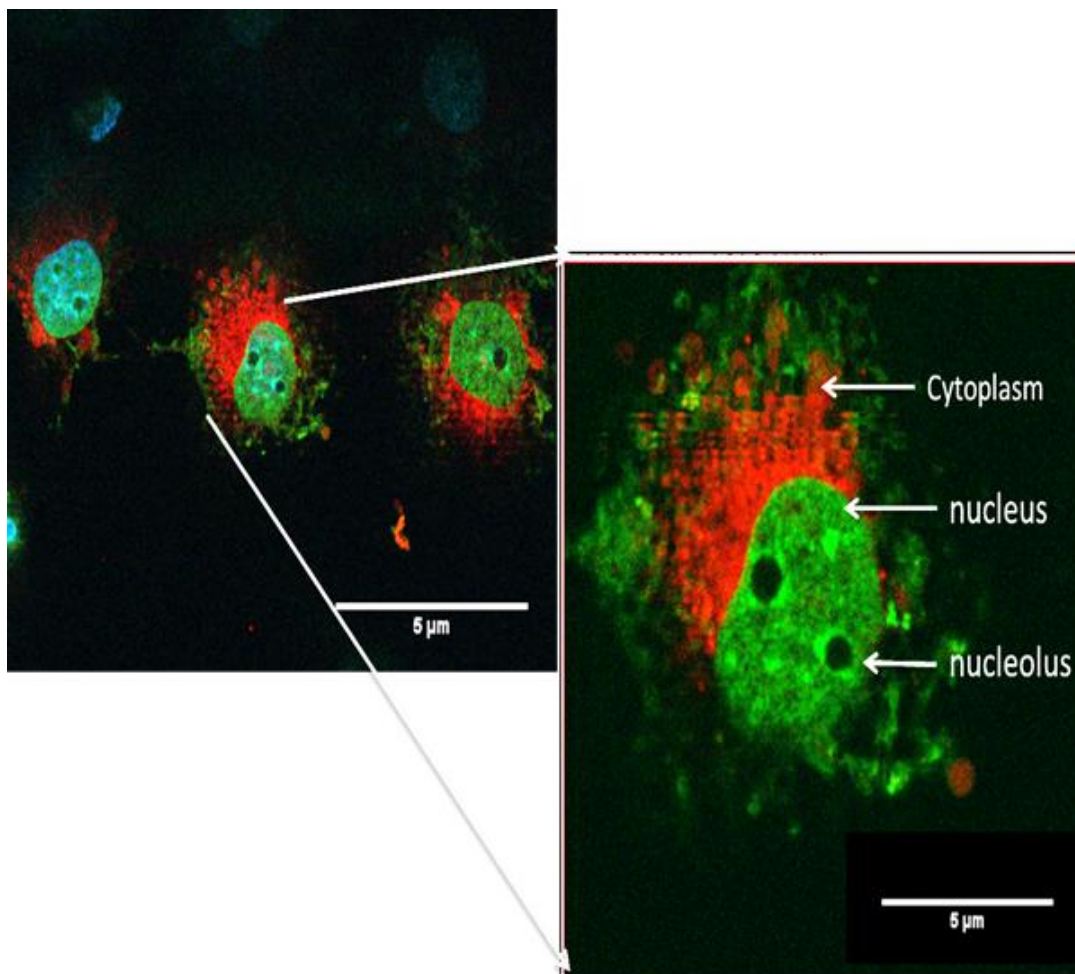


Figure 4.3.5.2.3B; fixed Fluorescence emerge images taken by confocal microscope for DOX treated COS-7 cells at early stage of apoptosis. Cells expressed RGN-GFP and then treated with (7 μ M) DOX for 1 h and then stained with 1 μ g/ml Hoechst (blue) and 0.5 μ M Mito-tracker red stain.

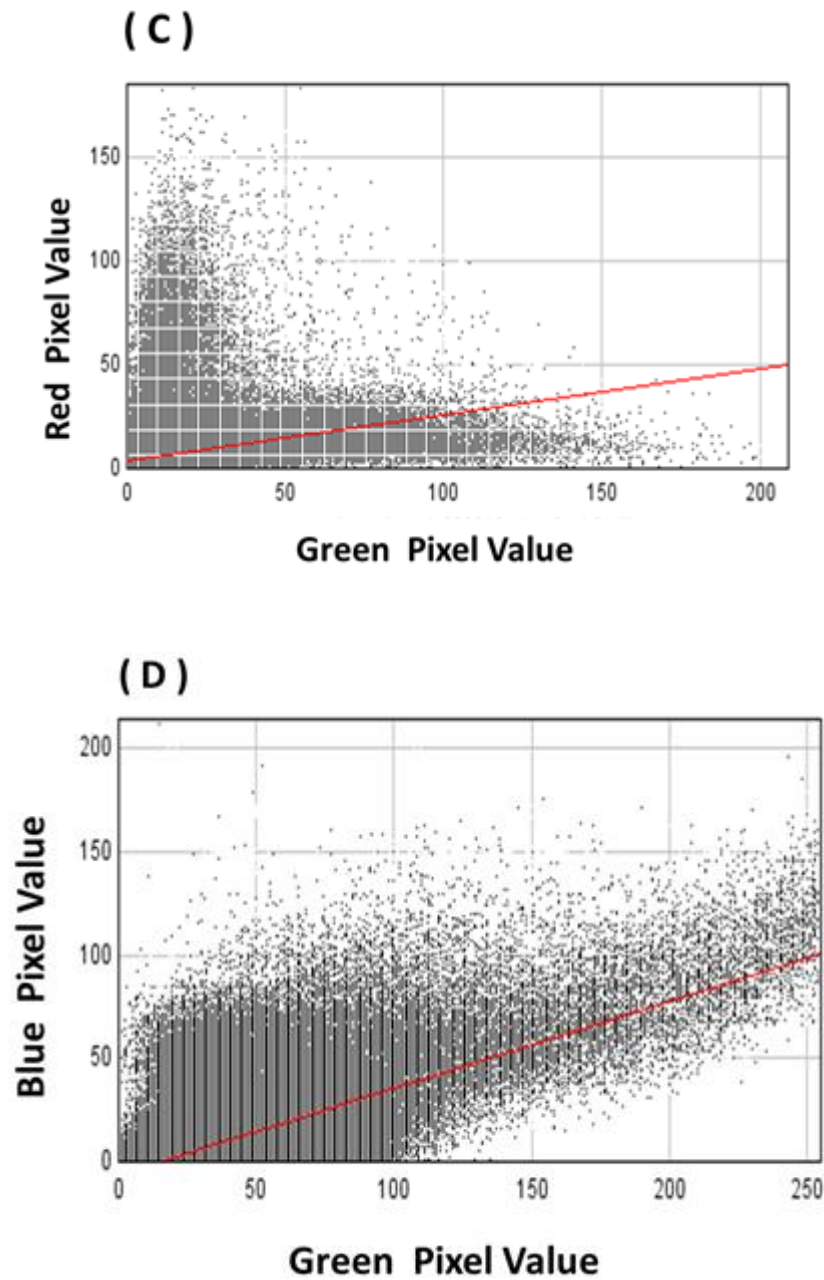


Figure 4.3.5.2.3C and D; colocalization analysis of RGN-GFP transfected COS-7 cells treated with DOX for a short time of period. (C) scatter plot of green and red pixel intensities (PCC 0.301), D scatterplot of green and blue pixel intensities (PCC 0.605), of RGN-GFP transfected COS-7 cells and treated with DOX.

4.3.6 Treating HepG2 cells with different calcium concentration

4.3.6.1 Measuring RGN expression by western blot

The level of liver RGN was shown to increase when rats were fed with a diet of high calcium (Misawa and Yamaguchi, 2002; Yamaguchi, 2009). In these experiments we aimed to investigate whether calcium levels in the media could affect RGN levels in HepG2 cells. Therefore, HepG2 cells were seeded on 6 well plate and left for 24 hrs to attach to the surface, then cells were treated with media containing different calcium concentrations (0 mM, 1.8 mM, and 10 mM). After 48 hrs the cells were washed with PBS and cell lysates were prepared and the protein concentration estimated. Western Blot were performed, each lane loaded with the same amount of protein (30 µg), and labelled with the anti-RGN primary antibody. The results in figure 4.3.6.1 shows that with no Ca^{2+} in the media the intensity of band for RGN which is considerably lower than cells in group (1.8 mM Ca^{2+}) or (10 mM Ca^{2+}) respectively. Therefore, these results indicate that increasing the calcium concentration in the media could increase the level of RGN expresses in HepG2 cells.

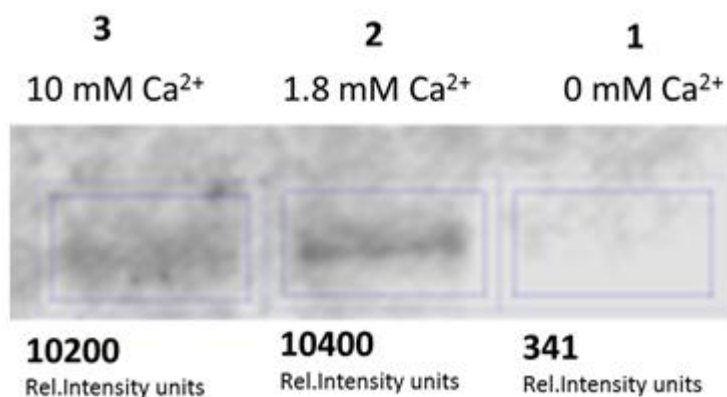


Figure 4.3.6.1; western blotts of RGN expression in HepG2 cells. 30 µg cell lysate were resolved on a 10% SDS-PAGE gels then transferred on to nitrocellulose. The anti-mouse RGN was used to probe the membrane. (1) indicated cells grown with no Ca^{2+} media, (2) cells grow in 1.8 mM Ca^{2+} media, while group (3) cells grown in 10 mM Ca^{2+} media.

4.4 Discussion

In this chapter I investigated the role of regucalcin (RGN) in protecting against cell death using two different versions of human RGN (SMP30, RGN-GFP). The study started by testing the role of RGN in decreasing the nephrotoxicity of the chemotherapy drugs (Etoposide, Cisplatin, and DOX) in COS-7 cells and the hepatotoxicity of DOX in HepG2 cells. Later, the effect of RGN on the cells viability, cell proliferation and localisation were studied.

We found that COS-7 cells that overexpressed SMP30 (without the GFP tag) had the ability to decrease the toxicity of the chemotherapy drugs such as Etoposide, Cisplatin, and DOX. The LC_{50} of PCDNA alone transfected cells were 200, 50 and 3 μ M, respectively, and these were shifted to > 500, > 300 and 20 μ M in SMP30 overexpressing cells treated with Etoposide, Cisplatin, and DOX, respectively. This therefore suggests the protective role for RGN in cell death. Our findings is supported by other studies, which showed a suppressive effect of RGN on apoptosis in kidney cells treated with TNF- α , LPS, Bay K 8644 or thapsigargin (Nakagawa and Yamaguchi, 2005 b). Accordingly, RGN has an important role in minimizing the amount of apoptotic cell through various signaling factors (Yamaguchi, 2013). Since TNF- α enhanced the mRNA expression of caspase-3 in cloned normal rat kidney proximal tubular epithelial cells (NRK52E), and the overexpression of RGN shows suppressor effect, therefore, RGN might also cause a decrease of the caspase-3 mRNA expression. This could support, in part, our findings that these chemotherapy drugs causes apoptosis via activating caspase-3 protein and RGN could reduce this. In accordance to our previous funding in chapter 3, it was shown that these drugs mediate various types of cell death (apoptosis, necrosis and autophagy), we therefore hypothesis that RGN might also play a role in protecting cells not just through apoptosis but also through the other forms of cell death (necrosis and autophagy) as well. This has not been suggested before and could open up new research into how this protein controls these other types of cell death.

COS-7 cells transfected with either RGN-GFP or SMP30 showed a significant decrease in cell number compared to PCDNA alone transfected cells ($p > 0.001$). Therefore, RGN shows it has a role to play in suppressing/slowing down cell proliferation and this

finding is supported by several other studies (Yamaguchi, 2012) that have suggested that cell proliferation may be regulated by RGN by causing cell cycle arrest at G1 and G1/M phase (Nakagawa et al., 2005).

Co-localization experiments and time-lapse photography to visualize the movement of RGN under cell stress (figure 4.3.5.1) has shown the movement of RGN towards the cell body when DOX was added to COS-7 cells within a very short time of about 25 min. Therefore, more detailed experiments were necessary, to investigate this behaviour further. The results in figure 4.3.5.2.1A show that RGN is normally distributed within the cytoplasm and nucleus, but limited within the mitochondria. COS-7 cells treated with DOX and in late apoptosis showed a very significant co-localisation with mitochondria, but only limited-colocalisation within nuclei (see figure 4.3.5.2.1D, E and F), and this also was the case when cells were treated with Etoposide. This suggests that RGN is usually distributed mostly in cytosol and nuclei in normal conditions, however this protein appear to move from the nuclei to the mitochondria during the latter stage of apoptosis possible trying to protect cells from cell death, by potentially altering mitochondrial mediated processes.

Cells in the early stages of apoptosis which is still have a normal structure, appeared to show possibly more colocalisation within nuclei, these results could be explained by the fact that RGN is a transcription factor regulator and participates in gene regulation at the nuclear level (Yamaguchi et al., 2003, Sawada et al., 2005). This observation appears to be the first reported case that RGN can translocate to the mitochondria during severe cell stress. RGN is able to increase Ca^{2+} uptake in mitochondria, which could also contribute to cell death (Takahashi and Yamaguchi, 2000 and Omura and Yamaguchi, 1999). Such a translocation of RGN from the cytoplasm to mitochondria could explain, the fact that as both DOX and etoposide induce oxidative stress (Kanchana Gang et al., 2013; Deaval, 2012 and Zhou 2001), therefore, RGN going to the mitochondria may be trying to control this oxidative stress (Ichikawa and Yamaguchi, 2004).

Another interesting observation, in RGN-transfected cells that have been treated with DOX to a limited extent, is that although the cells show a normal cell structure, there is appears to be clear accumulation of RGN around the nucleolus (see figure 4.3.5.2.3B). This finding is also novel and could suggest the involvement of RGN in some of the

roles of the nucleolus, such as ribosome biogenesis, regulation of mitosis, cell cycle progression and proliferation (Michel-Boisvert et al., 2007, Lempiäinen and Shore, 2009). However, further study is required to assess this in more detail.

After demonstrating the protective role of RGN to drug-induced toxicity, a more natural approach to increasing the expression of RGN was considered. As previous studies had shown that treating rats with a high Ca^{2+} diet caused an increased the expression of RGN in rat liver (Shimokawa and Yamaguchi, 1992), we tested the effects of Ca^{2+} in the media on RGN expression in cells in culture.

In cultured HepG2 cells, the results presented here clearly shows that Ca^{2+} in the culture media can affect the level of RGN expression, although the response appears to saturate after 2 mM Ca^{2+} , which is the normal range seen in plasma. Further experiments are required to assess whether other factors such as hormones (i.e. Calcitonin) can elevate RGN levels in cells (Isogai and Yamaguchi, 1995). If modulation of RGN levels in patients could be achieved by simple means such as increasing serum Ca^{2+} by ingestion and the use of hormones, this could potentially have beneficial effects, since a recent study on patients with pancreatic cancer showed a better prognosis if the tumor biopsy showed elevated level of RGN (Yamaguchi and Murata, 2015).

CHAPTER 5

SERCA and SPCA expression in
COS-7 cells and drug treatment

5 SERCA and SPCA expression in COS-7 cells and drug treatment

5.1 Introduction

Calcium ions are second messengers, involved in various cellular function including cell proliferation and death (Chemaly et al., 2013). It is well documented that interfering with the sequestration of Ca^{2+} into intracellular can trigger apoptosis as a part of a stress response (Orrenius et al., 2003), and many chemotherapy drugs such as Cisplatin can lead to this stress response (Foufelle and Froment, 2016). Several recent studies using Cisplatin and Doxorubicin have shown that they are able to cause a rise in intracellular $[\text{Ca}^{2+}]$ levels (Shen et al., 2016; Bartlett et al., 2016; Al-Taweel et al., 2014). This rise in intracellular $[\text{Ca}^{2+}]$ levels has been potentially attributed to their effects on a number of Ca^{2+} transporters such as the voltage operated Ca^{2+} channels (Al-Taweel et al., 2014); IP_3 receptors (Shen et al., 2016; Splettstoesser et al., 2007); Ryanodine receptors (Hanna et al., 2014); SERCA2a Ca^{2+} pumps (Hanna et al., 2014) and plasma membrane Ca^{2+} pumps, PMCA2 (Peters et al., 2016).

A recent study in heart has shown that overexpressing SERCA2a can reduce the cardiotoxicity induced by Doxorubicin (Mattila et al., 2016). In the Michelangeli lab a similar effect was also noted, where the toxic effects of a number of environmental pollutants on neuroblastoma cells could be reduced if the cells were transfected to overexpress SERCA (Al-Mousa, PhD thesis 2010).

In this study, the focus is on determining whether elevated Ca^{2+} plays a role in Cisplatin- and Doxorubicin-induced cell death in COS-7 cells. In addition, this chapter also focusses on whether overexpressing endoplasmic reticulum Ca^{2+} pump (SERCA 1b and 2b) as well as the Golgi localized secretory pathway Ca^{2+} pump (SPCA1 and SPCA2) in COS-7 cells (a kidney-derived cell line), can reduce the toxicity caused by Cisplatin and Doxorubicin, which are known to be nephrotoxic (Miller et al., 2010 and Lahoti et al., 2012).

In order to more easily assess the expression levels of these Ca^{2+} pumps, as well as determine their intracellular localization, green fluorescent protein constructs of SERCA and SPCA were used. The plasmids used for the expression of these fluorescence versions of the various Ca^{2+} pumps have already been characterized in detail and shown

to produce functional Ca^{2+} pumps with respect to Ca^{2+} dependent ATPase activity and or Ca^{2+} uptake (Newton et al., 2003; Wootton, 2004; Lai, 2009, Al-Mousa, PhD thesis, 2010, Baron et al., 2010).

5.2 Effect of BAPTA-AM on DOX-induced cell death in COS-7 cells

To determine whether cell death caused by DOX is via calcium-mediated process, BAPTA-AM, an intracellular calcium chelator, was used. Figure 5.2 shows COS-7 cells were incubated with BAPTA-AM (10 μM) for 5 hrs and then the cells were exposed to DOX (10 μM). The Cells were then incubated for 48 hrs and then MTT assays were performed. This figure that pre-incubation with BAPTA has little effect upon cell viability. Also shown is that 10 μM DOX causes a decreases in cell viability of approx. 60%. However, if the cells were first pre-treated with BAPTA-AM, then significantly more cells remained viable ($p < 0.05$).

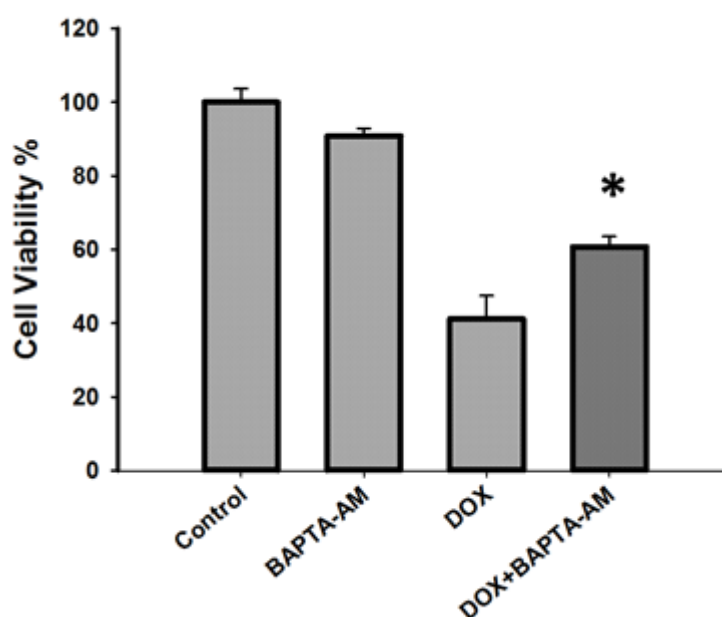


Figure 5.2; shows the effects of Doxycubicin with and without BAPTA-AM pre-treatment in COS-7 cells. The cells were pretreated with or without BAPTA-AM (10 μM) for about 5 hours and then exposed to DOX (10 μM) for 48 hrs at 37°C. Data represents the mean \pm S.D of 3-4 determinations. (* value points were significant different from the controls, $p \leq 0.05$), using the t-test.

5.3 The effects of BAPTA-AM on Cisplatin-induced cell death in COS-7 cells

Again in order to determine whether cell death caused by Cisplatin is calcium-dependent BAPTA-AM was used. Figure 5.3 shows COS-7 were pre-treated with BAPTA-AM (10 μ M) for 5 hr and then treated with cisplatin (65 μ M) at 37 °C for 48 hrs. BAPTA-treated cells had significantly higher cell viability than cells treated with cisplatin alone, under the same conditions ($p < 0.05$).

Taken together, these results with BAPTA-AM pre-treatment would suggest that both Cisplatin and DOX causes COS-7 cell death, at least in part, through a Ca^{2+} -dependent process and is therefore consistent with the previous findings that also suggested a role for Ca^{2+} in the toxicity by DOX and Cisplatin (Mattila et al., 2016, Shen et al., 2016 and Al-Taweel et al., 2014).

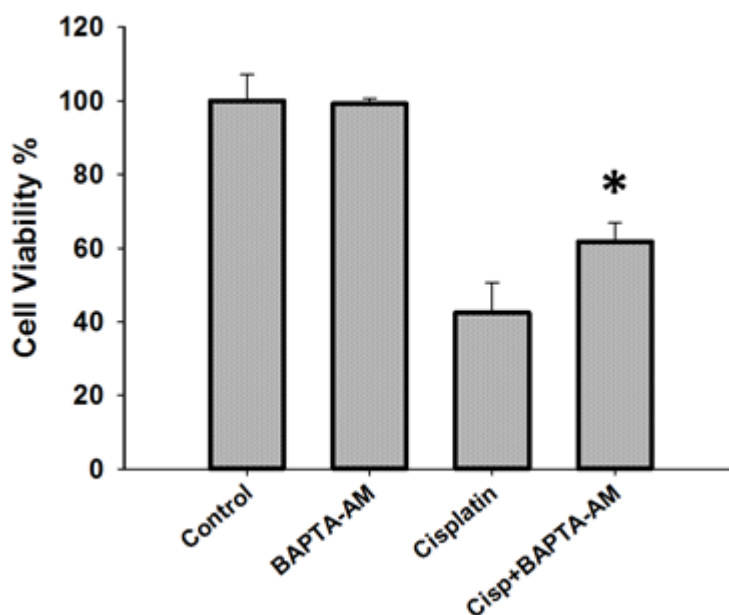


Figure 5.3; shows the effects of Cisplatin with and without BAPTA-AM pre-treatment in COS-7 cells. Cells were exposed to the Cisplatin (65 μ M) for 48 hrs at 37 °C. Data represents the mean \pm SD of 3-4 determinations. (* value points were significant different from the controls, $p \leq 0.05$), using the t-test.

5.4 SERCA detection, over-expression and cytoprotection

Two different SERCA isoforms were used (SERCA 1b and SERCA2b) tagged with GFP. For these studies the COS-7 cell line was used because we already had a substantial amount of data with regards the nephrotoxicity of the chemotherapy drug and they were also the easiest and most consistent to culture and transfect.

The mammalian expression plasmids for the Ca^{2+} ATPases used were as follows:

pcDNA3.1 Rabbit SERCA1b-N-GFP (Newton et al., 2003, Wotton, PhD thesis 2005, Al-Mousa, PhD thesis, 2010)

pcDNA6.2 Human SERCA2b-N-GFP (Baron et al., 2010)

pcDNA6.2 Human SPCA1a-N-GFP (Baron et al., 2010)

pcDNA6.2 Human SPCA2-N-GFP (Baron et al., 2010)

The plasmid identities were confirmed through diagnostic restriction enzyme analysis.

5.4.1 SERCA detection in normal cells

Figure 5.4.1 shows successful detection of SERCA expression in normal (un-transfected) HepG2 and COS-7 cells. The cell lysates were prepared and the extracts run by SDS-PAGE transferred onto nitrocellulose membranes and then probed with the pan-SERCA primary antibody (Y1F4 at 1/1000 dilution). These cells clearly expressed SERCA of the correct MW i.e. approximately 100KDa. Since natural levels of SERCA were already relatively high in these cells, it was decided that GFP tagged Ca^{2+} ATPases be used for over-expression studies so that cells expressing higher SERCA levels could be clearly identified post transfection.

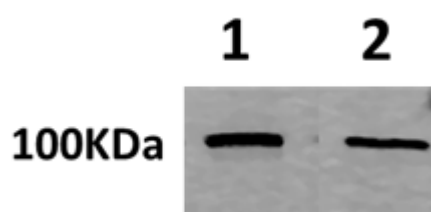


Figure 5.4.1; western blot of HepG2 (1) and COS-7 (2) cell lysate for SERCA. Total amount of protein loaded into each cell was 100 μ g. The cells were incubated with the pan –SERCA primary mouse antibody, Y1F4.

5.4.2 Overexpression of SERCA

COS-7 cells were transfected with SERCA1-GFP and SERCA2b-GFP expressing plasmids. The cells were seeded on to 6 well plates and then transfected with two different conditions (1 μ g DNA+4 μ l TR; condition 1:4) and (1 μ g DNA+ 2 μ l TR; condition 1:2). The transfected cells were examined under fluorescence microscopy after 24 and 48 hrs. After counting the total number of cells compared to those that were fluorescent, condition 1:2 was found to be the best condition and therefore used for the series of next experiments. Figure 5.4.2 shows COS-7 cells transfected under different SERCA1-GFP conditions, 24 hrs after transfection. Table 5.4.2 shows the transfection efficiency using both conditions, for both SERCA1-GFP and SERCA2b-GFP expression.

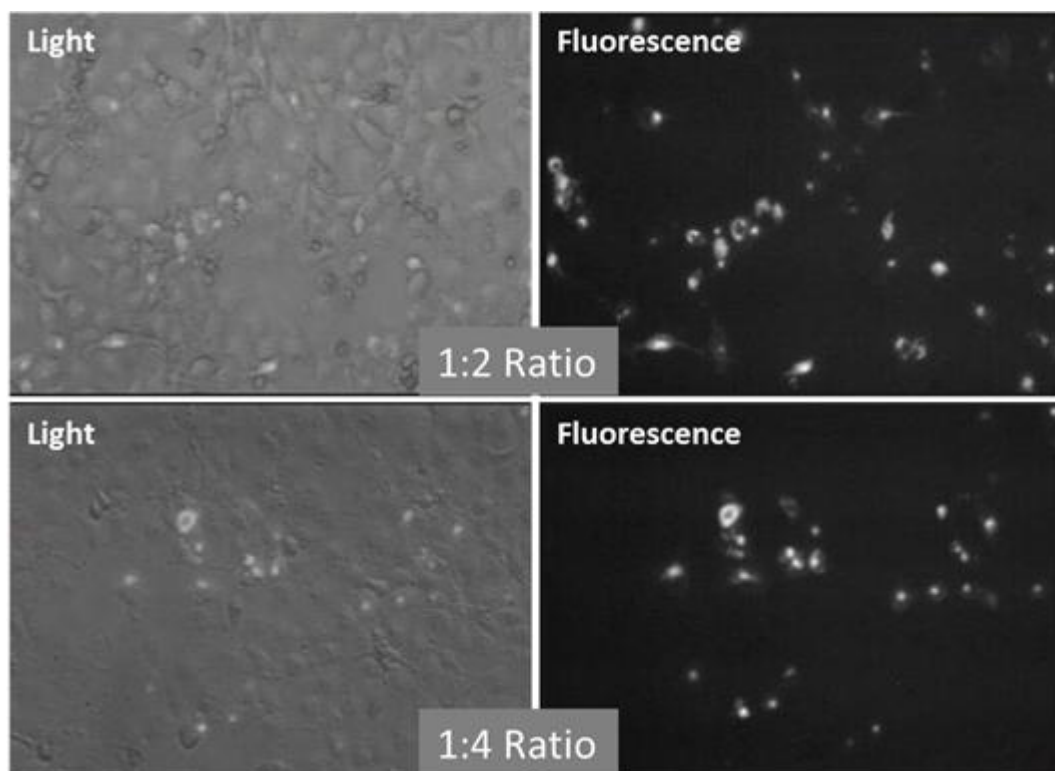


Figure 5.4.2; transfected of COS-7 cells with the two different condition of SERCA1-GFP plasmid. Ratio of 1 μ g SERCA1-GFP/2 μ l TR and 1 μ g SERCA1GFP/4 μ l TR were used to transfect cells. Fluorescence micrographs and light micrographs of the same field-of-view were used to determine the percentage of transfected cells (transfection efficiency).

Table 5.4.2; the transfection efficiency of the two different conditions of SERCA plasmid. Condition (1:2) and (1:4) refer to (μ g DNA plasmid+ μ l TR). The transfection efficiency was determined by counting the percentage of fluorescent cells against the total number of cells in the white light field. The data are from average of three different field-of-views in three replicate wells.

Transfection condition	1 μ g+2 μ l	1 μ g+4 μ l
Transfection efficiency	%	%
SERCA1-GFP	45	33
SERCA2B-GFP	35	25

5.4.3 High resolution visualisation of the localisation of SERCA-GFP using fluorescence microscopy

Both Ca^{2+} pump proteins (SERCA1 and SERCA2b) used in this project contained a GFP tag, which allowed for their localisation in the cell to be observed. COS-7 cells were transfected on to glass-bottomed dishes for high-magnification microscopy purposes. The nuclei were also stained with Hoechst 33342 stain. Figure 5.4.3 shows the location of SERCA1 and SERCA2b. The SERCAs showed a diffused distribution throughout the cytoplasm, as well as on the outside of the nuclear membrane, which is consistent with an ER location.

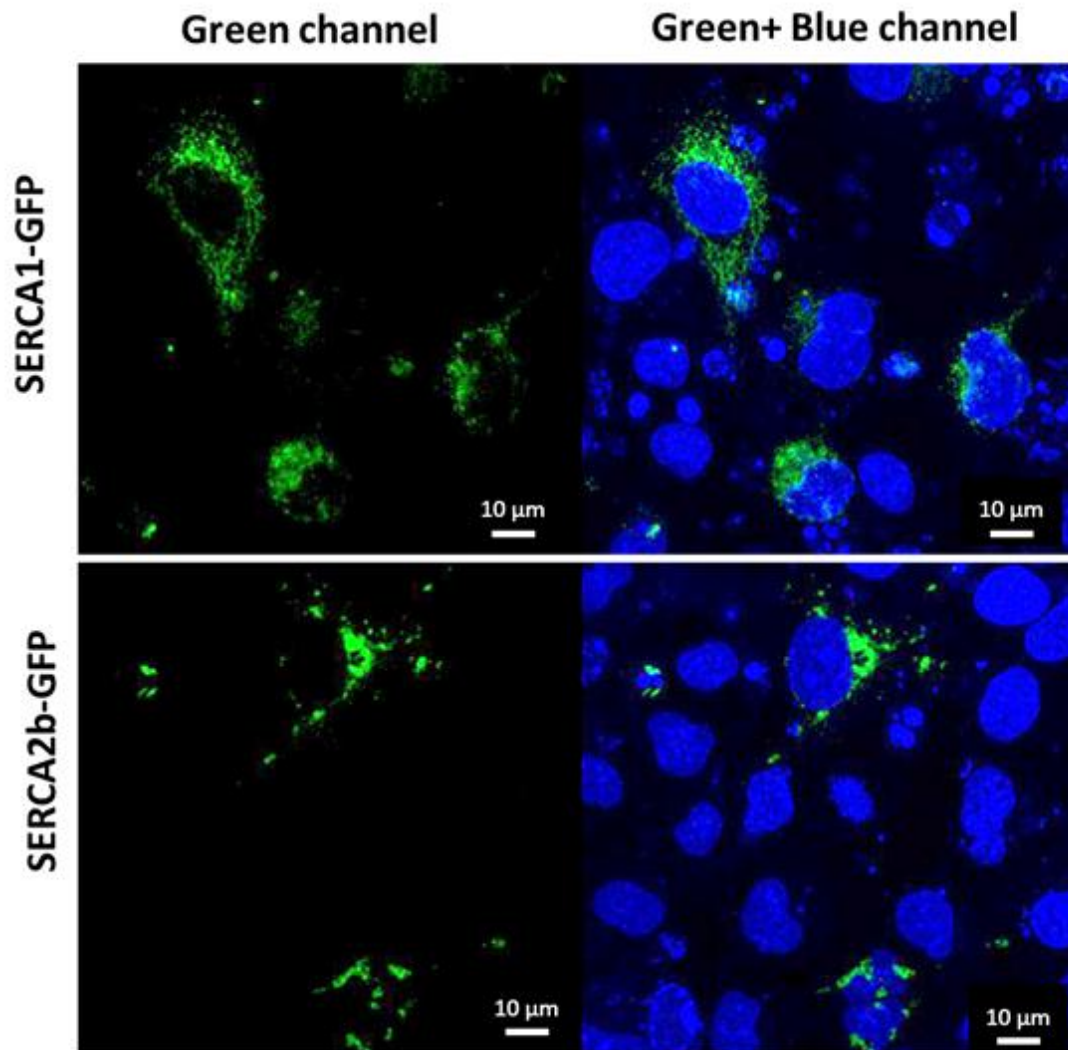


Figure 5.4.3; fluorescence images showing the localisation of SERCA1-GFP and SERCA2b-GFP in COS-7 cells. The cells were transfected with plasmid and the nuclei were also stained with Hoechst stain, allowing the nucleus to be visualised using the DAPI filter. The cells were visualised at 600x magnification. SERCA1-GFP and SERCA2b-GFP showed diffuse staining in the cell that resembles ER localisation. (These images were taken in association with Shi Ern, an MSc student).

5.4.4 The effects of SERCA-GFP overexpression on COS-7 cell viability

5.4.4.1 The effect of SERCA1-GFP overexpression on COS-7 cell viability when treated with chemotherapy drugs

To investigate whether SERCA1-GFP overexpression would decrease the nephrotoxicity of chemotherapy drugs COS-7 cells were overexpressed with SERCA1-GFP and PCDNA (empty vector) for 48 hrs with (1µg plasmid + 2µl TR), later on the cells were treated with different concentrations of either Cisplatin or DOX. MTT assays were then performed after 24 hrs of treatment.

Figure 5.4.4.1A shows the effects of DOX on cell viability were significantly different between the two groups (PCDNA and SERCA1-GFP) with a $p < 0.05$ at both 1 µM and 10 µM DOX concentrations. Therefore, this suggests that SERCA1 overexpression is reducing the toxicity by this drug.

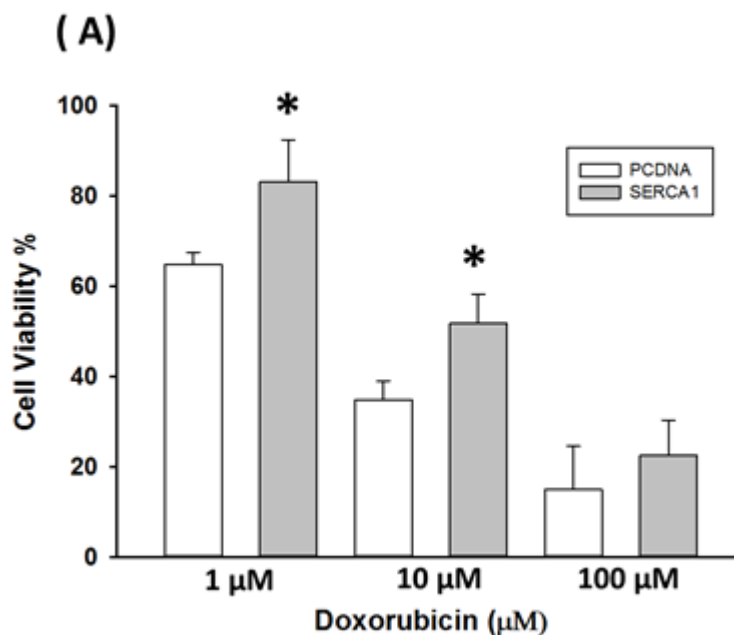


Figure 5.4.4.1A; the effect of DOX on COS-7 cell viability in the present of (SERCA1-GFP and PCDNA). Cells were transfected with SERCA1-GFP and then treated with DOX. MTT assays were carried out to determine the cell viability in both groups. The data pointed represent the mean \pm SD of 3-4 determines. (* $p < 0.05$, compared to PCDNA transfected cells).

Figure 5.4.4.1B shows the effects of Cisplatin on the viability COS-7 cells as measured using the MTT assay. In this case there was no significant difference between the two groups (PCDNA and SERCA1-GFP) at all concentrations tested. Therefore, this suggests that SERCA1 overexpression does not affect the toxicity by this drug.

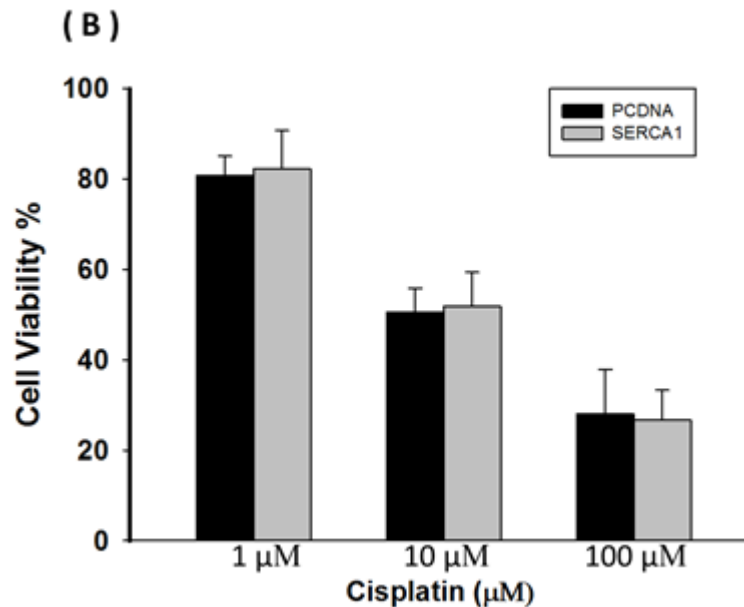


Figure 5.4.4.1B; the effect of Cisplatin on COS-7 cell viability in the presence of (SERCA1-GFP and PCDNA alone). Cells were transfected with SERCA1-GFP or PCDNA alone, when cells reached transfection efficiency 60% the cells were treated with the drug. MTT assay were then carried out to determine the cell viability in both groups. The data represent the mean \pm SD of 3-4 determines.

5.4.4.2 The effect of SERCA2b-GFP overexpression on COS-7 cell viability when treated with chemotherapy drugs

Figure 5.4.4.2A shows COS-7 cells were transfected with SERCA2b-GFP and PCDNA alone using the (1:2) ratio condition for 48 hrs, then cells were treated with DOX at different concentrations (0.1, 1, 10 and 100 μM). After 24 hrs, MTT assays were performed to measure the cell viability. The results show that SERCA2b significantly increased the viability of cells treated with DOX ($p < 0.05$).

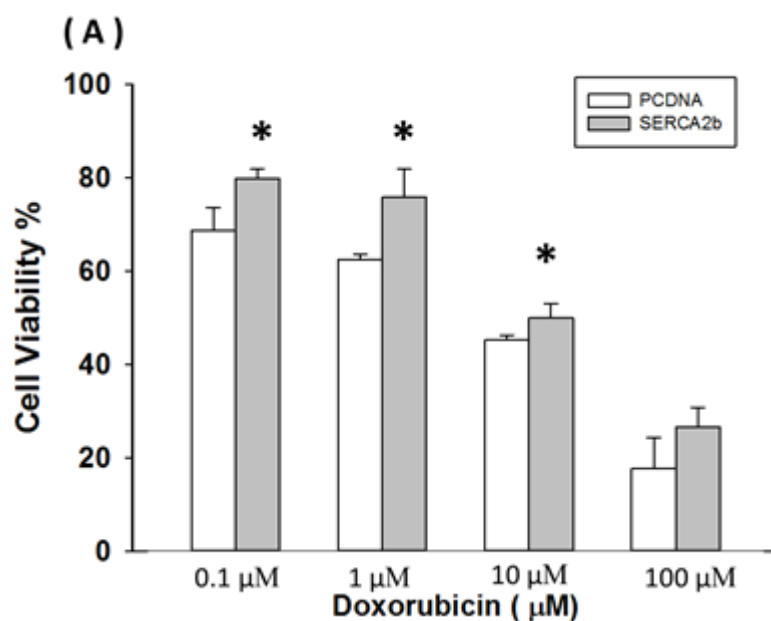


Figure 5.4.4.2A; the effect of DOX on cell viability of COS-7 cells in the present of SERCA2b. COS-7 cells were grown in 48 well plates and then cells were transfected after achieving 40-50% cell confluency. 1 μg of plasmid and 2 μl of TR (turbofect) were used to transfect cells with either SERCA2b or PCDNA plasmid, then cells were left for 48 hrs. Cells were then treated with DOX (0.1, 1, 10 and 100 μM), followed by MTT assays after 24 hrs. The data points represent the mean \pm SD of 3-5 determinations, (* $p \leq 0.05$, compared to their corresponding values in empty plasmid group).

Figure 5.4.4.2B shows the viability COS-7 cells following transfection with SERCA2b-GFP or PCDNA empty vector and then treated with Cisplatin. The results show that no protective effect was seen with this drug.

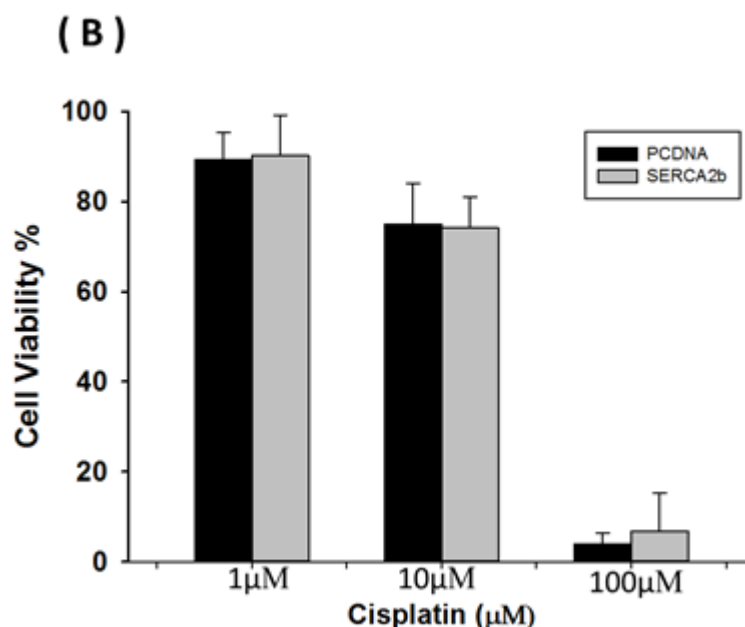


Figure 5.4.4.2B; shows COS-7 cell viability in the presence of SERCA2b-GFP or PCDNA and treated with Cisplatin. Cells were first transfected with SERCA2b-GFP or PCDNA empty plasmid and then treated with the drug. MTT assays were performed to determine the cell viability. The data pointed represent mean \pm SD of 3-4 determines.

5.5 SPCA transfection, detection and cyto-protection

5.5.1 Overexpression of SPCA

Kidney cells (COS-7 cells) were transfected with SPCA1a-GFP and SPCA2-GFP. Cells were seeded in 6 well plates and then transfected with two different conditions (1 μ g DNA+ 4 μ l TR) and (1 μ g DNA+ 2 μ l TR). Transfected cells were visualized under the fluorescence microscopy at 48 hrs. After counting the cell proportions under fluorescent and white light, condition 1:2 ratio was found to be the best and used for the next experiments. Table 5.5.1 shows the transfection efficiency for both conditions.

Table 5.5.1; the transfection efficiency of SPCA plasmids after 24 hrs .Two different conditions (1:2) and (1:4) (μg DNA plasmid: μl TR) were used. The transfection efficiency was determined by counting the percentage of fluorescent cells compared to the total number of cells in bright-field. The data represent the average of three replicates.

Transfection condition	1 μg +2 μl	1 μg +4 μl
Transfection efficiency	%	%
SPCA1a-GFP	43	21
SPCA2-GFP	45	43

5.5.2 The visualisation of the localisation of SPCA-GFP using fluorescence microscopy

Expression of GFP tagged SPCAs were used in these experiments, which allowed their localisation in the cell to be observed. COS-7 cells were transfected in glass-bottomed dishes for high-magnification microscopy purpose. The nuclei were also stained with Hoechst 33342 stain. Figure 5.5.2 shows the location of SPCA1a and SPCA2 which appear to be more highly distributed around the nuclei, which is consistent with the location of the Golgi Apparatus. This is consistent with other studies of SPCA location (Wootton et al., 2004, Baron et al., 2010).

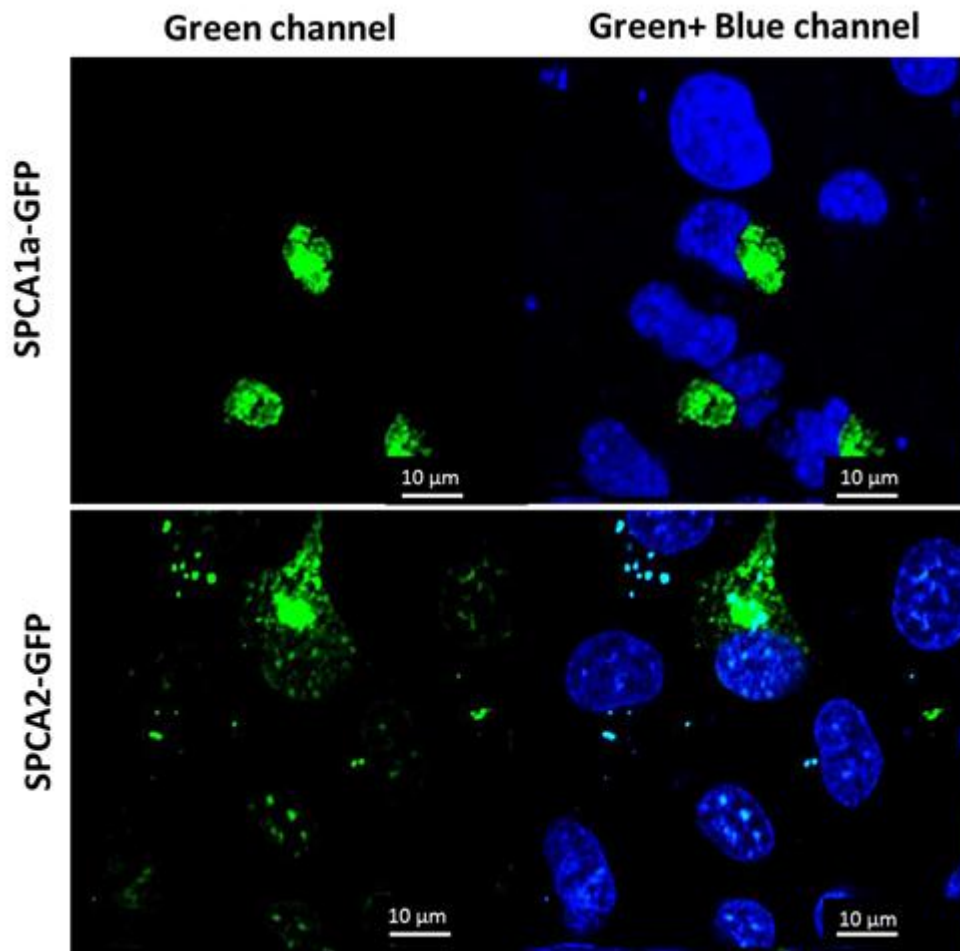
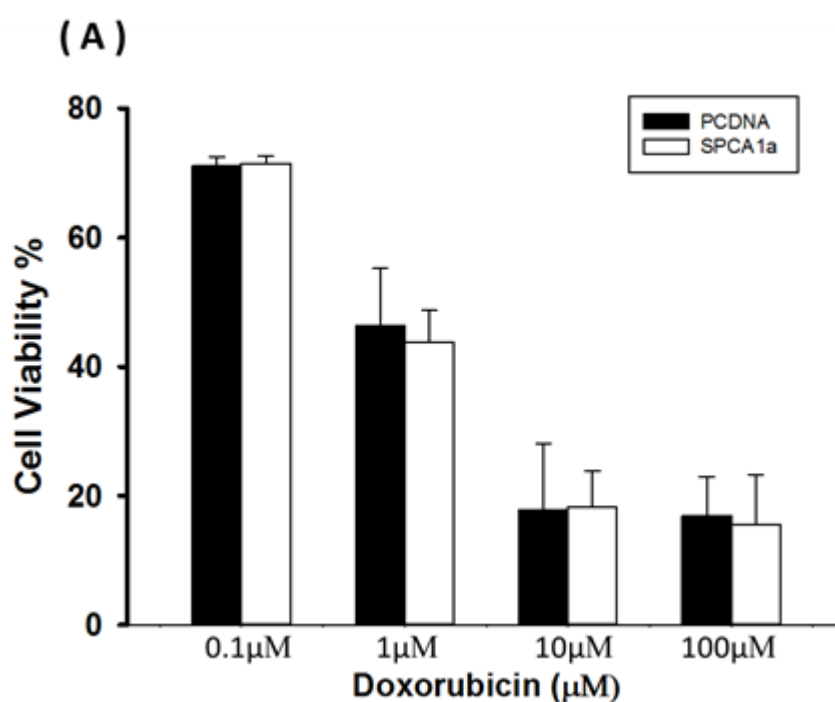


Figure 5.5.2; fluorescence images shows the localisation of SPCA1a-GFP and SPCA2-GFP in COS-7 cells. The cells were transfected with plasmids and the nuclei were also stained with a Hoechst stain, allowing the nucleus to be visualised using the DAPI filter. SPCAs appeared to be concentrated around the nucleus consistent with a Golgi Apparatus location.

5.5.3 The effect of overexpression of SPCA-GFP on COS-7 cells treated with chemotherapy drugs Doxorubicin and Cisplatin

5.5.3.1 The effect of overexpression of SPCA1a –GFP on COS-7 cells treated with Doxorubicin and Cisplatin

Figure 5.5.3.1A shows SPCA1a-GFP transfected COS-7 cells treated with different DOX concentrations for 24 hrs. The results show no significant change in cell viability in the presence of SPCA1a-GFP even with low concentrations compared to cells transfected with PCDNA alone. Figure 5.5.3.1B shows overexpressed cells with SPCA2b and transfected with cisplatin for 24 hrs, the results shows also no effect of this plasmid on protecting cells.



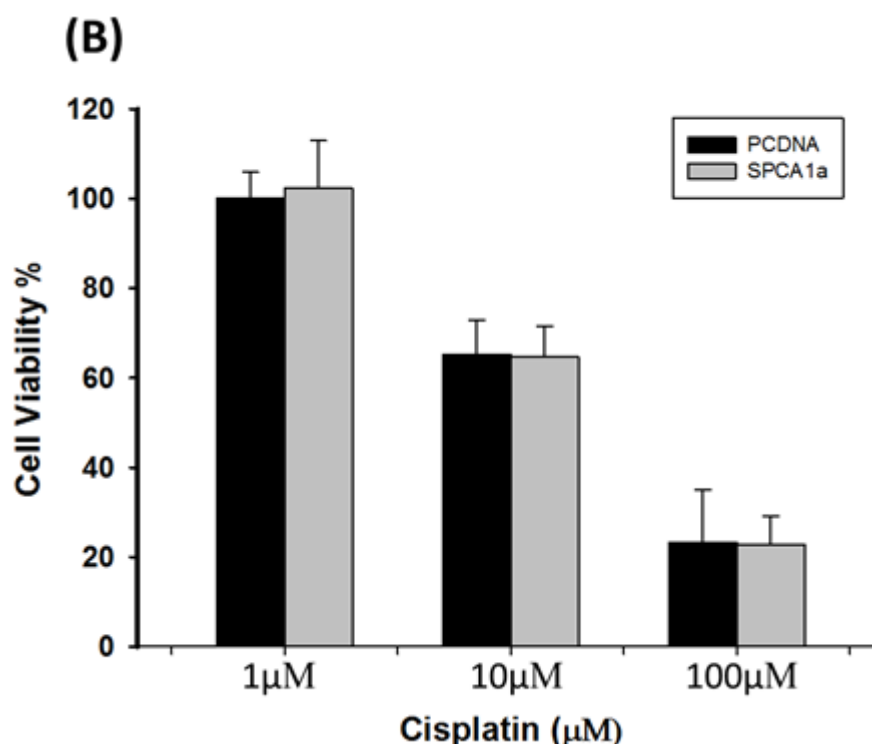


Figure 5.5.3.1A and B; the effects of DOX and Cisplatin on cell viability of COS-7 cells overexpressing SPCA1a-GFP or PCDNA alone. COS-7 cells were grown in 48 well plates in 1 ml media and then the cells were transfected, (1 μ g of plasmid and 2 μ l of TR in 0.5 ml). The transfect cells (either PCDNA or SPCA1a-GFP) were left for 48 hrs to allow for expression. Cells were then treated with DOX or Cisplatin and then MTT assays performed after 24 hrs to determine cell viability. The data points represent the mean \pm SD of 3-5 determinations.

5.5.3.2 The effect of SPCA2-GFP overexpression on COS-7 cells treated with Doxorubicin and Cisplatin

Figure 5.5.3.2A and figure 5.5.3.2B show COS-7 cells were transfected with SPCA2b and PCDNA for 48 hrs and treated with DOX and Cisplatin, respectively. Cells were treated with the drugs for 24 hrs and then MTT assay was carried out. Both figures were showed no changes in cell viability after drug treatment.

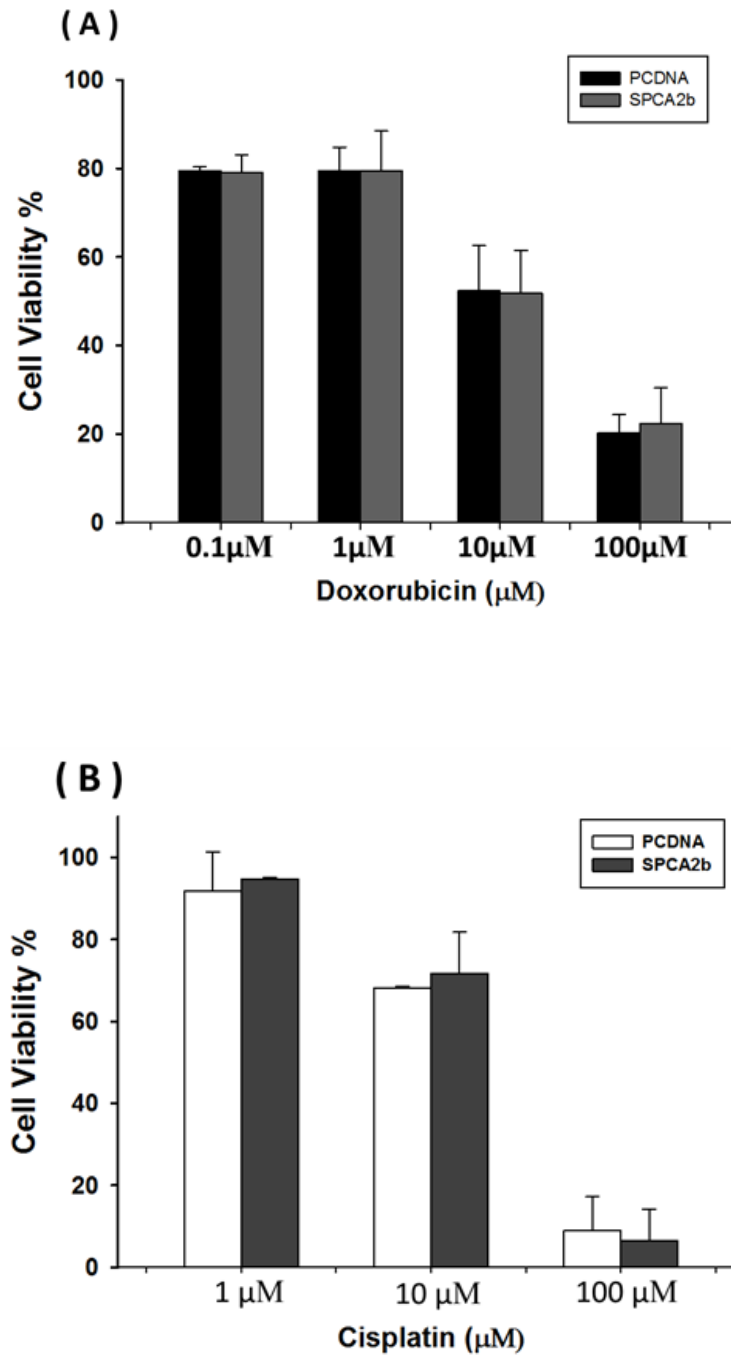


Figure 5.5.3.2A and B; the effects of Doxorubicin and Cisplatin on COS-7 cell viability, in cells overexpressing SPCA2-GFP. COS-7 cells were transfected with SPCA2b-GFP or PCDNA alone for 48 hrs, then the cells were treated with different concentrations of DOX or Cisplatin for 24 hrs and then MTT assays were carried out. The data points represent the mean \pm SD of 3-5 determinations.

5.6 The effect of Ca^{2+} concentrations in the culture media on SERCA expression

An investigation on whether changing calcium concentrations in the media surrounding COS-7 cells could have an effect on the SERCA expression was undertaken. COS-7 cells were seeded in 6 well plates and left for 24 hrs to attach, then cells were incubated with DMEM media containing different calcium concentrations; 0 mM , 1.8 mM and 10 mM. After 48 hrs the cells were washed with PBS and cell lysates were prepared and the protein concentrations estimated. SDS-PAGE was performed with the lanes loaded with the same amounts of cell lysate proteins (100 μg) from the cells grown in different conditions. Following transfer onto membranes, Western Blotting was undertaken using the anti-SERCA antibody Y1F4 to detect SERCA levels. The results in figure 5.6 shows that with no Ca^{2+} present in the media, SERCA was present in the cell lysate (lane 1, which is noted as 100%), although at lower levels than in cell lysates prepared in the presence of Ca^{2+} in the media.

Analysis of the bands using imageJ to determine band intensity showed that when the cells were grown in normal media containing 1.8 mM Ca^{2+} , the relative intensity had increased to 145% of that in the absence of added Ca^{2+} (lane 2). Upon increasing the Ca^{2+} level in the media to 10 mM, the relative increase in SERCA was shown to increase further to 161% of that observed in the absence of added Ca^{2+} . This result suggests that increasing Ca^{2+} concentrations within the media is causing an increase in SERCA expression within the cells.

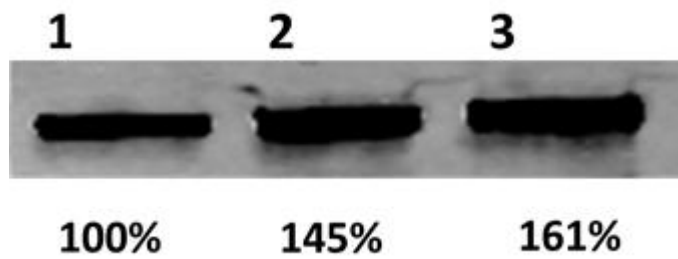


Figure 5.6; detection of SERCA in COS-7 cells incubated in media with different calcium concentrations. Cells were incubated for 48 hrs with (0 mM, 1.8 mM, and 10 mM) calcium in the media. Lane 1 = No Ca^{2+} in media, Lane 2 = 1.8mM in media and Lane 3 = 10 mM in media). Western blots were used with anti-SERCA YIF4 mouse primary antibody and anti-mouse 800 secondary antibody. ImageJ was used for analysis of band intensity.

5.7 Discussion

Doxorubicin (DOX) is widely used in treating various cancer such as Hodgkin and non-Hodgkin lymphomas, Kaposi's sarcoma, soft tissue sarcomas and osteosarcomas (Minotti et al., 2004; Al-Saedi et al., 2015). Cisplatin is another commonly used cancer drug that is used to treat lymphomas, head and neck carcinomas and bladder cancers (Dasari and Tchnounwou, 2014). However, the nephrotoxicity of these drugs is well documented as they are known to accumulate in kidney as well as liver, small intestines and heart. DOX is also well known to cause severe cardio-toxicity as a serious side-effect (Deman et al., 2001, Boonsanti et al., 2006, Mattila et al., 2016).

In this study it has been shown that the toxicity caused by both DOX and Cisplatin, is at least in part, by a Ca^{2+} -dependent process in kidney-derived COS-7 cells. These findings are consistent with other recent studies on these drugs using a variety of cell types (Shen et al., 2016, Bartlett et al., 2016, Al-Taweel et al., 2014). Since other studies have reported that both these drugs can affect a range of Ca^{2+} transporters within cells, here an investigation of the effects of these drugs on cell viability was undertaken in COS-7 cells overexpressing the intracellular Ca^{2+} pumps SERCA and SPCA.

In this study it was shown that SERCA1b and SERCA2b overexpression in COS-7 cells were able to reduce the cytotoxicity of DOX. One of the major reported side-effects of DOX is that it causes abnormalities within the sarcoplasmic reticulum (SR) (Fischer et al., 1991) and induces abnormal increases in cytosolic concentration of Ca^{2+} in cells (Kim et al., 2006; Olson, et al., 2005; Mattila et al., 2016). Since SERCA transfers calcium from the cytosol to the lumen of the ER in the cell, this can prevent any excessive rise in cytosolic Ca^{2+} which could lead to overload of calcium in the mitochondria leading to mitochondrial-mediated death via the intrinsic pathway of apoptosis (Pinton et al., 2008). Ca^{2+} transporters that have been shown to be specifically affected by DOX include both Ryanodine receptors (RyRs), which is activated, (Zorzato et al., 1985, Hanna et al., 2014) and SERCA, which is inhibited (Hanna et al., 2014, Vile and Winterbourn, 1990, Zhang et al., 2014 and Ondrias et al., 1990). However, since studies on COS-7 cells have shown that they do not express RyRs (Treves et al., 2002, Al-Mousa and Michelangeli, 2009), the most likely effect of DOX could be inhibition of SERCA. Therefore overexpressing SERCA would likely afford some

protection against Ca^{2+} -dependent cell death, by increasing the capacity to remove Ca^{2+} from the cytosol into the ER. However, this cannot be the full explanation since overexpression of SPCA does not protect against DOX-induced cell death. It is known that the Ca^{2+} uptake activity of SPCA is not as high as SERCA (Wuytack et al., 2002 and Wootton et al., 2004), which could explain this observation or it could also be that the ER-associated Unfolded Protein Response (UPR) cell stress pathway (which is activated upon Ca^{2+} depletion of the ER, Bravo et al., 2013), also plays a role, since SPCA would only refill the Golgi with Ca^{2+} and not the ER. Therefore further experiments to distinguish these possibilities would be required.

As shown here and in other studies (Chen et al., 2016), Cisplatin-induced cell death is partially through a Ca^{2+} -dependent process, however, the results presented here has also shown no protection when SERCA1a and SERCA2b are overexpressed. This was also the case when overexpressing SPCA as well. This would appear to be at odds with the previous explanation, except that Cisplatin appears to cause a rise in intracellular Ca^{2+} levels by directly activating the IP_3 receptors (IP_3Rs) (Shen et al., 2016; Splettstoesser et al., 2007). It is known that COS-7 cells have an abundance of the type III isoform of the IP_3R (Hattori et al., 2004). The capacity of IP_3Rs to release Ca^{2+} into the cytosol from the ER is considerably high (i.e. approximately 1.5 million $\text{Ca}^{2+}/\text{sec}/\text{channel}$) (Taylor and Traynor, 1995), compared to SERCA which can only transport about 20 $\text{Ca}^{2+}/\text{sec}/\text{pump}$ (Taylor and Traynor, 1995) in the opposite direction. Therefore even increasing the level of SERCA massively, would have little effect in reducing cytosolic Ca^{2+} levels, of the cell, or refilling of the ER lumen, especially if the IP_3R channels remained open (Figure 5.7). Therefore the addition of IP_3R channel blockers such as 2-APB (Bilmen et al., 2002), should protect against Cisplatin-induced, Ca^{2+} -mediated cell death, which is what has been observed in HeLa cells (Splettstoesser et al., 2007).

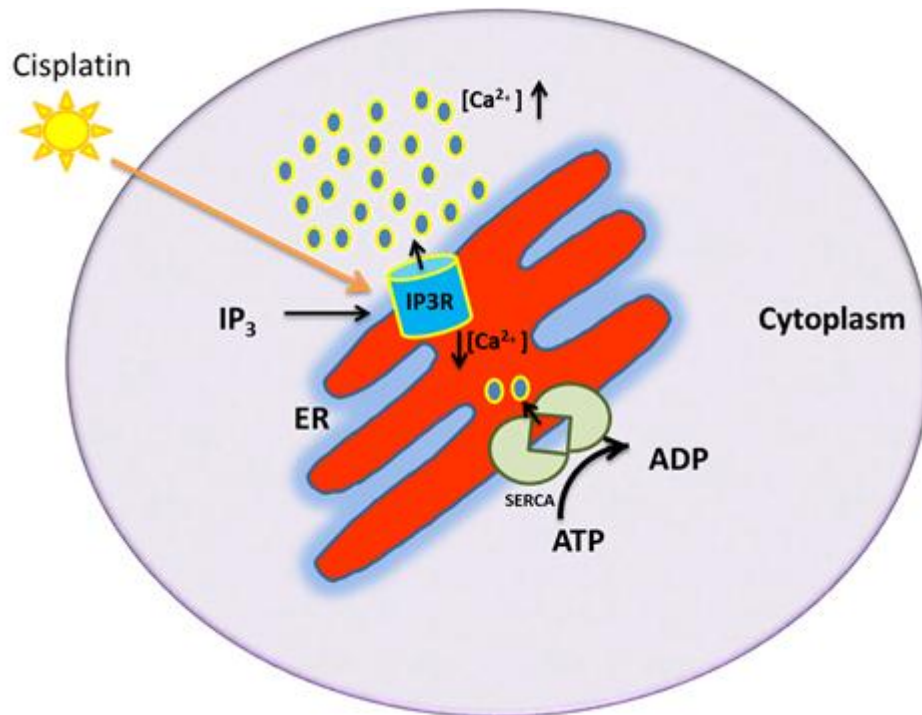


Figure 5.7; the effect of Cisplatin on ER. Cisplatin causes IP3R channels to open and decreases Ca^{2+} concentration inside the ER and this can cause elevation of cytosolic Ca^{2+} .

In this chapter we have also shown that increasing Ca^{2+} concentration in the media appears to increase SERCA expression in COS-7 cells. The levels of expression were determined to be about 60% higher than the SERCA levels in Ca^{2+} free media. Some studies have linked the expression and regulation of SERCA to many different factors such as; excessive muscle contraction, hormonal regulation (via thyroid hormone) and age (Periasamy et al., 2008), but not on external calcium concentration, which we have shown. We and others have shown that increased extracellular Ca^{2+} levels can increase the expression of regucalcin (Shimokawa and Yamaguchi, 1992) and elevated cellular regucalcin levels has recently been shown to also increase the expression of SERCA (Lai et al., 2011). Therefore more experiments to test this idea are required. It would also be interesting to see whether increased plasma Ca^{2+} concentrations could also induce higher levels of SERCA expression in whole organs within an organism, which could then provide protection against the effects of some cytotoxic drugs.

CHAPTER 6

General discussion and future works

6 General discussion and future works

6.1 General discussion

Despite cancer chemotherapy treatments having undergone many considerable advances in recent years which have led to significant improvements in the patient's survival, however, hepatotoxicity and nephrotoxicity remains an important complication of some of these drugs.

Four of the most commonly used chemotherapeutic drugs were chosen in this study, Methotrexate, Etoposide, Cisplatin and Doxorubicin. MTX drug was shown to have limited toxicity and mostly affected cell proliferation rather than cell death, because this drug inhibits the enzyme tetrahydrofolate reductase which is important for DNA synthesis (Weinsterin, 1990). However, other drugs showed a significant toxicity in both liver and kidney cell lines and they were able to cause cell death involving several pathways (ie apoptosis, necrosis and autophagy) (see table 6.1A). DOX drug was the most toxic drug compared to the others tested, showing potent toxicity at very low concentrations (see table 3.2). Cisplatin also showed toxicity in all cell lines used but at higher concentrations, and Etoposide was the least toxic of the drugs used in this study. Interestingly, in this study we found that Etoposide has a weak effect on cells with regards to apoptosis, necrosis and autophagy, compared to Cisplatin, which has showed a very strong effect on apoptosis, necrosis and autophagy for most cells tested. While DOX, has a reasonably strong effect on apoptosis (especially kidney cells), no effect on necrosis and some effect in autophagy as shown in the table 6.1A.

To summarize, chemotherapy drugs causes cell death in both liver and kidney cells by different pathways. Therefore clinicians must be aware with the hepatotoxicity and nephrotoxicity that these drugs may induce and we recommend a relationship between the oncologists and both nephrologist and hepatologist when it comes in treating any cancers with these drugs.

Table 6.1A; summary of the different cell death pathways and different chemotherapeutic drugs used in this study.

Cell death	Apoptosis			Necrosis			Autophagy		
Drugs Cell lines	Etop	Cisp	DOX	Etop	Cisp	DOX	Etop	Cisp	DOX
COS-7	++	+++	+++	+	+++	–	+	+++	++
HK2	+	+++	+++	–	++	–	ND	ND	ND
HepG2	+	+++	++	+	+++	–	+	+++	+++
Huh7.5	++	+++	++	–	+++	–	ND	ND	ND

- = Little or no effect

+ = A small but significant effect

++ = A substantially significant effect

+++ = A strong effect

ND = Not determined

The cyto-protective role of RGN has been known for a while. More recently a study reported the role of RGN in protecting against cardiotoxicity caused by DOX (Miyata et al., 2013). Based on the results of this study, I have also shown the protective role of RGN against several other chemotherapeutic drugs (Etoposide, Cisplatin and DOX) to a significant level (see table 6.1B), in both liver and kidney cell lines. The mechanism by which RGN protects cells from death is unknown. It is known that RGN is a transcription factor regulator and can be located within the nuclei and cytoplasm in normal cells. However, in my studies, when cells undergo stress through the treatment with chemotherapeutic drugs, RGN most likely moves to the mitochondria to possibly protect cells from mitochondrial mediated death. My data has also shown some accumulation of RGN around the edge of the nucleolus, which is a novel finding and suggests that this protein could also be involved in ribosome formation and therefore translation. I have also shown that increasing Ca^{2+} concentration in the media surrounded HepG2 cells increases the expression of RGN, which supports previously studies, which have shown that in rats treated with the calcitonin hormone and Ca^{2+} rich diet enhanced the expression of RGN by up to 300% (Isogai and Yamaguci, 1995). Furthermore, looking at my data in detail, since cisplatin causes cell death by apoptosis, necrosis and autophagy, I therefore also suggest that RGN could not only protect cells from apoptosis but possibly necrosis and autophagy cell death as well (Figure 6.1C). Therefore, RGN could be a new therapeutic target protein to reduce the hepatotoxicity and nephrotoxicity when patients are treated with these chemotherapeutic drugs, although further animal studies are required, to see if increased RGN in living organisms also has a protective role.

The nephrotoxicity of chemotherapy drugs is well documented and many studies have demonstrated that DOX can accumulate in kidney, liver and heart (Deman et al., 2001, Boonsanti et al., 2006). In this study I have shown that the nephrotoxicity of DOX and Cisplatin are calcium dependent, consistent with other studies. Both increases in expression of SERCA1 and SERCA2b have the ability to reduce the cytotoxicity of DOX but not cisplatin (see table 6.1B). DOX has been shown in several studies to cause SERCA inhibition (Hanna et al., 2014, Vile & Winterbourn, 1990, Zhang et al., 2014 and Ondrias et al., 1990), and therefore overexpression of this protein would help minimize this effect and aid removal Ca^{2+} from the cytosol to the ER. However, SPCAs

showed no protection against DOX toxicity, possibly because SPCA activity is much less than SERCA activity (Wootton et al., 2004 and Wuytack et al., 2002), or possibly that low ER [Ca²⁺] could cause the ER stress response (Mekahli et al., 2011).

Cisplatin toxicity was shown not to be protected by either SERCAs or SPCAs overexpression. This could be explained by the fact that this drug can cause a rise in intracellular Ca²⁺ level through opening the IP3R (Shen et al., 2016; Splettstoesser et al., 2007), therefore even by increasing SERCAs level substantially would have little effect upon Ca²⁺ leakage from the ER.

Another observation that can be made from the results presented here is that SERCA overexpression could have a protective role in apoptosis cell death but not necrosis, since DOX induces cell death by apoptosis, but not necrosis (Figure 6.1C).

Table 6.1B; summarized the different Ca²⁺ binding proteins and their protection, against chemotherapy drugs in COS-7 cells.

Proteins Drugs	SMP30	RGN-GFP	SERCA1	SERCA2b	SPCA1a	SPCA2b
DOX	+	+	+	+	–	–
Cisplatin	+	ND	–	–	–	–
Etoposide	+	ND	+	ND	ND	ND

– = No effect

+

= Positive protective effect

ND = Not determined

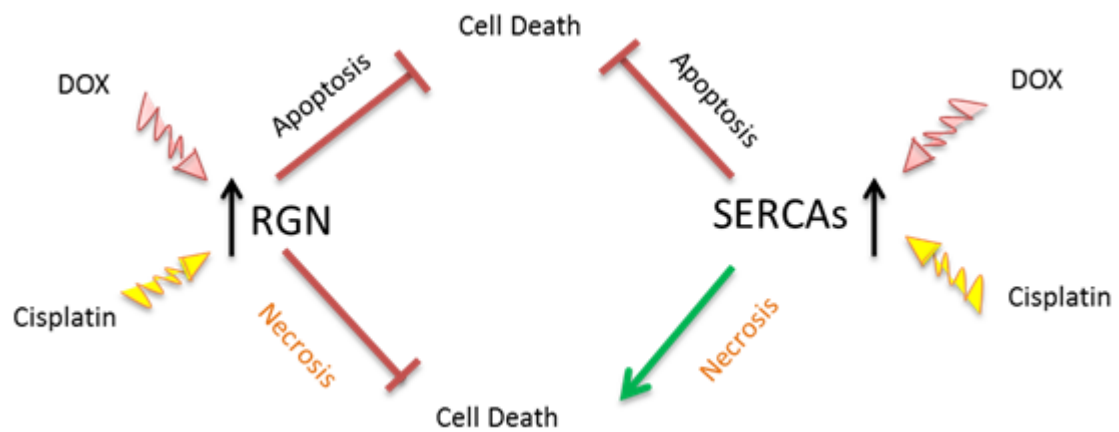


Figure 6.1C; schematic showing summary of this study. Increasing the expression of RGN in COS-7 cells, protect cells from apoptosis and necrosis cell death, induced by either DOX or Cisplatin. While SERCA overexpression in the same cells can inhibit apoptosis, but not necrosis, when cells exposed to such drugs.

6.2 Future Works

Since this study has shown different cell death mechanisms, between a range of cell lines that have originated from different organs when responding to the same chemical stresses induced by chemotherapeutic drugs, I think it will be a good idea to try a more extensive range of cells (both cell lines and primary cells) from different organs to see whether they also utilize the same cell death mechanisms. It will be also interesting to use a more extensive range of different chemotherapeutic drugs to see whether they also utilize different cell death mechanisms. As one of the key novel findings from this study is that some of the more commonly used chemotherapeutic drugs can cause autophagic cell death, it will be much better if this could be further confirmed by using other different techniques such as investigating the effects of autophagy inhibitors to see whether they can reduce chemotherapy drug induced cell death.

Regucalcin, was shown to protect cells from some chemotherapy drug toxicity, and this study could be extended to incorporate a wider range of drugs, to see if all cytotoxic drug classes are protected by RGN. In addition, compounds that are known only to cause cell death by a single pathway (ie apoptosis, necrosis or autophagy), could also be used to see how efficient RGN is at protecting against specific pathways. Given the fact that from my studies it was shown that RGN localizes around the nucleolus, it would also be interesting to investigate whether RGN affects any of the functions carried out by this intra-nuclear structure.

The research that has been discussed in chapter 5 has explored that increased expression of SERCAs, but not SPCAs, can protect COS-7 cells from DOX –induced cytotoxicity. Other questions that can be easily addressed include: Is this protection also seen in other cell types? Which other drugs can increased SERCA expression, protect against? Does the cell death pathway protected by increased SERCA, involve ameliorating the effects of elevated cytosolic $[Ca^{2+}]$ levels or decreased ER luminal $[Ca^{2+}]$ levels or both?

Finally, are the cyto-protective effects of RGN and SERCA additive? Can increasing the expression of both these Ca^{2+} binding proteins, in patients through dietary and hormonal means, protect them from drug induced toxicity?

References

7 References

- Abou-Elella, A., Siendones, E., Padillo, J., Montero, J., De la Meta, M., Relate, j. (2002) Tumour necrosis factor-alpha and nitric oxide mediate apoptosis by D-galactosamine in a primary culture of rat hepatocyte: Exacerbation of cell death by cocultured Kuppercell. *Can.J.Gastroenterol.* 16, pp.791-799.
- Agus, Z., Gardner, L., Beck, L., Goldberg, M., (1973). Effects of parathyroid hormone on renal tubular reabsorption of calcium, sodium, and phosphate. *Am J Physiol.* 224(5), pp.1143–1148.
- Ahlberg, J. Marzella, L. Glaumann, H. (1982). Uptake and Degradation of Proteins by Isolated rat live lysosomes. Suggestion of a microautophagic pathway of proteolysis, *Lab. Invest.* 47, pp.523–532.
- Akhter, T., Sawada, N., Yamaguchi, M. (2006) Regucalcin increases Ca^{2+} -ATPase activity in the heart mitochondria of normal and regucalcin transgenic rats. *M. Int J Mol Med* 18, pp.171–176.
- Alcântara, A., Vitor, R., Vieira, E., & Martins, I. (2010). Simultaneous detection of three antineoplastic drugs on gloves by liquid chromatography with diode array detector. *Brazilian Journal of Pharmaceutical Sciences*, 46(4), pp. 731-740.
- Al-Mousa, F. (2010). ‘Neurotoxicity of Environmental Pollutants’ PhD thesis, University of Birmingham, Birmingham, UK.
- Al-Mousa, F. and Michelangeli, F. (2009). Commonly used ryanodine receptor activator, 4-chloro-m-cresol (4CmC), is also an inhibitor of SERCA Ca^{2+} pumps. *Pharmacol Rep.* 61(5), pp.838-42.
- Alnemri, E., Livingston, D., Nicholson, D., Salvesen, G., Thornberry, N., Wong, W. and Yuan, J. (1996). Human ICE/CED-3 Protease Nomenclature. *Cell*, 87(2), p.171.
- Al-Taweel, N., Varghese, E., Florea, A., and Büsselberg, D. (2014). Cisplatin (CDDP) triggers cell death of MCF-7 cells following disruption of intracellular calcium ($[\text{Ca}^{2+}]_i$) homeostasis. *The Journal of Toxicological Sciences (J. Toxicol. Sci.)* 39(5), pp. 765-774.
- An Rijn, J., Heimans, J., vanden Berg, J., vander Valk, P. and Slotman, B. (2000). Survival of Human Glioma Cells treated with Various combinations of Temozolomide and X-rays. *International Journal of Radiation Oncology* Biology* Physics* 47(3), pp.779-784.

- Andersen,A. Bendixen,C.andWestergaard, O.(1996). DNA Topoisomerases DNA Replicationin Eukaryotic Cells. Cold Spring Harbor LaboratoryPres-87969-459-9/96.
- Arcamone,F. (1981). Doxorubicin Structure, ACADEMIC PRESS. (17).
- Arita, K., Utsumi, T., Kato, A., Kanno, T., Kobuchi, H., Inoue, B., Akiyama, J., Utsumi, K.(2000). Mechanism of dibucaine-induced apoptosis in promyelocytic leukemia cells (HL-60). *Biochem Pharmacol.* 60(7),pp.905-15.
- Armstrong,J.andDass,C.(2015) .Doxorubicinactiononmitochondria:relevance to osteosarcoma therapy?Curr DrugTargets.
- Asara, Y., Marchal,J., Bandiera,P., Mazzarello, V., Delogu,L., Sotgiu,M., Montella, A. and Madeddu,R.(2012). Cadmiuminfluencethe 5-Fluorouracilcytotoxic effectson breast cancer cells. *EurJHistochem.* 56(1), p.1.
- Assouline, S.,Buccheri,V., Delmer, A., Gaidano,G., McIntyre,C.,Brewster,M.,Catalani, O., Hourcade-Potelleret,F., Sayyed,P. andBadoux, X. (2015). Pharmacokinetics andsafety of subcutaneousrituximabplusfludarabineandcyclophosphamidefor patientswithchroniclymphocytic leukaemia.British Journalof Clinical Pharmacology, p.n/a-n/doi:10.1111/bcp.12662. [Epub ahead of print]. *Autophagy*1.pp. 66–74.
- Baehrecke,E.(2002). How death shapes life during development.*NatRevMolCellBiol.*3(10), pp.779-87.
- Baldwin,E.,and Osheroff,N.(2005). Etoposide,topoisomeraseII and cancer.CurrMedChem Anticancer Agents.5(4), pp.363-72.
- Baron, S., Vangheluwe, P., Sepúlveda, M., Wuytack, F., Raeymaekers, L., Vanoevelen, J.(2010). The secretory pathway Ca(2+)-ATPase 1 is associated with cholesterol-rich microdomains of human colon adenocarcinoma cells. *Biochim Biophys Acta*;1798(8),pp.1512-21.
- Bartlett, J., Trivedi, P. Yeung, P., Kienesberger, P. Pulinilkunnil, T. (2016). Doxorubicin Impairs Cardiomyocyte Viability by Suppressing Transcription Factor EB Expression and Disrupting Autophagy. *Biochem J.* pii: BCJ20160385. [Epub ahead of print]
- Baskar, R., Lee,K., Yeo, Yeoh,R. (2012). Cancer and Radiation Therapy: Current Advances and Future Directions. *Int J Med Sci.* 9(3), pp.193-199.
- Baskar, R., Lee, K., Yeo, R., Yeoh, K.(2012). Cancer and Radiation Therapy: Current Advancesand Future Directions.*Int JMedSci.* 9(3), pp.193-199.

- Bath,K.Brar, K.,Forouhar. A., Wu,Y.(2014). A review of Methotrexate-Associated Hepatotoxicity. *Journal of Digestive Diseases*.15 (10), pp. 517–524.
- Behne, M.J., Tu, C.L., Aronchik, I., Epstein, E., Bench, G., Bikle, D.D., Pozzan T., and Mauro, T.M. (2003). Human keratinocyte ATP2C1 localizes to the Golgi and Controls Golgi Ca²⁺ stores. *J Invest Dermatol*. 121, pp.688-694.
- Bellomo, G., Perotti, M., Taddei, F., Mirabelli, F., Finardi, G., Nicotera, P., Orrenius, S. (1992). Tumor necrosis factor alpha induces apoptosis in mammary adenocarcinoma cells by an increase in intranuclear free Ca²⁺ concentration and DNA fragmentation. *Cancer Res*. 1;52(5),pp.1342-6.
- Berghe,T.,Linkermann,A.,Jouan-Lanhouet,S.,Walczak,H.andVandenabeele,P. (2014). Regulatednecrosis: The Expanding Networkof Non-apoptoticcell Death Path Ways. *Nature Reviews Molecular CellBiology*.15(2), pp.135-147.
- Bhattacharjee,A., Basu,A., Biswas, J. and Bhattacharya, S.(2015). Nano-Sea ttenuates Cyclophosphamide-Inducedpulmonary Injury Through Modulation of Oxidative Stress and DNA damagein Swissalbinomice. *Mol Cell Biochem*. 405(1-2), pp.243-256.
- Bilmen, J., Wootton, L., Godfrey, R., Smar,t O., Michelangeli F. (2002) Inhibition of SERCA Ca²⁺ pumps by 2-aminoethoxydiphenyl borate (2-APB). 2-APB reduces both Ca²⁺ binding and phosphoryl transfer from ATP, by interfering with the pathway leading to the Ca²⁺-binding sites. *Eur. J. Biochem*. 269:3678–3687.
- Bobe R, Bredoux R, Corvazier E, Andersen JP, Clausen JD, Dode L, Kovács T, Enouf J. (2004). Identification, Expression, Function, and Localization of a Novel (sixth) iso form of the Human Sarco/Endoplasmic reticulum Ca²⁺ATPase 3 gene. *J Biol Chem*. 279, pp.24297-306.
- Bolte, S., & Cordelières, F. (2006). A guided tour into subcellular colocalization analysis in light microscopy, *Journal of Microscopy*. 224(3), pp. 213-232.
- Boonsanit D, Kanchanapangka S, Buranakarl, C. (2006). L-carnitineameliorates Doxorubicin-Induced Nephrotic Syndrome in Rats. *Nephrology*. 11(4), pp.313-320.
- Bootman, M. D., Collins, T. J., Peppiatt, C. M., Prothero, L. S., Mackenzie, L., De Smet, P., Travers, M., Tovey, S. C., Seo, J. T., Berridge, M. J., Ciccolini, F. & Lipp, P. (2001). Calcium signalling – an overview. *Seminars in Cell & Developmental Biology*. 12, pp.3-10.

- Brandl J, deLeon S, Martin R, MacLennan H.(1986). Adult forms of the Ca^{2+} -ATPase of Sarcoplasmic Reticulum. Expression in Developing Skeletal Muscle. *J Biol Chem.* 262, pp.3768-74.
- Bravo, R., Parra, V., Gatica, D., Rodriguez, A., Torrealba, N., Paredes, F., Lavandero, S. (2013). Endoplasmic Reticulum and the Unfolded Protein Response: Dynamics and Metabolic Integration. *International Review of Cell and Molecular Biology.* 301, pp.215–290.
- Brini, M and Carafoli, E. (2009). Calcium pumps in Health and Disease. *Physiol.Rev.* 89, pp.1341-1378.
- Brittig, F., Hargita, M., Marton, E., Kecskés, L., and Tehenes, S. (1993). Busulfanlung Simulating tumor, *Orv Hetil.* 134(13), pp.697-9.
- Brooks, C. L., and Gu, W. (2010). New insights into p53 activation. *Cell Research.* 20(6), pp.614–621.
- Brunello, A., Basso, U., Rossi, E., Stefani, M., Ghiotto, C., Marino, D., Crivellari, G. and Monfardini, S. (2007). Ifosfamide-Related Encephalopathy in Elderly Patients. *Drugs & Aging.* 24(11), pp.967-973.
- Burk SE, Lytton J, MacLennan DH, Shull GE. (1989). CDNA Cloning, Functional Expression, and mRNA Tissue Distribution of a Third Organellar Ca^{2+} pump. *J Biol Chem.* 264, pp.18561-68.
- Butler, M. (2004). The Role of Natural Product Chemistry in Drug Discovery†. *J. Nat. Prod.*, 67(12), pp.2141-2153.
- Calcraft, P. J., Ruas, M., Pan, Z., Cheng, X. T., Arredouani, A., Hao, X. M., Tang, J. S., Rietdorf, K., Teboul, L., Chuang, K. T., Lin, P. H., Xiao, R., Wang, C. B., Zhu, Y. M., Lin, Y. K., Wyatt, C. N., Parrington, J., Ma, J. J., Evans, A. M., Galione, A. & Zhu, M. X. (2009). NAADP Mobilizes Calcium From Acidic Organelles Through Two-pore Channels. *Nature*, 459, 596-U130.
- Candé, C., Cecconi, F., Dessen, P., Kroemer, G. (2002). Apoptosis-Inducing Factor (AIF): Key to The Conserved caspase-Independent Path Way of Cell death?. *Journal of Cell Science*, 115(24), pp.4727-4734.
- Carafoli E. (1994). Biogenesis: Plasma Membrane Calcium ATPase: 15 Years of Work on The Purified Enzyme. *JFASEB* 8, pp.993-1002.
- Carafoli, E., Santella, L., Brance, D., and Brisi, M. (2001). Generation, Control, and Processing of Cellular Calcium Signals. *Crit Rev Biochem Mol Biol.* 36, pp.107-260.

- Cardoso, S., Santos,R.,Carvalho,C.,Correia, S.Pereira,G., Pereira, S.,Oliveira, P., Santos, M.,Proenca,T.,Moreira,P.(2008). Doxorubicin increases the susceptibility of Brain Mitochondriato Ca(2+)-induced Permeability Transition and Oxidative damage. *Free Radi cBiolMed*. 45, pp.1395–1402.
- Carvajal,D.(2005). Activation of p53 by MDM2 Antagonists Can Protect Proliferating Cells from MitoticInhibitors.*Cancer Research*. 65(5),pp.1918-1924.
- Carvalho,C.,Santos,R.,Cardoso,S.,Correia,S., Oliveira,P.,Santos,M., Moreira,P. (2009) Doxorubicin: The Good, The Badand The Ugly Effect. *Curr Med Chem*. 16, pp.3267–3285.
- Cavaletti,G.(2008). Peripheral neuro toxi city of platinum-based chemotherapy. *Nat RevCancer*, 8(1).
- Cavaletti,G., Tredici,G., Petruccioli,M.,Dondè,E.,Tredici, P.,Marmioli, P.,Minoia,C., Ronchi,A., Bayssas,M.and Griffon Etienne,G. (2001). Effects of different schedules of Oxaliplatin Treatment on The Peripheral nervous system of therat.*European Journal of Cancer*. 37(18), pp.2457-2463.
- Cerella,C.,Diederich,M., andGhibelli,L.(2010). The Dual Role of Calcium as Messenger and Stressorin Cell Damage, Death, and Survival. *International Journal of Cell Biology*. (14).
- Chagaluka,G.,Stanley,C.,Banda,K.,Depani,S.,Nijram'madzi,J.,Katangwe,T.,Israels, T., Bailey, S., Mukaka, M. and Molyneux, E. (2014). Kaposi'ssarcoma in children: Anopen Randomisedtrial of Vincristine, Oraletoposide and acombination ofvincristine and bleomycin. *European Journal of Cancer*. 50(8), pp.1472-1481.
- Chakraborti, S. & Bahnson, B. (2010). Crystal Structure of Human Senescence Biochemistry, 75,pp. 5435-5442.
- Chang, H., Yang, X. (2000) Proteases for cell suicide: functions andregulation of caspases. *Microbiol Mol Biol Rev*. 64,pp.821-26.
- Chemaly, E.R, Bobe, R., Adnot, S., Hajjar, R.J, Lipskaia, L. (2013). Sarco (Endo) Plasmic Reticulum Calcium Atpases (SERCA) Isoforms in the Normal and Diseased Cardiac, Vascular and Skeletal Muscle. *J Cardiovasc Dis Diagn*. 1, pp.113.
- Chen, J.-Y., Tang, Y.-A., Li, W.-S., Chiou, Y.-C., Shieh, J.-M., & Wang, Y.-C. (2013). A Synthetic Podophyllotoxin Derivative Exerts Anti-Cancer Effects by Inducing Mitotic Arrest and Pro-Apoptotic ER Stress in Lung Cancer Preclinical Models. *PLoS ONE*. 8(4), e62082.

- Chen, M., Wu, X., Gu, J., Guo, Q., Shen, W., Lu, P. (2011). Activation of AMP-Activated Protein Kinase Contributes to doxorubicin-induced cell death and apoptosis in Cultured Myocardial H9c2 cells. *Cell Biochem Biophys.* 60, pp.311–322.
- Chen, I., Beisner, D., Degterev, A., Lynch, C., Yuan, J., Hoffmann, A. and Hedrick, S. (2008). Antigen-mediated T cell expansion regulated by parallel pathways of death. *Proceedings of the National Academy of Sciences.* 105(45), pp.17463-17468.
- Chipuk, J., Maurer, U., Green, D. and Schuler, M. (2003). Pharmacologic Activation of p53 Elicits Bax-Dependent Apoptosis in the Absence of Transcription. *Cancer Cell.* 4(5), pp.371-381.
- Cho JH, Ko KM, Singaravelu G, Ahn J. (2005). Caenorhabditis E PMR1, a P-type Calcium ATPase, is Important for Calcium/Manganese Homeostasis and Oxidative Stress response. *FEBS Lett.* 579, pp.778–782.
- Christenson, E., James, T., Agrawal, V., & Park, B. (2015). Use of Biomarkers for the Assessment of chemotherapy-induced cardiac toxicity. *Clinical Biochemistry.* 48(0), pp.223–235.
- Ciavarella, S., Milano, A., Dammacco, F. and Silvestris, F. (2010). Targeted Therapies in Cancer. *BioDrugs.* 24(2), pp.77-88.
- Clarke, P. and Clarke, S. (1995). Historic apoptosis. *Nat Dev.* 378, 230.
- Clarke, P. and Clarke, S. (1996). Nineteenth century research on naturally occurring cell Death and Related Phenomena. *Anatomy and Embryology,* 193(2).
- Cohen, G. (1997). Caspases: The Executioners of Apoptosis. *Biochem J* 326(1), pp.1-16.
- Cohen, J. and Duke, R. (1984). Glucocorticoid activation of a calcium-dependent endonuclease in thymocytes nuclei lead to cell death. *J. Immunol.* 132, pp.38-42.
- Cooper, G.M. (2000). *The Cell: A Molecular Approach.* 2nd edition. Sunderland (MA): Sinauer Associates; the Eukaryotic Cell Cycle. Available from: <http://www.ncbi.nlm.nih.gov/books/NBK9876/>.
- Cornelison, T., Reed, E. (1993). Nephrotoxicity and hydration management for cisplatin, carboplatin, and ormaplatin. *Gynecol Oncol.* 50(2), pp.147-58.
- Cornelison, T. and Reed, E. (1993). Nephro Toxicity and Hydration Management for Cisplatin, Carboplatin, and Ormaplatin, *Gynecologic Oncology.* 50(2), pp.147-158.

- Cory,S.andAdams,J. (2002). TheBcl2family:regulatorsofthecellularlife-or-death switch. *Nat Rev Cancer*2. pp.647–56.
- Cragg,G., Kingston,D.,Newman,D.,(2005). *Anticancer Agents from Natural Products*.Brunner-Routledge Psychology Press.
- Csordás,G. and Hajnóczy,G. (1987). SR/ER-mitochondrial local communication: calcium and ROS. *Biochimicaet Biophysica Acta*. 1787(11). pp.1352–1362.
- Cuellar,M.andEspinoza,L.(1997). Methotrexate use inpsoriasis and psoriaticarthritis.*Rheum Dis Clin North Am*, 23.pp.797-809.
- Cuervo,M.and Dice,F.(1996). Areceptor for These Lectiveup Take and Degradation of Proteins by Lysosomes.*Science* 273, pp.501–503.
- Danial, N. and Korsmyer, S. (2004). *Cell Death:Critical Control Points*. 116(2), pp.205-219.
- Danko S, Yamasaki K, Daiho T, Suzuki H. (2004). Distinct natures of Beryllium Fluoride-Bound, Aluminum Fluoride-Bound, and Magnesium Fluoride-Bound Stable Snalogues of an ADP-Insensitive Phosphoenzyme Intermediate of Sarcoplasmic Reticulum Ca²⁺-ATPase: Changes in Catalytic and Transport Sites During phosphoenzyme hydrolysis. *J Biol Chem*. 279(15), pp.14991-508.
- Dasari, S. and Tchounwou, P. (2014). Cisplatin in cancer therapy: molecular mechanisms of action. *European journal of pharmacology*. 0, pp. 364-378.
- Davies,S.(2001). Therapy-Related Leukemia Associated with alkylating agents. *Med.Pediatr*.
- De Alencar,T., Wilmart-Gonçalves,T.,Vidal,L.,Fortunato,R.,Leitão,A.andLage,C. (2014). Bipyridine(2,2'-dipyridyl) Potentiates Escherichiacolilethality Induced by Nitrogen Mustard Mechlorethamine. *Mutation Research/Fundamental and MolecularMechanisms of Mutagenesis*, 765, pp.40-47.
- Debatin, K. (1997). Cytotoxic drugs, programmed cell death, and the immune system: defining new roles in an old play. *J Natl Cancer Inst*. 4;89(11),pp.750-1.
- Debatin, K. M. (1997). Cytotoxic Drugs,Progeammed Cell Death, and The Immune System :Defining New Roles in an Old Play.*J Natl Cancer Inst*. 89(11), pp.750-1.
- Debnath, J., Baehrecke,E. ,and Kroemer, G.(2005). Does autophagycontributeto celldeath?

- Deconlie, R., Toftness, B., Lange, B. and Creasey, W. (1973). Clinical and Pharmacological Studies With cis-Diamminedichloroplatinum (II). *Cancer Res.* 33, pp.1310-1315.
- Defranco, A., Locksley, R., Robertson, M., (2007). *Immunity: The Immune Response in Infectious and Inflammatory Disease, Primers in Biology*. New Science Press, Chapter 5 (146) 387 pages.
- Degterev, A., Huang, Z., Boyce, M., Li, Y., Jagtap, P., Mizushima, N., Cuny, G., Mitchison, T., Moskowitz, M. and Yuan, J. (2005). Chemical Inhibitor of non apoptotic cell Death With therapeutic Potential for Ischemic Brain Injury. *Nature Chemical Biology.* 1(2), pp.112-119.
- Degterev, A., Maki, J. and Yuan, J. (2012). Activity and Specificity of necrostatin-1, Small-Molecule inhibitor of RIP1 kinase. *Cell Death and Differentiation.* 20(2), pp.366-366.
- Di Leva, F., T. Domi, L. Fedrizzi, D. Lim and E. Carafoli (2008). "The Plasma Membrane Ca^{2+} ATPase of Animal Cells: Structure, Function and Regulation." *Arch Biochem Biophys.* 476(1), pp.65-74.
- Dode L, Andersen JP, Vanoevelen J, Raeymaekers L, Missiaen L, Vilsen B, Wuytack F. (2006). Dissection of The Functional Differences Between Human Secretory Pathway Ca^{2+} /Mn $^{2+}$ -ATPase (SPCA) 1 and 2 Isoenzymes by Steady-State and Transient Kinetic Analyses. *J Biol Chem* 281, pp.3182–3189.
- Donovan, M. and Cotter, T. (2004). Control of Mitochondrial Integrity by Bcl-2 Family Members and Caspase-Independent Cell Death. *Biochimica and Biophysica Acta*, 1644, pp. 133-147.
- Doroshov, J., Locker, G., Gaasterland, D., Hubbard, S., Young, R. and Myers, C. (1981). *Drosophila* central nervous system midline. *Curr Biol.* 5(7), pp.784-790.
- Dyer, J.L., Michelangeli, F. (2001). Inositol 1,4,5-Trisphosphate Receptor Iso Forms Show Similar Ca^{2+} Release Kinetics. *Cell Calcium.* 30(4), pp.245-50.
- Dyer, J. and Michelangeli, F. (2001). Inositol 1,4,5-trisphosphate receptor isoforms show similar Ca^{2+} release kinetics. *Cell Calcium.* 30(4), pp.245-50.
- Elisa A. Durham (1991). The Pharmacology of Methotrexate. *JAMA CUTAN MED SURG.* 25 .pp.306-318.

- Ellis,H.,Horvitz,H.(1986).Geneticcontrol of Programmed Cell Death Inthenematode C.elegans. Cell. 44(6), pp.817-829.
- Ellis,H.andHorvitz,H.(1986). Genetic Control of Programmed Cell Death Inthenematode C. legans.Cel. 44(6), pp.817-829.
- Ewees,M., Abdelghany,T., Abdel-Aziz,A, Abdel-Bakky,M., (2015). All-Trans Retinoic Acid Mitigates Methotrexate-Induced Liver Injury in Rats; Relevance of Retinoic Acid Signaling pathway.Naunyn-Schmiedeberg's Archives of Pharmacology. 388(9), pp.931-938.
- Ewend,M.,Brem, S.,Gilbert,M.,Goodkin,R.,Penar, P.,Varia,M.,Cush, S.and Carey,L. (2007). Treatmentof Single Brain Metastasiswith Resection, Intracavity Carmustine PolymerWafers, and Radiation Therapy Is Safe and Provides ExcellentLocal Control.Clinical Cancer Research. 13(12), pp.3637-3641.
- Falco, P.,Bringen, S.,Avonto,I.,Gay,F.,Morabito,F.,Boccadoro, M.and Palumbo,A. (2007).Melphalananditsrole Inthemanagement of Patients with Multiple Myeloma.Expert Reviewof Anticancer Therapy.7(7), pp.945-957.
- Fan, Z., Beresford, P., Zhang, D., Lieberman, J. (2002). HMG2 interacts with the nucleosome assembly protein SET and is a target of the cytotoxic T-lymphocyte protease granzyme A. Mol Cell Biol.22(8),pp.2810-20.
- Ferris, C.D., Cameron, A.M., Bredt, D.S., Haganir, R.L., Snyder, S.H. (1992). Autophosphorylation of Inositol 1,4,5-Trisphosphate Receptors. J Biol Chem. 267(10), pp.7036-41.
- Ferrucci, P., Minchella, I., Mosconi, M., Gandini, S., Verrecchia, F., Cocorocchio, E., Passoni,C., Pari,C.,Testori,A.,Coco,P.andMunzone,E.(2015). Dacarbazinein combinationwithbevacizumab for the treatmentof unresectable/metastatic melanoma.MelanomaResearch. 25(3), pp.239-245.
- Fill M, Copello JA. (2002). Ryanodine Receptor Calcium Release Channels. Physiol Rev. 82, pp. 893-922.
- Fink, S. and Cookson, B., (2005). Apoptosis, Pyroptosis, and Necrosis: Mechanistic Description of Dead and Dying Eukaryotic Cells. Infect. Immun. (73)4, pp.1907-1916.
- Fleischer S (2008). Personal Recollections on the Discovery of the Ryanodine Receptors of Muscle .Biochem Biophys Res Commun. 369, pp.195-207.
- Fontanella,C.Aita, M.,Cinausero, M.,Aprile, G.,Baldin,M.,Dusi,V.,Lestuzzi,C.,Fasol, G., ugli1,G.(2014). Capecitabine-Induced

Cardiotoxicity: more evidence or clinical approaches to protect the patients' heart? *Onco Targets Ther.* 29(7), pp.1783-1791.

- Formigli, L., Papucci, L., Tani, A., Schiavone, N., Tempestini, A., Orlandini, G.E., Capaccioli, S., and Orlandini, S. Z. (2000). Aponecrosis: Morphological and Biochemical Exploration of a Syncretic Process of Cell Death sharing Gapoptosis and Necrosis. *J Cell Physiol.* 182, pp.41–49.
- Foufelle, F. and Fromenty, B. (2016). Role of Endoplasmic Reticulum Stress in Drug-Induced
- Fraser, S., Karimi, R., Michalak, M. and Hudig, D. (2000). Perforin Lytic Activity Is Controlled by Calreticulin. *The Journal of Immunology.* 164(8), pp.4150-4155.
- Frei, E., Eder, J. (2003). Combination Chemotherapy. In: Kufe DW, Pollock RE, Weichselbaum RR, et al., editors. *Holland-Frei Cancer Medicine*. 6th edition. Hamilton. Available from: <http://www.ncbi.nlm.nih.gov/books/NBK13955/>.
- Frosch, P., Czarnetzki, B., Macher, E., Grundmann, E. and Gottschalk, I. (1979). Hepatic Failure in a patient treated with dacarbazine (DTIC) for malignant melanoma. *J Cancer Res Clin Oncol.* 95(3), pp.281-286.
- Fujita, T., Inoue, H., Kitamura, T., Sato, N., Shimosawa, T., Maruyama, N. (1998). Senescence marker protein-30 (SMP30) rescues cell death by enhancing plasma membrane Ca(2+)-pumping activity in Hep G2 cells. *Biochem Biophys Res Commun.* 250(2), pp.374-80.
- Funderburk, S., Wang, Q., and Yue, Z. (2010). Beclin 1-VPS34 complex – At the Crossroads of Autophagy and Beyond. *Trends in Cell Biology.* 20(6), pp.355–362.
- Gandikota, N., Hartridge-Lambert, S., Migliacci, J., Yahalom, J., Portlock, C. and Schöder, H. (2015). Very Low Utility of Surveillance imaging in early-Stage Classic Hodgkin Lymphoma Treated With a combination of Doxorubicin, Bleomycin, Vinblastine, and Dacarbazine and Radiation Therapy. *Cancer.*
- Gewirtz, D. (1999). A critical evaluation of the mechanisms of action proposed for the antitumor effects of the anthracycline antibiotics adriamycin and daunorubicin. *Biochem Pharmacol.* 57, pp.727-741.
- Gilani, S., Khan, D., Khan, F., Ahmed, M. (2012). Adverse Effects of Low Dose Methotrexate in Rheumatoid Arthritis Patients. *J. Coll. Phys. Surg. Pak.* 22, pp.101-102.

- Gilman, A. and Philips, F. (1946). The Biological Actions and Therapeutic Applications of the B-Chloroethyl Amines and Sulfides. *Science*, 103(2675), pp.409-436.
- Goede, V., Eichhorst, B., Fischer, K., Wendtner, C. and Hallek, M. (2014). Past, Present and Future Role of Clorambucil in the treatment of chronic lymphocytic leukemia. *Leukemia & Lymphoma*. pp.1-8.
- Goodsell, D.S. (2006). The molecular perspective: Cisplatin. *The oncologist*, 11, pp.316-317.
- Green, D. R. (2011). *Apoptosis: Physiology And pathology*. Cambridge: Cambridge University Press.
- Green, D. (2006). At the gates of death. *Cancer Cell*. 9(5), pp.328-30.
- Groopman, J. and Itri, L. (1999). Chemotherapy-Induced Anemia in Adults: Incidence and Treatment. *JNCI J Natl Cancer Inst.* (19), pp.1616-1634.
- Gustafsson AB, Gottlieb RA. (2003). Mechanisms of Apoptosis in The Heart. *Journal of Clinical Immunology*. 23(6), pp.447-59.
- Halestrap AP, Connern CP, Griffiths EJ, Kerr PM. (1997). Cyclosporin A Binding to Mitochondrial Cyclophilin Inhibits the Permeability Transition Pore and Protects Hearts from Ischaemia/Reperfusion Injury. *Mol Cell Biochem*. 174 (1-2), pp.167-72.
- Hammill, A., Uhr, J. and Scheuermann, R. (1999). Annexin V Staining Due to Loss of Membrane Asymmetry Can Be Reversible and Precede Commitment to Apoptotic Death. *Experimental Cell Research*, 251(1), pp.16-21.
- Hande, K. (1996). The Importance of Drug Scheduling in Cancer Chemotherapy: Etoposide as an Example. *Stem Cells*. 14(1), pp.18-24.
- Hanna, A., Lam, A., Tham, S., Dulhunty, A. and Beard, N. (2014). Adverse Effects of Doxorubicin and Its Metabolic Product on Cardiac RyR2 and SERCA2A. *Mol. Pharmacol.* 86, pp. 438-449.
- Harvey, K., Xu, Z., Saadatzadeh, M., Wang, H., Pollok, K., Cohen-Gadol, A. and Siddiqui, R. (2015). Enhanced anticancer properties of lomustine in conjunction with docosahexaenoic acid in glioblastoma cell lines. *Journal of Neurosurgery*. 122(3), pp.547-556.
- Hattori, M., Suzuki, A., Higo, T., Miyauchi, H., Michikawa, T., Nakamura, T., Inoue, T. & Mikoshiba, K. (2004). Distinct Roles of Inositol 1,4,5-Trisphosphate Receptor Types 1 and 3 in Ca²⁺ Signaling' *Journal of Biological Chemistry*. 279(12), pp. 11967-11975

- Hayashi,T., S.,Goto,D., Matsumoto,I.andSumida,T.(2010). Elevated Levelof Serum Cystatin-concentration is ausefulpredictor for myelo suppression induced by methotrexate for treatmen to frheumatoid arthritis. *ModernRheumatology*. 20(6), pp.548-555.
- He,A.(2015).Efficacy of S-1vscapecitabine for the treatment of gastric cancer:Ameta-analysis. *WJG*, 21(14), p.4358.
- Henderson, B., and Feigelson, H. (2000). Hormonal Carcinogenesis.*Carcinogenesi*. 21(3), pp.427-433.
- Henderson, I., and Shapiro, C.(1991). Hexamethylmelamine use in the treatment of metastatic breast cancer.*Cancer Treat Rev*.pp.91-98.
- Hengartner ,M.(2000). Thebiochemistry of Apoptosis. *Nature*. 12. 407(6805), pp.770-776.
- Herold,M.,Scholz,C.,Rothmann,F.,Hirt,C.,Lakner,V.andNaumann,R.(2015). Long-Term Follow-up of Rituximab Plus First-Line Mitoxantrone, Chlorambucil, Prednisolone and interferon-alpha as maintenance therapy infollicular lymphoma. *JCancer Res Clin Oncol*.141(9),pp.1689-95.
- Hill, H., Hill, G., Szramowski, J.(1979). Dacarbazine Andmelphalan. Enhancement by Dosage Schedulingof The Effect Incombination Treatment on The Harding-Passey Melanoma in C3D2F1 mice.114(2), pp.135-8.
- Hirsova,P.andGores,G.(2015). Death Receptor-Mediated Cell Death and Proinflammatory Signalingin Nonalcoholic Steatohepatitis,CMGHC ellular and Molecular Gastroenterology and Hepatology, 1(1).pp.17-27.
- Hodgson, S., Foulkes, W., Eng, C., Maher, E. (2013). A Practical Guide to Human Cancer Genetics.Springer Science & Business Media, 420 pages.
- Holler, N.,Holler1,N.,Zaru1,R.,Micheau1,O.,Thome1,M., Attinger1,A., Valitutti1,S.,Bodmer1,J.,Schneider1,P.,Seed,B.,& Tschopp, J.(2000). Fas Triggersan Alternative,Caspase-8-Independent Cell Death Path Way Using Thekinase RIPas Effect or Mlecule.*Nature Immunol*. 1, pp.489–495.
- Hovnanian, A. (2007). SERCA Pumps and Human Diseases.*Subcell Biochem* 45, pp.337-363 109 17.
- Hu, Z. L., Bonifas, J. M., Beech, J., Bench, G., Shigihara, T., Ogawa, H., Ikeda, S., Mauro, T. & Epstein, E. H. (2000). Mutations in ATP2C1, encoding a calcium pump, cause Hailey-Hailey disease. *Nature Genetics*. 24, pp.61-65.

- Huang,C.,Luo,Y.,Zhao,J.,Yang,F.,Zhao,H.,Fan,W.andGe,P.(2013). Shikonin Kills Glioma Cells through Necroptosis Mediated by RIP-1. *PLoS ONE*. 8(6), pp.e66326.
- Idriss, H., and Naismith, J. (2000). TNF α and the TNF receptor superfamily; structure-function relationship(s). *Microscopy Res. Tech.* 50,pp. 184–195.
- Imajoh, H. Sugiura, S. Oshima,H. (2004). Morphological Changes Contribute to Apoptotic Cell Death and are Affected by Caspase-3 and Caspase-6 Inhibitors During Red Sea Bream iridovirus permissive replication *Virology*. 322, pp.220-230.
- Imtiaz,S.,Muzaffar,N.(2010). Ifosfamide neurotoxicity in a young female with aremarkable Functions. *Biochemistry*, 49,pp. 3436-3444.
- Inesi, G. (1985). Mechanism of calcium transport. *Annu Rev Physiol.* 47, pp.573-601.
- Ishigami,A., Fujita,T., Handa,S., Shirasawa,T., Koseki,H. Kitamura,T., Enomoto,N. Sato,N., Shimosawa,T., Maruyama,T., (2002). Senescence Marker Protein-30 Knockout Mouse Liver Is Highly Susceptible to Tumor Necrosis Factor- α and Fas-Mediated Apoptosis *American Journal of Pathology*. 161(4).
- Isoda, T.,Ito,S., Kajiwara, M. AndNagasawa,M.(2007).Successful High-Dose methotrexate Chemotherapy Inpatient With Acute lymphocytic leukemia who developed acute renal failure during the initial treatment. *Pediatrics International*. 49(6), pp.1018-1019.
- Izumi, T. and Yamaguchi, M.(2004). Overexpression of regucalcin suppresses cell death and apoptosis in cloned rat hepatoma H4-II-E cells induced by lipopolysaccharide, PD 98059, dibucaine, or Bay K 8644. *J Cell Biochem.* 15;93(3) ,pp.598-608.
- Izumi, T., Tsurusaki,Y., Yamaguchi, M. (2003). Suppressive effect of endogenous regucalcin on nitric oxide synthase activity in cloned rat hepatoma H4-II-E cells overexpression regucalcin. *J. Cell Biochem.* 89,pp.800-807.
- Jacobson,M.,Wei,M.,Raff,M.(1997) . Programmed cell death in animal development. *Cell*. 88(3), p.347-354.
- Jaskiewicz,K.,Voigt, H.,Blakolmer,K.(1996). Increased matrix protein, collagen and transforming growth factor are early marker of hepatotoxicity inpatient so nlong- term methotrexate therapy. *J-Toxicol.* 34, pp.301-305.
- Jeffes,EWBIII,McCullough,J.,Pittelkow,M.,McCormick,A.,Almanzor,J.,Liu,G., Dang,M.,Voss,K.,chlotzhauer,A.,Weinstein,G.(1995). Methotrexate therapy

- Jensen, A. M., Sorensen, T. L., Olesen, C., Moller, J. V., and Nissen, P. (2006). Modulatory and Catalytic Modes of ATP Binding by the Calcium Pump. *EMBO J.* 25, pp.2305-2314.
- Jin, X., Wu, X., Nouh, M. and Kakehi, Y. (2007). Enhancement of Death Receptor 4 Mediated Apoptosis and Cytotoxicity in Renal Cell Carcinoma Cells by Subtoxic Concentrations of Doxorubicin. *The Journal of Urology.* 177(5), pp.1894-1899.
- Jones, K., Patel, S. (2000). A family physician's guide to monitoring methotrexate. *Am Fam Physician.* 262(7), pp.1607-1614.
- Kamada, Y., Funakoshi, T., Shintani, T., Nagano, K., Ohsumi, M., Ohsumi, M., Tori-mediated (2000). Induction of autophagy via an Apg1 protein kinase complex, *J. Cell Biol.* 150, pp.1507–1513.
- Kamesaki, S., Kamesaki, H., Jorgensen, T., Tanizawa, J., Pommier, Y., Cossman, J., (1993). Bcl-2 Protein inhibits topoisomerase II-induced apoptosis through its effect on events subsequent to topoisomerase II-induced DNA strand breaks and their repair. *Cancer Res.* 53, pp.4251–4256.
- Kang, Y., Kang, Y., Yi, M., Kim, M., Park, M., Bae, S., Kang, C., Cho, C., Park, I., Park, M., Rhee, C., Hong, S., Chung, H., Lee, Y., and Lee, S. (2004). Caspase-Independent Cell Death by Arsenic Trioxide in Human Cervical Cancer Cells: Reactive Oxygen Species-Mediated Poly(ADP-ribose) Polymerase-1 Activation Signals Apoptosis-Inducing Factor Release from Mitochondria. *Cancer Research.* 64(24), pp.8960-
- Kang, B., Kim, J., Kwon, O., Chung, H., Yu, W. (2014). Non-Platinum-Based Chemotherapy for Treatment of Advanced Gastric Cancer: 5-Fluorouracil, Taxanes, and Irinotecan. *WJG.* 20(18), p.5396.
- Kaplan, I. (2014). Carvacrol and Pomegranate Extract in Treating Methotrexate-Induced Lung Oxidative Injury in Rats. *Medical Science Monitor.* 20, pp.1983-1990.
- Karadeniz, A., Simsek, N., Karakus, E., Yildirim, S., Kara, A., Can, I., Kisa, F., Emre, H. and
- Kasri, N.N., Holmes, A.M., Bultynck, G., Parys, J.B., Bootman, M.D., Rietdorf, K., Missiaen, L., McDonald, F., De Smedt, H., Conway, S.J., Holmes, A.B., Berridge, M.J., Roderick, H.L. (2004). Regulation of InsP3 receptor activity by neuronal Ca²⁺-binding proteins. *J EMBO.* 23(2), pp.312-21.
- Kass, N. and Orrenius, S. (1999). Calcium Signaling and Cytotoxicity. *Environmental Health Perspectives.* 107, pp. 25–35.

- Kawasaki,H., Taira, N.,Ichi,T., Yohena, T., Kawabata, T.,Ishikawa,K. (2014). Weekly Chemotherapy Withcisplatin,Vincristine,Doxorubicin, and Etoposide Followed by surgery for thymiccarcinoma. *EurJ Surg Oncol.* 40(9). pp.1151-5.
- KawasakiH,OnukiR,Suyama E,TairaK.(2002). Identification of Genesthat Functionin The TNF α -mediated Apoptotic pathway using an domized hybrid ribozyme libraries. *Nat Biotechnol.* 20(4). pp.376-80.
- Kerr, J. and Harmon,B.(1991). Definition and Incidence of Ooptosis :Anhistorical
- Kerr, J. (1971). Shrinkage necrosis: A distinct Mode of Cellular Death. *The Journal of*
- Kerr, J., Winterford, C.,Harmon ,B.(1994). Apoptosis.Its Significanceincancerand Cancer Therapy. *Cancer*, 73(8). pp. 2013-2026.
- Kerr,J.,Wyllie,A. ,andCurrie,A. (1972). Apoptosis:a Basic Biological Phenomenon With Wide-Ranging Implications in Tissuekinetics. *Br JCancer.* 26, pp. 239–57.
- King, P. and Perry, M. (2001). Hepatotoxicity of chemotherapy. *Oncologist.* 6(2),pp.162-76.
- King, P. Perry, M. (2001). Hepatotoxicity of chemotherapy. *Oncologist*;6(2),pp.162-76.
- King,D.P.andPerry,M.(2001). Hepatotoxicity of Chemotherapy.Theoncologist. 6, pp.162-176.
- Klionsky, J. (2004). The molecular machinery of autophagy: unanswered questions. *J Cell Sci.* 118(Pt 1), pp.7–18.
- Klosterhalfen, B., Töns, C., Hauptmann, S., Tietze,L., Offner,F., Küpper, W., Kirkpatrick, C. (1996). Influence of heat shock protein 70 and metallothionein induction by Zinc-Bis-(DL-Hydrogenaspartate) on the release of inflammatory mediators in a porcine model of recurrent endotoxemia, *Biochemical Pharmacology*, 52 (8), pp. 1201-1210.
- Kobayashi, S., Volden, P., Timm, D., Mao, K., Xu, X., Liang, Q. (2010). Transcription factor GATA4 inhibits doxorubicin-induced autophagy and cardiomyocyte death. *J Biol Chem* 285,pp.793–804.
- Kohn, E. C., Reed, E., Sarosy, G., Christian, M., Link, C. J., Cole, K., Figg, W. D., Davis, P. A., Jacob, J., Goldspiel, B. and Liotta, L. A. (1996). 'Clinical Investigation of a Cytostatic Calcium Influx Inhibitor in Patients with Refractory Cancers', *Cancer Research.* 56(3), pp.569-573.
- Koler,D.and Forsgren,A.(1958). Hepatotoxicity Duetochlorambucil Repost of Case.*JAMA.*167.pp.316-317.

- Kondo, Y., Kanzawa, T., Sawaya, R., and Kondo, S. (2005). The role of Autophagy in cancer Development and Response to Therapy. *Nat. Rev. Cancer.* 5, pp. 726–734.
- Kruger, S., Boeck, S., Heinemann, V., Laubender, R., Vehling-Kaiser, U., Waldschmidt, D., Kettner, E., Märten, A., Winkelmann, C., Klein, S., Kojouharoff, G., Gauler, T., Fischervon Weikersthal, L., Clemens, M., Geissler, M., Greten, T., Hegewisch-Becker, S., Modest, D., Stintzing, S. and Haas, M. (2015). Impact of Hand-Foot Skin Reaction on Treatment outcome in patients receiving capecitabine plus erlotinib for advanced Pancreatic cancer: A subgroup Analysis from AIO-PK0104. *Acta Oncol.* pp. 1-8.
- Kufe, D., Pollock, R., Weichselbaum, R., et al., (2003). Editors. *Holland-Frei Cancer Medicine*. 6th edition. Hamilton (ON): BC Decker.
- Kurz, T. and Terman, A. (2008). Lysosomes in iron metabolism, Ageing and Apoptosis. *Histochem Cell Biol.* 129, pp. 389-406.
- Kwon, H., Shin, H., Lee, J., Park, S., Kwon, M., Panneerselvam, S., Lee, C., Kim, S., Kim, J., Choi, S. (2015). Etoposide Induces Necrosis Through p53-Mediated Antiapoptosis in Human Kidney Proximal Tubule Cells. *Toxicol Sci*; 148(1), pp. 204-19.
- Lahoti, T., Patel, D., Thekkemadom, V., Beckett, R., Ray, S. (2012). Doxorubicin-induced in vivo nephrotoxicity involves oxidative stress-mediated multiple pro- and anti-apoptotic signaling pathways. *Curr Neurovasc Res.* 9(4), pp. 282-95.
- Lai P, Michelangeli F. (2009). Changes in Expression and Activity of the Secretory Pathway Ca²⁺ ATPase 1 (SPCA1) in A7r5 Vascular Smooth Muscle Cells Cultured at Different Glucose Concentrations. *Biosci Rep.* 29, pp. 397–404.
- Lai, P. (2009). ‘SPCA1 & Regucalcin: Expression, Activity & Regulation In Mammalian Ca²⁺ Homeostasis’ PhD thesis, University of Birmingham, Birmingham, UK.
- Lai, P. and Michelangeli, F. (2012). Bis(2-hydroxy-3-tert-butyl-5-methyl-phenyl)-methane (bis-phenol) is a potent and selective inhibitor of the secretory pathway Ca²⁺ ATPase. *Biochem Biophys Res Commun.* 3;424(3), pp. 616-9.
- Lai, P., Yip, N., Michelangeli, F. (2011). Regucalcin (RGN/SMP30) alters agonist- and thapsigargin-induced cytosolic [Ca²⁺] transients in cells by increasing SERCA Ca²⁺ATPase levels, *FEBS Letters.* 585(14), pp. 2291-2294.
- Laken, H. and Leonard, M. (2001). Understanding and Modulating Apoptosis in Industrial Cell Culture. *Current Opinion in Biotechnology.* 12, pp. 175-179.

- Lal,S.,Mahajan,A.,Chen,W.,Chowbay,B.,(2010). Pharma cogenetics of target genes across doxorubicin disposition pathway :areview.CurrDrugMetab. 11, pp.115–128.
- Laohapand,Charlie,EmvaleeArromdee,and Tawesak Tanwandee.(2015). 'Long-TermUse Of Methotrexate Does Not Result In Hepatitis B Reactivation In Rheumatologic Patients'. Hepatology International. 9(2).pp.202-208.
- Lapidus RG, Sokolove PM. (1994). The Mitochondrial Permeability Transition. Interactions of Spermine, ADP, and Inorganic Phosphate. J Biol Chem. 269(29), pp.18931-18936.
- Lawerence, E. Broder, M. and Stephen, K. (1973). Pancreatic Islet cell carcinoma II :Results of therapy with streptozotocin in 52 patients. Annals of internal medicin, 79,pp.108-118.
- Lee, A. G. (2002). A calcium Pump Made Visible. Curr Opin Struct Biol. 12, pp.547-554.
- Lee,T.,Lau,T.,Ng,I.(2002). Doxorubicin-Induced apoptosis and chemosensitivity in hepatoma cell lines. Cancer Chemother Pharmacol. 49, pp. 78–86.
- Leist, M. and Jaattela, M. (2001). Four deaths and a funeral: from caspases to alternative mechanisms. Nature Reviews Molecular Cell Biology, 2(8), pp.589-598.
- Lenz,T.(2012). Lessening Chemotherapy Side Effects With Life style Medicine. AmericanJournal of Life Style Medicine. 6(3), pp.219-221.
- Lervik,A., Bresme, F., Kjelstrupad, S.(2012). Molecular Dynamics Simulations of The Ca²⁺-Pump: a Structural Analysis. Phys. Chem. Chem. Phys. 14, pp.3543-3553.
- Leung,L.andWang,T.(1999). Differential Effects of Chemotherapeutic agent son the Bcl-2/Bax apoptosis pathway inhuman breast cancer cell line MCF-7.BreastCancer Res Treat.55, pp.73–83.
- Levine, B., Yuan, J. (2005). Autophagy in cell death: an innocent convict?. 115(10), pp. 2679-2688.
- Lieberman,J.(2003). The ABC So Fgranule-Mediated Cytotoxicity: New Weaponsinthe Arsenal. Nat RevImmunol. 3(5), pp.361-370.
- Litterst,CL. (1981). Alterations in the toxicity of cis-dichlorodiammin eplatinumII and in tissue localization fplatinum asa function f NaCl concentration in the vehicle of administration Toxicol Appl Pharmacol. 61, pp.99–108.

- Liu, M., Acres, B., Balloul, J., Bizouarne, N., Paul, S., Slos, P., Squiban, P. (2004). Gene-Based vaccines and immuno Therapeutics, *Proc Natl Acad Sci.* 101(2), pp.14567–14571.
- Lizama, C., Ludwig, A. and Moreno, R. (2011). Etoposide Induces Apoptosis and Upregulation of TACE/ADAM17 and ADAM10 In an invitro Male Germ Cellline Model. *Biochimica et Biophysica Acta (BBA)-Molecular Cell Research.* 1813(1), pp.120-128.
- Locksley, R., Killeen, N., and Lenardo, M. (2001). The TNF and TNF Receptor Super Families:
- Lodish, H., Berk, A., Zipursky, S., (2000). *Molecular Cell Biology.* 4th edition. New York: W. H. Freeman; Section 24.1, Tumor Cells and the Onset of Cancer.
- Loft, S., Høgh Danielsen, P., Mikkelsen, L., Risom, L., Forchhammer, L., Møller, P. (2008). Biomarkers of oxidative damage to DNA and repair *Biochem. Soc. Trans.* 36, pp. 1071–1076.
- Lohrer, P. (1991). Etoposide therapy for testicular cancer. *Cancer.* 67(S1), pp.220-224.
- Loike, J. and Horwitz, S. (1976). Effects of podophyllotoxin and VP-16-213
- Lomovskaya, N., Otten, S. L., Doi-Katayama, Y., Fonstein, L., Liu, X.-C., Takatsu, T. Hutchinson, C. R. (1999). Doxorubicin Overproduction in *Streptomyces Peucetius*: Cloning and Characterization of the *dnrU* Ketoreductase and *dnrV* Genes and the *doxA* Cytochrome P-450 Hydroxylase Gene. *Journal of Bacteriology.* 181(1), pp.305–318.
- Lompre, A. M., M. Anger and D. Levitsky (1994). "Sarco (endo) Plasmic Reticulum Calcium Pumps in the Cardiovascular System: Function and Gene Expression." *J Mol Cell Cardiol.* 26(9), pp.1109-1121.
- Lowe, S., Ruley, H., Jacks, T. and Housman, D. (1993). P53-dependent Apoptosis Modulates the Cytotoxicity of Anticancer Agents. *Cell.* 74(6), pp.957-967.
- Lukovic, D., Akira K., Beverly, P., and David, U., (2003). Caspase Activity is not Sufficient to Execute Cell Death. *Experimental Cell Research,* 289, pp. 384-395.
- Lytton, J, Westlin, M., Hanley, M. (1991). Thapsigargin inhibits the sarcoplasmic or endoplasmic reticulum Ca²⁺-ATPase family of calcium pumps. *J Biol Chem.* 266, pp.17067-71.
- Ma, X., Yu, H. (2006). Global Burden of Cancer. *The Yale Journal of Biology and Medicine.* 79(3-4), pp.85-94.

- MacLennan, D., Brand, C., Korczak, B., Green, N. (1985). Amino-acid sequence of a Ca^{2+} + Mg^{2+} -dependent ATPase from rabbit muscle sarcoplasmic reticulum, deduced from its complementary DNA sequence. *Nature*. 316,pp.696-700.
- MacLennan,D.H.(1970). "Purification and Properties of an Adenosine Triphosphate from Sarcoplasmic Reticulum." *J Biol Chem*. 245(17), pp.4508-4518.
- Majno G., andJoris,I.(1995). Apoptosis,Oncosisandnecrosis.Anover View of Cell Death.*Am.J.Path*.146,pp.3–15.
- Malatjalian,D.,Ross,J., Williams,C.,Colwell,S.,Eastwood,B.(1996).Methotrexate Transaminitisinpsoriasis: Reports of 104 Patients from Nova Scotia With Analysis ofrisksfromobesity,diabetesandalcoholconsumptionduring longtermfollow- up. *Can JGastroenterol*.10,pp.369–375.
- Maor,Y.andMalnick,S.(2013). Liver Injury Induced by Anticancer Chemo therapy and Radiation Therapy.*International Journal of Hepatology*. pp.1-8.
- Martin, N., Borchellini, D., Coso, D., Gastaud, L., Boscagli, A., Saudes, L., Re, D., Gutnecht,J.,Garnier,G.,Petit,E.,Barriere,J.,Naman,H.,Rossignol,B.,Thyss, A.andPeyrade,F.(2015). High-Dosechemo Therapy with Carmustine, Etoposide, Cytarabine and Melphalan Followed by Autologous Stem Cell Transplant is an Effective Treatment For elderly patients with poor-Prognosis lymphoma. *Leukemia & Lymphoma*, pp.1-9.
- Martin,S.,Reutelingsperger,C.,McGahon,A.Rader,J.,vanSchie,R.,LaFace,D.,Green, D. (1995).Earlyredistribution of Plasmamembranephosphatidylserinei Sageneral Feature of Apoptosisre gardl Essoftheinitiating Stimulus:Inhibitionby over Expression ofBcl-2and Abl. *JournalofExperimental Medicine*,182(5), pp.1545-1556.
- Mattila, M., Koskenvuo, J., Söderström, M., Eerola, K., Savontaus, M.(2016). Intramyocardial injection of SERCA2a-expressing lentivirus improves myocardial function in doxorubicin-induced heart failure. *J Gene Med*.18(7),pp.124-33.
- McGuire,M.,Lipsky, P.andThiele,D.(1992). Purification and Characterizationof dipeptidyl peptidaseIfrom humanspleen. *ArchBiochem Biophys*, 295(2). pp.280-285.
- McGuire,M.,Lipsky, P.andThiele,D.(1993). Generation of Active myeloidandlymphoid Granule Serine Proteases Requires Processing by The Granule Thiol Protease Dipeptidyl PeptidaseI. *J BiolChem*. 268(4).pp.2458-1267.

- Mekahli, D., Bultynck, G., Parys, J., De Smedt, H., & Missiaen, L. (2011). Endoplasmic-Reticulum Calcium Depletion and Disease. *Cold Spring Harbor Perspectives in Biology*, 3(6), a004317.
- Messori, L. and Merlino, A., (2016). Cisplatin Binding to Proteins: A structural Perspective *Coord. Chem. Rev.* 315, pp.67–89.
- Mestrlil, R., Chi, H., Sayen, M., O'Reilly, K., AND Dillman, W., (1999). Expression of inducible stress protein 70 in rat heart myogenic cells confers protection against stimulated ischemia-induced injury. *J. Clin. Invest.* 93, pp.759-767.
- Michael, A., Barry, Catherine, A., Bechnke and Alan, E. (1990). (Activation of Programmed Cell Death (Apoptosis) by Cisplatin, Other anticancer drugs, Toxicants and Hyperthermia. *Biochemical Pharmacology*. 40(10), pp. 2353-2362.
- Michelangeli F, Ogunbayo OA, Wootton LL, Lai PF, Al-Mousa F, Harris RM, Waring RH, Kirk CJ. (2008). Endocrine Disrupting Alkylphenols: Structural Requirements for Their Adverse Effects on Ca²⁺ Pumps, Ca²⁺ Homeostasis & Sertoli TM4 cell viability. *Chem Biol Interact.* 176, pp.220-26.
- Michelangeli, F., J. East. M., (2011). A diversity of SERCA Ca²⁺ Pump Inhibitors *Biochem Soc Trans.* 39(3), pp 789–797.
- Michelangeli, F., Di Virgilio, F., Villa, A., Podini, P., Meldolesi, J., Pozzan, T. (1991). Identification, kinetic properties and intracellular localization of the (Ca²⁺)-Mg²⁺)-ATPase from the intracellular stores of chicken cerebellum. *J Biol Chem.* 275, pp. 555-61.
- Michelangeli, F., Ogunbayo, O., Wootton, L. (2005). A plethora of Interacting Organellar Ca²⁺ Stores. *Curr Opin Cell Biol.* 2005 April. 17(2), pp.135–140.
- Miller, R., Tadagavadi, R., Ramesh, G., Reeves, W. (2010). Mechanisms of Cisplatin Nephrotoxicity. *Toxins.* 2(11), pp.2490-2518.
- Minev, B. (2011). *Cancer management in man.* Dordrecht: Springer.
- Mitchell KJ, Tsuboi T, Rutter GA. (2004). Role for Plasma Membrane-Related Ca²⁺-ATPase-1 (ATP2C1) in Pancreatic β -Cell Ca²⁺ Homeostasis Revealed by RNA Silencing. *Diabetes.* 53, pp.393–400.
- Mitigates Methotrexate –Induced Liver Injury in Rat, Relevance of Retinoic Acid Signalling Path Way. *Naunyn-Schmiedeberg's Arch Pharmacol.* 015, pp.1130-1135.

- Miyata, M., Suzuki, S., Misaka, T., Shishido, T., Saitoh, S., Ishigami, A., Takeishi, Y. (2013). Senescence Marker Protein 30 Has a Cardio-Protective Role in Doxorubicin-Induced Cardiac Dysfunction. *PLoS ONE*, 8(12), e79093.
- Mizushima, N. (2005). The Pleiotropic Role of Autophagy: from Protein Metabolism to Bactericide. *Cell Death Differ.* 12, pp.1535-1541.
- Mizushima, N., Ohsumi, Y., Yoshimori, T. (2002). Autophagosome formation in mammalia. *Cell structure and function*. 27, pp.421-429.
- Mohammed, G., Tamer, M., Abdel-Aziz, H., Mohamed, S. (2015). All-Transretinoic acid
- Molina, J., Yang, P., Cassivi, S., Schild, S., Adjei, A. (2008). Non-small lung cancer: epidemiology, Risk factors, treatment and survivorship. *Mayo Clin Proc.* 83, pp.584-599.
- Moller, J. V., Juul, B., and le Maire, M. (1996). Structural Organization, Ion Transport, and Energy Transduction of P-type ATPases. *Biochim Biophys Acta.* 1286, pp.1-51.
- Moller, J. V., Nissen, P., Sorensen, T. L., and le Maire, M. (2005). Transport Mechanism of The Sarcoplasmic Reticulum Ca^{2+} -ATPase Pump. *Curr Opin Struct Biol.* 15, pp.387-393.
- Moore, A., London, C., Wood, C., Williams, L., Cotter, S., L'Heureux, D. and Frimberger, A. (1999). Lomustine (CCNU) for the Treatment of Resistant Lymphoma in Dogs. *Journal of Veterinary Internal Medicine.* 13(5), pp.395-398.
- Morimoto, R., Santoro, G. (1998) Stress-inducible responses and heat shock proteins: new pharmacologic targets for cytoprotection. *Nat Biotechnol.* 16, pp.833–838.
- Mrozek-Orlowski, M., Frye, D., Sanborn, H. (1999) Capecitabine: Nursing implications of a New Oral Chemotherapeutic Agent. *Oncol Nurs Forum.* 26(4), pp.753-762.
- Mullauer, B., Kessler, J., and Medema, J. (2009). Betulinic acid induce cytochrome c release and Apoptosis in a Bax/Bak-Independent, Permeability Transition pore Dependent Fashion Apoptosis, 14(2). pp. 191–202.
- Musser, M., Quinn, H. and Chretien, J. (2012). Low apparent risk of CCNU (lomustine)-Associated Clinical Hepatotoxicity in cats. *Journal of Feline Medicine and Surgery*, 14(12), pp.871-875.

- Nagler, A., Labopin, M., Gorin, N., Ferrara, F., Sanz, M., Wu, D., Gomez, A., Lapusan, S., Irrera, G., Guimaraes, J., Sousa, A., Carella, A., Vey, N., Arcese, W., Shimoni, A., Berger, R., Rocha, V., Mohty, M. (2014). Intravenous Busulfan For Autologous Stem Cell Transplantation In Adult Patients With Acute Myeloid Leukemia: A Survey Of 952 Patients On Behalf Of The Acute Leukemia Working Party Of The European Group For Blood And Marrow Transplantation. *Haematologica* 99, pp.1380-1386.
- Nakagawa, T., Yamaguchi, M. (2005). Overexpression of Regucalcin enhances its nuclear localization and suppresses L-type Ca channel and calcium-sensing receptor mRNA expressions in cloned normal rat kidney proximal tubular epithelial NRK52E cells. *J Cell Biochem* 99(4), pp.1064-77.
- Nakagawa, T. and Yamaguchi, M. (2005b). Overexpression of Regucalcin Suppresses Apoptotic Cell Death in Cloned Normal Rat Kidney Proximal Tubular Epithelial NRK52E Cells: Change in Apoptosis-Related Gene Expression. *J Cell Biochem*. 96(6), pp.1274-85.
- Nakagawa, T., Sawada, N., Yamaguchi, M. (2005). Overexpression of Regucalcin Suppresses Cell Proliferation of Cloned Normal Rat Kidney Proximal Tubular Epithelial NRK52E Cells. *Int. J. Mol. Med.* 16, pp.637-643.
- Nakagawa, T. and Yamauchi, M. (2008). Nuclear Localization of Regucalcin is Enhanced in Culture With Protein Kinase C Activation in Cloned Normal Rat Kidney Proximal Tubular epithelial NRK25E cells. *Int. J. Mol. Med.* 21, pp.605-610.
- Neves, H., and Kwok, H. (2015). Recent Advances in The Field of Anti-Cancer Immunotherapy. *BBA Clin.* 3, pp.280–288.
- Newton, K., Petfalski, E., Tollervey, D., Cáceres, J. (2003). Fibrillarin is essential for early development and required for accumulation of an intron-encoded small nucleolar RNA in the mouse. *Mol Cell Biol.* 23(23), pp.8519-27.
- Nieto, Y., Vaughan, W., (2004). Pharmacokinetics of high-Dose chemo Therapy. *Bone Marrow Transplant.* 33, pp.259–369.
- Niggli, V., E. Sigel and E. Carafoli (1982). "The purified Ca²⁺ pump of human erythrocyte 147 membranes catalyzes an electroneutral Ca²⁺ exchange in reconstituted liposomal systems." *J Biol Chem* 257(5), pp.2350-2356.
- Nowsheen, S., and Yang, E. S. (2012). The Intersection Between DNA Damage Response and Cell Death Pathways. *Experimental Oncology.* 34(3), pp.243–254.

- Obregón-Henao, A., Duque-Correa, M., Rojas, M.(2012) Stable Extracellular RNA Fragments of Mycobacterium tuberculosis induce early Apoptosis in human Monocytes Via caspase-8 Dependent Mechanism. PLoS One. 7(1), pp.29970.
- Ocular irritation from high-dose methotrexate therapy: Pharmacokinetics of Drug in the Tear Film. Cancer. 48(10), pp.2158-2162.
- of Psoriasis: Differential Sensitivity of Proliferating Cells to the Cytotoxic and Growth-Inhibitory Effects of Methotrexate. J Invest Dermatol. 104, pp.183–188.
- Omura, M. & Yamaguchi, M. (1999). Regulation of Protein Phosphatase Activity by Regucalcin Localization in Rat liver Nuclei. Journal of Cellular Biochemistry, 75, p.437-445.
- Omura, M., and Yamaguchi, M.(1998). Inhibition of Ca²⁺/calmodulin-dependent phosphatase activity by regucalcin in rat liver cytosol: involvement of calmodulin binding. J Cell Biochem. 71(1), pp.140-8.
- Omura, M. & Yamaguchi, M. 1999. Regulation of protein phosphatase activity by regucalcin localization in rat liver nuclei. Journal of Cellular Biochemistry, 75, pp.437-445.
- Orrenius, S., Zhivotovsky, B., and Nicotera, P. (2003). Calcium , Regulation of Cell Death: The Calcium–Apoptosis Link. Nature Reviews Molecular Cell Biology. 4, pp.552-565.
- Oyanagi, H. I., Ichikawa, H., Kosugi, S., Banba, T., Hanyu, T., Hirashima, K., Ishikawa, T., Kameyama, H., Kobayashi, T., Minagawa, M., Koyama, Y., Wakai, T. (2015). Three cases of esophageal carcinoma Achieve a pathological complete response after neoadjuvant chemotherapy with Cisplatin and 5-Fluorouracil. Gan To Kagaku Ryoho, 42(4), pp. 497-501.
- Oztürk, Z., Gurbinar, T., Vural, K., Boyacıoğlu, S., Korkmaz, M. and Var, A. (2015). Effects of Selenium on endothelial dysfunction and metabolic profile In low dose Streptozotocin induced diabetic rats fed a high fat diet. Biotechnic & Histochemistry, pp.1-10.
- Paglin, S., Hollister, T., Delohery, T. (2001). A novel response of Cancer cells to radiation involves Autophagy and Formation of Acidic vesicles. Cancer Res. 61, 2, pp.439-444.
- Palmgren, M. G. and K. B. Axelsen (1998). "Evolution of P-type ATPases." Biochim Biophys Acta. 1365(1-2), pp.37-45.

- Papiez, M., (2013). The influence of Curcumin on the Action of Etoposide in Acute Myeloid Leukemia cell line. *Folia Med Cracov.* 53 (2), pp.1-72.
- Patel, S., Joseph, S.K, Thomas, A.P. (1999). Molecular Properties of Inositol 1,4,5-Trisphosphate Receptors. *Cell Calcium.* 25(3), pp.247-64.
- Payne, S. and Miles, D. (2008). Scott-Brown's Otorhinolaryngology: Head and Neck Surgery 7th Ed. 34-46 (chapter 4 Mechanisms of Anticancer Drugs).
- Pereira, M., Millot, J., Sebillé, S., Manfait, M., (2002). Inhibitory effects of extracellular Mg^{2+} on intracellular Ca^{2+} dynamic changes and thapsigargin-induced apoptosis in human cancer MCF7 cells. *Mol Cell Biochem.* 2002 Jan;229(1-2), pp.163-71.
- Periasamy, M., and Kalyanasundaram, A. (2007). SERCA Pump Isoforms: Their Role in Calcium Transport and Disease. *Muscle Nerve.* 35, pp.430-442.
- Pestell KE, Hobbs SM, Titley JC, Kelland LR and Walton MI. (2000). Effects of p53 status on sensitivity to platinum complexes in a human ovarian cancer cell line. *Mol Pharmacol* 57, pp.503–511.
- Peters, A., Michael, J., Milevskiy, G., Lee, W., Curry, M., Smart, C., Saunus, J., Reid, L., Silva, L., Marcial, D., Dray, E., Brown, M., Lakhani, S., Roberts-Thomson, S. & Monteith, G. (2016). The calcium pump plasma membrane Ca^{2+} -ATPase 2 (PMCA2) regulates breast cancer cell proliferation and sensitivity to doxorubicin. *Sci. Rep.* 6, 25505.
- Petrelli, F., Cabiddu, M. and Barni, S. (2012). 5-Fluorouracil or Capecitabine in the Treatment of Advanced Colorectal cancer: a pooled-analysis of randomized trials. *Med Oncol*, 29(2), pp.1020-1029.
- Pierobon, N., Renard-Rooney, D.C., Gaspers, L.D. and Thomas, A.P. (2006). Ryanodine Receptors in Liver 281(45), pp.34086-34095.
- Pinton, P., Giorgi, C., Siviero, R., Zecchini, E., Rizzuto, R. (2008). Calcium and apoptosis: ER-mitochondria Ca^{2+} transfer in the control of apoptosis. *Oncogene.* 27(50), pp.6407-6418.
- Post, R. L., Hegyváry, C., and Kume, S. (1972). Activation by Adenosine Triphosphate in the Phosphorylation Kinetics of Sodium and Potassium Ion Transport Adenosine Triphosphatase. *J Biol Chem.* 247, pp.6530-6540.
- Preedy, V. (2015). Fluorine: Chemistry, Analysis, Function and Effects. Royal Society of Chemistry P328.

- Proctor,D., Gatto,N., Hong,S., andAllamneni,K.,(2007).Mode-of-Action Framework for Evaluating the Relevanceof Rodent Forestomach Tumorsin Cancer Risk AssessmentToxicol. Sci. 98.pp. 313-326.
- Proskuryakov, S.,Konoplyannikov,A.andGabai,V.(2003).Necrosis:a Specific Form of Programmed Celldeath?.Experimental Cell Research. 283(1), pp.1-16.
- Qian,T.,Herman,B., andLemasters,J.(1999).The mitochondrial permeability Transition Mediates Bothnecrotic and Apoptotic Death of Hepatocytesexposed to Br-A23187. Toxicology and Applied Pharmacology. 154(2). pp.117–125.
- Raffray,M.and Cohen,M., C. (1997).Apoptosis and Necrosis Intoxicology:Acontinuumor Distinct Modes of Celldeath?.Pharmacology&Therapeutics. 75(3).pp.153-177.
- Raji,M.(2005).Managementofchemotherapy-inducedside-effects.TheLancetOncology.6(6), pp.357.
- Ramadori, G. and Cameron, S. (2010) Effect of Systematic Chemotherapy on the Liver.ANNALS of Hepatology. 9(2), pp. 133-143.
- Ramadori, G., Cameron, S., Tschechne, B. (2010). Long-Lasting Tumor Response in Patients with Panitumumab Monotherapy for Chemorefractory Metastatic Colorectal Carcinoma - A Report of Two Cases .Case Rep Oncol. 7;3(2),pp.154-159.
- Randall, R. D. & Thayer, S. A. (1992). Glutamate-Induced Calcium Transient Triggers Delayed Calcium Overload and Neurotoxicity in Rat Hippocampal. Journal of Neuroscience. 12, pp.1882-1895.
- Rani,V., and Yadav, U.(2014). Free Radicals in Human Health and Disease. Spring India.pp.11
- Reinhardt, T. A., Filoteo, A. G., Penniston, J. T. & Horst, R. L. (2000).Ca²⁺-ATPase Protein Expression in Mammary Tissue. American Journal of Physiology-Cell Physiology. 279, pp. C1595-C1602.
- response to thiamine .JPak Med Assoc, 60 (10), pp.867-69.
- Rheumatol, J. (1995) .The effect of age and renal function on the efficacy and toxicity of methotrexate in rheumatoid arthritis. Rheumatoid Arthritis Clinical Trial Archive Group.22,pp.218–223.
- Rheumatol,J.(1995).The Effect of age and renal function on the efficacy and toxicity of methotrexate inrheumatoid arthritis. Rheumatoid Arthritis Clinical Trial Archive Group. 22, pp.218–223.

- Richter, C.(1993) .Pro-oxidants and mitochondrial Ca^{2+} : their relationship to apoptosis and oncogenesis. *FEBSLetters*. 325(1-2), pp.104–107.
- Ringer S. (1882 a.). Regarding the Action of Hydrate of Soda, Hydrate of Ammonia, and Hydrate of Potash on the Ventricle of the Frog's Heart. *J Physiol*. 3, pp.195–202.
- Rosado, J., Lopez J., Harper, A., Harper.M., Redondo, P., Pariente, J., Sage, S, Salido, G.(2004). Two Pathways for Store-Mediated Calcium Entry Differentially Dependent on the Actin Cytoskeleton in Human Platelets. *J Biol Chem*. 279(28), pp.29231-5.
- Rosen, G.,Lurain,J. and Newton, M.(1987). Hexamethylmelamine in ovarian cancer after failure of cisplatin-based multiple-agent chemotherapy. *Gynecologic Oncology*, 27(2), pp.173-179.
- Rossi, A. E. and R. T. Dirksen (2006). "Sarcoplasmic Reticulum: The Dynamic Calcium Governor of Muscle." *Muscle Nerve*. 33(6), pp.715-731.
- Rossini,A.,Like,A.,Chick,W.,Appel,M.and Cahill,G.(1977). Studies of Streptozotocin-Induced in sulitis and diabetes. *Proceedings of the National Academy of Sciences*,74(6), pp.2485-2489.
- Rozenzweig,M.,VonHoff, D., Slavik,M.,Muggia,F. (1977). Cis-diamminedichloroplatinum(II).*Annals of Internal Medicine*. 86(6), p.803.
- Rudolph, H.K., Antebi, A., Fink, G.R., Buckley, C.M., Dorman, T.E., LeVitre, J., Davidow, L.S., Mao, J.I., and Moir, D.T. (1989) The Yeast Secretory Pathway is Perturbed by Mutations in PMR1, a Member of a Ca^{2+} ATPase Family. *Cell*. 58, pp.133-145.
- Sagara Y, Inesi G. (1991). J Inhibition of the Sarcoplasmic Reticulum Ca^{2+} transport ATPase by Thapsigargin at Subnanomolar Concentrations. *J Biol Chem*. 266(21), pp.13503-506.
- Sanders E., and Wride, M. (1995). Programmed Cell Death in Development. *Int.Rev.Cytol*.163 .pp.105–173.
- Saunders, J. (1966). Death in Embryonic Systems.*Science*. 154(3749), pp.604-612.
- Savill,J.,andFadok,V.(2000).Corpseclearedefinesthemeaningofcelldeath.*Nature* 407.pp. 784–788.
- Sawada, N., Nakagawa, T., Murata, T., Yamaguchi, M. (2005). Nuclear localization of a novel protein, RGpPR-p117, in cloned normal rat kidney proximal tubular epithelial cells.*Int. J. Mol*.16 ,pp.809-814.

- Schein,P.,O'Connell,M.,Blom, J., Hubbard,S.,Magrath,I.,Bergevin,P., Wiernik,P., Ziegler,J.andDevita,V.(1974).Clinical anti tumor activity andt oxicity of streptozotocin (NSC-85998).Cancer. 34(4), pp.993-1000.
- Segal-Bendirdjian,E. andJacquemia-Sablon(1995). CisplatinResistance ina Murine Leukemia Cell Line Is Associated with a Defective Apoptotic Process. Experimental Cell Research. 218(1), pp.201-212.
- Segalini, G., Labiania, R., Berretta, G. (1987). Cardiotoxicity of 5-FU - personal cases and review of literature. G Ital Cardiol .17,pp.781-5.
- Serpi, R., Piispala, J., Jarvilehto, M., Vahakangas, K. (1999). Thapsigargin has similar effecton p53 protein response to benzo (a) pyrene DNA adducts as TPA in mouse skin.Carcinogenesis 20, pp.1755–176.
- Shamberger,R.,Rosenberg, S., Seipp,C.etal.(1981). Effects of High-Dose Methotrexateand Vincristin on Ovarian and Testicularfunction in Pateints Undergoing Postoperative Adjuvat Treatmentofosteosarcoma. Cancer Treat Rep., 65.pp.739-746.
- Shen, L., Wen, N., Xia, M., Zhang, Y., Liu, W., Xu, Y., & Sun, S. (2016) .Calcium efflux from the endoplasmic reticulum regulates cisplatin-induced apoptosis in human cervical cancer HeLa cells. Oncology Letters. 11(4), pp.2411-2419.
- Shi,L.,Mai,S.,Israels,S.,Browne,K.,Trapani,J.,Greenberg,A.(1997). GranzymeB (GraB) Autonomously crosses the cell membrane and perforin initiates apoptosis and GraBnuclear localization. JExp Med, 185(5). pp. 855-66.
- Shimizu, S., Kanaseki,T., Mizushima, N., Mizuta, K., Arakawa-Kobayashi, S.,Thompson,C. and Tsujimoto, Y.(2004)Aroleof Bcl-2 Family of Proteins in Nonapoptotic Programmed cell death Dependent onautophagy Genes.Nat.Cell.Biol.6, pp.1221–1228.
- Shin, H. Kwon, H., Lee, J., Gui, X., Achek, A., Kim, J., Choi, S. (2015). Doxorubicin-induced necrosis is mediated by poly-(ADP-ribose) polymerase 1 (PARP1) but is independent of p53. Sci Rep. 5:15798.
- Shord, S.Bernard,S.,Lindley,C.,Blodgett,A., Mehta,V., Churchel,M., Poole, M., Pescatore, S.,Luo, F.,Chaney, S.. (2002).Oxaliplatin Biotransformation and Pharmacokinetics: a pilot study to determine the possible relationship to neurotoxicity. Anti cancer Res. 22, pp.2301–2309
- Shore, N. (2014). PROSTVAC® Targeted Immune Therapy Candidate for Prostate Cancer.

- Short, M., Goldstein, D., Halkett, G., Reece, W., Borg, M., Zissiadis, Y., Kneebone, A. and Spry, N. (2013). Impact of Gemcitabine Chemotherapy and 3-Dimensional Conformal Radiation Therapy/5-Fluorouracil on Quality of Life of Patients Managed for Pancreatic Cancer. *International Journal of Radiation Oncology* Biology* Physics*. 85(1), pp.157-162.
- Shoshan V, MacLennan DH. (1981). Quercetin Interaction with the $(Ca^{2+} + Mg^{2+})$ -ATPase of Sarcoplasmic Reticulum. *J Biol Chem*. 256(2), pp.887-92.
- Shull GE, Greb J. (1988). Molecular Cloning of two Isoforms of the Plasma Membrane Ca^{2+} -Transporting ATPase from Rat Brain. Structural and Functional Domains Exhibit Similarity to Na^{+} , K^{+} - and other Cation Transport ATPases. *J Biol Chem*. 263(18), pp.8646-57.
- Shull, G., Okunade, G., Liu, L. Kozel, P., Periasamy, M., Lorenz, J., Prasad, V. (2003). Physiological functions of plasma membrane and intracellular Ca^{2+} pumps revealed by analysis of null mutants. *Ann NY Acad Sci*. 986, pp.453-60.
- Sinha, B. (1995). Topoisomerase Inhibitors. *Drugs*, 49(1), pp.11-19.
- Sionov, R., Hayon, I., Haupt, Y. (2000). The Regulation of p53 Growth Suppression. In: Madame Curie Bioscience Database [Internet]. Austin (TX): Landes Bioscience; Available from: <http://www.ncbi.nlm.nih.gov/books/NBK6412>
- Skeel, R. and Khleif, S. (2011). Handbook of Cancer Chemotherapy (Lippincott Williams and Wilkins Handbook Series, p. 832.
- Skeel, T. & Khleif, S. (2011). Handbook of cancer chemotherapy. (8th edition)
- Sokolove PM, Albuquerque EX, Kauffman FC, Spande TF, Daly JW. (1986). Phenolic Antioxidants: Potent inhibitors of the $(Ca^{2+} + Mg^{2+})$ -ATPase of Sarcoplasmic Reticulum. *FEBS Lett*. 203(2), pp.121-26.
- Sorensen, T. L., Moller, J. V., and Nissen, P. (2004). Phosphoryl Transfer and Calcium Ion Occlusion in the Calcium Pump. *Science*. 304, pp.1672-1675.
- Souhami, R., Spiro, S., Rudd, R., Elvira, M., James, L., Gower, N., Lamont, A. and Harper, P. (1997). Five- Day Oral Etoposide Treatment for Advanced Small-Cell Lung Cancer: Randomized Comparison With Intravenous Chemotherapy. *JNCI Journal of the National Cancer Institute*. 89(8), pp.577-580.
- Spletstoeser, F., Florea, A., & Büsselberg, D. (2007). IP3 receptor antagonist, 2-APB, attenuates cisplatin induced Ca^{2+} -influx in HeLa-S3 cells and prevents activation of calpain and induction of apoptosis. *British Journal of Pharmacology*. 151(8), pp. 1176–1186.

- Sudbrak, R., Brown, J., Dobson-Stone, C., Carter, S., Ramser, J., White, J., Healy, E., Dissanayake, M., Larregue, M., Perrussel, M., Lehrach, H., Munro, C. S., Strachan, T., Burge, S., Hovnanian, A. & Monaco, A. P. (2000). Hailey-Hailey Disease is Caused by Mutations in ATP2C1 Encoding a Novel Ca²⁺ Pump. *Human Molecular Genetics*. 9, pp.1131-1140.
- Swift, L. H., & Golsteyn, R. M. (2014). Genotoxic Anti-Cancer Agents and Their Relationship to DNA Damage, Mitosis, and Checkpoint Adaptation in Proliferating Cancer Cells. *International Journal of Molecular Sciences*. 15(3), pp.3403–3431.
- Szabo, T., Vanderheyden, V., Parys, J.B., De Smedt, H., Rietdorf, K., Kotelevets, L., Chastre, E., Khan, F., Landegren, U., Soderberg, O., Bootman, M.D., Roderick, H.L. (2008). *Proc Natl Acad Sci USA*. 105(7), pp.2427-32.
- Tacar, O. and Dass, C. (2013). Doxorubicin-Induced death in tumour cells and cardiomyocytes: is autophagy the key to improving future clinical outcomes? *Journal of Pharmacy and Pharmacology*. 65(11), pp.1577–1589.
- Takahashi, H., Yamaguchi, M. (2000). Stimulatory effect of regucalcin on ATP-dependent Ca²⁺ uptake activity in rat liver mitochondria. *J Cell Biochem*. 78(1), pp.121-30.
- Takahashi, Y., Coppola, D., Matsushita, N., Cui, H., Sun, M., Sato, C., Liang, J., Jung, Y., Cheng, J., Mul, J., Pledger, W., Wang, H. (2007) Bif-1 interacts with Beclin1 through UVRAG and regulates autophagy and tumorigenesis. *Nat. Cell Biol.* 9, pp. 1142–1151.
- Tan, M., Choong, P., and Dass, C. (2009). Review: Doxorubicin delivery systems based on chitosan for cancer therapy. *Pharmazie*. 64(12), pp. 131-142.
- Tassa, A., Roux, M., Attai, D., Bechet, D. (2003) Class III phosphoinositide 3-kinase beclin1 complex mediates the amino acid-dependent regulation of autophagy in C2C12 myotubes. *Biochem. J.* 376, pp.577–586.
- Taylor, C. and Traynor, D. (1995). Calcium and inositol trisphosphate receptors. *The Journal of Membrane Biology*. 145(2), pp. 109–118.
- Taylor, O., Hockenberry, M., McCarthy, K., Gundy, P., Montgomery, D., Ross, A., Scheurer, M. and Moore, I. (2015). Evaluation of Biomarkers of Oxidative Stress and Apoptosis in Patients with Severe Methotrexate Neurotoxicity: A Case Series. *Journal of Pediatric Oncology Nursing*.

- Teixeira,A.,Santos,R., Poersch,A., Carrara,H.Andrade,J.,Takahashi,C.(2009). DNA Repairin Etoposide-InducedDNA DamageI Breast Cancerpatients and Healthy-WomenInt J Clin Exp Med 2, pp.280-288.
- Tenev, T.,Bianchi,K.,Darding, M.,Broemer,M.,Langlais, C., Wallberg,F.,Zachariou,A., Lopez,J.,MacFarlane,M.,Cain,K.andMeier,P.(2011). The Ripoptosome,a Signaling Plat form that Assemblesin Responseto Genotoxic Stress and Loss of IAPs. Molecular Cell. 43(3), pp.432-448.
- Thavaramara,T.,Tangjitgamol, S.,Manusirivithaya, S.,Leelahakorn,S.(2009) .Oral etoposide for refractoryorre current epithelial ovarian cancer. JMedAssocThai.92(11), pp. 1397-405.
- Thompson, G., and van Bel, A. (2012). Phloem: Molecular Cell Biology, Systemic Communication, Biotic Interactions. John Wiley & Sons.pages.386.
- Thoreen, C., Kang, J., Chang, Q., Liu, Zhang, Y., Gao, Y. (2009). "An ATPcompetitive mammalian target of rapamycin inhibitor reveals rapamycin-resistant functions of mTORC1." J Biol Chem 284(12),pp. 8023-8032.
- Tiseo,M.,Buti,S.,Boni,L.,Mattioni,R.andArdizzoni,A.(2014). Prognosticrole of Hyponatremia in 564 Smallcelllung Cancer Patient streated with topotecan.Lung Cancer. 86(1), pp.91-95.
- Ton VK, Mandal D, Vahadji C, Rao R. (2002). Functional Expression in Yeast of the Human Secretory Pathway Ca(2+), Mn(2+)-ATPase Defective in Hailey-Hailey Disease. J Biol Chem. 277(8), pp.6422-27.
- Tooze,S.A.(2012). Emerging details shed light on mammalian autophagy: Molecules and Membranes.Biochemist. 24,2. pp.4-7.
- Torrisi,J., Schwartz,L.,Gollub,M.,Ginsberg,M.,Bosl,G. andHricak,H. (2011). CT Findings of Chemotherapy-Induced Toxicity :What Radiologists Need to Know about the Clinicaland Radiologic Manifestations of Chemotherapy Toxicity 1.Radiology. 258(1), pp.41-56.
- Toyoda,K.,Abe,Y.,Tsuda,M.,Haji,S.,Choi,I.,Suehiro,Y.,Kiyasu,J.,Ohshima,K., Uike,N.(2014). Successful treatment with oral low-dose sobuzoxane andetoposide combined with rituximabinan elderly patient with HHV -8-negative primary effusion lymphoma-like lymphoma]. Rinsho Ketsueki. 55(7), pp.815-819.
- Toyoshima C, Inesi G. (2004). Structural Basis of Ion Pumping by Ca²⁺-ATPase of the Sarcoplasmic Reticulum. Annu Rev Biochem.73, pp.269-92.

- Toyoshima, C., and Mizutani, T. (2004). Crystal Structure of the Calcium Pump with a Bound ATP Analogue. *Nature*. 430, pp.529-535.
- Toyoshima, C., M. Nakasako, H. Nomura and H. Ogawa (2000). "Crystal Structure of The Calcium Pump of Sarcoplasmic Reticulum Bat 2.6 Å Resolution." *Nature*. 405(6787), pp. 647-655.
- Toyoshima, C., Nakasako, M., Nomura, H., Ogawa, H. (2000). Crystal structure of the calcium pump of sarcoplasmic reticulum at 2.6 Å resolution. *Nature*. 405, pp.647-55.
- Tran, A., Housset, C., Boboc, B., Housset, C., Boboc, B., Tourani, M., Carnot, F., Berthelot, F. (1991) Etoposide (VP-213) Induced hepatitis. Report of Three Cases Following Standard-Dose treatments. *J Hepatol*. 12 (1). pp.36-39.
- Treves, S., Pouliquin, R., Moccagatta, L., Zorzato, F. (2002). Functional properties of EGFP-tagged skeletal muscle calcium-release channel (ryanodine receptor) expressed in COS-7 cells: sensitivity to caffeine and 4-chloro-m-cresol. *Cell Calcium*. 31(1), pp.1-12.
- Tsang, W.P., Chau, S.Y., Kong, S.K., Fung, K.P., Knowk, T.T. (2003). Reactive Oxygen Species Mediate Doxorubicin Induced-p53-Independent Apoptosis. *73* (16), pp.2046-2058.
- Tsujimoto Y, Shimizu S. (2007). Role of The Mitochondrial Membrane Permeability Transition in Cell Death. *12*, pp.835-840.
- Tsujimoto, Y. (1998). Role of Bcl-2 Family Proteins in apoptosis: Apoptosomes or Mitochondria? *Genes Cells*. 3(11), pp. 697-707.
- Tunwell, R. A. and Lai, F.A. (1996). Ryanodine Receptor Expression in the Kidney and A non-Excitable kidney Epithelial Cells. *Journal of Biological Chemistry*. 271(47), pp.29583-29588.
- Turkeli, M. (2011). Royal Jelly Modulates Oxidative Stress and Apoptosis in Liver and Kidneys of Rats Treated With Cisplatin. *Oxidative Medicine and Cellular Longevity*. pp.1-10.
- Tutkun, A., İnanlı, S., Caymaz, O., Ayanoğlu, E. and Duman, D. (2001). Cardiotoxicity of 5-Fluorouracil: Two Case reports. *Auris Nasus Larynx*. 28(2), pp.193-196.
- Twelves, C., Scheithauer, W., McKendrick, J., Seitz, J., Van Hazel, G., Wong, A., Diaz-Rubio, E., Gilberg, F. and Cassidy, J. (2011). Capecitabine Versus 5-Fluorouracil/Folinic acid as adjuvant therapy For stage III Colon Cancer: Final Results from the X-ACT Trial with analysis by Age and preliminary Evidence

- of a pharmacodynamic marker of efficacy. *Annals of Oncology*. 23(5), pp.1190-1197.
- Tzifi, F., Economopoulou, C., Gourgiotis, D., Ardavanis, A., Papageorgiou, S. and Scorilas, A. (2012). The Role of BCL2 Family of Apoptosis Regulator Proteins in Acute and Chronic Leukemias. *Advances in Hematology*. pp.1-15.
- Ueno, M., Kakinuma, Y., Yuhki, K., Murakoshi, N., Iemitsu, M., Miyauchi, T., Yamaguchi, I. (2006). Doxorubicin induces apoptosis by Activation of Caspase-3 in cultured Cardiomyocytes invitro and rat cardiac ventricles in vivo. *J Pharmacol Sci*. 101, pp.151-158
- Underwood, J., Shahani, R., Blackburn, E. (1971). Jaundice after treatment of leukemia with busulphan. *Br Med J*. 6(1), pp.556-557.
- Van Baelen K, Vanoevelen J, Missiaen L, Raeymaekers L, Wuytack F. (2001). The Golgi PMR1 P-Type ATPase of *Caenorhabditis Elegans*. Identification of the Gene and Demonstration of Calcium and Manganese Transport. *J Biol Chem*. 276(14), pp.10683-691.
- Van Baelen, K., Dode, L., Vanoevelen, J., Callewaert, G., De Smedt, H., Missiaen, L., Parys, J.B., Raeymaekers, L., and Wuytack, F. (2004). The $\text{Ca}^{2+}/\text{Mn}^{2+}$ pumps in the Golgi apparatus. *Biochim Biophys Acta*. 1742, pp.103-112.
- Vandecaetsbeek, I., Vangheluwe, P., Raeymaekers, L., Wuytack, F. and Vanoevelen, J. (2011). The Ca^{2+} pumps of the endoplasmic reticulum and Golgi apparatus. *Cold Spring Harb Perspect Biol*. 2011 May 1;3(5). pii: a004184.
- Vandecaetsbeek, I., Vangheluwe, P., Raeymaekers, L., Wuytack, F. and Vanoevelen, J. (2011).
- Vander Most, R., Robinson, B., Lake, R., Baldwin, E. and Osheroff, N. (2005). Etoposide, Topoisomerase II and Cancer. *CMCACA*. 5(4), pp.363-372.
- Vavra, J., Deboer, C., Dietz, A., Hanka, L., and Sokosiki, W. (1959). Streptozotocin, A new antibacterial antibiotic. *Antibiot Annu*. 7, pp.230-5.
- Victor, M., Migulel, A., Carlos A. and Jose M. (2001). Cisplatin-Induced cell death always produced by apoptosis. 59(4). pp.657-663.
- Vile, G., and Winterbourn, C. (1990). dl-N,N'-dicarboxamidomethyl-N,N'-dicarboxymethyl-1,2-diaminopropane (ICRF-198) and d-1,2-bis(3,5-dioxopiperazine-1-yl)propane (ICRF-187) inhibition of Fe^{3+} reduction, lipid peroxidation, and CaATPase inactivation in heart microsomes exposed to Adriamycin. *Cancer Res*, 50(8), pp.2307-10.

- Vogelstein, B., Lane, D., Levine, A.J. (2000). Surfing the P53 Network. *Nature*. 408, pp.307-301.
- Von Hoff, D., Evans, D., and Hruban, R. (2003). *Pancreatic cancer*. Jones and Bartlett learning, p.188 pages 838.
- Wagner-Dobler, I., Beil, W., Lang, S., Meiners, M., Laatsch, H. (2002) Integrated Approach to Explore the Potential of Marine Microorganisms for the Production of Bioactive Metabolites. *Advances in Biochemical Engineering/Biotechnology*. 74, pp. 208-238.
- Walker, P., Smith, C., Youdale, T., Walker, R., Smith, C., Youdale, T., Leblanc, J., Whitfield, J., Sikorska, M. (1991) Topoisomerase II-Reactive Chemotherapeutic Drugs induce Apoptosis in Thymocytes. *Cancer Res*. 51, pp.1078–1085.
- Walsh, C., Chvanov, M., Haynes, L., Petersen, O., Tepikin, A., Burgoyne, R. (2010). Role of phosphoinositides in STIM1 dynamics and store-operated calcium entry *Biochem. J.*, 425, pp. 159–168
- Wang, J., Whiteman, M., Lian, H., Wang, G., Singh, A. (2009) A non-canonical MEK/ERK signaling pathway regulates autophagy via regulating Beclin 1. *J Biol Chem* 284, pp. 21412–21424.
- Wang, S., Konorev, E., Kotamraju, S., Joseph, J., Kalivendi, S., Kalyanaraman, B. (2004). Doxorubicin induces apoptosis in normal and tumor cells via distinctly different mechanisms. Intermediacy of H₂O₂- and p53-dependent pathways. *J Biol Chem*. 279, pp. 25535–25543.
- Wang, X., Zelenski, N., Yang, J., Sakai, J., Brown, M., Goldstein, J. (1996). Cleavage of sterol regulatory element binding proteins (SREBPs) by CPP32 during apoptosis. *Embo J.* 15(5). pp. 1012-1020.
- Warlick, C. A., Sweeney, C. I. and McIvor, R. S. (2000). Maintenance of Differential Methotrexate Toxicity Between C-Cell Sex-Pressing Drug-Resistant and Wild-Type Dihydrofolate Reductase Activities in the Presence of Nucleosides through Nucleoside Transport Inhibition. *Biochemical Pharmacology*. 59(2), pp. 141-151.
- Warwick, P. (1963). The Mechanism of Action of Alkylating Agents *Cancer Res*. 23, pp. 1315-1333.
- Waseem, M., Bhardwaj, M., Tabassum, H., Raisuddin, S. and Parvez, S. (2015). Cisplatin Hepatotoxicity Mediated by Mitochondrial Stress. *Drug and Chemical Toxicology*, pp. 1-8.

- Wei,P.,Zhang,Z.,Li,L.,Du,X.,Shan,C.andSheng,X.(2015). Clinicalobservational Study of Conformal Radiotherapy Combined With Topotecan Chemotherapy in Patients with Platinum-Resistan Trecurren to Varian cancer. *Genet.Mol.Res.* 14(2), pp.3833-3842.
- Weinstein,G.,Jeffes,E.andMcCullough,J.(1990). Cytotoxicand Immunologic Effects of
- Weiss, R., James, W., Major, W., Porter,M.,Allegra, C.and Curt,G. (1986).Skinreactions Induced by Trime Trexate,Ananalog of Methotrexate.*Investigational New Drugs*,4(2).
- Weiss,R.(1992). The anthracyclines: will we ever find a better doxorubicin?*Semin Oncol*, 19.pp. 670-686.
- Wictome M, Khan YM, East JM, Lee AG. (1995). Binding of Sesquiterpene Lactone Inhibitors to The Ca^{2+} -ATPase. *J Biol Chem*. 310, pp.859-68.
- Wictome M, Michelangeli F, Lee AG, East JM. (1992b). The Inhibitors Thapsigargin and 2,5-di(tert-butyl)-1,4-Benzohydroquinone Favour the E2 Form of the Ca^{2+} ,Mg(2+)-ATPase.*FEBS Lett*. 304(2-3), pp.109-13.
- Williams AJ, West DJ, Sitsapesan R. (2001). Light at The End of the Ca^{2+} -Release Channel Tunnel: Structures and Mechanisms Involved in Ion Translocation in Ryanodine Receptor Channels. *Q Rev Biophys*. 34(1),pp.61-104.
- Wilson,C.andBrowning,J.(2002).Death of HT29a Denocarcinoma Cell Sinduced by TNF Family Receptor Activationiscaspase-Independent and Displays Features of Both Apoptosis and Necrosis. *Cell Death and Differentiation*. 9(12), pp.1321-1333.
- Wojcikiewicz, R.J, Luo, S.G. (1998). Phosphorylation of Nositol 1,4,5-Trisphosphate Receptors by cAMP-Dependent Protein Kinase. Type I, II, and III Receptors are Differentially Susceptible to Phosphorylation and are Phosphorylated in Intact Cells. *J Biol Chem*. 273(10), pp.5670-77.
- Woo, M., Hakem ,R., and Mak, T.(2000). Executionary Pathway for Apoptosis: Lessons From Mutant Mice.*Cell Res*. 10(4), pp.267-278.
- Wootton LL, Argent CC, Wheatley M, Michelangeli F. (2004). The Expression, Activity and Localisation of the Secretory Pathway Ca^{2+} -ATPase (SPCA1) in Different Mammalian Tissues. *Biochim Biophys Acta*.1664(2), pp.189-97.
- Wootton LL, Michelangeli F. (2006). The Effects of the Phenylalanine 256 to Valine Mutation on the Sensitivity of Sarcoplasmic/Endoplasmic Reticulum Ca^{2+} ATPase (SERCA) Ca^{2+} Pump Isoforms 1, 2, and 3 to Thapsigargin and other Inhibitors. *J Biol Chem*. 281(11), pp.6970-976.

- Wootton, L., Cymone, C. Wheatley, A., Michelangeli, F. (2004). The expression, activity and localisation of the secretory pathway Ca^{2+} -ATPase (SPCA1) in different mammalian tissues, *Biochimica et Biophysica Acta (BBA) – Biomembranes*. 1664(2).pp. 189-197.
- Wuytack F, Raeymaekers L, Missiaen L. (2003). PMR1/SPCA Ca^{2+} pumps and the Role of the Golgi Apparatus as a Ca^{2+} store. *Pflugers Arch*. 446(2), pp148-53.
- Wuytack, F., Raeymaekers, L., Missiaen, L. (2002). Molecular physiology of the SERCA and SPCA pumps. *Cell Calcium*.32(5-6),pp.279-305.
- Wyllie, A.(1980).Glucocorticoid-Induced thymocyte Apoptosisisassociated with Endogenous Endonuclease Activation. *Nature*. 284, pp.555–556.
- Yamaguchi, M (2013) The Anti-Apoptotic Effect of Regucalcin is Mediated Through Multisignaling Pathways.*Apoptosis*. 18(10), pp1145-1153.
- Yamaguchi, M. & Yamamoto, T. (1978). Purification Of Calciumbinding Substance From Soluble Fraction Of Normal Ratliver.*Chemical &Pharmaceutical Bulletin*, 26,1915-1918.
- Yamaguchi, M. (2012). *Regucalcin Genomics, Cell Regulation and Diseases*. New York, Nova Science Publishers.
- Yamaguchi, M. and Murata, T. (2015). Suppressive effects of exogenous regucalcin on the proliferation of human pancreatic cancer MIA PaCa-2 cells in vitro. *Int J Mol Med* ;35(6),pp.1773-8.
- Yamaguchi, M. and Shibano, H. (1987). Effect of Calcium-Binding Protein on the Activation of Phosphorylase α in Rat Hepatic Particulate Glycogen by Ca^{2+} . *Chemical and Pharmaceutical Bulletin*.35 (6) ,pp. 2581-2584.
- Yamaguchi, M.(2005). Role of regucalcin in maintaining cell homeostasis and function (review). *Int J Mol Med*. 15(3), pp.371-89.
- Yamaguchi, M., Mori, S., Kato, S. (1988) Calcium-binding protein regucalcin is an activator of $(\text{Ca}^{2+}\text{-Mg}^{2+})$ -adenosine triphosphatase in the plasma membranes of rat liver. *Chem Pharm Bull* 36,pp. 3532–3539.
- Yang,H.,Zhang,Q.,He, J., andLu.W. (2010).Regulation of Calciumsignaling Inlung Cancer *JThoracDis*. 2(1),pp.52–56.
- Yardley, A. (2013). Drug Resistance and the Role of Combination Chemotherapy in Improving Patient Outcomes, *International Journal of Breast Cancer*. Volume 2013 (2013), <http://dx.doi.org/10.1155/2013/137414p>.137- 414.

- Yeh,E., Tong,A., Daniel,M., Lenihan,J.,Yusuf,S.,Swafford, J., Champion,C.,Durand,J.Gibbs,H., fZafarmand,A., Ewer,M., (2004).Reviews: Current Perspectives Cardiovascular Complications of Cancer Therapy Diagnosis, Athogenesis,and Management.109, pp.3122-3131.
- Yoo,Y.,Yoon,Y.,Lee,J., Song,Y., Oh, J., Park,B., Kwon,T.,Park,C.,Choi,Y., And Yoo,Y. (2012). Etoposide induces amixed type of programmed cell death and overcomes the resistance conferred by Bcl-2 in Hep3B hepatoma cells. *IntJOncol*.41.pp. 1443-1454.
- Youn,H.,Kim,H.,Jeon,M.,Lee,J., Seo,Y.,Lee,Y.,Lee,J.(2005). Induction of Caspase-Independent ApoptosisinH9c2 Cardiomyocytesby adriamycintreatment.*MolCell Biochem* . 270.pp. 13–19.
- Yu, X., and Li,Z.(2015) New insights into MicroRNAs involves in drug resistance in diffuse large B cell lymphoma. *Am J Transl Res*. 7(12),pp. 2536-2542.
- Yu,L.,Alva,A.,Su,H.,Dutt,P., Freundt,E., Welsh,S., Baehrecke, E.andLenardo,M. (2004). RegulationofanATG7-Beclin1 Program of Autophagic Cell Deathby Caspase-8. *Science*. 304.pp.1500–1502.
- Zamble, D.and Lippard,S.(1995).CisplatinandDNArepairincancerchemotherapy.Trends in Biochemical Sciences. 20(10), pp.435-439.
- Zelivianshi, S., Spellman, M., Kellerman, M.,Kakitelashvilli, V., Zhou,X., Lugo, E., Lee, M., Taylor, R., Daris, T., Hauke, R., Lin, M.(2003).ERK inhibitor PD 98059 enhances docetaxel-induced apoptosis of androgen-independent human prostate cancer cells.*Int.J.Cancer* 107,pp.478-485.
- Zhang,J.,John,R.,Clark,J.,Eugene,H.,Herman,andVictor,J.(1996). Doxorubicin- induced Apoptosisin Spontaneously HypertensiveRats: Differentia lEffectsin Heart,Kidney and Intestine,andInhibition byICRF-187. *JournalofMolecularand CellularCardiology*. 28(9), pp.1931-1943.
- Zhen,W.,Link.C.,Oconnor,P.Reed,E., Parker,R.,Howell,S.,Bhor,A.(1992) .Inceasedgene- Specific Repairof Cisplatin Inter Stand Cross-Link in Cisplatin-Resistant Human Ovarian Celllines.*Molcell Biol*. 12,pp.3669-3698.
- Zhou,L., Hashimi, H., Schwartz,L., Nambu, J.(1995). Programmed cell death in the the Drosophila central nervous system midline.*Curr Biol*. 1;5(7), pp.784-90.
- Zhu,J., Wang,C.andXu, Y. (2011). Lycopene Attenuatesendothelialdys function in streptozotocin-induced diabetic rats by reducing oxidative stress.*Pharmaceutical Biology*. 49(11), pp.1144-

- Zinzani, P., Pellegrini, C., Broccoli, A., Casadei, B., Argnani, L. and Pileri, S. (2013). Fludarabine-Mitoxantrone-Rituximab Regimen Inuntreated Intermediate/High-Risk Follicular non-Hodgkin's lymphoma: Experience on 142 Patients. *American Journal of Hematology*. 88(11), pp.E273-E276.
- Zitvogel, L., Kepp, O. and Kroemer, G. (2010). Decoding Cell Death Signals in Inflammation and Immunity. *Cell*. 140(6), pp.798-804.
- Zoratti M, Szabo I. (1995). The Mitochondrial Permeability Transition. *Biochimica et Biophysica Acta (BBA)- Reviews on Biomembranes*. 1241(2), pp.139-176.
- Zorov, D., Filburn, C., Klotz, Q., Zweier, J. and Sollott, S. (2000). Reactive Oxygen Species (ROS)- induced ROS release: a new phenomenon accompanying Induction of the Mitochondrial Permeability transition in cardiac Myocytes," *Journal of Experimental Medicine*. 192(7), pp. 1001–1014.
- Zorzato, F., Salviati, G., Facchinetti, T., and Volpe, P. (1985). Doxorubicin induces calcium release from terminal cisternae of skeletal muscle. A study on isolated sarcoplasmic reticulum and chemically skinned fibers. *J Biol Chem*. 260 .pp.7349–7355.